Novel Glycopolymer Architectures

For Biological Applications:

A Supramolecular Approach

Under the Supervision of

Dr. C. Remzi Becer

Dr. Julien Gautrot

Yamin Abdouni

Submitted in partial fulfilment of the requirements of the Degree of Doctor of Philosophy

School of Engineering and Materials Science
Queen Mary, University of London
September 2019

This project has received funding from the European Union's Horizon 2020 research and innovation programme under the Marie Skłodowska-Curie grant agreement No 642083

Statement of originality

I, *Yamin Abdouni*, confirm that the research included within this thesis is my own work or that where it has been carried out in collaboration with, or supported by others, that this is duly acknowledged below and my contribution indicated. Previously published material is also acknowledged below.

I attest that I have exercised reasonable care to ensure that the work is original, and does not to the best of my knowledge break any UK law, infringe any third party's copyright or other Intellectual Property Right, or contain any confidential material.

I accept that the College has the right to use plagiarism detection software to check the electronic version of the thesis.

I confirm that this thesis has not been previously submitted for the award of a degree by this or any other university.

The copyright of this thesis rests with the author and no quotation from it or information derived from it may be published without the prior written consent of the author.

Signature:

Date:

Details of collaborations:

- Parts of this work has been carried out in close collaboration with Gökhan Yilmaz at Nottingham University, Nottingham, UK.
- Parts of this work has been carried out in close collaboration with Anna K. Blakney and Robin J. Shattock at Imperial College, London, UK
- Parts of this work has been carried out in close collaboration with Gijs M. ter Huurne, Anja R. Palmans and E. W. Meijer at the TU Eindhoven, Eindhoven, The Netherlands

Parts of this work have been published in:

- Abdouni, Y., Yilmaz, G. & Becer, C. R. Sequence and Architectural Control in Glycopolymer Synthesis. *Macromol. Rapid Commun.* **38**, 1700212 (2017).
- Abdouni, Y., Yilmaz, G. & Becer, C. R. Sequence and Architectural Control in Glycopolymer Synthesis. in *Sequence-Controlled Polymers* 229–256 (Wiley-VCH Verlag GmbH & Co. KGaA, 2017).
- Abdouni, Y., Yilmaz, G. & Becer, C. R. Sequence Controlled Polymers from a Novel β-Cyclodextrin Core. *Macromol. Rapid Commun.* **38**, 1700501 (2017).
- Oz, Y., Abdouni, Y., Yilmaz, G., Becer, C. R. & Sanyal, A. Magnetic glyconanoparticles for selective lectin separation and purification. *Polym. Chem.* **10**, 3351–3361 (2019).
- Redondo-Gómez, C., Abdouni, Y., Becer, C. R. & Mata, A. Self-Assembling Hydrogels Based on a Complementary Host–Guest Peptide Amphiphile Pair. *Biomacromolecules* **20**, 2276–2285 (2019).

This project has received funding from the European Union's Horizon 2020 research and innovation programme under the Marie Skłodowska-Curie grant agreement No 642083

Abstract

This work reports the synthesis and use of novel glycopolymeric structures synthesised *via* polymer and supramolecular chemistry for lectin-binding studies.

A novel *β*-cyclodextrin initiator was developed for the polymerisation of sequence-controlled star-shaped polymers. Three distinct methods were explored, using well known 'click' or 'click-like' reactions after which it was found that radical thiol-*ene* offers the best initiator. Subsequently, this *β*-cyclodextrin based initiator was used for the sequence-controlled polymerisation of three different acrylates *via* single-electron transfer – living radical polymerisation (SET-LRP).

In a second project, the influence of arm number and arm length of star-shaped glycopolymers was investigated towards a series of lectins found on dendritic and Langerhans cells. Novel star shaped initiators were synthesised and characterised and subsequently used for the polymerisation of glycomonomers *via* SET-LRP. Lectin-binding affinity for the synthesised glycopolymers was finally investigated *via* surface plasmon resonance (SPR)

The third project describes the synthesis of novel glycopolymeric structures starting from commercially available polyethylenimine (PEI) *via* a supramolecular approach. Firstly, commercially available PEI was modified to contain appending adamantane units. Secondly a *β*-cyclodextrin was modified to contain seven appending mannose sugars, and also a *β*-cyclodextrin based mannose star-shaped glycopolymer was synthesised. Subsequently mannosylated PEI's (*glyco*PEI) were achieved by host-guest complexation between the adamantyl residues and the *β*-cyclodextrin based mannose compounds. Finally the *glyco*PEIs were used as a self-amplifying RNA (saRNA) delivery platform both *in vitro* and *ex vivo*.

Finally, the synthesis and characterisation of single-chain glycopolymeric nanoparticles achieved *via* a supramolecular approach were described. Mannose and ethyl hexyl acrylate containing amphiphilic glycopolymers with appending chiral benzene-1,3,5-tricarboxamide (BTA) units were synthesised *via* SET-LRP. After dissolution, heating and sonication, these polymeric compounds formed single-chain polymeric nanoparticles (SCPNs). These SCPNs were subsequently physically characterised *via* DLS, CD and SAXS and furthermore tested for their lectin binding efficiency *via* SPR towards a series of lectins found on dendritic and Langerhans cells.

Acknowledgement

I would like to express my appreciation towards all the people who've helped me during the past years scientifically, but also my friends who've been a constant support throughout these tough years.

First of all, I would like to thank my supervisor *Dr*. Remzi Becer for giving me the opportunity to work in his team, for his constant supervision and help. Without you I would not have been where I am today. The decision you've made in 2015 changed my life completely.

Secondly I would also like to thank all my friends with whom I've worked together in the lab. Jacky and Luka, xiè xiè for teaching me Chinese and those delicious mooncakes! Thank you Resat, for your constant unconditional help whenever I needed it in the lab, you are a great chemist! Alessandra and Ben, thank you both for cheering me up during my last year in the lab, and my apologies for all the singing in the lab. Thank you Cigdem for teaching me my first words in Turkish. And muito obrigado to my Brasilian friends Frederico and Martina for bringing that bit of samba to the lab. I really want to express my appreciation to my friend *Dr*. Gokhan Yilmaz, with whom I had a really great time in the lab and who was a constant source of help and support for me, even in the darkest times. I really appreciate all the help you've given me, resulting in many papers together! Teşekkürler!

A PhD does not only happen in the lab, but fruitful discussions and friendships are made in the PhD offices too. I'd like to thank everyone from 'our office' on the first floor. Isil, Dina, Jasmin and James, lunches without our lunch breaks, I don't know if I would've survived the busy days at QMUL. Isil, you were the first to get your PhD of 'our group' but most definitely you won't be the last! Thank you very much Pavel, Ilanna, Szymon and Ryley, you guys really know well, when to pick the worst moments to discuss science, if you know what I mean. Thank you Pavel for the help with all the mathematical problems. Carlitos muchísimas gracias for your friendship throughout the years. I'm really glad to know you both on a scientific and friendship level resulting in an awesome collaboration. Hopefully more in the future?

Lastly at Queen Mary, there's the mother of all PhD students, our mama bear, Mouna. Thank you very much for all your mental support throughout the years. I'm really happy to have met you, always laughing with stupid stuff, even when our lives are sometimes difficult.

I would like to thank all the people who helped me and worked with me at the Eindhoven University of Technology. Special thanks to prof. Dr. Bert Meijer and prof. Dr. Anja Palmans. It was a pleasure to work in your lab, a truly amazing experience. A big thank you to all the friends I've made in the Netherlands, Gijs, Elisabeth, Patricia, Marcin, Brigitte, Mathijs, Ghislaine, Andreas, Julian and Silvia. You are always welcome to visit whichever country I'll be living in.

I would furthermore like to thank all my Belgian friends, who came and supported me throughout not only my PhD but also my time at Ghent University. Special thanks to my best Belgian friends, Esther, Anne-mare, Greet, Sofie, Jens, Jessie, William and Maarten! Let's make more memories together. Special tribute to you Esther, you were always there whenever I needed you! You guys often came to visit and made Belgium feel even closer to London than it already is.

Big thanks to all the other friends I've made in London over the years and who supported me whenever I needed it, Ryan, Lida, Giusella, Jean-Paul, Hélène, Erwin, Xawa, Marifer, Jennifer, Olga, Nigar, Mo, my Filipino friends Brandon, Aldo, Lorenzo and Vincent, my two Belgian friends in the UK, Annelies and Wing Fai and also my flatmates and 'Birmingham crew', Bianca, Ioli, Lubo, Dominik, Isabelle an Charley.

Lastly I'd like to express my appreciation towards my family. Merci Mama, vo mie olsan gesteund t'in deur gjil min leven en mie gepusht t'in a'k kljinne woare. Zonder gie zou'n ik, Nordine en Kheira nooit gerakt zijn woar dawe nu zijn. Oeveel mamas kun der zeggen dase under kind ip eigen houtje kunn ipvoeden in tot doctor? Khoop daj trots ip mie zit ma ik ook ip joe. Aussi merci à toi Papa, pour tout ton aide pendant mon doctorat. Tu étais quand même toujours la quand j'avais besoin de toi. Comme tu sais il y avait beaucoup de moments où je pensais de quitter mais t'as quand même toujours réussi à augmenter ma morale. Spécialement merci, pour ton aide financièrement pendant ma dernière année. Aussi pour toi, j'espère que tu sois fière sur ton fils.

Thank you to anyone I might have forgotten. If you've helped me during these last years, please do know I appreciate you and thank you for everything.

Table of Contents

Abbreviations

^{1}H-NMR	Proton nuclear magnetic resonance spectroscopy
Ac	Acetyl
Ad	Adamantane
*ada*PEI	Adamantane bearing PEI
ARGET	Activators ReGenerated by Electron Transfer'
ASSET	Anchored Secondary scFv Enabling Targeting
ATRP	Atom Transfer Radical Polymerisation
BA	*n*-Butyl acrylate
BIBB	α-Bromoisobutyryl bromide
BMDO	5,6-Benzo-2-methylene-1,3-dioxepane
BTA	Benzene1,3,5-tricarboxamide
BTA-OH	BTA bearing alcohol
CAM	Cell adhesion molecule
CD	*β*-Cyclodextrin
CD	Circular dichroism
CD-(*p*Man_8)$_7$	Polymeric mannose bearing β-cyclodextrin
CD207	Langerhans cell-specific C-type lectin
CD209	Dendritic cell-specific intracellular adhesion molecules -3 grabbing non-integrin
CD209L	Liver/lymph node-specific ICAM-3 grabbing non-integrin
$CDCl_3$	Deuterated chloroform
CD-Man_7	Heptamannose-*β*-cyclodextrin
cDMEM	Complete Dulbecco's Modified Eagle's Medium

$CHCl_3$	Chloroform
CHO	Carbohydrate
CLEC-1	C-type lectin-like receptor -1
ConA	Concanavalin A
C_p	Complex at the primary rim region
CRD	Carbohydrate recognition domain
CRP	Controlled radical polymerisation
C_s	Complex at the secondary rim region
CTA	Chain transfer agent
CTLD	C-type lectin-like domain
Cu(0)-LRP	Copper (0) mediated living radical polymerisation
CuAAC	Copper (I) Catalysed Azide-Alkyne Cycloaddition
d	Doublet
Đ	Dispersity
DCM	Dichloromethane
DC-SIGN	Dendritic cell-specific intercellular adhesion molecule-3-grabbing non integrin
DC-SIGNR	Liver/lymph node-specific ICAM-3 grabbing non-integrin
DCTB	Trans-2-[3-(4-tert-Butylphenyl)-2-methyl-2-propenylidene]malononitrile
dd	Doublet of doublets
DEC205	Dendritic and epithelial cell receptor
DEGEEA	Di(ethylene glycol) ethyl ether acrylate
DLS	Dynamic Light Scattering
DMF	Dimethyl formamide

DMSO	Dimethyl sulfoxide
DNA	Deoxyribonucleic acid
DNGR-1	Dendritic cell natural killer (NK) lectin group receptor 1
DPA	2-diisopropylaminoethyl methacrylate
E	Entgegen
EA	Ethyl acrylate
EBiB	Ethyl α-bromoisobutyrate
EDTA	Ethylenediaminetetraacetic acid
EHA	2-Ethylhexyl acrylate
ER	Endoplasmatic reticulum
EWG	Electron withdrawing group
FRP	Free radical polymerisation
Fuc	Fucose
Gal	Galactose
GalNAc	N-acetylgalactosamine
GAMA	2-Gluconamidoethyl methacrylate
GFP	Green fluorescent protein
Glc	Glucose
*glyco*PEI	Glycosylated PEI
gp120	Glycoprotein 120
gp41	Glycoprotein 41
GPC	Gel permeation Chromatography
HEPES	4-(2-Hydroxyethyl)-1-piperazineethanesulfonic acid
HIV	Human immunodeficiency viruses

ICAR	Initiators for Continuous Activator Regeneration
ISET	Inner sphere electron transfer
ITC	Isothermal Calorimetry
ITP	Iodine transfer polymerisation
K_a	Association constant
K_D	Dissocation constant
KTFA	Potassium trifluoroacetate
LAMA	2-Lacto-bionamidoethyl methacrylate
Langerin	Langerhans cell-specific C-type lectin
LCST	Lower critical solution temperature
LNP	Lipid nanoparticle
L-SIGN	Liver/lymph node-specific ICAM-3 grabbing non-integrin
m	Multiplet
MA	Methyl acrylate
MALDI-TOF MS	Matrix assisted Laser Desorption Ionisation – Time of Flight Mass spectrometry
Man	Mannose
MBL	Mannose binding lectin
Me_6TREN	Tris[2-(dimethylamino)ethyl]amine
MEHQ	Mequinol
MeOH	Methanol
M_n	Number average molar mass
M_p	Peak molecular weight
*m*RNA	Messenger RNA
MTBE	Methyl *tert*-butyl ether

NBS	N-bromosuccinimide
NHS	N-hydroxysuccinimide
NK	Natural killer
NMP	Nitroxide mediated polymerisation
NMP	N-methyl-2-pyrrolidone
NMR	Nuclear magnetic resonance
NOESY	Nuclear Overhauser enhancement spectroscopy
Nu	Nucleophile
OEGMEA	Oligo(ethylene)glycol methyl ether acrylate
OSET	Outer sphere electron transfer
PAcManA	Poly(2-acryloylethyl-α-D-mannopyranoside)
PBA	Poly(n-butylacrylate)-
PDEAEMA	Poly(2-(diethylamino)ethyl methacrylate)
PDEGMA	Poly(diethylene glycol methacrylate)
*p*DNA	Plasmid DNA
PEG	Polyethylene glycol
PEI	Polyethylenimine
PEO	Poly(ethylene oxide)
Ph_3P	Triphenylphosphine
PHEMA	Poly(hydroxyethyl acrylate)
PMAGlc	Poly(3-O-methacryloyl-a,b-D-glucopyranose)
PMDETA	N,N,N’,N’,N”-pentamethyldiethylenetriamine
PMMA	Poly(methyl methacrylate)
PNA	Peanut agglutinin
PNIPAM	Poly(N-isopropylacrylamide)

PVDF	Polyvinylidene difluoride
PVP	Poly(4-vinylpyridine)
quin	Quintuplet
RAFT	Reversible addition-fragmentation chain-transfer polymerisation
RCA_{120}	Ricinus communis agglutinin
R_G	Radius of gyration
R_H	Hydrodynamic Radius
RID	Refractive index detector
RLU	Relative Light Unit
RNA	Ribonucleic acid
ROP	Ring-opening polymerisation
R_p	Free space radius at the primary rim region
RPM	Rotations per minute
R_s	Free space radius at the secondary rim region
SARA ATRP	Supplemental Activator and Reducing Agent ATRP
*sa*RNA	Self-amplifying RNA
SAXS	Small-angle X-ray scattering
SCPN	Single-chain polymeric nanoparticles
SEC	Size Exclusion Chromatography
SET-LRP	Single-electron transfer – living radical polymerisation
scFv	Single-chain variable fragment
SG1	*N*-tert-butyl-1-diethylphosphono-2 2-dimethylpropyl nitroxide
*si*RNA	Small interfering RNA

SPAAC	Strain-promoted azide-alkyne cycloaddition
SP-D	Surfactant protein-D
SPR	Surface Plasmon Resonance
t	Triplet
TEA	Triethyl amine
TEM	Transmission electron microscope
TEMP	Tetramethyl piperidinyloxyl
TFEMA	2,2,2-Trifluoroethyl methacrylate
Theo	Theoretical
THF	Tetrahydrofuran
TMPA	Tris(2-pyridylmethyl)amin
UK	United Kingdom of Northern Ireland and Great-Britain
VWD	Variable wavelength detector
WGA	Wheat Germ Agglutinin
Z	Zusammen
β-CD-$(Br)_7$	*Per*-(6-deoxy-6-bromine)-β-cyclodextrin
β-CD-$(N_3)_7$	*Per*-(6-deoxy-6-azido)-β-cyclodextrin
β-CD-$(SH)_7$	*Per*-(6-deoxy-6-thio)-β-cyclodextrin

List of Figures

List of Schemes

List of Tables

Chapter 1

Introduction to glycopolymer synthesis

Glycopolymers are synthetic carbohydrate containing materials capable of interacting and binding to specific targeting lectins, which are crucially important in many biological processes. Over the last decade, advances in synthetic chemistry and polymerisation techniques have enabled the development of sequence and architecturally controlled glycopolymers for different types of bioapplications such as drug delivery and release purposes, gene therapy, lectin-based biosensors and much more. These precision glycopolymers are able to mimic structural and functional features of the naturally existing glycocalyx. This introductory chapter will focus on synthesis methods, recent advances in precision synthesis and intermolecular and intramolecular self-assembly of glycopolymers.

Parts of this chapter have been published:

Abdouni, Y., Yilmaz, G. & Becer, C. R. Sequence and Architectural Control in Glycopolymer Synthesis. *Macromol. Rapid Commun.* **38**, 1700212 (2017).

I Introduction to glycopolymer synthesis

I.1 Controlled Radical Polymerisation Techniques

One of the most important mile stones in polymer synthesis is undoubtedly the development of the living polymerisations by Michael Szwarc in 1956.[1,2] Szwarc firstly demonstrated the principle with an anionic polymerisation of styrene in an alkali metal / naphthalene system in THF. He found that the viscosity of the system would increase gradually after the initial addition of the monomer to the initiator system which is perfectly in line with polymer chain growth. However, after addition of 'new' monomer to the system he found another increase in viscosity which indicated that the polymer chains had yet again grown and concluded the polymerisation had never been terminated. The term living polymerisation was then denoted as a chain growth polymerisation for which termination and/or transfer reactions were absent.

The first living polymerisations were based on anionic and cationic polymerisation techniques. Due to the fact that equal charges do not react with one another, termination and transfer reactions can be excluded, resulting in the preservation of the active chain ends. The main drawbacks though, are the incompatibility of such techniques to certain functional groups, the low number of compatible monomers and the need for stringent reagent preparation and reaction conditions.

Free radical polymerisations (FRP) on the other hand enabled the synthesis of high molecular weight polymers owing to their mild reaction conditions and high tolerance toward solvents, impurities and several functional groups.[3] Unlike living polymerisations, FRP still suffers from a lack of control over most important polymer features such as molecular weight, end-group functionality and dispersity. All essential elements for well-defined organic polymeric materials.

I.1.1 Introduction to Controlled Radical Polymerisation methods

In order to resolve the above mentioned problems with FRP, controlled radical polymerisation techniques (CRP) were developed over the past 20 years.[4] These methods offer an exceptional control over the polymerisation process, which allows the development of well-defined polymers with a good control over molecular weight, composition, dispersity, overall architecture and end-group functionality.

The observed limited control during the FRP process is mainly caused by the high concentration of radicals $[P^{\bullet}]$ in the reaction mixture. The biradical termination reaction during radical polymerisations displays a second rate order (quadratic relation with the concentration of radicals in the reaction medium, $R_t = k_t[P^{\bullet}]^2$), while propagation is a first order rate process.[5] In general all controlled radical polymerisation techniques rely on a dynamic equilibrium between the active propagating radicals and various dormant species. Hence, resulting in a dramatic decrease in concentration of active propagating radicals. At concentrations in the range of ppm to ppb, termination reactions are negligible. The fast equilibrium between active and dormant species results in all polymer chains propagating at the same rate enabling the synthesis of homogeneous products. Another way to achieve a controlled radical polymerisation consists of a degenerative exchange process (**Scheme I.1.1**).

$$R_p = k_p[P_n^{\bullet}][M]$$

$$R_t = 2k_t[P^{\bullet}]^2$$

R_p = Propagation rate

R_t = Termination rate

k_p = Propagation rate coefficient

k_t = Termination rate coefficient

$[P_n^{\bullet}]$ = Radical concentration

$[M]$ = Monomer concentration

Several CRP methods have been developed based on these general mechanisms, and the most widely used ones can be listed as nitroxide mediated polymerisation (NMP), reversible chain transfer polymerisation, and Cu-mediated polymerisation.[6–9]

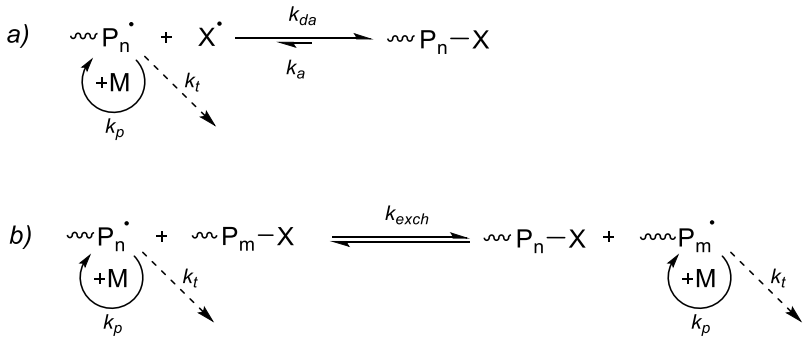

Scheme I.1.1 Controlled radical polymerisation mechanism: a) Deactivation/activation process; b) Degenerative exchange process.

In general, nitroxide mediated polymerisation (NMP) relies on the dissociation of an initiator into two radicals $R^{\bullet}$. Subsequently these radicals can react in an irreversible way with vinyl monomers, thereby starting the polymerisation process. Generation of the dormant species is in this case achieved by the reaction of a radical chain end with a stable persistent nitroxide radical in the reaction medium. Typically tetramethyl piperidinyloxy (TEMPO) or N-*tert*-butyl-1-diethylphosphono-2 2-dimethylpropyl nitroxide (SG1) are used (**Figure I.1.1**). Although a high control over polymer properties is achieved, the required (high) reaction temperature and low monomer compatibility limit the applicability, since mostly styrenic or acrylic derivatives are used.[10]

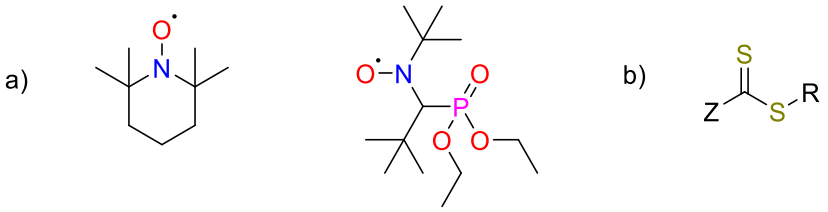

Figure I.1.1 a) Nitroxide stabile radicals applied in NMP: TEMPO (left) and SG1 (middle); b) Thiocarbonylthio compounds used in RAFT polymerisations (right).

I.1.1.1 Reversible chain transfer polymerisation

Reversible chain transfer polymerisation encompasses several polymerisation techniques, including iodine transfer polymerisation (ITP), which is more thoroughly explained in a review on iodo compounds in radical polymerisations, and reversible addition-fragmentation chain-transfer polymerisation (RAFT).[11] RAFT was first reported in 1998 by Rizzardo *et al.* and the group of Charmot. The wide range of functional

monomers which are polymerisable *via* RAFT and the possibility to introduce different end-group functionalities at the α-terminus *via* the chain transfer agent (CTA) enables the synthesis of well-defined complex macromolecules.

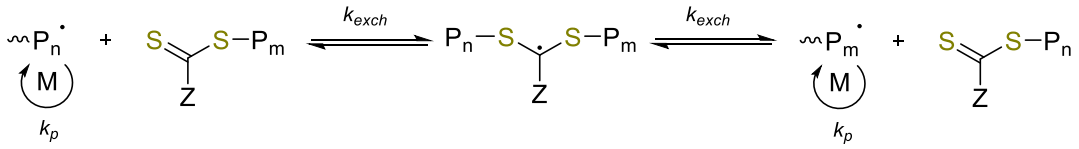

Scheme I.1.2 Reversible chain transfer in RAFT polymerisations

RAFT relies on a degenerative exchange process whereby a thiocarbonylthio compound is used as a chain transfer agent (CTA), creating a free living radical polymerisation system. A wide variety of thiocompounds have been reported as CTA's including dithioesters, dithiocarbamates, trithiocarbonates and xanthates. Mechanistically, the RAFT process involves a series of addition-fragmentation steps. At first, the addition of a propagating radical $P_n^\bullet$ to the CTA results in the formation of a polymeric thiocarbonylthio compound and a new radical $R^\bullet$.This newly formed radical readily reacts with surrounding monomers forming a new propagating radical $P_m^\bullet$. The fast equilibrium between the active propagating radicals and the dormant polymeric thiocarbonylthio compounds provides polymers with a low dispersity *Đ*. A more detailed explanation of these methods can be found in a number of reviews. [6,7,10,11]

I.1.2 Cu-Mediated Polymerisation

In the following section, copper catalysed controlled radical polymerisation techniques will be more thoroughly examined. At first, Atom Transfer Radical Polymerisation, aka ATRP, will be discussed, subsequently the more novel Cu^0-mediated polymerisation will be addressed.

I.1.2.1 Atom Transfer Radical Polymerisation

Atom Transfer Radical Polymerisation (ATRP) is one of the most commonly controlled radical polymerisation techniques used in modern day research. ATRP was developed in 1995 by two separate groups independently, namely the groups of

Sawamoto[12] and Matyjaszewski[13]. The name Atom Transfer Radical Polymerisation refers to the key step reaction which ensures a good control and uniform chain growth, the atom transfer step.

The general mechanism of ATRP relies on a reversible redox process which creates radicals in the system. A transition metal complex (M_t^n/L) in its lower oxidation state catalyses the formation of active radicals abstracting a halogen atom X homolytically of an ATRP initiator $(R-X)$.[14] The reaction generates an alkyl radical $R^{\bullet}$, while the metal complex is transformed into its higher oxidation state $(X-M_t^{n+1}/L)$. The newly active radical species can then propagate with vinyl monomer species, be reversibly transformed into a dormant species (P_n-X) through the addition of a halogen atom or undergo a termination reaction (radical-radical coupling or disproportionation). The low levels of active species however make that the termination reactions are negligible.[15]

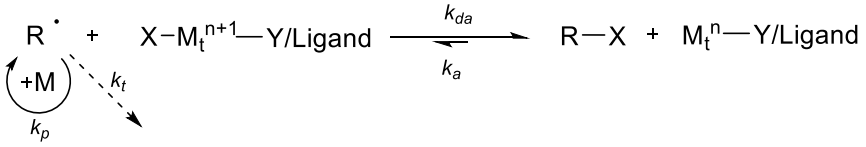

Scheme I.1.3 Main ATRP equilibrium, shifted to the sleeping state. Propagation only occurs when activated.

Several transition metal complexes can be employed (e.g. molybdenum, iron, rhodium, palladium and copper). The metal complex needs to fulfil a few requirements:

- The complex needs to have a free coordination space, which is necessary for addition of the halogen atom to the complex.
- The metal's lower oxidation state should be more stable as compared to its higher oxidation state, this in order to achieve a lower radical concentration.
- The reversible redox process should occur fast.
- The complex should show high affinity towards halogen atoms and a low affinity towards other species in the system.

The most commonly used transition metal is copper, whereas certain iron and ruthenium complexes have also been reported. The wide use of copper is due to its high applicability with several monomers and the relatively low cost. A myriad of ligands have been extensively studied and used in Cu-mediated ATRP, the most important ligands include aromatic pyridine derivatives and aliphatic amines such as tris(2-pyridylmethyl)amine (TMPA) and *N,N,N',N',N"*-pentamethyldiethylenetriamine

(PMDETA).[16] This type of CRP has been successfully used with a whole range of monomer types, such as styrenes, (meth)acrylates, (meth)acrylamides and acrylonitriles leading to polymers with predetermined molecular weights, narrow dispersities and good control over the functionalities. ATRP of nitrogen containing monomers however, proves to be troublesome as monomer and polymer complexation with the catalyst can lower its activity.

Although well-defined polymers are readily obtained *via* ATRP, the major disadvantage of this system is the need for high amounts of transition metal catalyst. Despite several purification methods have been developed to address this problem, there was still a need for lower transition metal concentrations, as these purification methods were generally time-consuming and prohibitively expensive.

The development of three new concepts by Matyjaszewski *et al.* allowed for a reduction of catalyst while still maintaining a controlled polymerisation. The first concept 'Activators ReGenerated by Electron Transfer' (ARGET) ATRP makes use of an excess of reducing agent in the system (e.g. derivatives of hydrazine, ascorbic acid, sugars,…) that regenerates the active catalyst from the deactivating species that accumulate *via* unavoidable termination reactions. In the second concept which is called 'Initiators for Continuous Activator Regeneration' (ICAR) ATRP, the use of reducing agent (in ARGET) is replaced by radical initiators which continually reduce and regenerate Cu(I) species. Furthermore, the use of an externally applied electrochemical potential over the system, allows for a reversible activation of the copper catalyst for ATRP by a one-electron reduction of an initially added air-stable cupric species Cu(II)/L, and thus the *e*ATRP concept.[9,17] These methods allow for a vast reduction in catalyst amount to only a few ppm leading to near colourless products. Moreover, the reactions are less sensitive to the presence of air, which allows them to be performed without deoxygenation.

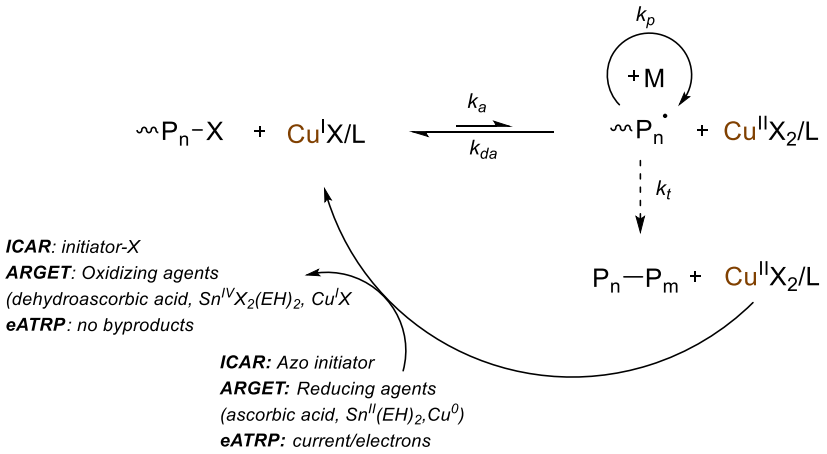

Scheme I.1.4 Main ICAR, ARGET and *e*ATRP equilibria. Compared to classic ATRP, a reductant is added in order to reduce the increasing amount of oxidised metal species due to termination reaction.

I.1.2.2 Cu^0-Mediated Living Radical Polymerisation

In 2006 Percec *et al.* reported a new concept solving the need for high catalyst amounts in ATRP.[18–20] This then relatively new technique, further referred to as Single Electron Transfer – Living Radical Polymerisation (SET-LRP), makes use of the initiators commonly used in ATRP, in combination with elemental copper as the active species, which makes it resemble ATRP mechanistically. By altering the reaction conditions favouring electron transfer and disproportionation of in situ produced Cu(I) and the change of active catalyst to Cu(0), a different polymerisation mechanism is acquired.

The proposed mechanism can be divided into four main steps:

- Activation of the initiator and dormant chains by Cu(0) *via* a heterogeneous single electron transfer (SET).
- Disproportionation of in situ produced Cu(I) into Cu(0) and Cu(II).
- Propagation of the growing polymer chains.
- Deactivation of the propagating polymer radicals by Cu(II) forming Cu(I), which instantly disproportionates.

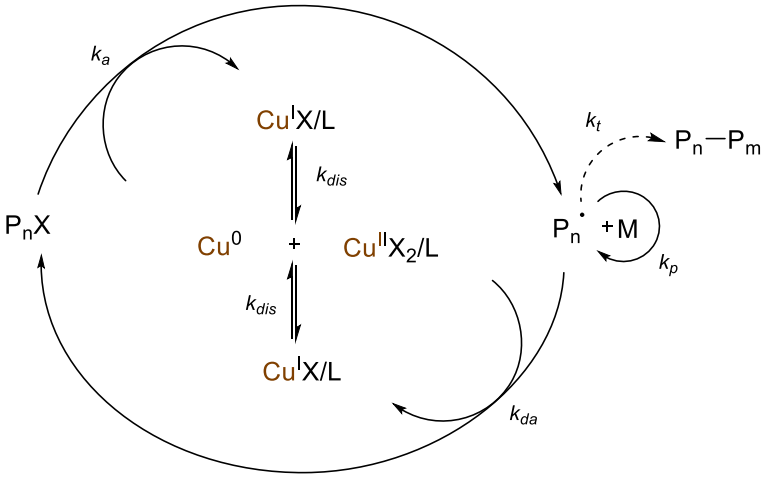

Scheme I.1.5 Proposed mechanism for the Cu0-mediated polymerisation

Essential to the Cu(0)-mediated system is the disproportionation step, which delivers both the activating and the deactivating species. In absence of this step, the polymerisation would not be sufficiently controlled due to the lack of deactivating Cu(II). In contrast to aqueous media, this disproportionation of Cu(I) does not happen necessarily. Rapid disproportionation can be attained by using suitable *N*-ligands, and can often be confirmed in a visual manner by the formation of a blue or green colour in the reaction mixture due to the presence of Cu(II).[21]

The solubility of the copper and halide ions in the reaction mixture are also strongly determined by the solvent composition. Generally, strongly polar or protic solvents give rise to dissociated Cu(I)X and Cu(II)X_2 salts and highly solvated ions. The addition of multidentate *N*-ligands such as Me_6TREN, TREN or PMDETA further enhances this dissociation, as the copper ions are stabilised as complexes.

I.1.2.3 Critical comparison of SARA ATRP and SET-LRP

Besides the mechanism proposed by Percec stated above, another concept developed by Matyjaszewski *et al.* called ‘Supplemental Activator and Reducing Agent ATRP’ (SARA ATRP) debates this principle. The main difference between these two concepts lies in the role of the different copper species during the polymerisation. Although the exact same components are used in both mechanisms, the difference lies in the contribution of each reaction which points out the differences in the major catalytic species.

In SARA ATRP Cu(I) is regarded as the major activator of alkyl halides. On the other hand, Cu(0) functions as a supplemental activator and a reducing agent of Cu(II) *via* comproportionation. In contrast to SET-LRP where the activation of the alkyl halides occurs by outer sphere electron transfer (OSET), the electron transfer in the activation step in SARA ATRP occurs *via* an inner sphere electron transfer (ISET).[19,22]

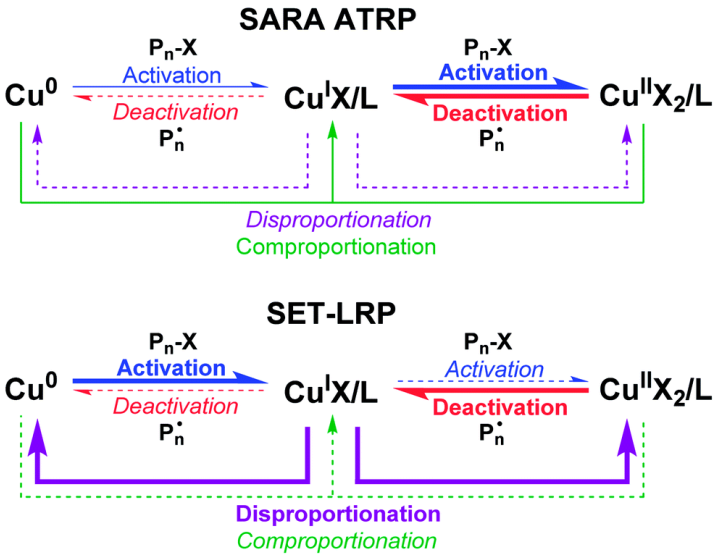

Scheme I.1.6 Proposed mechanisms for SARA ATRP and SET-LRP, showing the most contributing reactions in bold.[22]

In recent literature both research groups (Matyjaszewski and Percec) have made compelling arguments for either proposed mechanism, which are nicely summarised in the recent review by Haddleton *et al.*[19] However, a universally applicable mechanism should be identified in order to end this controversy, because this labelling of reactions, as Matyjaszewski stated, is comparable to differentiating between S_N1 and S_N2 reactions in traditional organic chemistry. Furthermore, for our research objectives, the resulting polymer features are way more important than the occurring reaction mechanism. For this reason, experimental methods in this thesis, are employed as they have been found in SET-LRP literature. The advantages of SET-LRP are first of all the simple removal of the copper catalyst from the polymer, as it is heterogeneous to the polymerisation system. Secondly the polymerisation rates are a lot quicker as compared to conventional ATRP, while using a lot less copper catalyst. However, the main advantage of using SET-LRP remains the high chain-end fidelity (even at 99% conversion), which makes this technique successful for the synthesis of functional macromolecules with complex architectures.

I.2 Click Reactions in Polymer Chemistry

At present, in material science, organic chemistry and pharmacological areas, there's an increasing demand for the preparation of structurally complex molecules through a rational design. From an industrial point of view, practical applications can only exist if the required synthetic route is both synthetically and economically viable. A synthetic route's success is mainly dependent on the success of the individual reactions. For this reason, a change in strategy was needed in order to provide reliable synthetic pathways.

This change in strategy had arrived in 2001 when the term 'click' chemistry was introduced by Sharpless *et al.*.[23] 'Click' chemistry encompasses a number of coupling procedures that comply with a set of stringent criteria: *"The reaction must be modular, wide in scope, give very high yields, generate only inoffensive byproducts that can be removed by non-chromatographic methods, and be stereospecific (but not necessarily enantioselective). The required process characteristics include simple reaction conditions (ideally, the process should be insensitive to oxygen and water), readily available starting materials and reagents, the use of no solvent or a solvent that is benign (such as water) or easily removed and simple product isolation. Purification –if required- must be by non-chromatographic methods, such as crystallization or distillation and the products must be stable under physiological conditions."* Chemically, this means a 'click' reaction should be orthogonal (highly specific and regioselective). A high thermodynamic driving force (usually above 20 kJ/mol) achieves these required characteristics. Such processes usually proceed rapidly to completion and tend to be highly selective. Most common examples of click chemistry include:

- Cycloadditions to unsaturated species, notably 1,3-dipolar cycloaddition reactions, but also Diels-Alder type of cycloaddition reactions.
- Nucleophilic substitution reactions, especially ring-opening reactions of strained heterocyclic electrophiles such as epoxides, aziridines, *etc.*
- Carbonyl reactions (excluding aldol reactions): e.g. urea formation, amide formation, *etc.*
- Additions to carbon-carbon double bonds: oxidative reactions such as epoxidations, dihydroxylation, aziridination but also Michael addition reactions especially the thiol-*ene* reaction.

However, the term ‘click’ reaction has become such a powerful, relevant and commonly used term that articles and reviews use the term ‘click’ to describe reactions that often do not proceed to high conversions or require tedious purification methods. For this reason several polymer chemists have teamed up to defend the core ideas of ‘click’ chemistry and pointed out a set of requirements that should be fulfilled in order for a reaction to be labelled as ‘click’ in the context of macromolecular chemistry.[24] The additional polymer specific criteria include equimolarity and easy large-scale purification.

I.2.1 Copper(I) Catalysed Azide-Alkyne Cycloaddition

The most important and most frequently employed click reaction is undoubtedly the Huisgen 1,3-dipolar azide-alkyne cycloaddition. The popularity of this reaction can mainly be attributed to the fact that alkyne and azide components can easily be incorporated into a wide range of substituents. Additionally, this type of click reaction is very unique as the azide moiety is absent in almost all natural compounds and lacks reactivity towards other functional groups. However, the major drawbacks of the original, uncatalysed azide-alkyne (Huisgen) cycloaddition were that it proceeded rather slowly, requiring high temperatures or pressures and yielding a mixture of different (1,4- and 1,5-)triazoles, which was not in line with the simple reactions conditions and stereospecificity. These rather important drawbacks were successfully overcome by the introduction of the copper catalysed 1,3-dipolar cycloaddition reaction of azides and alkynes, independently reported by Meldal *et al*. and Sharpless *et al.*.[25,26] Using a Cu(I) catalyst, exclusively yields the 1,4-substituted 1,2,3-triazole and excessively accelerates the reaction, allowing room-temperature cycloadditions.

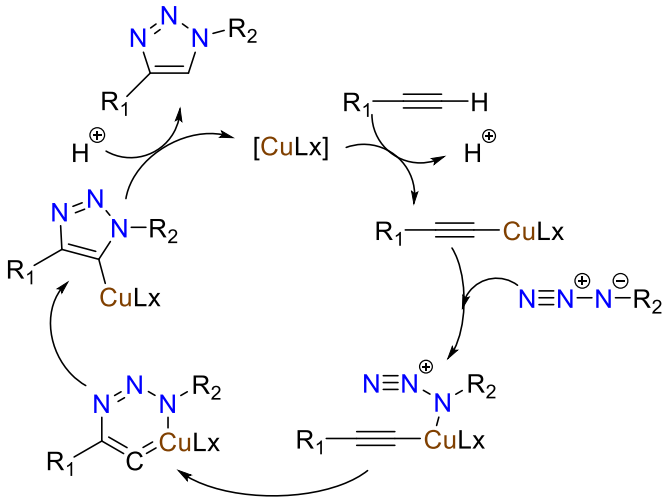

Scheme I.2.1 Proposed mechanism for the Cu(I)-catalysed azide-alkyne cycloaddition.

Unlike the thermal dipolar azide-alkyne cycloaddition which occurs through a concerted mechanism, the Cu(I) catalysed azide-alkyne click reaction is thought to proceed *via* a stepwise mechanism. It is mainly accepted that the stepwise catalytic cycle starts with the formation of a Cu(I) acetylide species *via* the *π*-complex. In addition to Cu(I), also other metal catalysts such as Ni(II), Pt(II) and Pd(II) have been investigated however, their catalytic activity seems much lower as compared to Cu(I). Ru(II) on the other hand is of particular interest as this metal allows the coupling of azides to internal alkynes whereas Cu(I) only catalyses the reaction on terminal alkynes. Moreover, the different catalytic mechanism of the Ru(II) catalyst results in only pure 1,5-substituted 1,2,3-triazoles when the azide is clicked with a terminal alkyne.

I.2.2 Metal-free Click Chemistry

Although, very efficient, disadvantages such as the need for metal catalyst and safety issues related to the use of azides have made this reaction quite unsuitable for biological and/or industrial applications. These drawbacks have inspired scientists to explore other ‘click’ inspired reactions fitting most of the philosophy, without the need for metal catalysts.

I.2.2.1 Strain-Promoted Azide-Alkyne Cycloadditions

The strain-promoted azide-alkyne cycloaddition (SPAAC) was first noted in 1961 by Wittig and Krebs who noticed that the reaction between cyclooctyne and phenylazide proceeded explosively fast (explosionsartig).[27] In 2004 Bertozzi *et al.* proposed to use this SPAAC reaction in chemical biology, however, the first generation of these unactivated cyclooctynes gave rather slow kinetics as compared to the CuAAC reaction.[28,29] This limitation was dramatically improved through the introduction of electron-withdrawing groups (such as fluoride) on the α-position of the triple bond. The high reactivity can be explained by the geometrical deformation of the alkyne bond due to the ring strain, along with the electron deficiency of the triple bond. However, considering the absence of regioselectivity (1,4- and 1,5-substituted triazoles) and the fact that the synthesis of these substituted cyclooctynes is rather demanding, it seems improbable that these reactions will fully replace the CuAAC reaction.

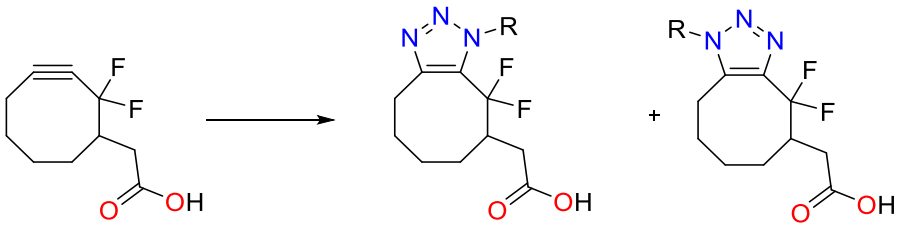

Scheme I.2.2 Strain-promoted azide-alkyne cycloaddition reaction of an azide with a cyclooctyne.

I.2.2.2 'Click'-Inspired Thiol-X Reactions

Thiols are inherently extremely reactive due to the high polarizability and available *d*-orbitals on the sulphur atom. This high reactivity has led to thiols being used for a variety of very efficient thiol-based reactions with a myriad of readily available and useful substrates. Thiolate anions, for example, can mainly be employed in nucleophilic reactions such as Michael additions to electron poor alkenes, but also reactions with isocyanates, epoxides and halogens. On the other hand, thiyl radicals find their substrates in an array of electron rich alkynes and alkenes. However, this high reactivity of thiols implies a restriction. Despite often being classified as a 'click' reaction, thiol-X reactions are not chemoselective or orthogonal towards solvents, reagents and functional groups other than the desired thiol-X reaction which is not in line with the original definition by Sharpless *vide supra.* The following two sections will discuss the

most important of thiol-X reactions, namely the radical thiol-*ene* reaction and the nucleophilic (Michael addition) thiol-*ene* reaction. For further information on other thiol related 'click' reactions, the reader is referred to the excellent review by Hoyle *et al.*[30]

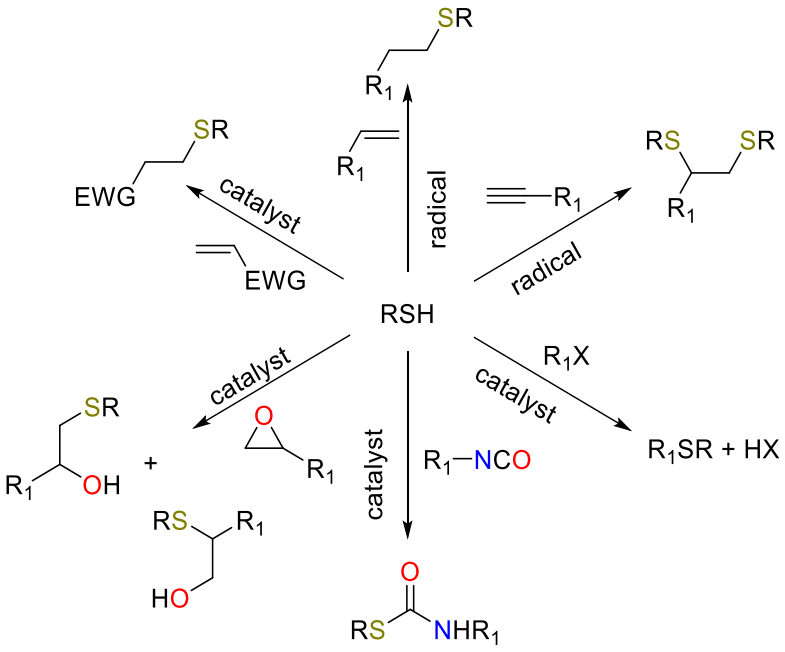

Scheme I.2.3 A variety of efficient thiol-X reactions. EWG=electron withdrawing group. X=Br, I and R_1=aliphatic or aromatic groups.[30]

Radical thiol-*ene* reaction. The thiol-*ene* reaction has first been mentioned as early as in 1905. Basically, the radical thiol-*ene* reaction consists of three parts: initiation, propagation and finally termination. Research conducted by Yağcı *et al*., pointed out that initiation is preferred to happen photochemically using type I photo initiators such as DMPA.[31] Following the formation of radicals, the thiol is converted into the corresponding thiyl radical through hydrogen abstraction. Subsequently the propagation follows two main steps. At first, the thiyl radical inserts itself into the carbon-carbon double bond resulting in a carbon centred radical. Secondly, the newly formed carbon radical abstracts a hydrogen from a thiol in close proximity, resulting in the formation of the anti-Markovnikov thiol-*ene* product and a new thiyl radical. Termination finally ensues by radical-radical coupling as happens in any radical process.

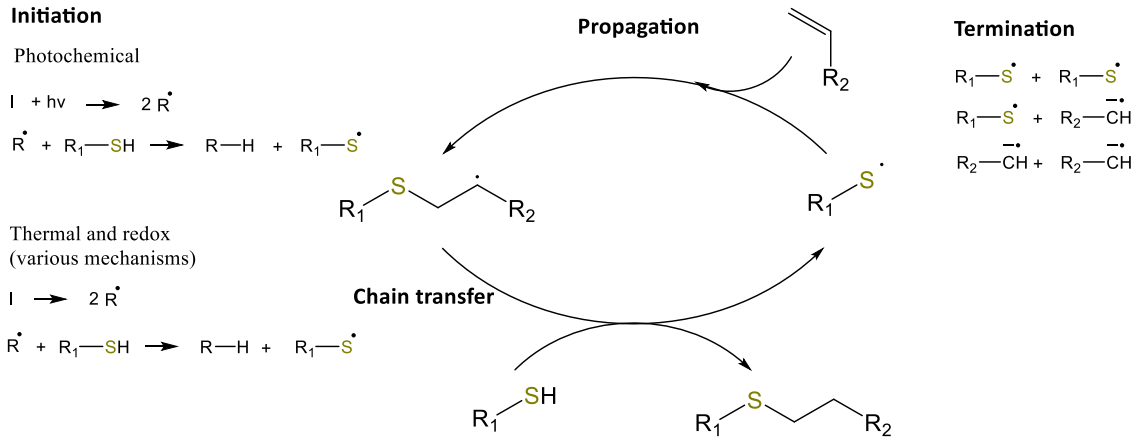

Scheme I.2.4 Mechanism for the radical Thiol-Ene reaction.

Radical thiol-*yne* reaction. Although similar to the radical thiol-*ene* reaction, the radical thiol-*yne* reaction offers a unique way of synthesizing dithiols with 1,2-regioselectivity. Analogous to the radical thiol-*ene* reaction, a thiyl radical is formed photochemically or thermally. This newly formed thiyl radical further undergoes immediate addition to the triple bond resulting in an intermediate thioether vinyl radical. Ensuing this first thiol-*ene* reaction, a second thiol is added radically in a rate three times faster as compared to the initial thiol-*yne* reaction.

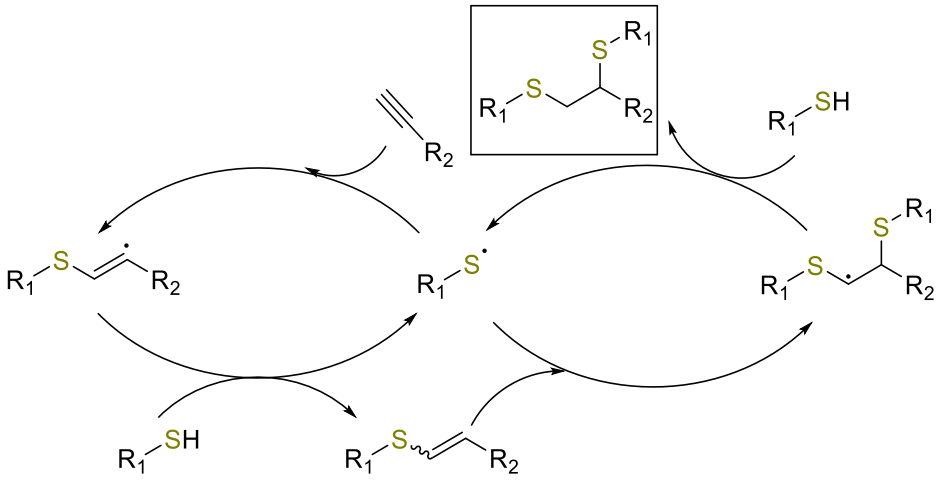

Scheme I.2.5 Proposed mechanism for the radical Thiol-Yne reaction.

Nucleophilic thiol-*ene* reaction. Apart from the radical mechanism *vide supra*, thiol-*ene* reactions can also occur *via* a 1,4-Michael addition to activated alkenes. This thiol-Michael addition reaction can easily be catalysed using catalytic amounts of either a nucleophile or a base. The base catalysed reaction occurs *via* three distinct steps. First, a thiolate anion is created by deprotonation of the thiol by the base. Secondly, the thiolate anion adds to the electron deficient alkene yielding an enolate anion. Lastly,

deprotonation of a protonated base or thiol results in the formation of the thioether end product. The yield and reaction kinetics of this base-catalysed system mainly depend on the concentration and strength of the base catalyst, the thiol pK_a, but also steric accessibility and nature of the electron withdrawing group.

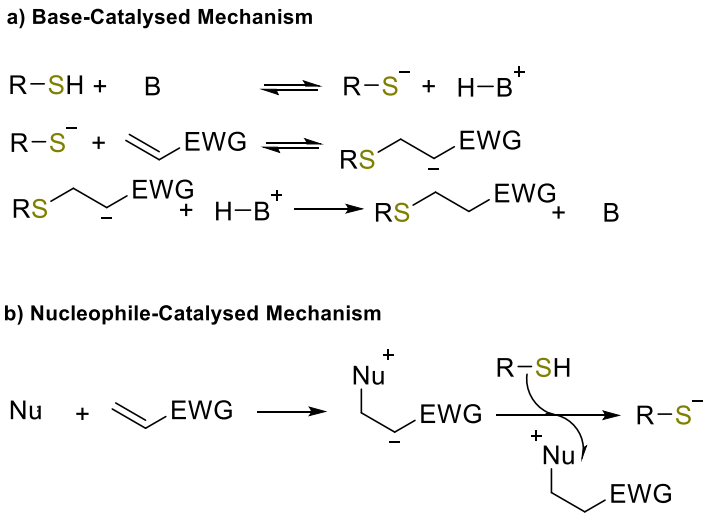

Scheme I.2.6 The base and nucleophile catalysed Michael addition reaction mechanisms.

In contrast to the base-catalysed reaction the nucleophile in the nucleophilic pathway does not really catalyse the reaction. It rather reacts with the electron-deficient alkene generating a strong base. The amount of active thiolate that is generated is strongly influenced by the nucleophilicity of the catalyst. For this purpose phosphines tend to be better catalysts as compared to several amines. Further information on thiol-*ene* reactions, regarding substrate reactivity for example can be found in a review by Bowman *et al*.[32]

I.3 Supramolecular Interactions

As the title of this PhD suggests, supramolecular interactions will form an important tool in the synthesis of our desired compounds and thus understanding the dynamic nature of these physicochemical interactions is essential. J.-M. Lehn defined the field as following: *Supramolecular chemistry, the chemistry beyond the molecule, is the designed chemistry of the intermolecular bond, just as molecular chemistry is that of the covalent bond.*[33] The field of supramolecular chemistry originates from back in the 1960s when new discoveries such as crown ethers (by Pedersen), cryptands (by Lehn) and spherands (by Cram) led scientists to realise that small, complementary molecules could be made to recognise each other *via* noncovalent interactions.[34–36] Noncovalent interactions include ionic interactions (ion-ion, ion-dipole, dipole-dipole), metal coordination, hydrogen bonding, Van der Waals forces, solvophobic interactions, etc. The relevant interactions important for this thesis will briefly be discussed, for further information and better understanding of the underlying principles in supramolecular chemistry, the reader is referred to an excellent review by Hans-Jörg Schneider.[37]

I.3.1 Host-guest interactions: Cyclodextrins

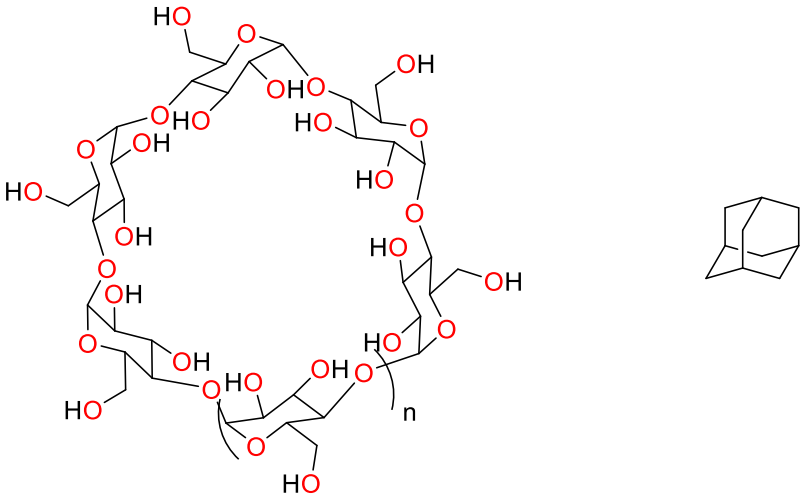

Figure I.3.1 Chemical structure of cyclodextrins (left): n=1 *α*-cyclodextrin, n=2 *β*-cyclodextrin and n=3 *γ*-cyclodextrin and chemical structure of adamantane (right)

Cyclodextrins are cyclic oligosaccharides which consist of six, seven, eight or even more glucopyranose units respectively called *α*-cyclodextrin, *β*-cyclodextrin and *γ*-cyclodextrin. X-ray structures revealed that in cyclodextrins, the secondary hydroxyl

groups (C_2 and C_3) are found on the wider edge of the ring while the primary hydroxyl groups (C_6) are on the other edge.[38] The apolar C_3 and C_5 hydrogens and ether-like oxygens are furthermore found at the inside of these torus-like molecules. These structural features result in a molecule displaying a hydrophilic exterior, dissolvable in water and an apolar cavity which acts as a hydrophobic matrix described as a 'micro heterogeneous environment.[39] The synthetically (enzymatically) most accessible of cyclodextrins is *β*-cyclodextrin and as a consequence the lowest-priced and generally the most useful. The most important properties of cyclodextrins can be found in **Table I.3-1.**

Table I.3-1 Cyclodextrin properties[39]

Property	*α*-cyclodextrin	*β*-cyclodextrin	*γ*-cyclodextrin
Number of glucopyranose units	6	7	8
Molecular weight (g/mol)	972	1135	1297
Solubility in water at 25˚C (%, w/v)	14.5	1.85	23.2
Outer diameter (Å)	14.6	15.4	17.5
Cavity diameter (Å)	4.7–5.3	6.0–6.5	7.5–8.3
Height of torus (Å)	7.9	7.9	7.9
Cavity volume ($Å^3$)	174	262	427

The most remarkable feature of cyclodextrins is their inherent capability to form host-guest complexes with a wide variety of solid, liquid and gaseous compounds. Guest molecules are held within the cavity of the respective cyclodextrin forming an intermolecular complex. The hydrophobic cavity of the cyclodextrin molecule displays a microenvironment which can accommodate appropriately sized apolar molecules. During the formation of the inclusion complex, no covalent bonds are broken or formed, however the main driving force of complex formation stems from the release of energy-rich water molecules from the cavity resulting in an increase of entropy. The hydrophobic guest molecules displace the water molecules resulting in an apolar-apolar association which furthermore decreases the cyclodextrin's ring strain, finally resulting in a more stable lower energy state. As all supramolecular interactions, host-guest complexation is not fixed but displays a rather dynamic equilibrium. This dynamic equilibrium highly depends on how well the host and guest 'fit' together and secondly on the thermodynamic interactions between the different components of the system (cyclodextrin, guest and solvent). A net energetic driving force is crucial to achieve complex formation.

Generally, four main interactions can be identified which help shift the equilibrium towards the inclusion complex. These comprise:

- The displacement of high energy water molecules from the cavity.
- An increase in hydrogen bonds as displaced water returns to the aqueous environment.
- A reduction in repulsive interactions between the (hydrophobic) guest and the aqueous environment.
- An increase in hydrophobic interactions between the guest and the apolar cavity.

Perhaps the most famous of all guest molecules is the hydrocarbon adamantane. Adamantane derivatives are capable of forming unusually strong complexes with *β*-cyclodextrin owing to the fact that the adamantyl residue perfectly fits inside the cavity and the water molecules thus not have any space inside the cavity. The adamantane residues have an approximate spherical shape with an estimated radius of 3.6 Å which is slightly larger than the free space radii (R_p and R_s) close to the H_3 and H_5 atoms (**Figure I.3.2**).[40] For this reason, two separate complexes can be formed with the adamantane guest located either at the primary rim region (complex c_p) or at the secondary rim region (complex c_s). Association constants of adamantane derivatives with *β*-cyclodextrin generally range around 3.52×10^4 for rimantadine (amino derivative of adamantane) and 1.42×10^5 for adamantyl methanol.

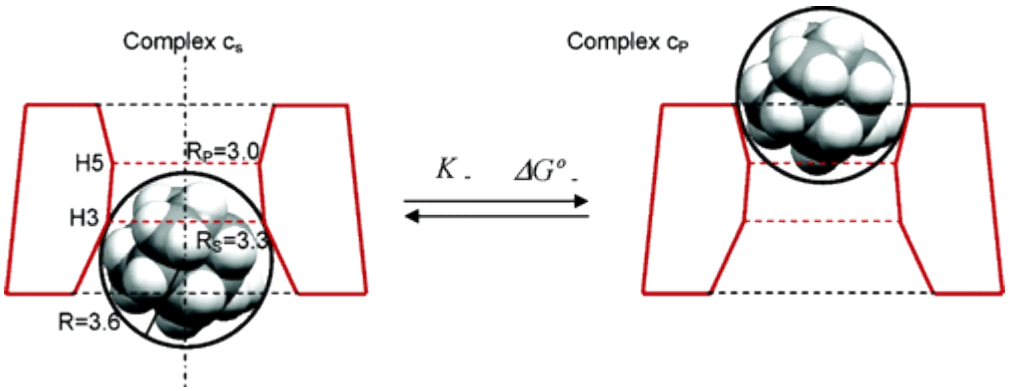

Figure I.3.2 Equilibrium between expected inclusion complexes formed by *β*-CD and adamantane derivatives, data in Å.[40]

I.3.2 Directional supramolecular motifs: Benzene-1,3,5- tricarboxamides

Besides *β*-cyclodextrin, another supramolecular system will be exploited further down in this thesis. The benzene-1,3,5-tricarboxamide moiety, further simply referred to as BTA, and its derivatives have been extensively studied over the past 20 years (**Figure I.3.3**).[41,42] BTAs have the inherent ability to self-assemble into helical supramolecular polymers which are stabilised by threefold hydrogen bonding.

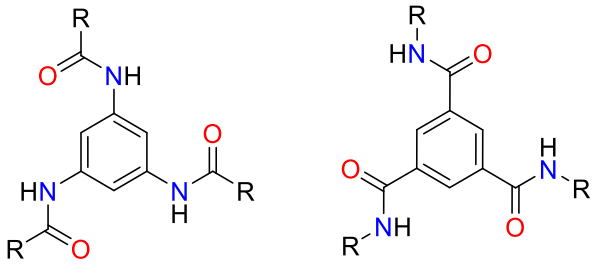

Figure I.3.3 General chemical structures of N- and C=O-centred benzene1,3,5-tricarboxamide (BTA) molecules.

The three amide moieties are able to form hydrogen bonds and (under selected conditions) they are capable of growing into one-dimensional supramolecular polymers (**Figure. I.3.4**). When a chiral centre is introduced into the alkyl side chains, helicity of the one-dimensional aggregates is achieved. This can be proved using circular dichroism (CD) spectroscopy in dilute apolar solutions, which shows a strong Cotton effect around 225 nm.

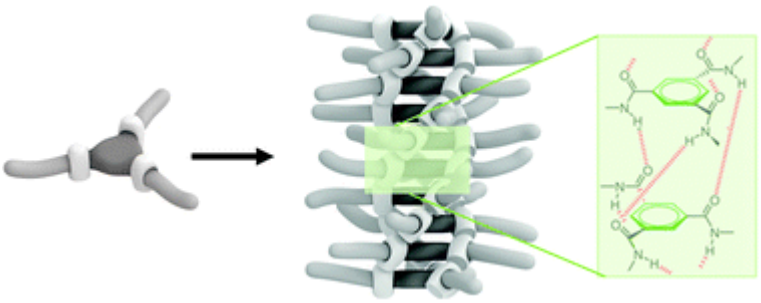

Figure I.3.4 Schematic representation of benzene-1,3,5-tricarboxamide into helical one-dimensional stacks.

Apart from self-assembly in apolar solvents, solubility and additionally self-assembly of the BTA moieties in water was also achieved *via* two distinct design strategies. The first and most straightforward strategy employs the replacement of the aliphatic chains of the BTA derivative by chiral poly(ethylene glycol) side chains, resulting in C_3 symmetrical bipyridine discotics which self-assemble in water using strong

directional *π*-*π* and strong hydrophobic interactions.[43] The second strategy, is based on the principle of hydrophobic shielding. [44] A BTA derivative containing an *L*-phenylalanine and aminobenzoate based spacer, provides a hydrophobic pocket in which the BTA core can still self-assemble using triple H-bonding. Water solubility, in this case, is furthermore achieved by a highly charged peripheral metal chelate complex.

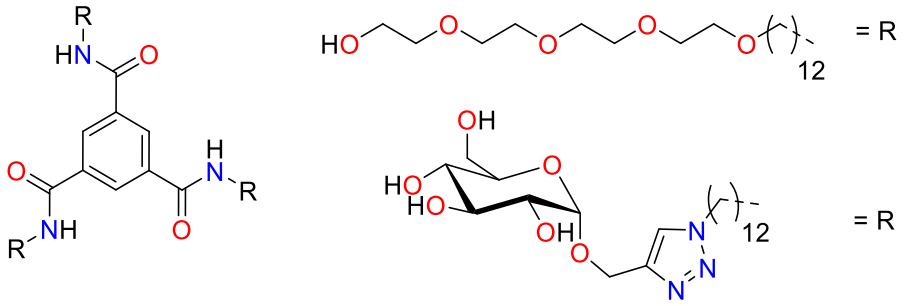

Figure I.3.5 Chemical structure of water soluble BTAs using tetra-ethyleneglycol and α-D-glucopyranoside.

More recently the same principle of a combination of hydrophobic shielding and the use of a water soluble group was employed in two distinct ways (**Figure I.3.5**). Hydrophobic shielding is achieved by using long chiral dodecyl alkyl spacers between the BTA and the water soluble group in both cases. Solubility in water was then achieved using water soluble tetra-ethylene glycol units, the second method (and most recent one) employs simple monosaccharides to achieve this water solubility.[45,46] Using shorter alkyl spacers reflects the need of hydrophobic shielding as the compounds with shorter alkyl spacers self-assemble into shorter one-dimensional aggregates or not even at all and are thus molecularly completely dissolved.

I.4 Glycopolymers and Lectin Recognition

Multivalent protein-carbohydrate interactions play a pivotal role in a wide range of complex biological processes, such as intercellular recognition, signal transduction and host-pathogen recognition.[47–51] Carbohydrates exhibit a great interaction capacity to specific lectins thanks to their monomeric units and their inherent highly branched nature.[52–54] This specific interaction is greatly enhanced by a multivalency effect of densely packed carbohydrate molecules with unique functionalities, which is known as the "glycocluster effect".[55,56] The interactions between carbohydrates and lectins are created by hydrogen bonding, van der Waals' interactions and hydrophobic stacking at the molecular level.[57,58] In contrast to other types of proteins, lectins are not products of the immune system and they display a great diversity in terms of their structure and size.[59–61] Glycopolymers, which are essentially synthetic carbohydrate containing macromolecules, are able to mimic structural and functional features of oligosaccharides thanks to variations in anomeric status, linkage positions, branching, and introduction of site specific substitutions.[62–66] A wide range of oligosaccharides have the capability of covering functionally important areas of lectins, of modulating the interactions with other biomolecules, and of affecting the rate of biological processes which in turn involves conformational changes thanks to their very sensitive sugar coding.[67,68] This special sugar coding system allows them to have crucial biological roles with unusual oligosaccharide sequences, unusual presentations of common terminal sequences and even modifications of the sugars themselves.[69,70] Hence, even though at present there has been great progress on the synthesis of well-defined glycopolymers and glyconanoparticles, there is still a demand for higher precision control on monomer sequences, compositions, and architectures in order to understand the nature of the carbohydrate-lectin interaction in more detail.

During the last decade, there has been a great deal of interest in the integration of carbohydrates in nanotechnology.[71–74] Advances in glyconanotechnology have allowed for the creation of different bioactive glyconanostructures for various health related applications such as drug delivery, gene therapy, pathogen detection, toxin inhibition and the development of lectin-based biosensors.[75–78] Nanoparticles functionalised with carbohydrates present a highly multivalent way for lectin interactions and allow for high local concentrations of ligands on a relatively small surface.[79,80] Glyconanoparticles as carbohydrate-based systems, provide a controlled platform for glycobiological studies because of their ability to mimic the behaviour of the naturally existing glycocalyx.[80] Therefore, the design and engineering of highly innovative

glyconanoparticles with unique physicochemical properties will help further enhancement of specific recognition properties on multivalent scaffolds in glycoscience.

In the last couple of years, “single chain technology” has been explored for a deeper understanding of the multivalent functions and the precise folding mechanism of naturally occurring single-chain architectures of macromolecules in biological systems, such as secondary and tertiary structures of proteins and enzymes.[81–83] In nature, many biomolecules exhibit reversible self-folding processes that are necessary for interfacial molecular recognition.[84,85] Therefore, the introduction of precise synthetic single polymer chain folding is an important step forward towards the creation of more complex macromolecules with specific functionalities and properties in order to imitate complex biological systems. Not only polymer chemists are interested in developments in single-chain collapse, but also researchers from various other areas, especially those in biology. Biologists are drawn to this field due to the inherent opportunities controlled folding would enable, in order to achieve synthetic polymers with specific biological functions.[86–88] In light of these developments, single-chain folding of glycopolymers was discussed as a the newest step forward.

I.4.1 Glycopolymers

The increasing interest in glycopolymer synthesis resulted in a myriad of synthetic polysaccharides used as carbohydrate-vaccines, drug delivery systems and even found applications in tissue engineering exhibiting molecular-recognition abilities, biocompatibility and biodegradability. As stated before, the use of sugars as small molecule inhibitors offers great potential in pharmacological applications. On the other hand most carbohydrate ligands bind to their protein receptor rather weakly (usually association constants are way below 10^6 M^{-1}). In order to achieve higher association constants, biology aggregated most saccharides into higher-order oligomeric structures of very high valency. The tight binding limitation was thus circumvented through multivalency. This phenomenon of enhancement in affinity by multivalency, noted by Lee et al. in 1995, is referred to as the ‘cluster glycoside effect’.[89]

Generally, strategies in glycopolymer synthesis are carried out either by post-glycosylation of preformed polymers or by direct polymerisation of glycomonomers. Several reviews have been published over the last decade by Stenzel, Haddleton, Cameron and recently Seto *et al*., reporting different glycopolymer architectures ranging

from linear to dendritic glycopolymers with different molecular weights, functional groups and carbohydrate densities.[90–93]

I.4.1.1 Direct polymerisation of glycomonomers

Glycopolymer synthesis *via* the direct polymerisation of saccharide containing monomers can be carried out by a range of polymerisation techniques. These include the ring-opening polymerisation (ROP), living anionic polymerisation, ring-opening metathesis polymerisation (ROMP), free-radical polymerisation (FRP), and furthermore controlled free-radical polymerisation techniques (CRP). This section will only encompass controlled radical polymerisation techniques, further information regarding other polymerisation techniques can be found in reviews by Stenzel, Haddleton, Becer and Albertin *et al.*.[90–92,94]

Nitroxide-Mediated Polymerisation (NMP). The first ever developed controlled radical polymerisation technique NMP has only been applied few times in glycopolymer synthesis. The main disadvantages the technique suffers from are the high temperatures needed to achieve homolytic cleavage of the alkoxyamine needed to initiate the polymerisation. Synthesis of glycopolymers *via* NMP was first described in 1998 by Fukuda *et al.* employing a styrenic monomer.[95] Big differences were observed when using either protected or unprotected galactoses. Polymerisation of the unprotected monomer yielded only low conversions and low molecular weight polymers, whereas the polymerisation of the protected monomer afforded uniform polymers while going to high conversions under the same conditions.

Atom transfer radical polymerisation (ATRP). Fukuda *et al*. further employed ATRP as a facile way of synthesizing glycopolymers.[96] The main advantage of ATRP over NMP is the lower polymerisation temperature. It is widely known that glycopolymers and their glycomonomers are unstable at temperatures higher than 120 °C. The main disadvantage of ATRP however, is the need for copper catalyst leaving toxic *Cu* ions which could potentially be harmful in biomedical applications. Glycopolymers thus have to be thoroughly purified before use. Haddleton and co-workers furthermore used ATRP

in combination with click chemistry to prepare glycopolymers. The group clicked different ratios of mannose and galactose based azides resulting in a change of epitope density which influenced the binding affinity of these glycopolymers to rat mannose-binding lectin (MBL).[97]

Reversible addition-fragmentation transfer (RAFT) polymerisation. RAFT has been a valuable tool for the preparation of glycomonomers which is reflected by the number of publications using this polymerisation technique to date. A typical RAFT polymerisation process employs temperatures in the range of 60 to 70 °C. Moreover, this method is highly applicable in biomedical engineering as the polymerisation can be performed in water and no toxic catalyst is needed. The use of a RAFT based glycomonomers furthermore pointed out that glycomonomer functionality is also important. The absence of bioactivity was shown when a glycopolymer containing mannose moieties did not show any significant binding affinity to ConA, not even after 8h.[98] This was attributed to the fact that the used methacryloyl functionality was introduced at the C_6 position. For this reason glycopolymers are frequently conjugated to the polymer backbone *via* their anomeric C_1 position. A recent article by Schubert *et al.* reported the synthesis of a new methacrylic fructose glycomonomer polymerised *via* RAFT which yielded glycopolymers showing an enhanced cellular uptake in to breast cancer cells as compared to other glycopolymers. These were shown using a Rhodamine B label utilising the thiol-functionality derived from the RAFT end group.[99]

Single Electron Transfer-Living Radical Polymerisation (SET-LRP). SET-LRP has recently become a valuable tool for the synthesis of well-defined glycopolymers because of its excellent control over polymer dispersity and its high chain end group fidelity. The importance of the SET-LRP technique, which unfortunately still needs the use of copper catalyst, can be shown by the high impact journals in which the articles are published. In 2013 Haddleton *et al.* published an article describing the synthesis of well-defined glycopolymers prepared *via* SET-LRP employing monomers synthesised by the copper catalysed azide-alkyne click reaction (CuAAC).[100] Both sequence-controlled co-polymers of mannose and glucose based monomers were synthesised, as sequence controlled glycopolymers of a mannose based monomer and di(ethylene glycol) ethyl

ether acrylate (DEGEEA). Furthermore, this report showed that glycopolymer backbone plays an important role in binding behaviour to lectins as two mannose based homopolymers showed different binding affinity. A homopolymer with an acrylic backbone displayed higher binding affinity than a homopolymer with a methacrylic backbone. In 2014 an article was published by Becer *et al.* describing the synthesis of cyclodextrin based glycoconjugates prepared *via* SET-LRP.[101] The synthesised star glycopolymers showed an unprecedented high binding affinity towards the lectin DC-SIGN. This exceptionally high binding affinity was attributed to the high valency of mannose moieties on the star polymer. Furthermore, the star glycopolymers showed high loading capacity of hydrophobic anti-cancer and anti-HIV drugs which renders them promising for HIV therapeutics and in smart drug delivery systems.

I.4.1.2 Post polymerisation glycosylation of synthetic polymers

Even though carbohydrate-containing monomers have been successfully polymerised, post-glycosylation of preformed polymers offers an excellent alternative for glycopolymer synthesis. Glycopolymer libraries of different architectures can easily be attained by attaching carbohydrate moieties to preformed polymer backbones. Crucial in this approach is the presence of a functional handle along the polymer scaffold through which the sugar moieties can be attached. Several of these post-functionalization approaches have nicely been reviewed and summarised by Klok *et al.*.[102]

The main focus of most preformed polymer modifications was put on aminosaccharides which yielded amide linkages between the carbohydrate and the polymer backbone. This focus can be justified because of the good nucleophilicity of amines as compared to other functional groups such as alcohols which are omnipresent in saccharides. Polymer scaffolds bearing active carbonyl moieties such as *N*-hydroxysuccinimide (NHS) esters, carboxylic acids and anhydrides have frequently been employed for glycosylation.

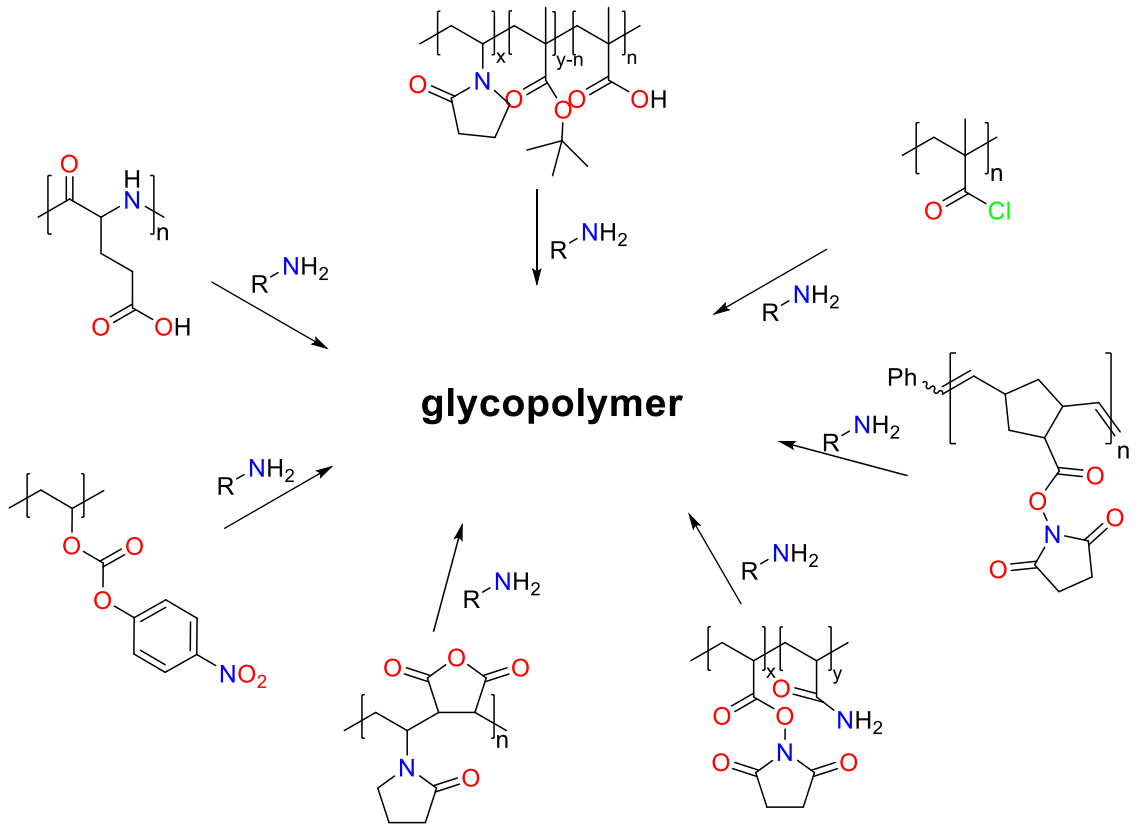

Figure I.4.1 Synthesis of glycopolymers using amide linkages. R= Sugar moiety

A different route of preparing glycopolymers consists of post-glycosylation using 'click' reactions. This approach has been nicely summarised in a review by Becer *et al.*.[92] The copper catalysed azide-alkyne cycloaddition reaction has been shown to be a very effective and versatile strategy for the preparation of glycomonomers. As mentioned before, the removal of copper catalyst still remains a challenge for biological applications. Regardless of this drawback, the reaction has been employed for the preparation of glycopolymers with different topologies and carbohydrate content.

Apart from the CuAAC reaction, also thiol-based 'click' reactions have extensively been employed. For this, thiol functional sugars were reacted with alkene, alkyne, chloro and epoxide groups yielding glycopolymers. The most interesting of these reactions perhaps, is the use of the thiol-*para*-fluoro 'click' reaction. This strategy has been utilised by Schubert *et al.* in combination with NMP yielding well defined homopolymers in a metal free manner.[103]

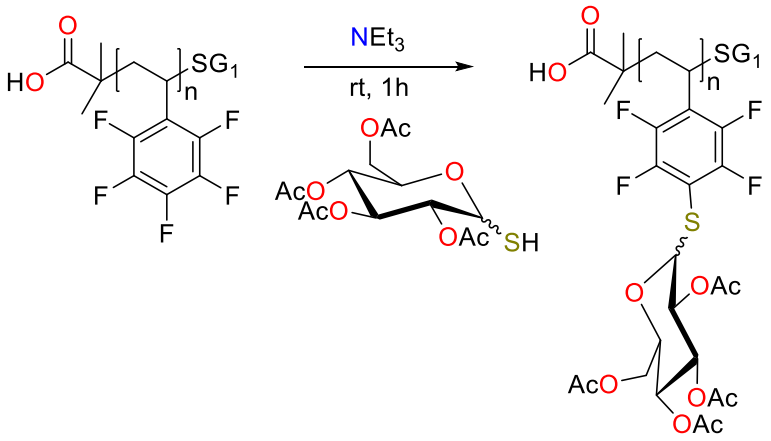

Scheme I.4.1 Synthesis of glycopolymers using thiol-para-fluoro 'click' reaction

I.4.2 Lectins

Lectins, a name derived from the past participle of the Latin verb *legere* which means to select or to choose, are defined as sugar-binding proteins which bind reversibly but with high specificity to carbohydrates.[90,104] Lectins have been demonstrated to be critical in a variety of life processes and essential for several viral infections and pathogeneses in numerous organisms. A wide range of different lectins have been identified to date, these lectins find their sources not only in plants but also in animals and even microorganisms. Although all these lectins have at least one thing in common, the ability to bind carbohydrates, they are still quite diverse in terms of structure and size. For this reason, lectins are often categorised in large families depending on their function or functional parameters. In what follows, the most important lectins will briefly be described.[90,104]

I.4.2.1 Plant lectins

The function of plant lectins is still uncertain although it is suggested that they play a role in plant germination and perhaps in the seed's survival itself.

Legumes. The largest family of lectins is the legume family which consists of over 70 lectins that have been isolated to date. Legumes usually have molecular weights that are below 40 kDa and often require the presence of divalent cations such as Ca^{2+} and Mn^{2+}. Legumes often consist of 2 or 4 subunits with at least 1 binding site each. The most important plant lectin, in a glycopolymer chemist point of view perhaps, is the lectin

Concanavalin A (ConA). ConA is a lectin which is extracted from jack beans, it is also the first ever lectin to be discovered and characterised, and the first ever lectin to be commercially available. More important perhaps, is the fact that ConA binds with strong affinity to mannose, but also glucose. Another important plant lectin is the lectin Peanut agglutinin (PNA). PNA has specific binding affinity towards galactose and preferably to galactosyl (*β*-1,3) *N*-acetylgalactosamine. PNA does not need divalent cations to bind galactose but binding is augmented in the presence of Ca^{2+}.

Cereal lectins. Cereal lectins are composed of two subunits which both have 2 binding sites (usually). Cereal lectins do not require the presence of divalent cations to have binding affinity and are known to be rich in disulphide bonds. The most important cereal lectin is Wheat Germ Agglutinin (WGA) which exists in three different isoforms, WGA1, WGA2 and WGA3. Each consists of two identical subunits and all of them are rich in cysteine (disulphide bonds). Moreover, WGA has a strong specificity for *N*-acetylglycosamine and *N*-acetylneuraminic acid (sialic acid).

Other lectins. Perhaps the most famous lectin, due to its appearance on the television show 'Breaking bad', is the lectin Ricin. Ricin and its closely related *Ricinus communis* agglutinin (RCA_{120}) are two lectins produced by the beans of the castor tree and are perhaps one of the most toxic lectins. Both lectins have a strong affinity to *β*-galactose.

I.4.2.2 Animal lectins

At present, animal lectins are categorised into many families based on their conserved structure of sequence motifs for sugar binding and carbohydrate specificities (**Table I.4.1**).[105] Animal lectins play an important role in a variety of functions. Some of the most important functions include: self- and non-self-recognition, acting as recognition molecules within the immune system, mediation of cellular growth, mediation of endocytosis, *etc.* In what follows, only *C*-Type lectins and Galectins will be discussed.[90,106]

Table I.4-1 Classification of animal lectins. [106]

Lectin	***Saccharide specificity***	***Core motif***	***Location***	***Direct Interaction to Viral components***
C-type lectin	Variable	C-type sequence motif	Extracellular, Cell membrane	Yes
Galectin	*β*-galactosides	S-type sequence motif	Extracellular, Cytoplasm	Yes
Calnexin	Glc_1Man_9	Calnexin sequence motif	ER	Yes
P-Type lectin	Mannose-6-P, others	P-type sequence motif	Cell membrane, Endosome	Yes
L-Type lectin	Variable	L-type sequence motif	ER, ERGIC, Golgi	Yes
I-Type lectin	Sialic acid, Variable	Ig-like domains	Cell membrane	No
M-Type lectin	Man_8	M-type sequence motif	ER	No
F-Type lectin	L-Fucose	F-type sequence motif	Extracellular	No
R-Type lectin	Variable	R-type sequence motif	Extracellular, Cell membrane	No
F-Box lectin	$GlcNAc_2$	F-box sequence motif	Cytoplasm	No
Chitinase-like lectin	Chito-oligosaccharides	TIM (Triose-phosphate isomerase) barrel-like structure	Extracellular	No
Intelectin	Gal, galactofuranose, pentoses	Intelectin sequence motif	Extracellular, Cell membrane	No

C-Type lectins. C-type lectins are lectins that are dependent on the presence of Ca^{2+} in order to interact with carbohydrates. Usually they consist of complex structures with carbohydrate recognition domains (CRD) of about 120 amino acids. In contrast to plant lectins previously discussed, C-type lectins can have a variable number of subunits with 1-8 binding sites each. C-type lectins are further divided into subfamilies. An example of such a C-type lectin is the hepatic asiologlycoprotein (hepatic lectin) which is specific for galactose/ *N*-acetylgalactosamine.

Another very important example is the animal lectin DC-SIGN which is the dendritic cell-specific intercellular adhesion molecule-3-grabbing non integrin that is expressed on dendritic cells, cells which take part of the immune system. DC-SIGN is an interesting target with high affinity for mannose and plays a role in the main pathway the

HIV virus uses to enter the dendritic cell during infection. The HIV virus uses its glycoprotein *gp*120, which is heavily glycosylated with mannose residues, to adhere to DC-SIGN, subsequently another helical glycoprotein called *gp*41 unfolds enabling the HIV virus to enter the dendritic cell. Another C-type lectin found on macrophages is the mannose receptor. The mannose receptor can also be found on hepatic and lymphatic endothelia, on tracheal smooth muscle cells, on mesangial cells in the kidneys and on retinal pigment epithelium. As the name suggests, there is a strong preference in binding to mannose, but also fucose and *N*-acetyl glucosamine have some binding affinity.

Selectins are a family of cell adhesion molecules (CAMs). Selectins are related to C-type lectins due to their related amino terminus and a calcium-dependent manner of binding. Selectins have a strong tendency to interact with sialyl-CD15 (a tetrasaccharide), which consists of sialic acid, galactose, fucose, and *N*-acetylgalactosamine. There are 3 subtypes of selectins which include: E-selectins (in endothelial cells), P-Selectins (in platelets and endothelial cells) and lastly L-selectins (in leukocytes).

Galectins (S-Type). Formerly called S-type lectins, galectins are suggested to play a role in cancer proliferation and roles in other functions such as inflammation. Most galectins have a high affinity for *β*-galactosides, with a strong preference to lactose and *N*-acetyl lactosamine. Galectins are divided into three subgroups. The first group comprises galectins in the dimeric form that consists of only carbohydrate recognition domains. The second group encompasses galectins where the CRD is attached at the *N*-terminus and which has a high sequence repetitive domain. The last group are galectins that consist of two tandemly connected CRDs.

I.4.3 Maximizing lectin recognition

For glycopolymers to achieve effective lectin binding and affect signal transduction, they must bind to at least one but usually multiple copies of their protein receptor. Glycopolymers thus have to be tailored to inhibit glycan interactions with a cell surface receptor or to cluster receptors for signalling. To achieve this, there are some glycopolymer features influencing activity, which need to be considered.[107]

Glycopolymer length, functional affinity and receptor clustering. The development of living polymerisations (with almost no termination) have enabled the

synthesis of polymers of defined length. A minimum length of glycopolymer is often required as lectins often consist of multiple subunits. Optimal binding usually needs at least two binding sites bridged by the glycopolymer. Furthermore, it should also be noted that when all accessible binding sites are occupied, an increase in polymer length will not further yield enhancements in functional affinity (avidity). Glycopolymer length not only influences functional affinity, but it also influences the ability to cluster multiple receptors and the amount clustered. It is sometimes found that clustering multiple receptors leads to more effectively transmitted signals and thus shows that glycopolymer length influences signal strength.

Density of the saccharide ligands. Altering the epitope density on the polymer backbone also has a strong influence on the glycopolymer functional affinity. There are two ways in which carbohydrate ligand density can be manipulated: copolymerisation of a sugar bearing monomer with a biologically inactive monomer, or post-polymerisation functionalization of a polymer with a biologically inert ligand and a sugar bearing ligand. Both methods allow for a variation in level of carbohydrate substitution. Although it is often the case that the highest saccharide substitution level gives the best binding affinity, this cannot be generalised. It is found that the spacing between two sugar units has the most important influence. The spacing between two carbohydrates should match that of the binding epitopes on the lectin.

Polymer backbone flexibility. The flexibility (or rigidity) of the polymer backbone has a strong impact on the glycopolymer's ability to bind receptors. Although rigid polymers would avoid an entropic penalty when binding, it is found that they are less capable of adapting to protein interfaces, lowering the binding affinity. However, polymers which are too flexible pay a big conformational penalty leading to a low binding affinity as well. Not only backbone flexibility plays a role, but also flexibility of the linker (which connects the saccharide to the backbone). It seems thus likely that the most active glycopolymers will be the ones that maintain a balance between rigidity and flexibility in order to adopt a conformation that leads to effective interactions.

I.5 Sequence-controlled glycopolymers

Until recently, glycopolymer synthesis was mainly limited to the synthesis of homomultivalent sugar containing polymers. In the last couple of years however, in polymer chemistry, there has been a shift towards absolute control over monomer sequence. Unlike for peptide synthesis, polymer synthesis had not yet been established in a sequence controlled manner up until now. New methods have been developed enabling good control over primary and secondary structures in polymer design. This was not different in glycopolymer design, where it is believed that a better control over glycopolymer architecture will not only lead to a better lectin binding affinity, but will also introduce a much desired selectivity towards specific lectins. That an improved control over architecture has significant influence on glycopolymer binding, has already been shown by the development of star glycopolymers, which showed to bind better to specific lectins compared to their linear counterparts.[101,108] Various research groups have contributed to this emerging field of precision glycopolymer synthesis in diverse approaches.

In 2013 Barner-Kowollik *et al.* described several approaches to acquire sequence controlled polymers.[109] Three different approaches were suggested, providing a degree of sequence control. The first approach consisted of the classical step-by-step synthesis yielding sequence-defined polymers, which are often prepared on solid-phase. The second approach relies on classical reversible-deactivation-based synthesis of block copolymers, this consists of the sequential polymerisation (with isolation of intermediate polymers) of sequentially added monomers. Thirdly Barner-Kowollik suggested the sequence-controlled polymerisation of different monomers in a one-pot process, without isolation steps *via* time-regulated chain extensions. For the synthesis of periodic polymers containing a sequence defined periodic repetition of monomers, two other approaches can be added. The fourth approach would be the polymerisation of a defined oligomer into a polymer with repeated sequence, these are often observed in Nature (e.g. glycosaminoglycans, collagen, etc.). The fifth approach would consist of the combination of one or multiple orthogonal reactions, either for the polymerisation or post-polymerisation modification of a polymer, resulting in a macromolecule with a repeated sequence.[110]

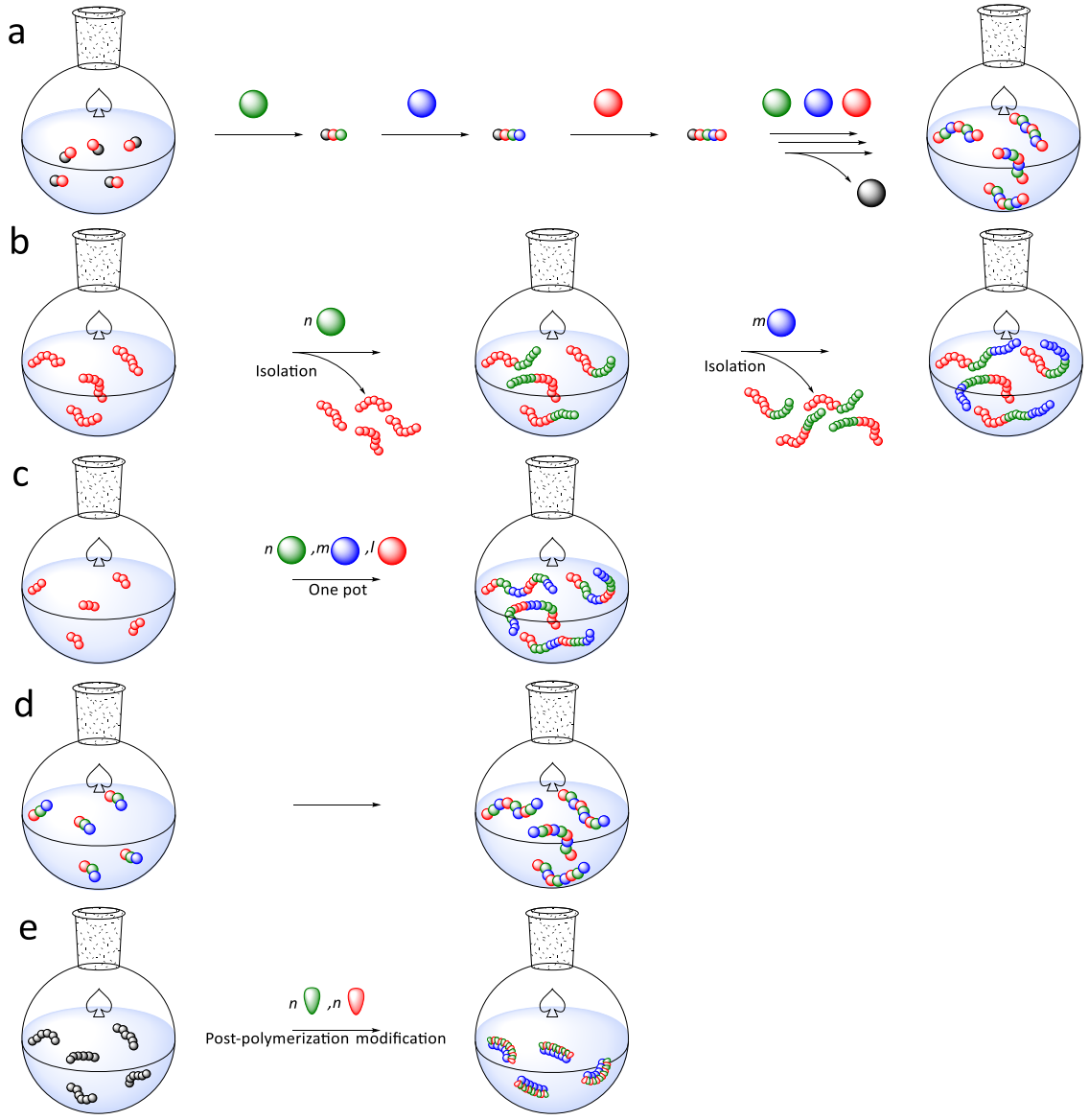

Figure I.5.1 a) Classical step-by-step synthesis of sequence-defined polymers. b) Sequential polymerisation (with isolation of intermediate polymers) of sequentially added monomers. c) Sequence-controlled polymerisation via time regulated chain extensions, without the need for isolation steps. d) Polymerisation of a sequence-defined oligomer into a periodic polymer. e) Post-polymerisation modification *via* orthogonal reactions resulting in a periodic polymer.[110]

I.5.1 Sequence-defined glycooligomers

This first approach was first introduced in glycopolymer synthesis by the group of Hartmann, who elegantly borrowed standard peptide synthesis coupling procedures combined with click reactions. In order to achieve these solid phase bound oligomers, different building blocks had to be prepared (**Scheme I.5.1**). The group designed various

blocks using a doubly protected diethylenetriamine key intermediate as an asymmetrical precursor capable of being functionalised at the secondary amine.[111–113]

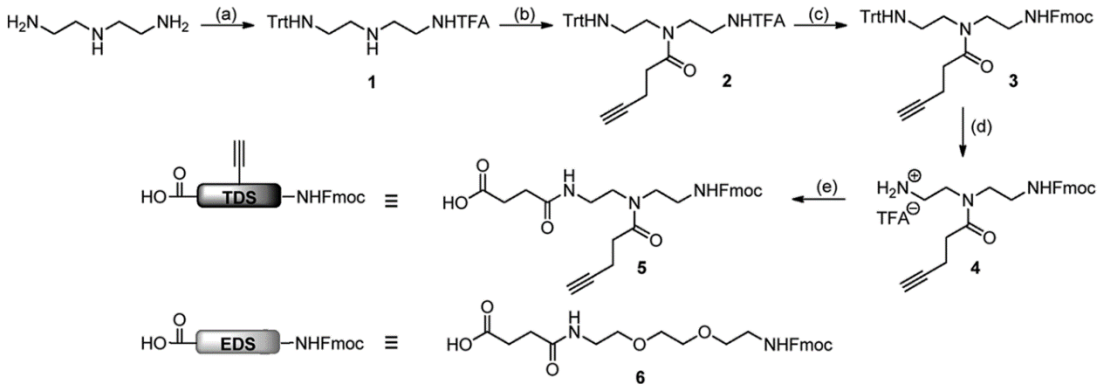

Scheme I.5.1 Building block synthesis: The Triple bond functionalized building block **(TDS)** with a Succinyl rest synthesized starting from Diethylenetriamine and an Ethylenedioxy building block **(EDS).**[111]

At first, homomultivalent glycooligomers presenting mannose were synthesised *via* an on-resin 1,3-dipolar cycloaddition to a scaffold composed of these building blocks (**Scheme I.5.2**). These mannose containing oligomers could show that binding affinity towards the lectin Con A was not only dependent on the number of presented sugars on the scaffold, but also on chemical composition of the scaffold and the spacing in between the ligands. The same technique has more recently been applied using fucose as the carbohydrate of interest.[114]

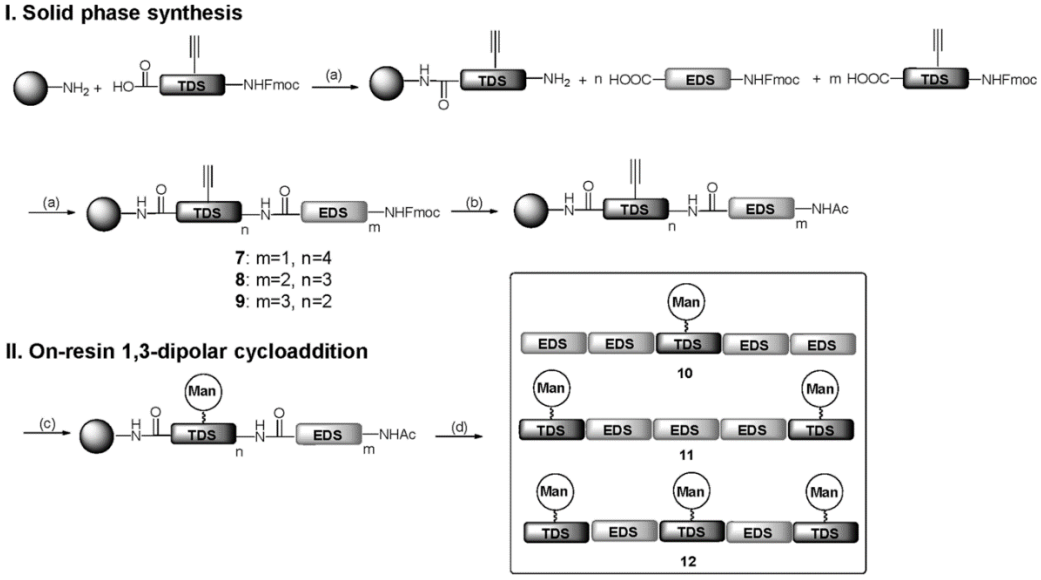

Scheme I.5.2 Solid-phase synthesis of glycopolymer segments.[111]

After the successful synthesis of these homomultivalent glycooligomers, more diverse heteromultivalent glycooligomers were prepared presenting different combinations of Man, Gal and Glc with a controlled number and position of ligands. These glycooligomers were further subject to evaluation for their binding behaviour towards the lectin ConA.[115] More interestingly maybe, was the combination of these building blocks with a new photoswitchable building block containing an azobenzene moiety.[116] Use of this building block provided a controlled reduction in binding affinity upon *E* → *Z* photoisomerization towards the galactophilic lectin (PA-IL), a tetrameric, calcium dependent lectin which specifically binds to *α*-galactosides. This *E* → *Z* photoisomerization provides to reversibly isomerise between an extended and planar form (*E*-isomer) and a more compact and twisted state (*Z*-isomer).

The same principle of building blocks combined with click reactions, was further explored using an in-flow conjugation of thioglycosides to a double-bond presenting diethylenetriamine precursor *via* thiol-*ene* chemistry.[113] The main difference here is that the building blocks were functionalised with glycosides prior to the solid phase synthesis. After glycosylation, these protected carbohydrate containing building blocks were coupled to the solid-phase resulting in monodisperse sequence-defined glycooligomers with different glycosylation patterns.

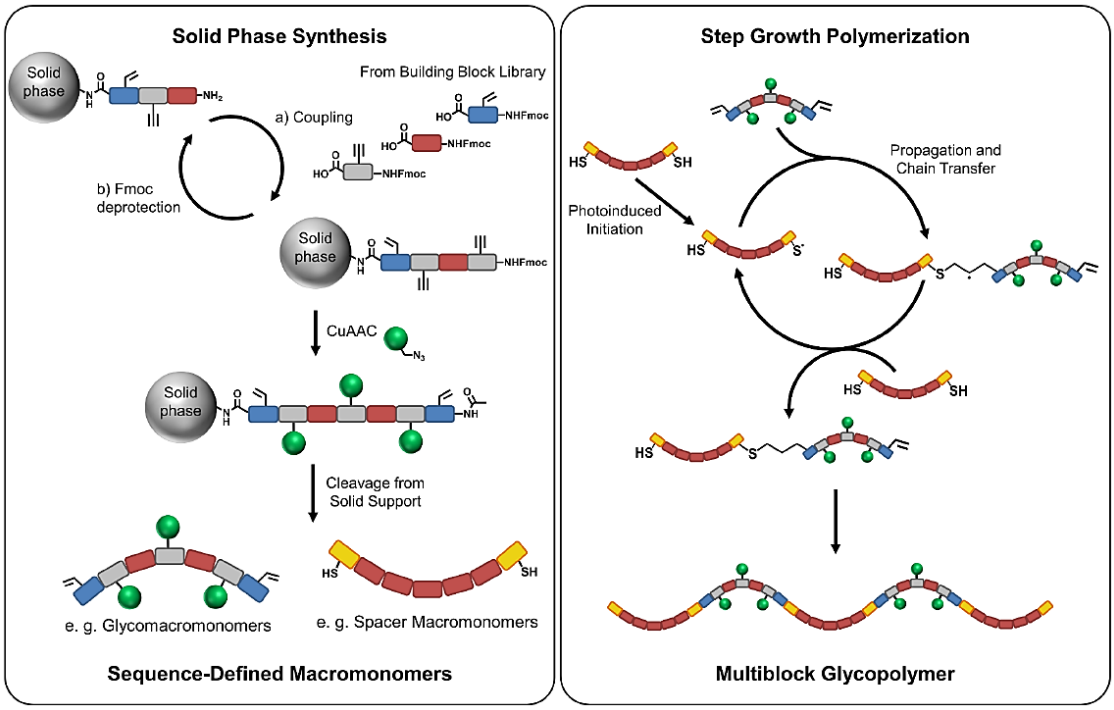

Figure I.5.2 Schematic presentation of the solid phase synthesis of end-functionalised macromonomers using tailor-made building blocks (left) and their step-growth polymerisation via thiol-ene coupling (right). [117]

The same group has now achieved to bring this approach one-step forward using a combination of solid phase synthesis and step-growth polymerisation by photoinduced thiol-*ene* coupling.[117,118] Firstly, two sets of macromonomers were prepared *via* solid phase assembly of functional building blocks introducing either a hydrophilic spacer block with thiol end groups or sugar-presenting blocks with varying number of sugar units in the side chain and alkene end groups. Subsequently, as seen in **Figure I.5.2**, photoinduced thiol-*ene* coupling step-growth polymerisation were undertaken to obtain specifically sequence-controlled glycopolymers with high molecular weight. Obviously, this advanced approach will lead to synthesise precision glycopolymers with higher molecular weight multiblock copolymers for polymer chemists in this field. The technique was recently optimised by introducing norbornene as an improved “ene”, yielding much higher molecular weights.[119]

I.5.2 Sequence-control *via* time regulated additions

Although solid-phase polymer synthesis allows for an absolute control over glycopolymer sequence and allows for the synthesis of monodisperse polymers, the fact that synthesis occurs on a solid-phase limits the application of this method on a larger scale. In 2007 Lutz *et al.* published a report in which they described a kinetic strategy allowing control over microstructure in radical chain-growth polymerisations.[120,121] The method relies on the time-regulated sequential addition of *N*-substituted maleimides during the chain growth polymerisation of styrenes. The great difference in monomer reactivity renders it possible to incorporate the maleimides at specific places along the polymer chain. In 2013 the group further used this technique for the synthesis of single chain sugar arrays (**Figure I.5.3**). They polymerised three different triple bond containing maleimides, each containing protecting groups of different lability, allowing for the selective deprotection of each set of monomers.[122] After each deprotection step different azide-functionalised hexoses were clicked to the polymer backbone. The method demonstrated that sugars could be placed at certain locations along a bioinert polystyrene backbone. Although this proposed technique does not deliver monodisperse sequence-defined glycopolymers, it does provide controlled polymers on a larger scale.

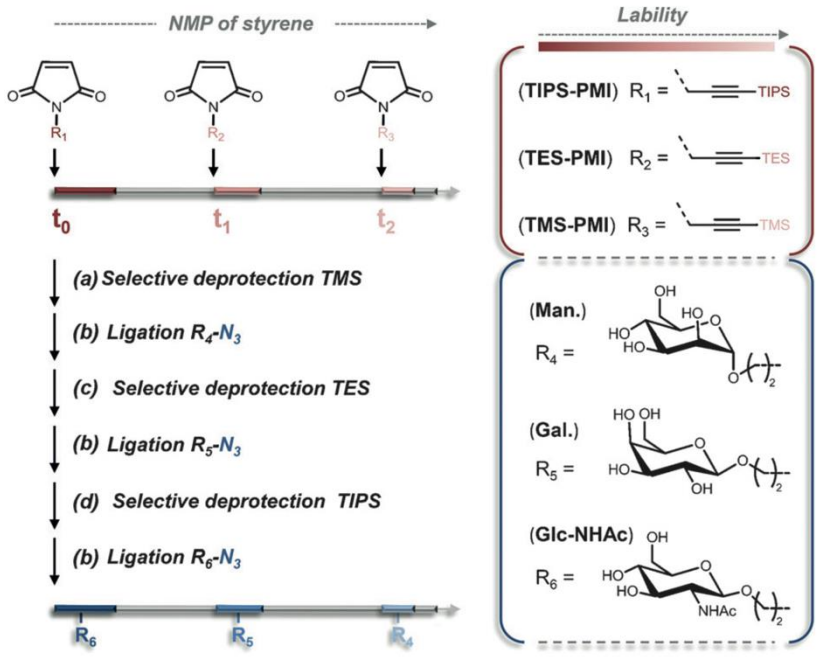

Figure I.5.3 General strategy for the synthesis of single-chain sugar arrays.[122]

I.5.3 Sequence-control *via* time regulated chain extensions

This first use of controlled radical polymerisations showed great potential in the development of sequence-controlled glycopolymers and was thus further exploited. Controlled radical polymerisations offered not only better polydispersities during chain growth, but copper mediated radical polymerisations also introduced a much better chain end fidelity. This increased chain end fidelity inspired Haddleton *et al.* for the synthesis of sequence controlled glycopolymers *via* copper(0) mediated living radical polymerisation (Cu(0)-LRP) as developed by Percec *et al.* in 2002/2006.[18,100,123] The group made use of the retention of the chain end to perform chain extensions after monomer consumption (**Scheme I.5.3**). Sequential addition of new monomer after consumption of each block provided sequence controlled block copolymers of well-defined length and with low dispersities.

This route was employed for the preparation of a whole range of different glycopolymers based on acrylate monomers containing sugar units synthesised *via* the 1,3-dipolar cycloaddition. These glycopolymers, containing mannose, glucose and fucose moieties, were examined for their binding behaviour towards DC-SIGN, a lectin highly present on dendritic cells. Higher-affinity binding was observed for polymers with a higher mannose content, although no effect of sequence on binding was detected.

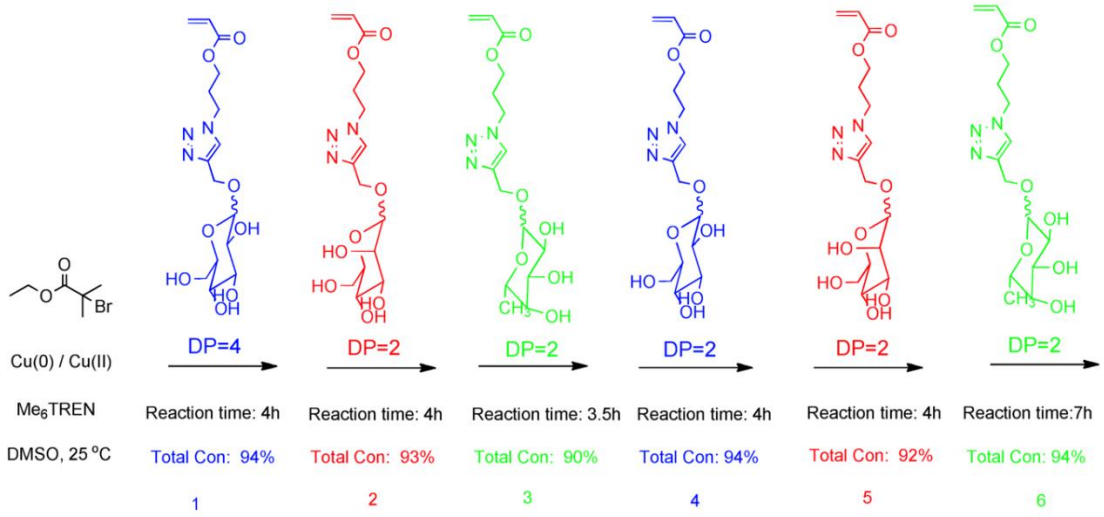

Scheme I.5.3 Schematic representation of the synthesis of multiblock glycopolymers by sequential addition of glycomonomers at defined periods of time *via* Cu(0)-LRP. [124]

The use of Cu(0)-LRP for the preparation of sequence-controlled glycopolymers was further adopted in combination with other 'click'-like reactions. In this case,

Haddleton et al. synthesised a sequence-controlled prepolymer that could selectively be glycosylated at different places.[124] The prepolymer was synthesised using an epoxide containing glycidyl acrylate and TMS protected propargyl acrylate. A post-polymerisation modification was carried out *via* thiol-X reactions using 1-thio-β-D-glucose tetraacetate. After this the TMS group was deprotected and subsequently the free triple bonds were used for conjugation of azide-functionalised mannose.

Qian *et al.* made use of sequential ATRP for the synthesis of triblock copolymer-grafted silica microparticles.[125] First, the authors immobilised ATRP initiators on the surface of the silica particles and afterwards the glycopolymers were grown on that surface (**Figure I.5.4**). Unlike with the previous approach (using Cu(0)-LRP) the silica particles were isolated and washed in between the polymerisation of each block. The glycopolymer grafted silica particles were then further used for efficient and selective enrichment of glycopeptides.

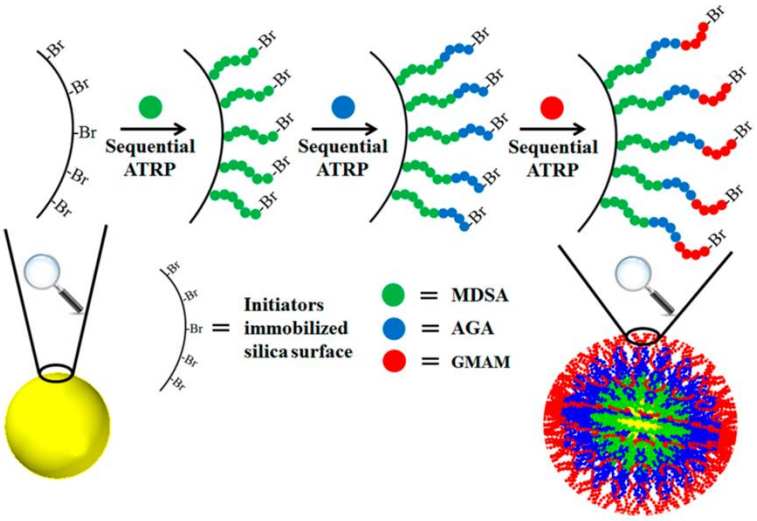

Figure I.5.4 Schematic overview of the preparation of triblock copolymer-grafted silica microparticles by sequential-ATRP. [125]

I.5.4 Sequence-control *via* orthogonal reactions

Lastly, the fourth approach was applied by Chen *et al.*[126] The group first prepared poly(methacrylic acid) *via* the RAFT polymerisation process. Subsequently the free pending acid groups were used in an Ugi reaction with gluco- or mannosamine, incorporating a first sugar into the chain, and propargyl isocyanoacetamide which tactfully introduced a terminal alkyne. These terminal alkynes were then finally employed to click gluco- or mannosyl azide onto the polymer chain (**Scheme I.5.4**).

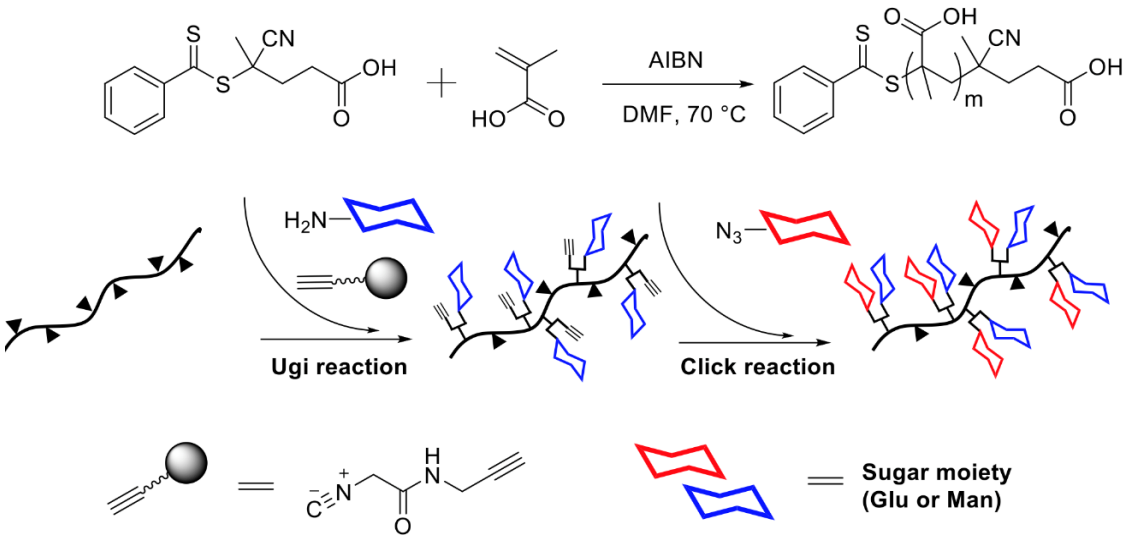

Scheme I.5.4 Modular synthesis of glycopolymers *via* Ugi reaction and click chemistry.

Although the last couple of years, the main focus of polymer chemistry has been the precise control over monomer sequence, this cannot really be interpolated towards glycopolymers for which the field is still in its infancy. Few research groups have currently attempted to tackle this problem, and each technique comes with its advantages and drawbacks. Perfect monodisperse sequence-defined polymers could readily be achieved *via* solid-phase glycopolymer synthesis, however multiple steps are required to achieve only small amounts of product. Keeping that in mind, chain growth polymerisation could be favoured. Lutz *et al.* demonstrated that sequence-controlled glycopolymers can be achieved based on a difference in monomer reactivity. However, also in this case several deprotection steps are required for the post-polymerisation glycosylations. Chain extensions *via* copper mediated polymerisations seem very promising as these techniques can easily be scaled up and occur in a one pot manner. Although there is a good control over sequence of the block copolymer, each block still has a distribution and in this aspect it is still inferior to the solid-phase synthesis approach regarding

‘control’. However, the dispersities of the blocks are relatively low, allowing for a well-controlled synthesis on a bigger scale.

I.6 Self-assembly of glycopolymers

Recently it has become more and more clear that presentation of the saccharide units is of great importance in achieving enhanced lectin-glycopolymer binding. Glyconanoparticles with different morphologies can readily be obtained depending on the hydrophilicity/hydrophobicity and the length of the different blocks in the block-copolymer which have an effect on the packing parameter.[127–129] Over the past decade a whole range of different self-assembling glycopolymers have been synthesised and their composition and presenting morphologies have been greatly summed up in a review by Chen *et al*.[130] In this section different methods will be summarised for the preparation of these assemblies, along with most important and recent publications.

I.6.1 Self-assembly based on amphiphilicity

The synthesis of glycopolymeric amphiphiles was first reported in 1999, by Li *et al*.[131] The authors prepared a set of block-copolymers based on polystyrene-*b*-poly[2-*β*-*D*-glycopyranosyloxy)ethyl acrylate]. By varying the composition, the solvent and the concentration, they were able to prepare different morphologies ranging from spherical micelles to cylindrical micelles and vesicles called polymersomes. Now more than 20 years later, many articles have been published on the synthesis of different amphiphilic glycopolymers, each one differing either in choice of the hydrophobic block, choice of the sugar and/or of course the polymerisation procedure.[130,132–136]

In the last few years, one of the most active groups working on glycopolymer self-assemblies and their use in biomedical applications is undoubtedly the group of Stenzel. The group prepared several glycopolymers *via* different methods. In 2014 the group published a collaborative report with the group of Du Prez, where they elegantly used the thiolactone strategy developed by Espeel *et al*. (**Scheme I.6.1**).[137] The authors firstly prepared a statistical copolymer of *N*-isopropyl acrylamide and *N*-homocysteine thiolactone acrylamide. The glycopolymers were prepared by using a one-pot procedure in which the thiolactone ring is opened by an aliphatic amine which releases a thiol that was subsequently reacted with a bromine functionalised saccharide already present in

the reaction mixture. The size of the obtained particles after dialysis could be tuned by varying the length of the amine side chains.

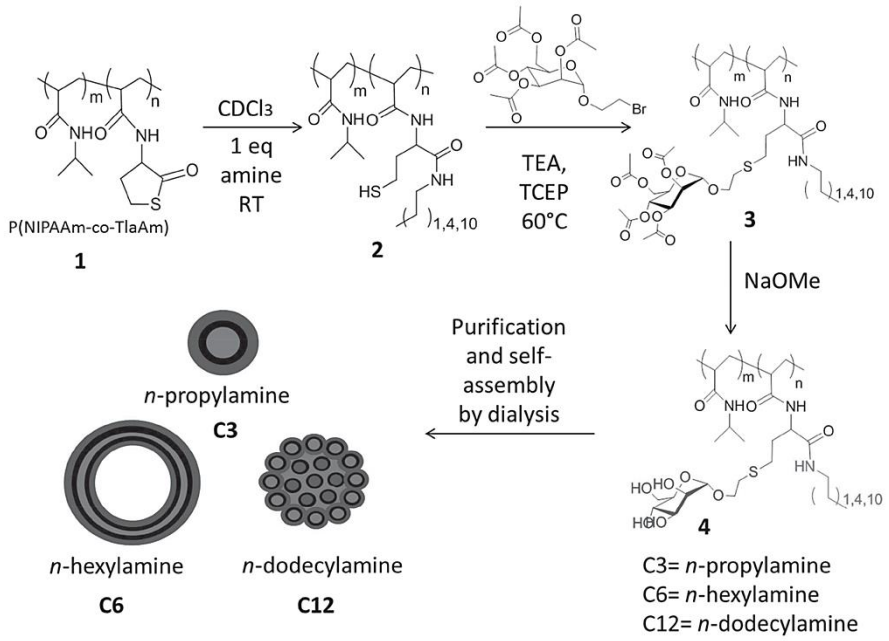

Scheme I.6.1 One-pot reaction pathway to glycopolymer-based nanoparticles, employing a double modification (aminolysis and nucleophilic substitution) of thiolactone-containing polyacrylamides. [137]

Another strategy in which the group managed to tune glycopolymer morphology was using two sets of block-copolymers and simply changing the mixing ratio (**Figure I.6.1**).[138] Two sets of block-copolymers were prepared, the first based on mannose acrylate and *n*-butyl acrylate. For the second, mannose acrylate was replaced by oligo(ethylene)glycol methyl ether acrylate (OEGMEA, M_n = 480 g mol^{-1}). It was observed that glycopolymer morphologies with higher mannose content had better cellular uptake which suggests that mannose concentration is more important than shape and size effects. The same group furthermore prepared biodegradable glycopolymer micelles as drug delivery platforms *via* RAFT.[139] In order to achieve biodegradability in the glycopolymer block, a 5,6-benzo-2-methylene-1,3-dioxepane (BMDO) monomer was copolymerised which introduced cleavable ester bonds.

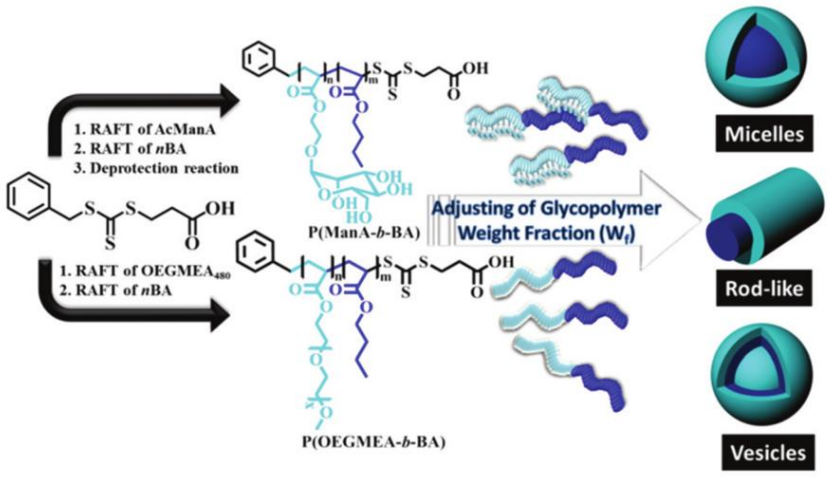

Figure I.6.1 Synthetic pathway for the preparation of glyco-nanoparticles with different morphologies. [138]

Zentel *et al.* employed active esters for the preparation of polymersomes forming block-glycopolymers.[140] The hydrophobic block of the copolymer consists of a statistical copolymer of lauryl methacrylate and 2-(2,2-dimethyl-1,3-dioxolane-4-yl)ethyl methacrylate. The incorporation of the last monomer provides a controlled pH responsive disintegration of the polymersomes, which can be used for controlled cargo release.

The group of Lecommandoux published several papers on the synthesis and self-assembly of amphiphilic glycopolypeptides.[141] Their approach was first introduced using two oligosaccharides, dextran or hyaluronan as the hydrophilic block combined with poly(*γ*-benzyl-*L*-glutamate) as the hydrophobic block (**Scheme I.6.2**).[142] Tree-like structures were prepared *via* the Huisgen cycloaddition reaction of an azide functionalised oligosaccharide and alkyne functionalised small propargyl glycine block. Another strategy they employed was again the use of a block-copolymer consisting of poly(γ-benzyl-L-glutamate) and polypropargylglycine.[143] Here the alkynes were clicked to azide functionalised iminosugars. The obtained glycopolypeptides were capable of self-assembling but the polymers did generate the tree-like structure. In a last publication the authors synthesised glycopolypeptides containing galactose based on the same principles.[144]

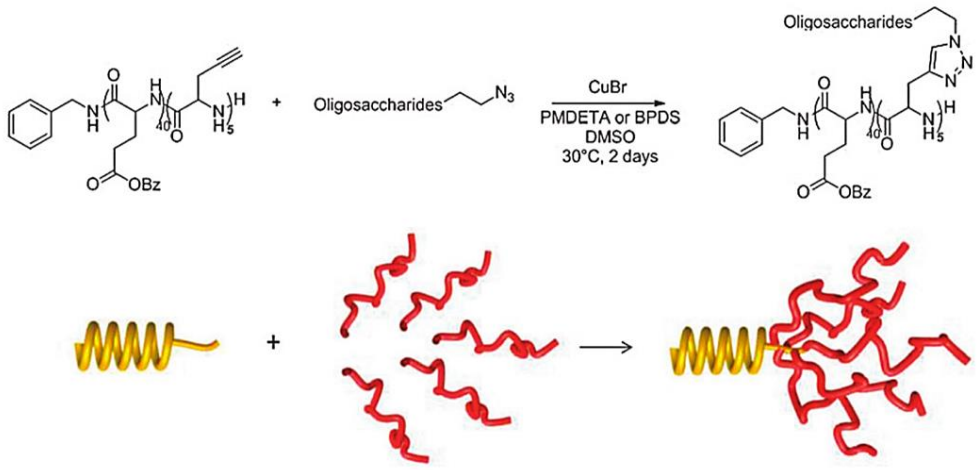

Scheme I.6.2 Oligosaccharides coupling onto poly(*γ*-benzyl-*L*-glutamate)-block-poly(propargyl glycine) by Huisgen cycloaddition. [142]

Apart from varying different block lengths, Satoh *et al.* prepared a range of miktoarm block-copolymers to obtain different glycopolymer morphologies.[145] A series of different miktoarm polymers was prepared in which the amount of arms per block was changed, this altered the packing parameter, resulting in a change in micelle size. The miktoarm polymers were prepared by clicking alkyne functionalised maltoheptaose using the copper catalysed azide-alkyne cycloaddition to azide functionalised poly-*ε*-caprolactones.

An interesting approach was used for the synthesis of gradient glycopolymers by Wei *et al*.[146] The group made use of the in situ enzymatic monomer transformation using Novozym 435. Gradient glycolymers were prepared *via* the RAFT polymerisation of 2,2,2-trifluoroethyl methacrylate (TFEMA) (**Scheme I.6.3**). The presence of Novozym 435 and 1,2:3,4-di-O-isopropylidene-*α*-*D*-galactopyranose resulted in the gradual conversion of TFEMA into 1,2:3,4-di-O-isopropylidene-6-O-methacryloyl-*α*-*D*-galactopyranose (DIMAG) in the reaction medium delivering a gradient glycopolymer as a final product. Comparison of the binding affinity of these galactose containing block-, gradient and statistical glycopolymers showed that binding affinity towards the lectin RCA_{120} was optimal for the glycopolymer with the block structure. The use of concurrent RAFT polymerisation and enzymatic monomer transformation was further used by the group of Tao for the synthesis of a multifunctional glycopolymer.[147]

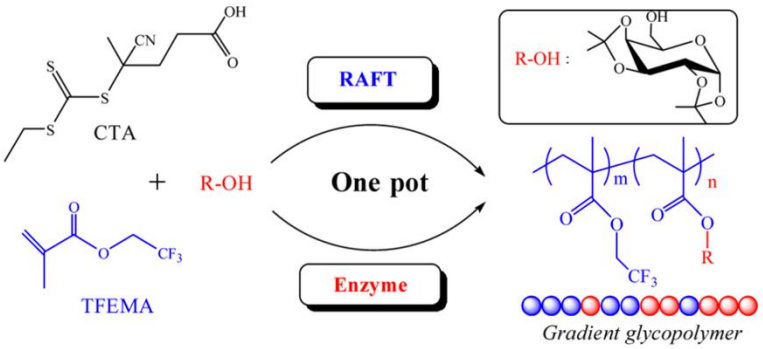

Scheme I.6.3 One-pot synthesis of the gradient glycopolymer via concurrent enzymatic monomer transformation and RAFT polymerisation. [146]

Self-assembly was also observed by Böker *et al*., for double-hydrophilic glycopolymers consisting of poly(hydroxyethyl acrylate) (PHEMA) and an *N*-acetyl glucosamine monomer (**Scheme I.6.4**).[148] The authors state that although their PHEMA block should have a cloud point of at least 32 °C and thus be water soluble, they still obtained formation of spherical nanoparticles.

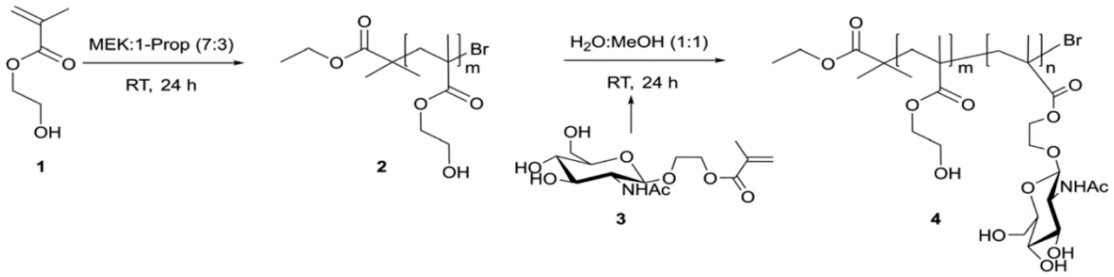

Scheme I.6.4 General scheme for the synthesis of PHEMA-b-PGlcNAcEMA. [148]

Self-assembled block-copolymers containing sugars are often used for drug delivery systems. However often little attention is drawn to the actual location of the drug inside the self-assembly or the effect of the drug on the polymer properties. Recently, Stenzel *et al*., have shown that their drug of choice (curcumin) was unexpectedly located in the shell of the micelle and furthermore showed that an accumulation of their drug in the hydrophilic block consequently led to changes in the morphology of the self-assembly. [149]

I.6.2 Temperature-triggered self-assemblies

Instead of using hydrophobic blocks in the design of the block-copolymer, several research groups have opted to use double hydrophilic blocks in which the non-saccharide block is a hydrophilic thermoresponsive block. Upon heating of the dissolved polymers in water, often based on poly(diethylene glycol methacrylate) (PDEGMA) and poly(*N*-isopropylacrylamide) (PNIPAM), the particles aggregate due to the LCST behaviour of the aforementioned polymers. The LCST or lower critical solution temperature is the critical temperature below which the components of a mixture are miscible for all compositions. LCST behaviour is entropy driven as hydrating water gets released into the bulk water and depends on the hydrophilic-hydrophobic balance of the polymer, the end groups, the polymer chain length, presence of salts and pH of the water. In 2008 Alexander *et al.* prepared block-copolymers of PDEGMA and poly(2-glucosyloxyethyl methacrylate) *via* several controlled radical polymerisation techniques (**Scheme I.6.5**).[150] By changing the temperature above or below the LCST of the PDEGMA, the authors were capable of controlling the size of the obtained vesicles. PDEGMA was further used by Stenzel and collaborators for the synthesis of thermoresponsive micelles first in combination with thiol-*ene* 'click'-like chemistry and further in combination with copper catalysed azide-alkyne 'click' chemistry.[151,152]

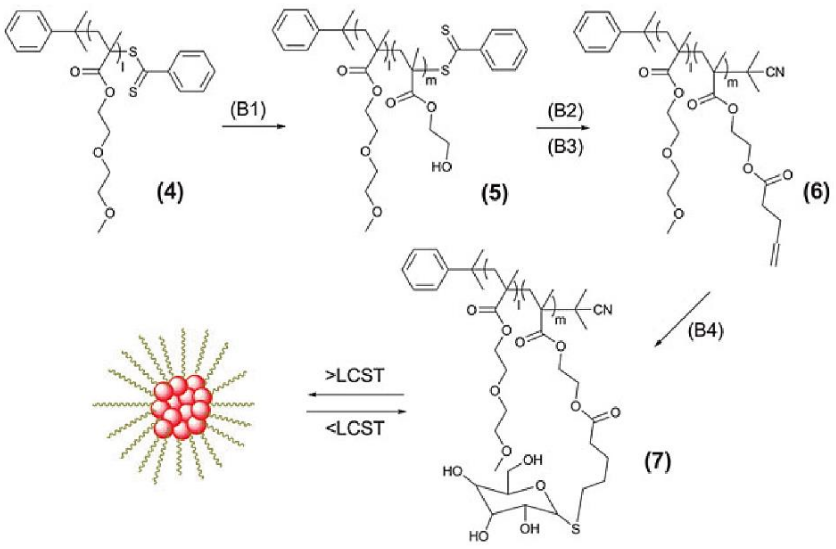

Scheme I.6.5 Synthetic strategies for the preparation of glucose functionalised (co)polymers. (B1) HEMA, AIBN, DMAc, 70 °C; (B2) AIBN, toluene, 80 °C; (B3) 4-pentenoic anhydride, DMAP, pyridine, DMF; (B4) UV, glucothiose, DMPA, DMF. [150]

Haddleton *et al*. further employed the novel aqueous SET-LRP for the synthesis of their double hydrophilic block-copolymers.[153] Rapid disproportionation of CuBr allows

for a fast polymerisation with high conversions. Diethylene glycol ethyl ether acrylate (DEGEEA) was polymerised in combination with mannose acrylate, yielding well defined polymeric nanoparticles above the LCST.

The other commonly used polymer with LCST behaviour, PNIPAM, was also employed for the synthesis of thermoresponsive glycopolymers. Zhu *et al.* prepared triblock glycopolymers consisting of two blocks of PNIPAM and a glucose containing block *via* RAFT.[154] Besides these polymers were further capable of self-assembling. The use of PNIPAM was further employed in combination with an adamantane containing block by Becer *et al*. (**Scheme I.6.6**).[155] The adamantane blocks were subsequently made more hydrophilic using the supramolecular interaction of adamantane and *β*-cyclodextrins decorated with mannose units in water.

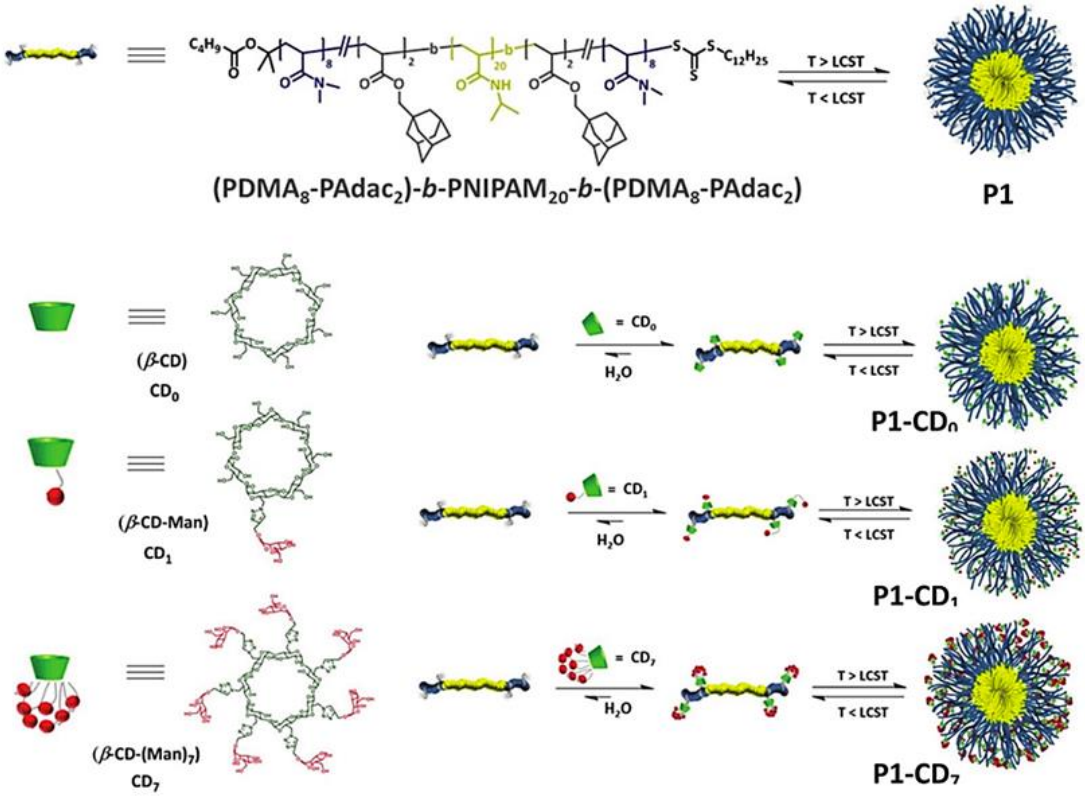

Scheme I.6.6 The triblock copolymer synthesised by sequential RAFT polymerisation and its host–guest interaction with self-assembly behaviour. [155]

I.6.3 *pH*-responsive self-assemblies

A potentially interesting feature, especially in regards to drug release, would be the integration of pH-responsive blocks controlling the self- and disassembly of block-glycopolymers. Armes *et al.* firstly reported the synthesis of these pH-responsive glycopolymers in 2003.[156] The group synthesised different triblock-glycopolymers *via* ATRP based on poly(ethylene glycol) (PEG) and 2 different sugar monomers 2-gluconamidoethyl methacrylate (GAMA) and 2-lacto-bionamidoethyl methacrylate (LAMA). The pH-sensitive blocks were composed of 2-(diethylamino)ethyl methacrylate (DEA) or 2-(diisopropylaminoethyl methacrylate (DPA). Self-assembly of glycopolymers could be triggered by changing the acidity below or above pH 7. The same GAMA monomer was further employed by Dong *et al.* for the fabrication of star-shaped polypeptide/glycopolymer biohybrids composed of poly(*γ*-benzyl-*L*-glutamate).[157] By using G_0-PAMAM as a core and by varying the pH, the size of the produced micelles could be tuned. Another group used dendronised lysine for this purpose.[158]

Wang *et* al. on the other hand produced pH-sensitive block glycopolymers of poly(2-(diethylamino)ethyl methacrylate) (PDEAEMA) and poly(3-O-methacryloyl-a,b-D-glucopyranose) (PMAGlc) *via* RAFT.[159] Spherical micelles were formed with PDEAEMA as the hydrophobic cores and PMAGlc as the hydrophilic shells in alkaline aqueous solution (**Fig. I.6.2**).

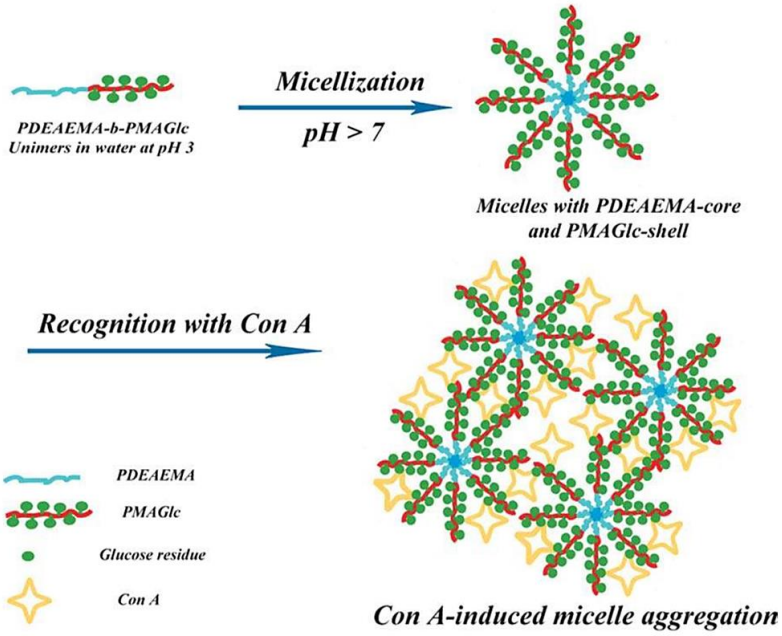

Figure I.6.2 Illustration of the micellization of PDEAEMA-*b*-PMAGlc block copolymer in water and recognition with protein Con A. [159]

Not only dis- or self-assembly can be triggered but also changes in various self-assembling morphologies can be achieved using pH-sensitive blocks. Change of morphology was obtained by Stenzel *et al.* based on a single triblock-copolymer of poly(2-acryloylethyl-*α*-*D*-mannopyranoside)-*b*-poly(n-butylacrylate)-*b*-poly(4-vinylpyridine) ($PAcManA_{70}$-*b*-PBA_{369}-*b*-PVP_{370}).[160] The obtained morphologies were quite interesting ranging from flower-like micelles, cylindrical micelles, raspberry-like morphologies to nanocaterpillars, all depending on the processing conditions (pH of the aqueous environment during dialysis) (**Scheme I.6.7**).

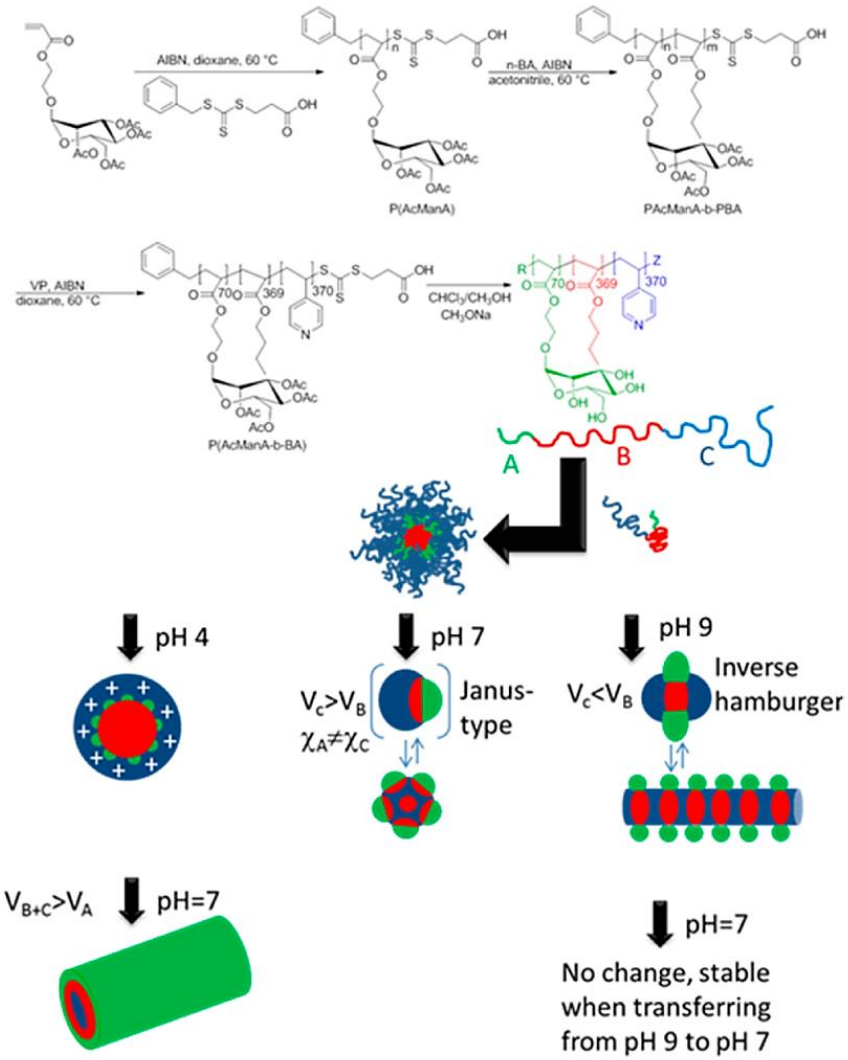

Scheme I.6.7 Synthesis of triblock copolymer and its self-assembly in methanol followed by dialysis against aqueous solutions of different pH values. [160]

3.4. Self-assembly based on electrostatic interactions

Ionic interactions are the strongest noncovalent interactions and can thus form a strong basis for the self-assembly or loading of glycopolymeric nanoparticles. Narain *et*

al. achieved nanoparticles by using the electrostatic interaction of negatively charged plasmid DNA and a cationic block-glycopolymer consisting of 3-gluconamidopropyl methacrylamide and 3-aminopropyl methacrylamide.[161] Wang et al. furthermore used a diblock glycopolymer consisting of 2-(methacrylamido) glucopyranose and methacrylic acid monomers synthesised *via* RAFT in combination with a quaternary ammonium chitosan as a cross-linker (**Figure I.6.3**).[162] Optimisation of the synthesis conditions resulted in the formation of glyconanogels with a compact ionic cross-linked core and a glucose corona as was confirmed by TEM.

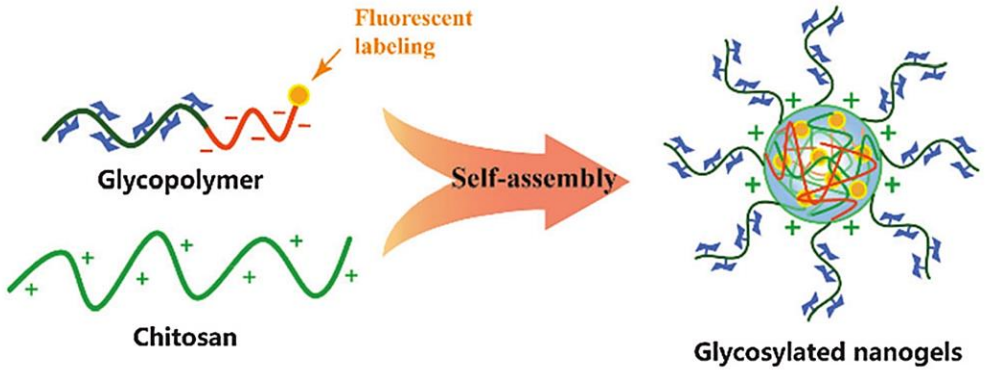

Figure I.6.3 Schematic illustration of the preparation of bioactive poly-electrolyte nanogels from natural and synthetic sugar polymers. [162]

The group of Chen, firstly synthesised a copolymer with dopamine and amino groups that were cable of self-assembling with zinc phthalocyanine into stable nanoparticles (**Scheme I.6.8**).[163] These positively charged nanoparticles were then further complexed with the same block-glycopolymer used by Wang *et al.* yielding glycopolymer decorated nano-phthalocyanine nanoparticles.

Although many different self-assembling glycopolymer structures have been achieved over the past two decades, the number of architectures is still limited, ranging from micelles to polymersomes for diblock based glycopolymers. More interesting structures could be achieved by using triblock copolymers as evidenced vide supra, however glycopolymer-lectin binding affinity showed to be more influenced by the density of the sugar ligands than the overall glycopolymeric architecture. Looking back to nature, these types of self-assembled architectures can be found on the scale of cells and organelles. Selectivity and specificity however, occur on the scale of proteins and receptors embedded in these nanostructures. It has become clear that in order to achieve the selectivity and specificity often observed in Nature, control should be performed on the smallest scale possible. As illustrated in the first section, control over

primary structure is possible, but what differs in comparison to natural glycosylated proteins is the absence of controlled single-chain folding.

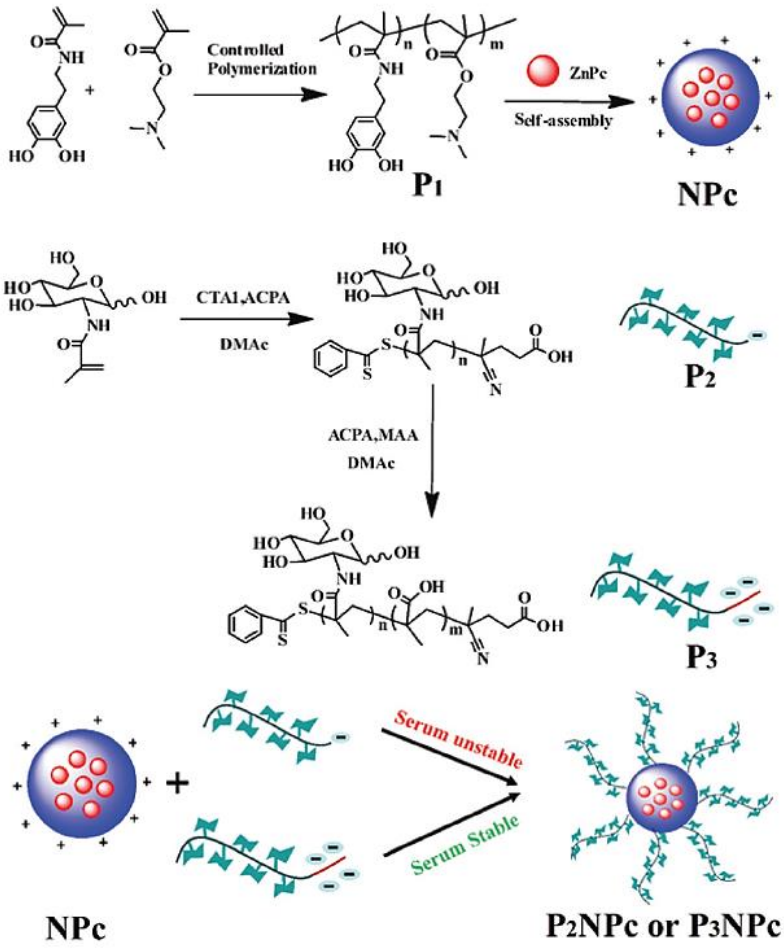

Scheme I.6.8 Synthesis of glycopolymer coated nano-phthalocyanine.[163]

I.7 Single-chain folding of glycopolymers

Single-chain polymeric nanoparticles (SCPNs), single polymeric chains capable of folding into a nanoparticle, have gained much interest over the past decade. Surprisingly, the new advances in this relatively young field have not yet extensively been applied in combination with glycopolymers. Taken in mind that glycopolymers are mainly soluble in water and primarily synthesised for biomedical applications, ranging from imaging probes to synthetic vaccines and drug-delivery carriers, it should be clear that single-chain folding must be able to occur in water. Interactions that can be used include covalent linkages, metal coordination, hydrogen bonds, ionic interactions and hydrophobic interactions as is common in Nature's protein folding.

Preparation of SCPNs can primarily be divided into two fundamentally distinct synthetic strategies, as introduced by Barner-Kowollik *et al*..[164,165] These two approaches are on the one hand '*selective point folding*' and on the other hand '*repeat unit folding*' (**Figure I.7.1**). Selective point folding of macromolecules makes use of complementary recognition units at predefined positions along the polymer chain to achieve extremely well-defined nanoparticles. On the other hand repeat unit folding offers a less-defined and chaotic collapse, although it should be noted that this approach is synthetically more accessible. In order to achieve folding as found in nature, selective point folding is preferred, especially for glycopolymer systems where individual distances in between saccharide units can have a great influence on lectin-binding.

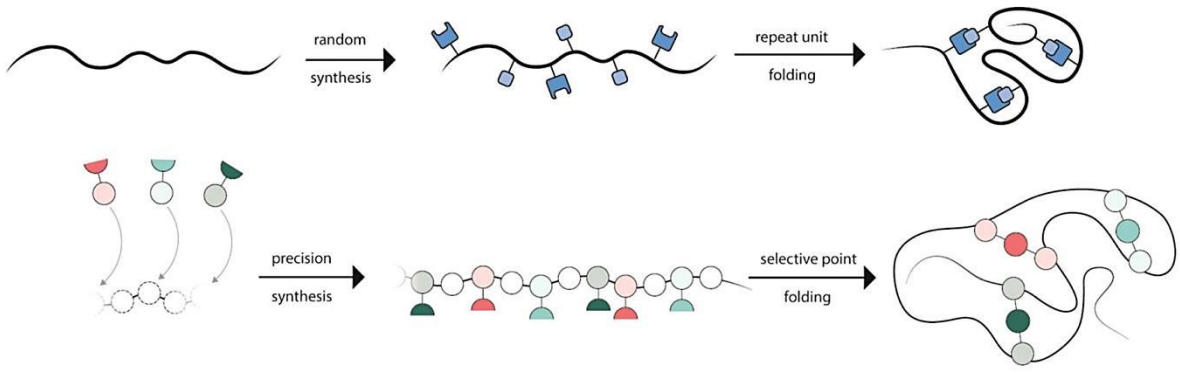

Figure I.7.1 Single-chain folding of well-defined synthetic polymers via repeat unit folding and selective point folding.[165]

I.7.1 Selective point folding

As previously stated, selective point folding is the preferred approach for the preparation of well-defined glycopolymeric structures. The field however is still young and most contributions have been conducted in non-competing solvents based on hydrogen bonding arrays. An interesting example of this selective point folding methodology was introduced by Barner-Kowollik using a combination of two orthogonal H-donors and acceptor units.[166] *Via* this approach based on the interaction of thymine and diaminopyridine and the self-association of cyanuric acid and the Hamilton wedge, the authors achieved an 8-shaped macromolecule. Although very elegant, this approach was conducted in a non-competing solvent which eliminates its use in water.

Approaches that can be combined with glycopolymers in aqueous environments are those based on metal-ligand interactions, host-guest interactions and covalent linkages. An important example of these host-guest interactions, is the well-known association between adamantane and *β*-cyclodextrin. Barner-Kowollik and coworkers successfully employed this interaction for the preparation of cyclic *α*-*ω*-functionalised poly(*N,N*-dimethylacrylamide).[86] Single-chain folding and dissociation were able to be monitored by dynamic light scattering (DLS) and nuclear Overhauser enhancement spectroscopy (NOESY). In NOESY, the nuclear Overhauser cross relaxation in the mixing period between nuclear spins is utilized to determine the correlations. A correlation is thus found between atoms which are closer than 5 Å in proximity. The same group further introduced metal-ligand complexation to achieve selective point folding.[167] Triphenylphosphine ligands were employed to afford single-chain metal complexes in the presence of Pd(II) ions at high dilution. Although the experiments were performed in chloroform and dichloromethane, it still proves the relevance of metal-coordination as a synthetic platform.

I.7.2 Repeat unit folding

In contrast to the '*selective point folding*' approach, '*repeat unit folding*' has received significant interest with numerous contributions and Pomposo *et al.* as one of the main contributors.[164,165,168] As mentioned before, single-chain folding of glycopolymers demands self-assembly in water in order to have significant applications. Many covalent links have been utilised to date for the formation of SCPNs *via* covalent bonds, these include thiol-*ene* and thiol-*yne* coupling,[169,170] Michael addition,[171–173] amide

formation,[174] tetrazine-norbornene reaction,[175] alkyne homocoupling,[176] tetrazole-ene ligation,[177] and disulphide linkages.[178] It is evident that the scope of covalent linkages is broad and that many other contributions are expected in the following years.

Furthermore the dynamic nature of supramolecular interactions can be useful for reversible and responsive glycopolymer synthesis. The most fascinating contributions in this field are undoubtedly from the group of Meijer and Palmans. The use of self-recognising motifs such as the benzene-1,3,5-tricarboxamides (BTA) proved to be very beneficial for SCNP formation even in water, as is evidenced by many contributions (**Scheme I.7.2**).[179–184] Upon reduction of temperature, BTA moieties self-assemble into helical aggregates inducing a collapse into an SCPN. Evidently, every major supramolecular interaction which has a high association constant in water could be used. Many options are still to be explored.

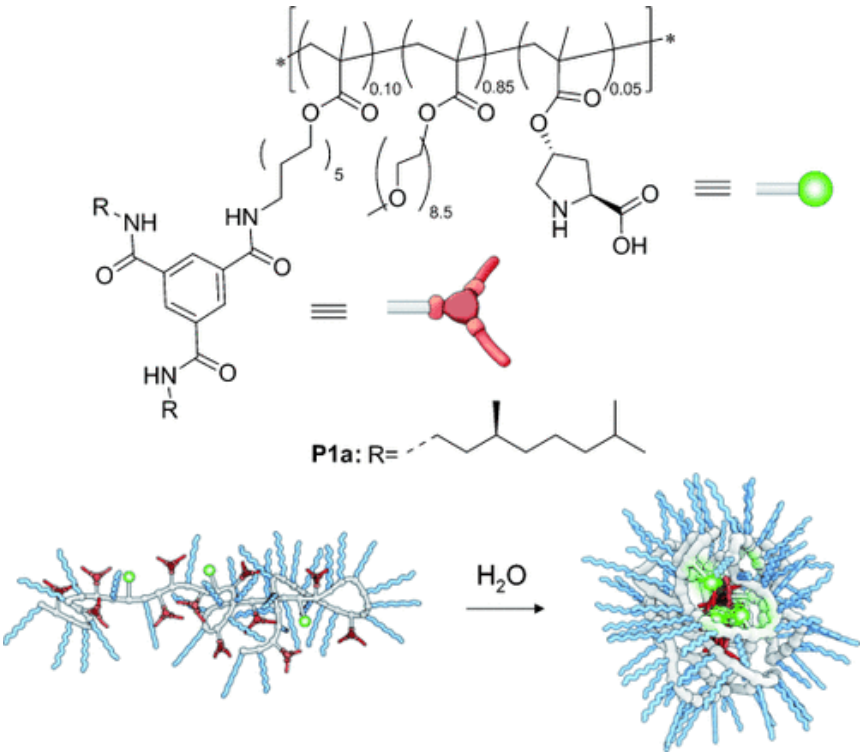

Figure I.7.2 Collapse of an *L*-Proline containing water soluble polymer, based on the self-assembly of BTA moieties.[184]

I.7.3 Single-chain folding glycopolymers

Although little applied in glycopolymer science, single-chain folding technology based on both covalent and non-covalent interactions has received a significant increase of interest as evidenced by myriad publications in recent years. In order to achieve specificity in lectin-glycopolymer binding it is clear that ‘selective point folding’ is preferred over ‘repeat unit folding’ in glycopolymer design and all of this in an aqueous environment. Only the precise synthesis of not only the correct sugar moieties along the polymer chain, but also the precise collapse into a nanoparticle will provide efficient control. Self-assembly into single-chain nanoparticles is found in nature on the scale of proteins and other biomacromolecules. It should thus be clear that further effort into the synthesis of these glyconanoparticles will most probably result in a gain in molecular understanding of lectin recognition events and be beneficial for future syntheses of glycopolymeric ligands.

The first scientific report describing the synthesis of single-chain folding glycopolymers stems from a collaboration of the groups of Stenzel and Barner-Kowollik.[185] The groups collaborated by synthesising fluorescent single-chain folding glycopolymers and reported their subsequent functionalisation onto nanodiamonds (**Scheme I.7.1**). Collapse of the synthesised glycopolymers was achieved by a post-polymerisation functionalisation step, which introduced profluorescent photoactive tretrazole groups and furan-protected maleimide moieties. By subsequently irradiating highly diluted aqueous solutions of the polymers, they managed to trigger intramolecular tretrazole-mediated cycloadditions yielding polymeric glyconanoparticles.

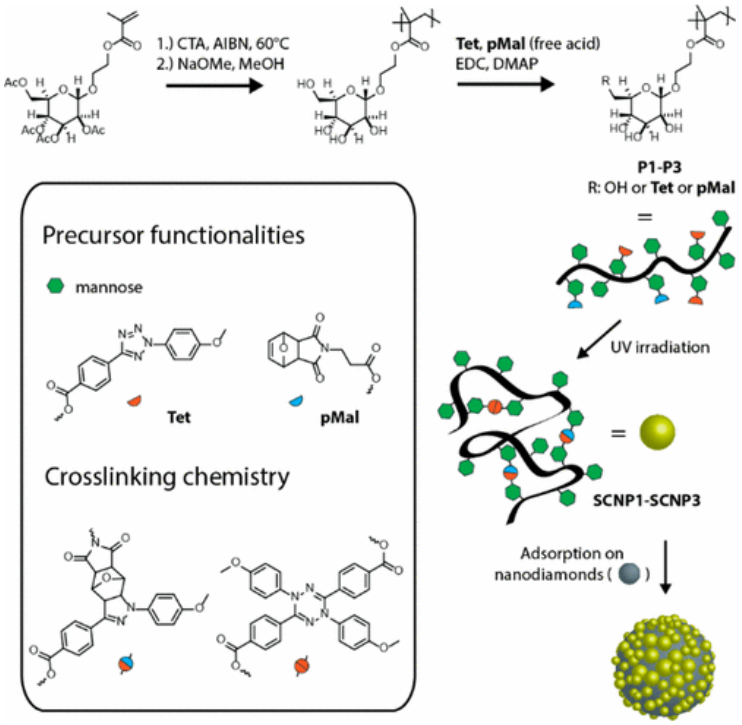

Figure I.7.3 Synthetic Approach for the Preparation of SCNP-Decorated Nanodiamonds. [185]

The second report of single-chain nanotechnology in glycopolymer science, was by Yilmaz *et al*.[186] In this report the group synthesised tri-block copolymers *via* RAFT containing adamantane and cyclodextrin at the rear ends of the polymer. The reversible single-chain folding of the glycopolymers was subsequently achieved by dissolving the polymers under high dilution in water and the self-assembly itself was then investigated using 2D NOESY. They were able to demonstrate an increase in lectin binding affinity as compared to unfolded linear structures (**Figure I.7.4**).

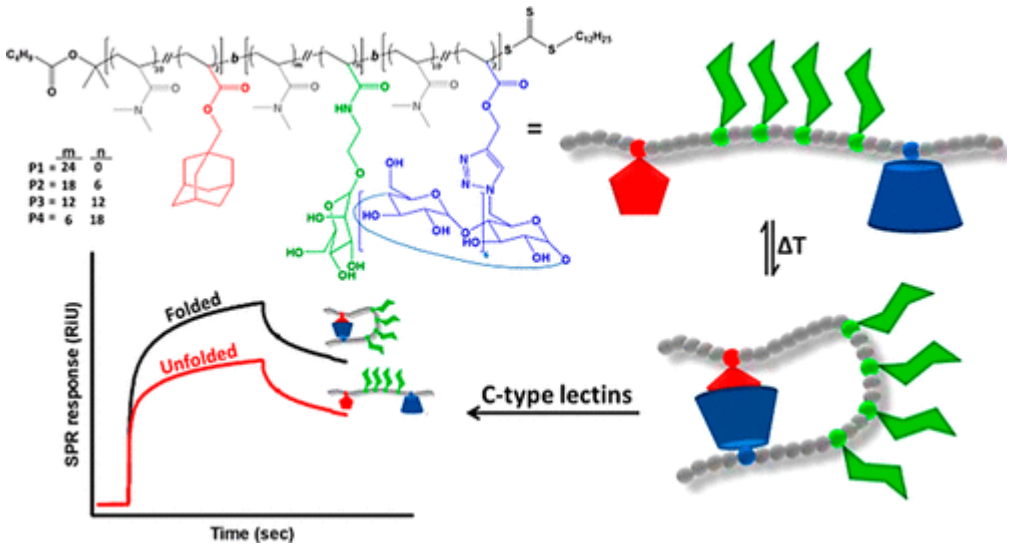

Figure I.7.4 Selective-point folding using adamantane and cyclodextrin.[186]

Finally, the last report (to the best of my knowledge) describes the synthesis of glucose containing single-chain folding glycopolymers, again by the group of Stenzel (**Figure I.7.5**).[187] As in their first report, here again the repeat unit folding method was used. Firstly, glycopolymers were synthesised containing protected thiols along the glycopolymer chain. Single-chain folding was then achieved by deprotection of the thiols using hydrazine and subsequently adding PEG diacrylate.

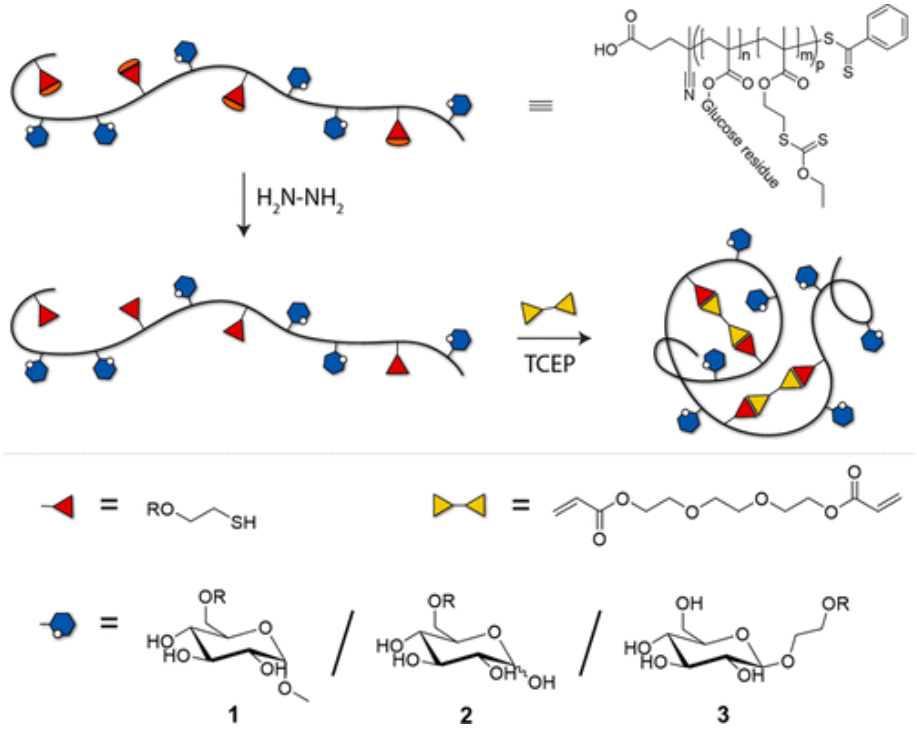

Figure I.7.5 Schematic Representation of single-chain glycopolymeric nanoparticles by thiol-Michael addition.[187]

I.8 References

(1) Webster, O. W. *Science (80-.).* **1991**, *251* (4996), 887.

(2) Szwarc, M. *Nature* **1956**, *178* (4543), 1168.

(3) *Handbook of Radical Polymerization*; Matyjaszewski, K., Davis, T. P., Eds.; John Wiley & Sons, Inc.: Hoboken, NJ, USA, 2002.

(4) Matyjaszewski, K.; Spanswick, J. *Mater. Today* **2005**, *8* (3), 26.

(5) di Lena, F.; Matyjaszewski, K. *Prog. Polym. Sci.* **2010**, *35* (8), 959.

(6) Nicolas, J.; Guillaneuf, Y.; Lefay, C.; Bertin, D.; Gigmes, D.; Charleux, B. *Prog. Polym. Sci.* **2013**, *38* (1), 63.

(7) Chiefari, J.; Chong, Y. K. (Bill); Ercole, F.; Krstina, J.; Jeffery, J.; Le, T. P. T.; Mayadunne, R. T. A.; Meijs, G. F.; Moad, C. L.; Moad, G.; Rizzardo, E.; Thang, S. H. *Macromolecules* **1998**, *31* (16), 5559.

(8) Ayres, N. *Polym. Rev.* **2011**, *51* (2), 138.

(9) Matyjaszewski, K.; Tsarevsky, N. V. *Nat. Chem.* **2009**, *1* (4), 276.

(10) Grubbs, R. B. *Polym. Rev.* **2011**, *51* (2), 104.

(11) David, G.; Boyer, C.; Tonnar, J.; Ameduri, B.; Lacroix-Desmazes, P.; Boutevin, B. *Chem. Rev.* **2006**, *106* (9), 3936.

(12) Kato, M.; Kamigaito, M.; Sawamoto, M.; Higashimura, T. *Macromolecules* **1995**, *28* (5), 1721.

(13) Wang, J.-S.; Matyjaszewski, K. *J. Am. Chem. Soc.* **1995**, *117* (20), 5614.

(14) Matyjaszewski, K.; Xia, J. *Chem. Rev.* **2001**, *101* (9), 2921.

(15) Braunecker, W. A. *Prog. Polym. Sci.* **2007**, *32* (1), 93.

(16) Tang, W.; Matyjaszewski, K. *Macromolecules* **2006**, *39* (15), 4953.

(17) Magenau, A. J. D.; Strandwitz, N. C.; Gennaro, A.; Matyjaszewski, K. *Science (80-.).* **2011**, *332* (6025), 81.

(18) Percec, V.; Guliashvili, T.; Ladislaw, J. S.; Wistrand, A.; Stjerndahl, A.; Sienkowska, M. J.; Monteiro, M. J.; Sahoo, S. *J. Am. Chem. Soc.* **2006**, *128* (43), 14156.

(19) Anastasaki, A.; Nikolaou, V.; Nurumbetov, G.; Wilson, P.; Kempe, K.; Quinn, J. F.; Davis, T. P.; Whittaker, M. R.; Haddleton, D. M. *Chem. Rev.* **2016**, *116* (3), 835.

(20) Rosen, B. M.; Percec, V. *Chem. Rev.* **2009**, *109* (11), 5069.

(21) Zhang, Q.; Wilson, P.; Li, Z.; McHale, R.; Godfrey, J.; Anastasaki, A.; Waldron, C.; Haddleton, D. M. *J. Am. Chem. Soc.* **2013**, *135* (19), 7355.

(22) Konkolewicz, D.; Wang, Y.; Krys, P.; Zhong, M.; Isse, A. A.; Gennaro, A.; Matyjaszewski, K. *Polym. Chem.* **2014**, *5* (15), 4396.

(23) Kolb, H. C.; Finn, M. G.; Sharpless, K. B. *Angew. Chem. Int. Ed.* **2001**, *40* (11), 2004.

(24) Barner-Kowollik, C.; Du Prez, F. E.; Espeel, P.; Hawker, C. J.; Junkers, T.; Schlaad, H.; Van Camp, W. *Angew. Chemie Int. Ed.* **2011**, *50* (1), 60.

(25) Tornøe, C. W.; Christensen, C.; Meldal, M. *J. Org. Chem.* **2002**, *67* (9), 3057.

(26) Rostovtsev, V. V.; Green, L. G.; Fokin, V. V.; Sharpless, K. B. *Angew. Chemie Int. Ed.* **2002**, *41* (14), 2596.

(27) Wittig, G.; Krebs, A. *Chem. Ber.* **1961**, *94* (12), 3260.

(28) Agard, N. J.; Prescher, J. A.; Bertozzi, C. R. *J. Am. Chem. Soc.* **2004**, *126* (46), 15046.

(29) Jewett, J. C.; Bertozzi, C. R. *Chem. Soc. Rev.* **2010**, *39* (4), 1272.

(30) Hoyle, C. E.; Lowe, A. B.; Bowman, C. N. *Chem. Soc. Rev.* **2010**, *39* (4), 1355.

(31) Uygun, M.; Tasdelen, M. A.; Yagci, Y. *Macromol. Chem. Phys.* **2010**, *211* (1), 103.

(32) Hoyle, C. E.; Bowman, C. N. *Angew. Chemie Int. Ed.* **2010**, *49* (9), 1540.

(33) Lehn, J.-M. *Angew. Chemie Int. Ed. English* **1990**, *29* (11), 1304.

(34) Pedersen, C. J. *J. Am. Chem. Soc.* **1967**, *89* (26), 7017.

(35) Dietrich, B.; Lehn, J. M.; Sauvage, J. P. *Tetrahedron Lett.* **1969**, *10* (34), 2885.

(36) Kyba, E. B.; Koga, K.; Sousa, L. R.; Siegel, M. G.; Cram, D. J. *J. Am. Chem. Soc.* **1973**, *95* (8), 2692.

(37) Schneider, H.-J. *Angew. Chemie Int. Ed.* **2009**, *48* (22), 3924.

(38) Szejtli, J. *Trends Biotechnol.* **1989**, *7* (7), 170.

(39) Del Valle, E. M. M. *Process Biochem.* **2004**, *39* (9), 1033.

(40) Carrazana, J.; Jover, A.; Meijide, F.; Soto, V. H.; Tato, J. V. *J. Phys. Chem. B* **2005**, *109* (19), 9719.

(41) Greef, T. F. A. De; Smulders, M. M. J.; Wolffs, M.; Schenning, A. P. H. J.; Sijbesma, R. P.; Meijer, E. W.; Counterpart, C. *Chem. Rev.* **2009**, *109* (11), 5687.

(42) Cantekin, S.; De Greef, T. F. A.; Palmans, A. R. A. *Chem. Soc. Rev.* **2012**, *41* (18), 6125.

(43) Brunsveld, L.; Lohmeijer, B. G. G.; Vekemans, J. A. J. M.; Meijer, E. W. *Chem. Commun.* **2000**, No. 23, 2305.

(44) Besenius, P.; van den Hout, K. P.; Albers, H. M. H. G.; de Greef, T. F. A.; Olijve, L. L. C.; Hermans, T. M.; de Waal, B. F. M.; Bomans, P. H. H.; Sommerdijk, N. A. J. M.; Portale, G.; Palmans, A. R. A.; van Genderen, M. H. P.; Vekemans, J. A. J. M.; Meijer, E. W. *Chem. - A Eur. J.* **2011**, *17* (18), 5193.

(45) Leenders, C. M. A.; Albertazzi, L.; Mes, T.; Koenigs, M. M. E.; Palmans, A. R. A.; Meijer, E. W. *Chem. Commun.* **2013**, *49* (19), 1963.

(46) Leenders, C. M. A.; Jansen, G.; Frissen, M. M. M.; Lafleur, R. P. M.; Voets, I. K.;

Palmans, A. R. A.; Meijer, E. W. *Chem. - A Eur. J.* **2016**, *22* (13), 4608.

(47) Pieters, R. J. *Org. Biomol. Chem.* **2009**, *7* (10), 2013.

(48) Gamblin, D. P.; Scanlan, E. M.; Davis, B. G. *Chem. Rev.* **2009**, *109* (1), 131.

(49) Ting, S. R. S.; Chen, G.; Stenzel, M. H. *Polym. Chem.* **2010**, *1* (9), 1392.

(50) Geng, J.; Biedermann, F.; Zayed, J. M.; Tian, F.; Scherman, O. A. *Macromolecules* **2011**, *44* (11), 4276.

(51) Wang, Q.; Dordick, J. S.; Linhardt, R. J. *Chem. Mater.* **2002**, *14* (8), 3232.

(52) Ghazarian, H.; Idoni, B.; Oppenheimer, S. B. *Acta Histochem.* **2011**, *113* (3), 236.

(53) Gabius, H.-J.; André, S.; Kaltner, H.; Siebert, H.-C. *Biochim. Biophys. Acta - Gen. Subj.* **2002**, *1572* (2–3), 165.

(54) Cairo, C. W.; Gestwicki, J. E.; Kanai, M.; Kiessling, L. L. *J. Am. Chem. Soc.* **2002**, *124* (8), 1615.

(55) Arnaud, J.; Audfray, A.; Imberty, A. *Chem. Soc. Rev.* **2013**, *42* (11), 4798.

(56) Kiessling, L. L.; Gestwicki, J. E.; Strong, L. E. *Angew. Chemie Int. Ed.* **2006**, *45* (15), 2348.

(57) Lee, R. T.; Lee, Y. C. *Glycoconj. J.* **2000**, *17* (7), 543.

(58) Holgersson, J.; Gustafsson, A.; Breimer, M. E. *Immunol Cell Biol* **2005**, *83* (6), 694.

(59) Kumar, K.; Chandra, K.; Sumanthi, J.; Reddy, G.; Shekar, P.; Reddy, B. V. R. *J. Orofac. Sci.* **2012**, *4* (1), 20.

(60) Geijtenbeek, T. B. H.; Gringhuis, S. I. *Nat. Rev. Immunol.* **2009**, *9* (7), 465.

(61) Etzler, M. E. *Annu. Rev. Plant Physiol.* **1985**, *36* (1), 209.

(62) Yilmaz, G.; Becer, C. R. *Eur. Polym. J.* **2013**, *49* (10), 3046.

(63) Yilmaz, G.; Becer, C. R. In *Carbohydrate Nanotechnology*; John Wiley & Sons, Inc, 2015; pp 137–173.

(64) Spain, S. G.; Gibson, M. I.; Cameron, N. R. *J. Polym. Sci. Part A Polym. Chem.* **2007**, *45* (11), 2059.

(65) Ilyas, R.; Wallis, R.; Soilleux, E. J.; Townsend, P.; Zehnder, D.; Tan, B. K.; Sim, R. B.; Lehnert, H.; Randeva, H. S.; Mitchell, D. A. *Immunobiology* **2011**, *216* (1–2), 126.

(66) Burke, S. D.; Zhao, Q.; Schuster, M. C.; Kiessling, L. L. *J. Am. Chem. Soc.* **2000**, *122* (18), 4518.

(67) Garegg, P. J.; Lindberg, A. A. *ACS Symp. Ser.* **1993**, *519* (519), 204.

(68) Kiessling, L. L.; Cairo, C. W. *Nat Biotech* **2002**, *20* (3), 234.

(69) Dove, A. *Nat Biotech* **2001**, *19* (10), 913.

(70) Ambrosi, M.; Cameron, N. R.; Davis, B. G. *Org. Biomol.* **2005**, *3* (9), 1593.

(71) Yilmaz, G.; Becer, C. R. *Front. Bioeng. Biotechnol.* **2014**, *2*.

(72) de la Fuente, J. M.; Penadés, S. *Biochim. Biophys. Acta - Gen. Subj.* **2006**, *1760* (4), 636.

(73) Marradi, M.; Martín-Lomas, M.; PenadÉs, S. *Adv. Carbohydr. Chem. Biochem.* **2010**, *64*, 211.

(74) Marradi, M.; Chiodo, F.; Garcia, I.; Penades, S. *Chem. Soc. Rev.* **2013**, *42* (11), 4728.

(75) Chiodo, F.; Marradi, M.; Calvo, J.; Yuste, E.; Penadés, S. *Beilstein J. Org. Chem.* **2014**, *10*, 1339.

(76) Mudshinge, S. R.; Deore, A. B.; Patil, S.; Bhalgat, C. M. *Saudi Pharm. J.* **2011**, *19* (3), 129.

(77) Ahmad, Z.; Shah, A.; Siddiq, M.; Kraatz, H.-B. *RSC Adv.* **2014**, *4* (33), 17028.

(78) García, I.; Marradi, M.; Penadés, S. *Nanomedicine* **2010**, *5* (5), 777.

(79) Yilmaz, G.; Becer, C. R. *Polym. Chem.* **2015**, *6* (31), 5503.

(80) Barrientos, Á. G.; de la Fuente, J. M.; Rojas, T. C.; Fernández, A.; Penadés, S. *Chem. – A Eur. J.* **2003**, *9* (9), 1909.

(81) Dobson, C. M. *Nature* **2003**, *426* (6968), 884.

(82) Dill, K. A.; MacCallum, J. L. *Science (80-.).* **2012**, *338* (6110), 1042.

(83) Perrier, S. *Nat Chem* **2011**, *3* (3), 194.

(84) Altintas, O.; Lejeune, E.; Gerstel, P.; Barner-Kowollik, C. *Polym. Chem.* **2012**, *3* (3), 640.

(85) Altintas, O.; Gerstel, P.; Dingenouts, N.; Barner-Kowollik, C. *Chem. Commun.* **2010**, *46* (34), 6291.

(86) Willenbacher, J.; Schmidt, B. V. K. J.; Schulze-Suenninghausen, D.; Altintas, O.; Luy, B.; Delaittre, G.; Barner-Kowollik, C. *Chem. Commun.* **2014**, *50* (I), 7056.

(87) Shishkan, O.; Zamfir, M.; Gauthier, M. A.; Borner, H. G.; Lutz, J.-F. *Chem. Commun.* **2014**, *50* (13), 1570.

(88) Schmidt, B. V. K. J.; Fechler, N.; Falkenhagen, J.; Lutz, J.-F. *Nat Chem* **2011**, *3* (3), 234.

(89) Lundquist, J. J.; Toone, E. J. *Chem. Rev.* **2002**, *102* (2), 555.

(90) Ting, S. R. S.; Chen, G.; Stenzel, M. H. *Polym. Chem.* 2010, pp 1392–1412.

(91) Ladmiral, V.; Melia, E.; Haddleton, D. M. *Eur. Polym. J.* **2004**, *40* (3), 431.

(92) Slavin, S.; Burns, J.; Haddleton, D. M.; Becer, C. R. *Eur. Polym. J.* **2011**, *47* (4), 435.

(93) Miura, Y.; Hoshino, Y.; Seto, H. *Chem. Rev.* **2016**, *116* (4), 1673.

(94) Ghadban, A.; Albertin, L. *Polymers (Basel).* **2013**, *5* (2), 431.

(95) Ohno, K.; Tsujii, Y.; Miyamoto, T.; Fukuda, T.; Goto, M.; Kobayashi, K.; Akaike, T.

.

(96) Ohno, K.; Tsujii, Y.; Fukuda, T. *J. Polym. Sci. Part A Polym. Chem.* **1998**, *36* (14), 2473.

(97) Geng, J.; Mantovani, G.; Tao, L.; Nicolas, J.; Chen, G.; Wallis, R.; Mitchell, D. A.; Johnson, B. R. G.; Evans, S. D.; Haddleton, D. M. *J. Am. Chem. Soc.* **2007**, *129* (49), 15156.

(98) Granville, A. M.; Quémener, D.; Davis, T. P.; Barner-Kowollik, C.; Stenzel, M. H. *Macromol. Symp.* **2007**, *255* (1), 81.

(99) von der Ehe, C.; Rinkenauer, A.; Weber, C.; Szamosvari, D.; Gottschaldt, M.; Schubert, U. S. *Macromol. Biosci.* **2016**, *16* (4), 508.

(100) Zhang, Q.; Collins, J.; Anastasaki, A.; Wallis, R.; Mitchell, D. A.; Becer, C. R.; Haddleton, D. M. *Angew. Chemie - Int. Ed.* **2013**, *52* (16), 4435.

(101) Zhang, Q.; Su, L.; Collins, J.; Chen, G.; Wallis, R.; Mitchell, D. A.; Haddleton, D. M.; Becer, C. R. *J. Am. Chem. Soc.* **2014**, *136* (11), 4325.

(102) Gauthier, M. A.; Gibson, M. I.; Klok, H.-A. *Angew. Chemie Int. Ed.* **2009**, *48* (1), 48.

(103) Becer, C. R.; Hoogenboom, R.; Schubert, U. S. *Angew. Chemie Int. Ed.* **2009**, *48* (27), 4900.

(104) Ambrosi, M.; Cameron, N. R.; Davis, B. G. *Org. Biomol.* 2005, pp 1593–1608.

(105) Liu, Y.; Liu, J.; Pang, X.; Liu, T.; Ning, Z.; Cheng, G. *Molecules* **2015**, *20* (2), 2272.

(106) Liu, Y.; Liu, J.; Pang, X.; Liu, T.; Ning, Z.; Cheng, G. *Molecules* **2015**, *20* (2), 2272.

(107) Kiessling, L. L.; Grim, J. C. *Chem. Soc. Rev.* **2013**, *42* (10), 4476.

(108) Xue, H.; Peng, L.; Dong, Y.; Zheng, Y.; Luan, Y.; Hu, X.; Chen, G.; Chen, H. *RSC Adv.* **2017**, *7* (14), 8484.

(109) Schmidt, B. V. K. J.; Barner-Kowollik, C. *Nat. Chem.* **2013**, *5* (12), 990.

(110) Abdouni, Y.; Yilmaz, G.; Becer, C. R. *Macromol. Rapid Commun.* **2017**, *38* (24), 1700212.

(111) Ponader, D.; Wojcik, F.; Beceren-Braun, F.; Dernedde, J.; Hartmann, L. *Biomacromolecules* **2012**, *13* (6), 1845.

(112) Wojcik, F.; Mosca, S.; Hartmann, L. *J. Org. Chem.* **2012**, *77* (9), 4226.

(113) Wojcik, F.; Lel, S.; O'Brien, A. G.; Seeberger, P. H.; Hartmann, L. *Beilstein J. Org. Chem.* **2013**, *9* (1), 2395.

(114) Bücher, K. S.; Babic, N.; Freichel, T.; Kovacic, F.; Hartmann, L. *Macromol. Biosci.* **2018**, *18* (12), 1800337.

(115) Ponader, D.; Maffre, P.; Aretz, J.; Pussak, D.; Ninnemann, N. M.; Schmidt, S.; Seeberger, P. H.; Rademacher, C.; Nienhaus, G. U.; Hartmann, L. *J. Am. Chem. Soc.* **2014**, *136* (5), 2008.

(116) Ponader, D.; Igde, S.; Wehle, M.; Märker, K.; Santer, M.; Bléger, D.; Hartmann, L.

Beilstein J. Org. Chem **2014**, *10*, 1603.

(117) Gerke, C.; Ebbesen, M. F.; Jansen, D.; Boden, S.; Freichel, T.; Hartmann, L. *Biomacromolecules* **2017**, *18* (3), 787.

(118) Camaleño de la Calle, A.; Gerke, C.; Chang, X. J.; Grafmüller, A.; Hartmann, L.; Schmidt, S. *Macromol. Biosci.* **2019**, *19* (6), 1900033.

(119) Gerke, C.; Jacobi, F.; Goodwin, L. E.; Pieper, F.; Schmidt, S.; Hartmann, L. *Macromolecules* **2018**, *51* (15), 5608.

(120) Pfeifer, S.; Lutz, J. F. *J. Am. Chem. Soc.* **2007**, *129* (31), 9542.

(121) Lutz, J. F.; Schmidt, B. V. K. . J.; Pfeifer, S. *Macromol. Rapid Commun.* **2011**, *32* (2), 127.

(122) Baradel, N.; Fort, S.; Halila, S.; Badi, N.; Lutz, J. F. *Angew. Chemie - Int. Ed.* **2013**, *52* (8), 2335.

(123) Percec, V.; Popov, A. V.; Ramirez-Castillo, E.; Monteiro, M.; Barboiu, B.; Weichold, O.; Asandei, A. D.; Mitchell, C. M. *J. Am. Chem. Soc.* **2002**, *124* (18), 4940.

(124) Zhang, Q.; Anastasaki, A.; Li, G.-Z.; Haddleton, A. J.; Wilson, P.; Haddleton, D. M. *Polym. Chem.* **2014**, *5* (12), 3876.

(125) Pan, Y.; Ma, C.; Tong, W.; Fan, C.; Zhang, Q.; Zhang, W.; Tian, F.; Peng, B.; Qin, W.; Qian, X. *Anal. Chem.* **2015**, *87* (1), 656.

(126) Xue, L.; Xiong, X.; Chen, K.; Luan, Y.; Chen, G.; Chen, H. *Polym. Chem.* **2016**, *7* (25), 4263.

(127) Van Dongen, S. F. M.; De Hoog, H. P. M.; Peters, R. J. R. W.; Nallani, M.; Nolte, R. J. M.; Van Hest, J. C. M. *Chem. Rev.* **2009**, *109* (11), 6212.

(128) Ahmed, F.; Photos, P. J.; Discher, D. E. *Drug Dev. Res.* **2006**, *67* (1), 4.

(129) Blanazs, A.; Armes, S. P.; Ryan, A. J. *Macromol. Rapid Commun.* **2009**, *30* (4–5), 267.

(130) Li, X.; Chen, G. *Polym. Chem.* **2015**, *6* (9), 1417.

(131) Li, Z.-C.; Liang, Y.-Z.; Li, F.-M. *Chem. Commun.* **1999**, *29* (16), 1557.

(132) Peng, K. Y.; Hua, M. Y.; Lee, R. S. *Carbohydr. Polym.* **2014**, *99*, 710.

(133) Babiuch, K.; Dag, A.; Zhao, J.; Lu, H.; Stenzel, M. H. *Biomacromolecules* **2015**, *16* (7), 1948.

(134) Yilmaz, G.; Messager, L.; Gleinich, A. S.; Mitchell, D. A.; Battaglia, G.; Becer, C. R. *Polym. Chem.* **2016**, *7* (41), 6293.

(135) Heller, P.; Mohr, N.; Birke, A.; Weber, B.; Reske-Kunz, A.; Bros, M.; Barz, M. *Macromol. Biosci.* **2015**, *15* (1), 63.

(136) Wang, Z.; Luo, T.; Sheng, R.; Li, H.; Sun, J.; Cao, A. *Biomacromolecules* **2016**, *17* (1), 98.

(137) Chen, Y.; Espeel, P.; Reinicke, S.; Du Prez, F. E.; Stenzel, M. H. *Macromol. Rapid Commun.* **2014**, *35* (12), 1128.
(138) Dag, A.; Lu, H.; Stenzel, M. H. *Polym. Chem.* **2015**, *6* (45), 7812.
(139) Ganda, S.; Jiang, Y.; Thomas, D. S.; Eliezar, J.; Stenzel, M. H. *Macromolecules* **2016**, *49* (11), 4136.
(140) Scherer, M.; Kappel, C.; Mohr, N.; Fischer, K.; Heller, P.; Forst, R.; Depoix, F.; Bros, M.; Zentel, R. *Biomacromolecules* **2016**, 1.
(141) Bonduelle, C.; Lecommandoux, S. *Biomacromolecules* **2013**, *14* (9), 2973.
(142) Bonduelle, C.; Huang, J.; Ibarboure, E.; Heise, A.; Lecommandoux, S. *Chem. Commun.* **2012**, *48* (67), 8353.
(143) Bonduelle, C.; Huang, J.; Mena-Barragan, T.; Ortiz Mellet, C.; Decroocq, C.; Etame, E.; Heise, A.; Compain, P.; Lecommandoux, S. *Chem. Commun.* **2014**, *50* (25), 3350.
(144) Bonduelle, C.; Oliveira, H.; Gauche, C.; Huang, J.; Heise, A.; Lecommandoux, S. *Chem. Commun.* **2016**, *52* (75), 11251.
(145) Isono, T.; Miyachi, K.; Satoh, Y.; Nakamura, R.; Zhang, Y.; Otsuka, I.; Tajima, K.; Kakuchi, T.; Borsali, R.; Satoh, T. *Macromolecules* **2016**, *49* (11), 4178.
(146) Lu, J.; Fu, C.; Wang, S.; Tao, L.; Yan, L.; Haddleton, D. M.; Chen, G.; Wei, Y. *Macromolecules* **2014**, *47* (14), 4676.
(147) Fu, C.; Bongers, A.; Wang, K.; Yang, B.; Zhao, Y.; Wu, H.; Wei, Y.; Duong, H. T. T.; Wang, Z.; Tao, L. *Polym. Chem.* **2016**, *7* (3), 546.
(148) Park, H.; Walta, S.; Rosencrantz, R. R.; Körner, A.; Schulte, C.; Elling, L.; Richtering, W.; Boker, A. *Polym. Chem.* **2015**, *7* (4), 878.
(149) Cao, C.; Zhao, J.; Chen, F.; Lu, M.; Khine, Y. Y.; Macmillan, A.; Garvey, C. J.; Stenzel, M. H. *Chem. Mater.* **2018**, *30* (15), 5227.
(150) Pasparakis, G.; Alexander, C. *Angew. Chemie - Int. Ed.* **2008**, *47* (26), 4847.
(151) Chen, G.; Amajjahe, S.; Stenzel, M. H. *Chem. Commun.* **2009**, *19* (10), 1198.
(152) Kumar, J.; McDowall, L.; Chen, G.; Stenzel, M. H. *Polym. Chem.* **2011**, *2* (8), 1879.
(153) Zhang, Q.; Wilson, P.; Anastasaki, A.; McHale, R.; Haddleton, D. M. *ACS Macro Lett.* **2014**, *3* (5), 491.
(154) Sun, K.; Bligh, S. W. A.; Nie, H.; Quan, J.; Zhu, L. *RSC Adv.* **2014**, *4* (66), Ahead of Print.
(155) Cakir, N.; Hizal, G.; Becer, C. R. *Polym. Chem.* **2015**, *6* (37), 6623.
(156) Narain, R.; Armes, S. P. *Biomacromolecules* **2003**, *4* (6), 1746.
(157) Qiu, S.; Huang, H.; Dai, X. H.; Zhou, W.; Dong, C. M. *J. Polym. Sci. Part A Polym. Chem.* **2009**, *47* (8), 2009.
(158) Boye, S.; Appelhans, D.; Boyko, V.; Zschoche, S.; Komber, H.; Friedel, P.;

Formanek, P.; Janke, A.; Voit, B. I.; Lederer, A. *Biomacromolecules* **2012**, *13* (12), 4222.

(159) Liu, L. I.; Zhang, J.; Wenhui, L. V.; Luo, Y. A. N.; Wang, X. *J. Polym. Sci. Part A Polym. Chem.* **2010**, *48* (15), 3350.

(160) Dag, A.; Zhao, J.; Stenzel, M. H. *ACS Macro Lett.* **2015**, *4* (5), 579.

(161) Deng, Z.; Ahmed, M.; Narain, R. *J. Polym. Sci. Part A Polym. Chem.* **2009**, *47* (2), 614.

(162) Yuan, F.; Wang, S.; Lu, W.; Chen, G.; Tu, K.; Jiang, H.; Wang, L.-Q. *J. Mater. Chem. B* **2015**, *3* (22), 4546.

(163) Chen, K.; Bao, M.; Muñoz Bonilla, A.; Zhang, W.; Chen, G. *Polym. Chem.* **2016**, *7* (14), 2565.

(164) Altintas, O.; Barner-Kowollik, C. *Macromol. Rapid Commun.* **2012**, *33* (11), 958.

(165) Altintas, O.; Barner-Kowollik, C. *Macromol. Rapid Commun.* **2016**, *37* (1), 29.

(166) Altintas, O.; Krolla-Sidenstein, P.; Gliemann, H.; Barner-Kowollik, C. *Macromolecules* **2014**, *47* (17), 5877.

(167) Willenbacher, J.; Altintas, O.; Roesky, P. W.; Barner-Kowollik, C. *Macromol. Rapid Commun.* **2014**, *35* (1), 45.

(168) Pomposo, J. A. *Polym. Int.* **2014**, *63* (4), 589.

(169) Chao, D.; Jia, X.; Tuten, B.; Wang, C.; Berda, E. B. *Chem. Commun.* **2013**, *49* (39), 4178.

(170) Perez-Baena, I.; Asenjo-Sanz, I.; Arbe, A.; Moreno, A. J.; Lo Verso, F.; Colmenero, J.; Pomposo, J. A. *Macromolecules* **2014**, *47* (23), 8270.

(171) Sanchez-Sanchez, A.; Akbari, S.; Etxeberria, A.; Arbe, A.; Gasser, U.; Moreno, A. J.; Colmenero, J.; Pomposo, J. A. *ACS Macro Lett.* **2013**, *2* (6), 491.

(172) Moreno, A. J.; Lo Verso, F.; Sanchez-Sanchez, A.; Arbe, A.; Colmenero, J.; Pomposo, J. A. *Macromolecules* **2013**, *46* (24), 9748.

(173) Sanchez-Sanchez, A.; Akbari, S.; Moreno, A. J.; Verso, F. Lo; Arbe, A.; Colmenero, J.; Pomposo, J. A. *Macromol. Rapid Commun.* **2013**, *34* (21), 1681.

(174) Sanchez-Sanchez, A.; Pomposo, J. A. *J. Nanomater.* **2015**, *2015*, 1.

(175) Hansell, C. F.; Lu, A.; Patterson, J. P.; O'Reilly, R. K. *Nanoscale* **2014**, *6* (8), 4102.

(176) Sanchez-Sanchez, A.; Asenjo-Sanz, I.; Buruaga, L.; Pomposo, J. A. *Macromol. Rapid Commun.* **2012**, *33* (15), 1262.

(177) Willenbacher, J.; Wuest, K. N. R.; Mueller, J. O.; Kaupp, M.; Wagenknecht, H. A.; Barner-Kowollik, C. *ACS Macro Lett.* **2014**, *3* (6), 574.

(178) Tuten, B. T.; Chao, D.; Lyon, C. K.; Berda, E. B. *Polym. Chem.* **2012**, *3* (11), 3068.

(179) Mes, T.; Van Der Weegen, R.; Palmans, A. R. A.; Meijer, E. W. *Angew. Chemie - Int. Ed.* **2011**, *50* (22), 5085.

(180) Hosono, N.; Palmans, A. R. A.; Meijer, E. W. *Chem. Commun.* **2014**, *50* (59), 7990.

(181) ter Huurne, G. M.; Gillissen, M. A. J.; Palmans, A. R. A.; Voets, I. K.; Meijer, E. W. *Macromolecules* **2015**, *48* (12), 3949.

(182) Hosono, N.; Kushner, A. M.; Chung, J.; Palmans, A. R. A.; Guan, Z.; Meijer, E. W. *J. Am. Chem. Soc.* **2015**, *137* (21), 6880.

(183) Hosono, N.; Gillissen, M. A. J.; Li, Y.; Sheiko, S. S.; Palmans, A. R. A.; Meijer, E. W. *J. Am. Chem. Soc.* **2013**, *135* (1), 501.

(184) Huerta, E.; Stals, P. J. M.; Meijer, E. W.; Palmans, A. R. A. *Angew. Chemie - Int. Ed.* **2013**, *52* (10), 2906.

(185) Wuest, K. N. R.; Lu, H.; Thomas, D. S.; Goldmann, A. S.; Stenzel, M. H.; Barner-Kowollik, C. *ACS Macro Lett.* **2017**, *6* (10), 1168.

(186) Yilmaz, G.; Uzunova, V.; Napier, R.; Becer, C. R. *Biomacromolecules* **2018**, *19* (7), 3040.

(187) Kröger, A. P. P.; Komil, M. I.; Hamelmann, N. M.; Juan, A.; Stenzel, M. H.; Paulusse, J. M. J. *ACS Macro Lett.* **2019**, *8* (1), 95.

Chapter 2

Development of a novel cyclodextrin based initiator and its sequence-controlled polymers

In this chapter, I discuss the synthesis and use of a novel β-cyclodextrin based SET-LRP initiator. Three different approaches towards the synthesis of this initiator, based on three 'click' like reactions (copper(I)-catalysed azide-alkyne cycloaddition, nucleophilic thiol-ene reaction and radical thiol-ene reaction), have been explored and discussed. Synthesis via radical thiol-ene proved to be most successful in achieving this. The β-cyclodextrin based initiator was subsequently used for the polymerisation of several acrylates in a controlled fashion yielding 7-arm multiblock-copolymers. The achieved sequence-controlled polymers exhibit low dispersities (≤ 1.12) and were completed under 6.5 h at high monomer conversion (≥95 %) for each block.

Section II.2.2 was performed by Dr. G. Yilmaz

Parts of this chapter have been published:
Abdouni, Y., Yilmaz, G. & Becer, C. R. Sequence Controlled Polymers from a Novel β-Cyclodextrin Core. *Macromol. Rapid Commun*. **38**, 1700501 (2017).

II Development of a novel cyclodextrin based initiator and it's sequence-controlled polymers

II.1 Introduction

Over the last decade, there has been an increased interest in the development of more structurally complex macromolecules both in terms of monomer sequence as in overall architecture.[1–3] Function in Nature's macromolecules is not only determined by its primary structure but also by its overall molecular architecture, displaying sophisticated properties such as molecular recognition and catalysis. For this reason, many different nonlinear molecular architectures have been established ranging from cyclic polymers to dendritic, graft, brush, hyperbranched and star-shaped (co)polymers.[4] These, together with advances in controlled polymerisation methods at the end of the last century, have paved the way for the recent explosion of novel precision macromolecules, specifically tailored to exhibit distinct features.[5,6]

Star polymers, in particular, can be prepared either *via* three distinct approaches namely *via* the arm-first approach, *via* the coupling-onto method or *via* the core-first approach. In light of architectural precision, a core-first approach offers an enhanced control over the number of arms, as the arm-first approach usually gives a broad distribution of number of arms per molecule.[7] The coupling-onto method, on the other hand, requires a high coupling efficiency often acquired *via* 'click' reactions after full conversion of the active chain end groups.

In 2001 Haddleton and co-workers introduced *β*-cyclodextrin (a homochiral cyclic oligosaccharide containing 7 glucopyranose units and thus 21 free hydroxyl groups), as a multifunctional core initiator for the preparation of well-defined star-shaped polymers *via* copper mediated controlled radical polymerisations.[8] However, more recent

publications have shown that full substitution of the 21 hydroxyl groups is not achieved and that a mixture of star initiators is obtained.[9] More recently, the group of Li employed a less substituted version of this *β*-cyclodextrin core initiator with only 4 initiating sites on average.[10–12]

Stenzel and coworkers introduced the use of a *β*-cyclodextrin derived star RAFT agent for the synthesis of spherical glycopolymer architectures (**Figure II.1.1**).[13,14] The interesting feature about this multifunctional *β*-cyclodextrin derived RAFT agent is that only the top face of the *β*-cyclodextrin is converted to RAFT agents, whereas the bottom face is not. This leaves the possibility for small molecules to access the hydrophobic core for potential host-guest complexations. Although RAFT has proven to be a very useful technique in the preparation of extremely well-defined multiblock-co-polymers by the group of Perrier, it was found not suitable for the synthesis of core-first star shaped polymers as it is prone to many termination reactions.[15–18].

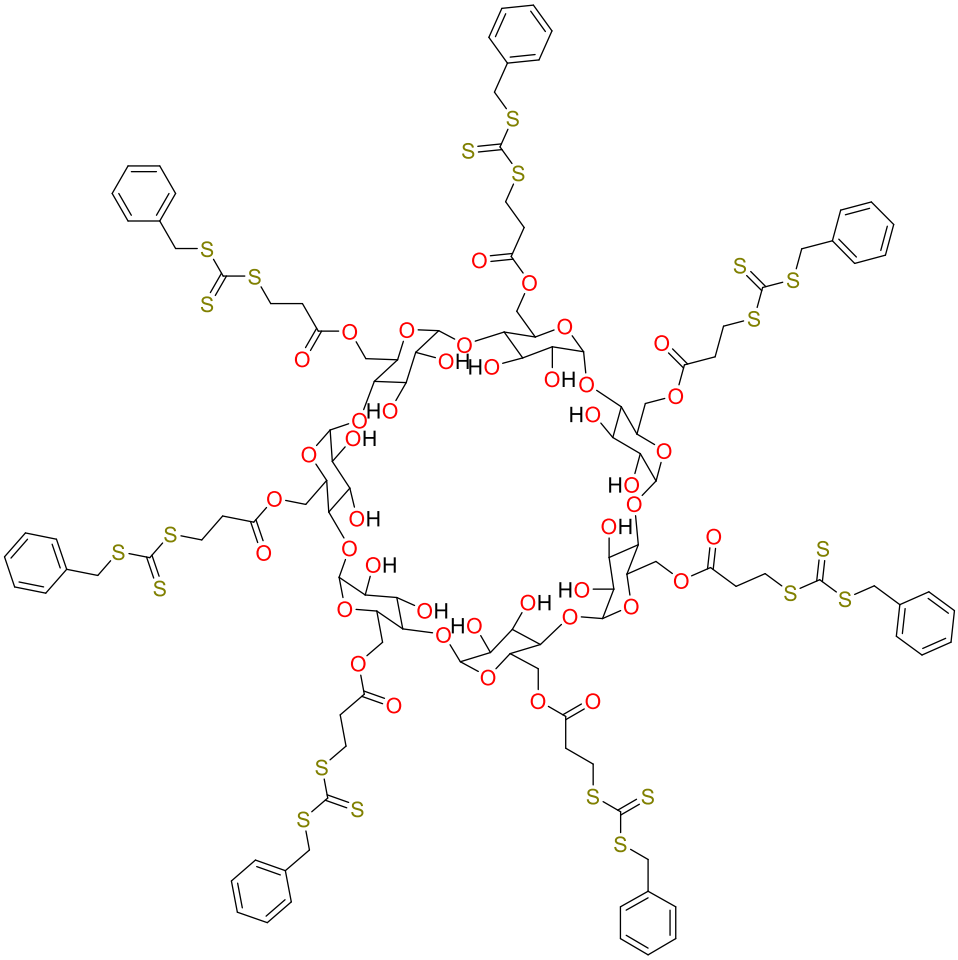

Figure II.1.1 β-Cyclodextrin-derived star RAFT agent.[13]

As mentioned *vide supra*, copper mediated controlled radical polymerisations offer an elegant way of achieving interesting architectures. The group of Haddleton has

used these techniques for the synthesis of sequence controlled polymers both in DMSO and in aqueous systems.[19–21] Encouraged by these results, our group was recently able to prepare star-shaped polymers *via* SET-LRP in DMSO and pentablock star shaped polymers in less than 90 minutes *via* aqueous SET-LRP starting from a water soluble glycerol core.[22,23]

Inspired by these findings and the interesting features a *β*-cyclodextrin core could provide, we have developed a novel *β*-cyclodextrin derived SET-LRP star initiator (*β*-CD initiator). This chapter describes the synthesis route towards this novel star initiator *via* 'click' like reactions as well as its use for the sequence-controlled polymerisation of different acrylates.[24,25]

II.2 Results and discussion

II.2.1 Synthesis of a *β*-cyclodextrin initiator

For the preparation of the *β*-cyclodextrin based initiator three different synthesis routes were explored of which the former two have proven not to be successful (**Scheme II.2.1**).

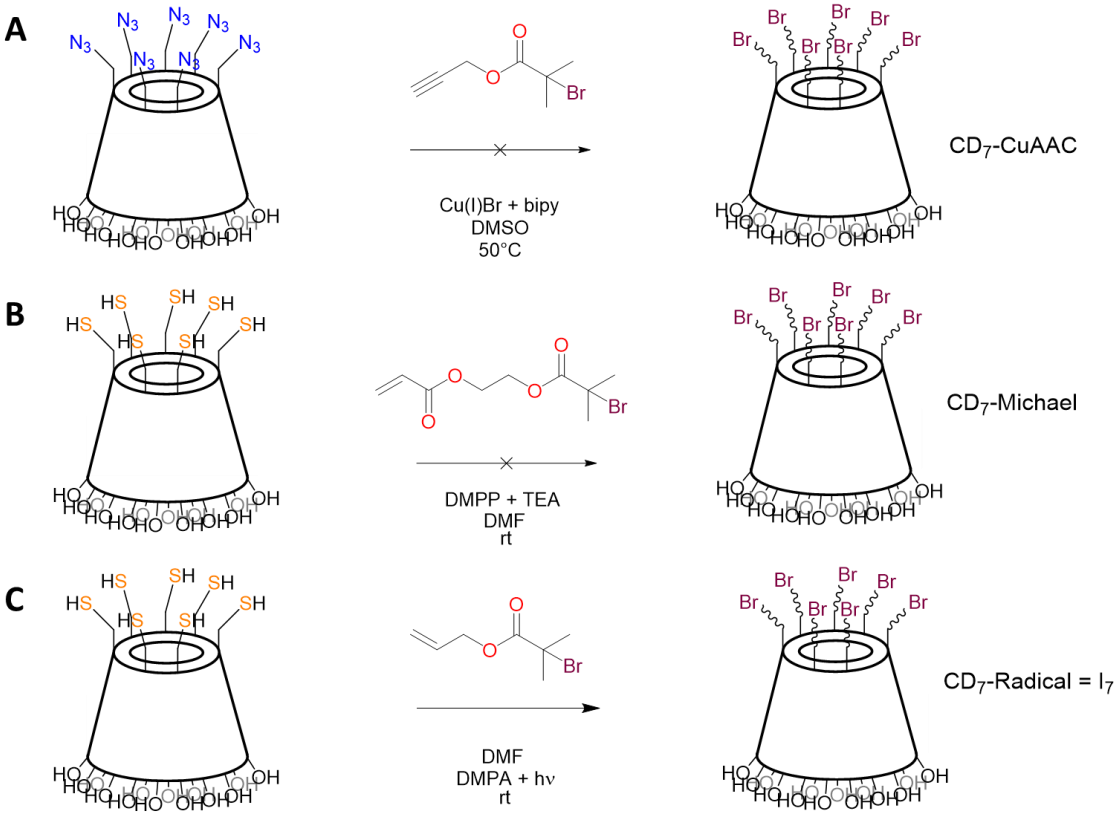

Scheme II.2.1 Schematic overview of the different approaches towards a monofacially functionalized cyclodextrin initiator.

The first synthesis route explored (**Scheme II.2.1A**), was based on the copper(I)-catalysed azide-alkyne cycloaddition (CuAAC), well-known as the 'click' reaction.[26] For this, the secondary hydroxyl groups on primary rim region of the *β*-cyclodextrin were selectively brominated using triphenylphosphine and *N*-bromosuccinimide and subsequently converted into azides *via* a simple azide nucleophilic substitution in dimethylformamide (DMF). A terminal alkyne containing SET-LRP initiator was synthesised by simple substitution reaction between propargyl alcohol and bromoisobutyryl bromide. This SET-LRP initiator was then 'clicked' to the *per*-(6-deoxy-

6-azido)-*β*-cyclodextrin, however gel permeation chromatography (GPC) and MALDI-TOF analysis showed the synthesis was prone to side reactions. **Figure II.2.1A** shows the MALDI-TOF mass spectrum or CD_7-CuAAC which shows a lot of side products with a higher molecular weight which have not been identified. These findings were confirmed in the GPC chromatogram, showing products at shorter retention times, thus confirming the higher molecular weight of the side products (**Figure II.2.1B**).

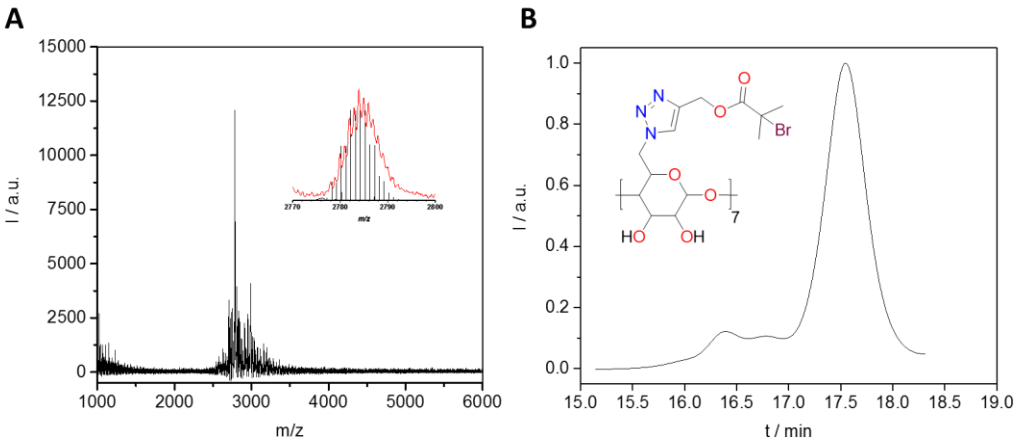

Figure II.2.1 A) MALDI-TOF mass spectrum of compound CD_7-CuAAC with the isotopic distribution of the peak of interest (red) and the theoretical isotopic distribution (black) A; B) GPC chromatogram of compound CD_7-CuAAC including the chemical structure of the desired compound CD_7-CuAAC.

For the second approach (**B**), the brominated cyclodextrin was thiolated using thiourea and subsequent hydrolysis and acidification yielded *per*-6-thio-*β*-cyclodextrin (*β*-CD-$(SH)_7$). Taking into account the oxidative instability of the thiols, this compound should be used as quickly as possible and be stored under argon. Subsequently the Michael addition was performed in DMF to 2-(2-bromoisobutyryloxy) ethyl acrylate as the Michael acceptor in the presence of triethylamine as a base catalyst and dimethyl phenyl phosphine as nucleophilic catalyst and doubling as a reductant for possible disulphide bridges.[27] Also for compound CD_7-Michael, a combination of MALDI-TOF analysis and GPC revealed that although the desired compound was achieved, many side products were observed which could be ascribed to a competitive nucleophilic thio-bromo reaction, illustrating why reactions involving thiols cannot be named ‘click’ reactions as described in section **I.2.2.2** (**Figure II.2.2**).

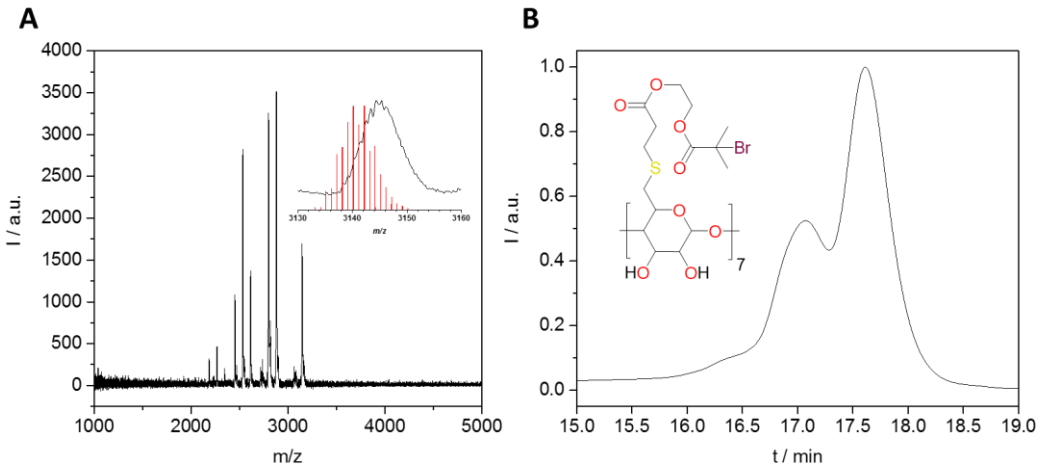

Figure II.2.2 A) MALDI-TOF mass spectrum of compound CD_7-Michael with the isotopic distribution of the peak of interest (black) and the theoretical isotopic distribution (red); B) GPC chromatogram of compound CD_7-Michael including the chemical structure of the desired compound CD_7-Michael.

The third approach proved to be the most successful (**C**), for this the thiolated *β*-cyclodextrin was reacted with a large excess of allyl 2-bromo-2-methylpropionate *via* the radical thiol-*ene* reaction in DMF.[28,29] To account for possible disulphide bridges, present in the starting product, two equivalents of dithiothreitol were added as a reductant 60 hours prior to the radical thiol-*ene* reaction. Also here, MALDI-TOF analysis and GPC were performed. The desired product was achieved, however the GPC chromatogram showed minor dimer formation (**Figure II.2.3**). As this product gave the best results, it was further used for the synthesis of sequence-controlled star polymers.

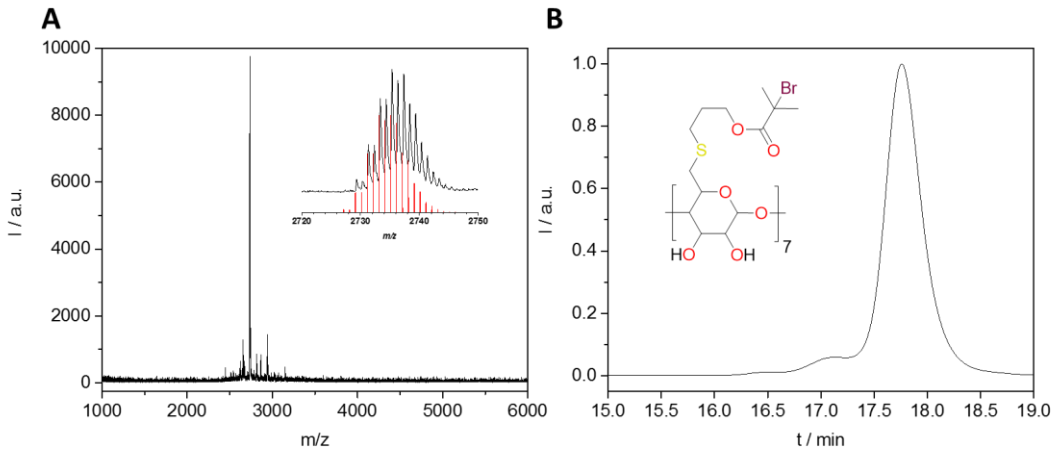

Figure II.2.3 A) MALDI-TOF mass spectrum of compound CD_7-Radical (I7) with the isotopic distribution of the peak of interest (black) and the theoretical isotopic distribution (red); B) GPC chromatogram of compound CD_7-Radical (I_7) including the chemical structure of the desired compound CD_7-Radical (I_7).

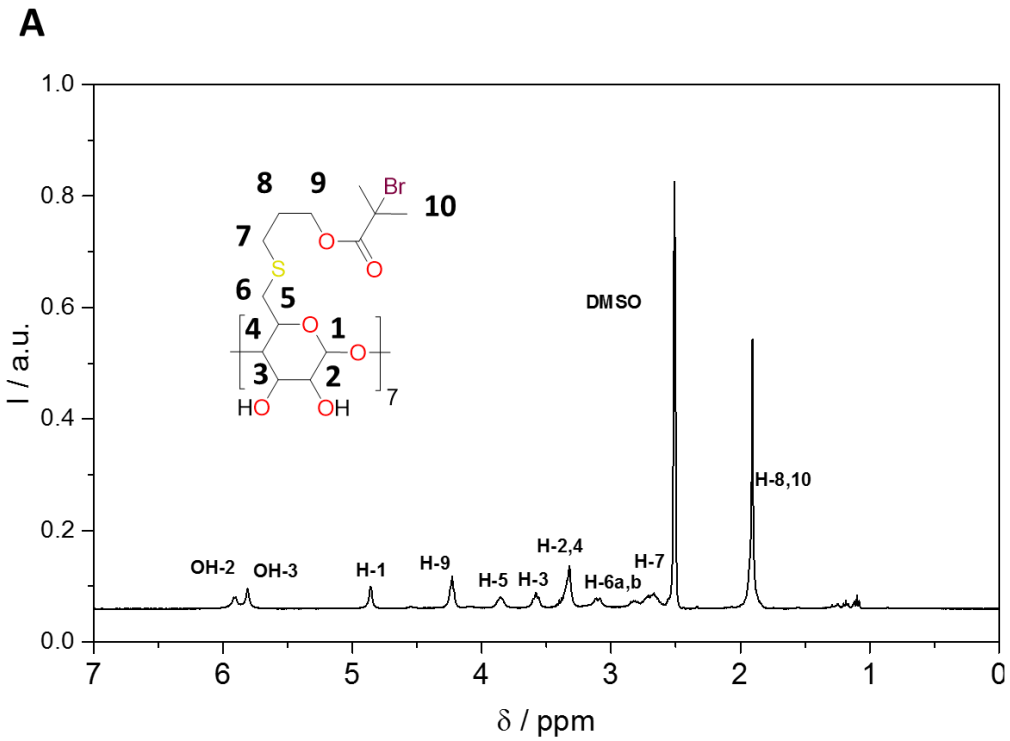

Figure II.2.4 A) ^{1}H-NMR spectrum (in DMSO-d_6) of per-6-deoxy-6-(thiopropyl-2-bromo-2-methylpropanoate)-β-cyclodextrin (CD_7-Radical (I_7)).

II.2.2 Sequence-controlled polymerisation of acrylates

The novel β-cyclodextrin based initiator CD_7-Radical (I_7) was subsequently used for the SET-LRP polymerisation of three different acrylates in DMSO (**Figure II.2.5**).[30] A variety of star multiblock copolymers based on methyl acrylate, ethyl acrylate and *n*-butyl acrylate were synthesised in various compositions demonstrating the versatility of the approach.

The multi-block copolymerisation was initiated with 60 repeating units of methyl acrylate (MA) per arm using the ratio of [MA] : [I] : [$CuBr_2$] : [Me_6TREN] = 60 : 1 : 0.04 : 0.19. A higher amount of monomers per arm was chosen for the first block, as it was found that using a smaller amount would result in elevated levels of terminating radical radical coupling. Typically a Schlenk tube was charged with same ratio of first block monomer methyl acrylate (MA), pre-activated Cu(0) wire (5 cm), $CuBr_2$ and Me_6TREN in DMSO (1 ml) and then the mixture was degassed by gentle bubbling of argon gas for

30 min. Pre-degassed *β*-CD initiator in 1 ml was then added *via* gas tight syringe sequentially. The Schlenk tube was sealed and the reaction mixture was allowed to polymerise at 25°C. After a polymerisation time of 1.5 h, NMR evidenced that the polymerisation reaction was terminated. The second block solution of 10 repeating units of ethyl acrylate (EA) per arm was then degassed with argon for 20 min and subsequently transferred *via* cannula to the Schlenk tube under argon protection and allowed to polymerise which was finished after 1.5 h. Finally, a third block of 10 repeating units of *n*-butyl acrylate (BA) per arm was added, for which the polymerisation was finished after 2.5 h.

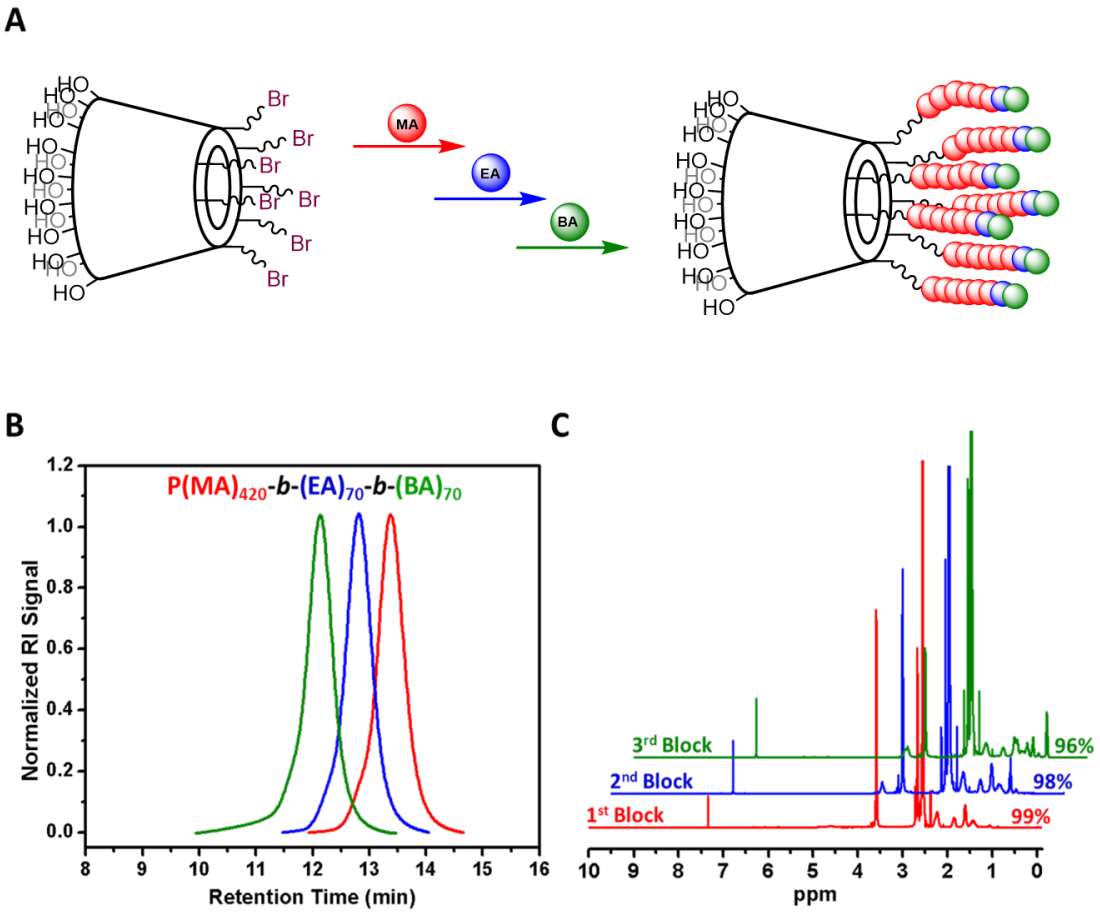

Figure II.2.5 A) Representative scheme for the obtained triblock *β*-CD initiated copolymer M42E7B7; B) SEC traces of M42E7B7; C) ^{1}H NMR spectra displaying full conversion for each block.

The obtained polymers were very well defined, demonstrating low polydispersities and radical-radical coupling and no tailing was observed (see section **II.4.3**). As previously described, four different multi-block copolymers were synthesised (**Table II.2.1**), demonstrating the versatility of the approach. We were able to keep the dispersity (*Đ)* of the multi-block copolymers below 1.12 with each block finished under

2.5 hours at monomer conversions over 95% and a total polymerisation time under 6.5 h. Number average molar masses (M_n) and dispersities were determined *via* THF GPC relative to PMMA standards. As often found for star polymers, measured molar masses were lower than theoretical molar masses.

Table II.2.1 Summary of monomer (MA = methyl acrylate, EA = ethyl acrylate, BA = n-butyl acrylate) conversions, number average molar masses (M_n) and molar mass distributions ($Đ$) of the synthesised triblock copolymers.

Code	Polymer	ρ^a (%)			$M_{n,NMR}{}^b$ (g.mol^{-1})	$M_{n,GPC}{}^c$ (g.mol^{-1})	$Đ$	*Time (h)*
		MA	**EA**	**BA**				
M42E7B7	P((MA)$_{420}$-*b*-(EA)$_{70}$)-*b*-(BA)$_{70}$)	99	-	-	38800	35600	1.06	1.5
		-	98	-	45800	43500	1.07	1.5
		-	-	96	54750	51200	1.12	2
M42B7E7	P((MA)$_{420}$-*b*-(BA)$_{70}$)-*b*-(EA)$_{70}$)	99	-	-	38800	35300	1.06	1.5
		-	-	97	47800	45700	1.09	2
		-	97	-	54750	50900	1.11	2.5
E42M7B7	P((EA)$_{420}$-*b*-(MA)$_{70}$)-*b*-(BA)$_{70}$)	-	99	-	44700	41900	1.07	1.5
		98	-	-	50750	48400	1.08	2
		-	-	95	59700	56200	1.11	2.5
E42B7M7	P((EA)$_{420}$-*b*-(BA)$_{70}$)-*b*-(MA)$_{70}$)	-	99	-	44700	41700	1.08	1.5
		-	-	96	53600	51100	1.10	2.5
		96	-	-	59500	56600	1.12	2.5

[a)] Conversion (ρ) obtained from ^{1}H NMR; b) $M_{n,NMR}$ = ([M]$_o$/[CD-initiator]$_o$ x conversion x M_{mon}) + $M_{CD\text{-}init}$; c) Determined by THF GPC (relative to PMMA stn.).

II.3 Conclusion

In conclusion, we have investigated several synthesis routes towards monofacially functionalized *β*-cyclodextrin based SET-LRP star initiators using ‘click’ and ‘click’ like reactions. It was found that the radical thiol-*ene* reaction proved to be most successful in achieving this. The other two synthesis routes not only gave too many side reactions, but the first synthesis route also produces copper residues that can further interfere in the copper mediated polymerisation processes. Furthermore we have demonstrated that this novel *β*-cyclodextrin based initiator can be used for the synthesis of core-first 7-arm multi-block star shaped polymers based on different acrylates. All synthesised multiblock-copolymers have excellent dispersities (≤ 1.12), even at high monomer conversions and were completed under 6.5 h. As the hydrophobic cavity of the *β*-cyclodextrin core should still be accessible, we hope to have drawn a basis for novel macrohost-guest reactions.

II.4 Experimental section

II.4.1 Materials

Methyl acrylate (MA) (99%, contains ≤100 ppm MEHQ as inhibitor), ethyl acrylate (EA) (99%, contains ≤100 ppm MEHQ as inhibitor) and butyl acrylate (BA) (99%, contains ≤100 ppm MEHQ as inhibitor were purchased from Sigma Aldrich Chemical Company (Dorset, UK). Tris(2-(dimethylamino)ethyl)amine (Me_6TREN) was previously synthesised within the group. All other reagents and solvents were obtained at the highest purity available from Sigma Aldrich Chemical Company. MA, EA and BA were passed through a basic alumina column to remove inhibitors prior to polymerisation.

II.4.2 Instruments and analysis

Proton (^{1}H-NMR) nuclear magnetic resonance spectroscopy (Bruker DPX-400/600) was used to determine the chemical structure of the synthesised initiators and polymers. Samples were dissolved at 10 mg/mL concentration in $CDCl_3$ or DMSO-d_6 as solvent.

Gel Permeation Chromatography (GPC) measurements were conducted on an Agilent 1260 infinity system operating in THF containing 2% triethylamine (TEA) and equipped with refractive index detector (RID) and variable wavelength detector (VWD), 2 PLgel 5 µm mixed-C columns (300×7.5mm), a PLgel 5 mm guard column (50x7.5mm) and an autosampler. The instrument was calibrated with linear poly(methyl methacrylate) (PMMA) standards.

Matrix assisted laser desorption/ionisation – time of flight mass spectroscopy (MALDI-TOF MS) was performed using a Bruker Daltonics Autoflex MALDI-ToF mass spectrometer, equipped with a nitrogen laser at 337 nm with positive ion ToF detection. Polymer samples were measured as follows; solutions in acetonitrile of trans-2-[3-(4-tert-Butylphenyl)-2-methyl-2-propenylidene]malononitrile (DCTB, ≥98%) as matrix (30 mg·mL^{-1}), potassium trifluoroacetate (KTFA) as cationisation agent (10 mg·mL^{-1}) and sample (10 mg·mL^{-1}) were spotted separately on the MALDI plate (0.7 µL each) and

mixed on the plate. Spectra were recorded in reflectron mode and the mass spectrometer was calibrated with a peptide mixture up to 6000 Da.

II.4.3 Experimental procedures

II.4.3.1 Synthesis of per-(6-deoxy-6-bromine)-β-cyclodextrin (β-CD-(Br)$_7$)

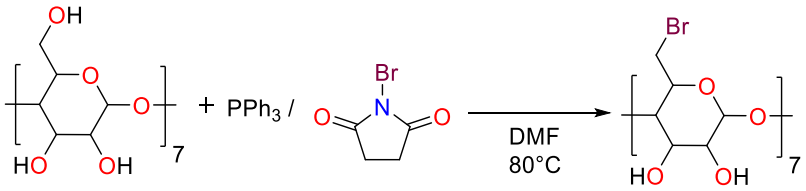

Scheme II.4.1 Schematic representation of the synthetic approach to β-CD-(Br)$_7$.

Triphenylphosphine (Ph_3P, 40.39 g, 154.0 mmol) was dissolved in anhydrous DMF (150 mL) under stirring and cooled down to 0 °C. *N*-bromosuccinimide (NBS, 27.41 g, 154.0 mmol) was dissolved in anhydrous DMF (40 mL) and the solution was added dropwise to the Ph_3P solution under Ar atmosphere and then stirred at ambient temperature for 30 min. *β*-Cyclodextrin (*β*-CD, 11.35 g, 10.00 mmol) (previously recrystallized three times from water and dried in a vacuum oven at 50 °C for two days) was dissolved in anhydrous DMF (150 mL). The obtained Ph_3P/NBS solution was then added dropwise to the *β*-cyclodextrin solution at ambient temperature after which the solution temperature was increased to 80 °C. The mixed brown solution was stirred under Ar atmosphere overnight at 80 °C. Afterwards MeOH (40 mL) was added at ambient temperature and stirring was continued for 30 min. The reaction mixture was then cooled to 0 °C and the pH was adjusted to 9 by adding sodium methoxide, while further stirring for 1 h. The reaction mixture was then poured into stirred ice-water (4 L) resulting in a fine precipitate which was filtered and washed with MeOH. *Heptakis* (6-deoxy-6-bromo)-*β*-cyclodextrin was obtained as beige solids and dried under vacuum for 1 day. Yield: 11.32 g, 70%).

^{1}H NMR (400 MHz, DMSO-d_6, 298 K, ppm): δ =6.02 (*d*, 7 H, 6.7 Hz), 5.89 (*d*, 7 H, 1.9 Hz), 4.98 (*d*, 7 H, 3.4 Hz), 4.00 (*d*, 7 H, 9.8 Hz), 3.82 (*t*, 7 H, 9.3 Hz), 3.65 (*m*, 14 H), 3.38 (*m*, 14 H, overlap with H_2O)

MALDI-TOF MS m/z: calculated for $C_{42}H_{63}Br_7O_{28}K^+$: 1614.73; found, 1614.74

II.4.3.2 Synthesis of *per*-(6-deoxy-6-azido)-*β*-cyclodextrin (*β*-CD-$(N_3)_7$)

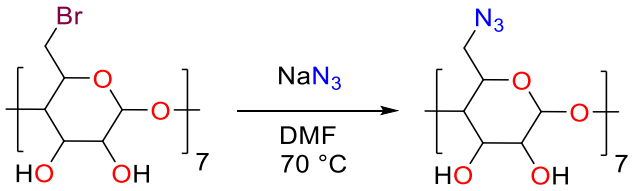

Scheme II.4.2 Schematic representation of the synthetic approach to *β*-CD-$(N_3)_7$.

Heptakis (6-deoxy-6-bromo)-*β*-cyclodextrin (10.0 g, 6.34 mmol) was dissolved in anhydrous DMF (80 mL) and NaN_3 (5.78 g, 88.8 mmol). The resulting suspension was stirred at 70 °C under Ar for 36 h. The suspension was then allowed to cool down and precipitated in 2 L of stirred ice-water. The precipitate was filtered, washed with water and redissolved in DMF (20 mL) and precipitated in 1L of stirred ice-water. The precipitate was filtered and washed with water and with little acetone. The resulting product was a white solid (yield: 7.2 g, 86.5 %) and was dried under vacuum overnight.

^{1}H NMR (400 MHz, DMSO-d_6, 298 K, ppm): δ =5.90 (*d*, 7 H, 6.8 Hz), 5.75 (*d*, 7 H, 2 Hz), 4.91(*d*, 7 H, 3,4 Hz), 3.74 (*m*, 14 H), 3.59 (*m*, 14 H), 3.36 (*m*, 14 H, overlap with H_2O).

MALDI-TOF MS m/z: calculated for $C_{42}H_{63}N_{21}O_{28}K^+$: 1348.37; found, 1348.27

II.4.3.3 Synthesis of propargyl-2-bromoisobutyrate

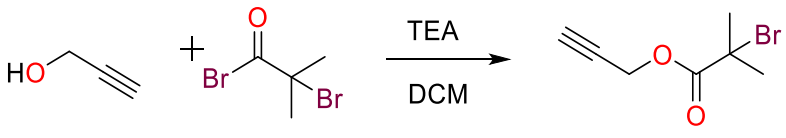

Scheme II.4.3 Schematic representation of the synthetic approach to propargyl 2-bromoisobutyrate.

Propargyl alcohol (7.50 mL, 7.22 g, 129 mmol) and triethylamine (28.7 mL, 20.8 g, 206 mmol) were dissolved in dichloromethane (DCM) (150 mL) and cooled down to 0 °C in an ice-water bath. A solution of *α*-bromoisobutyryl bromide (BIBB) (20.7 mL, 38.5 g, 167 mmol) in 20 mL DCM was added dropwise over a period of 20 min. The mixture was allowed to stir for 1 h at 0 °C after which it was allowed to reach room temperature and stirring was continued overnight. The solution was washed 3 x 50 mL 10% HCl solution, 3 x 50 mL saturated $NaHCO_3$ solution, 3 x 50 mL water and subsequently dried over $MgSO_4$. After evaporating the solvent *via* rotary evaporation, the product was purified by column chromatography on silica gel using DCM: hexane (1:3) affording a colourless oil. (yield: 75%, 20 g).

^{1}H NMR (400 MHz, $CDCl_3$, 298 K, ppm): δ = 4.78 (*d*, 2 H, 2.4 Hz), 2.52 (*t*, 1 H, 2.4 Hz), 1.96 (*s*, 6 H)

II.4.3.4 Synthesis of per-6-deoxy-6-((1,2,3-triazol-4-yl)methyl 2-bromoisobutyrate)-*β*-cyclodextrin (CD_7-CuAAC)

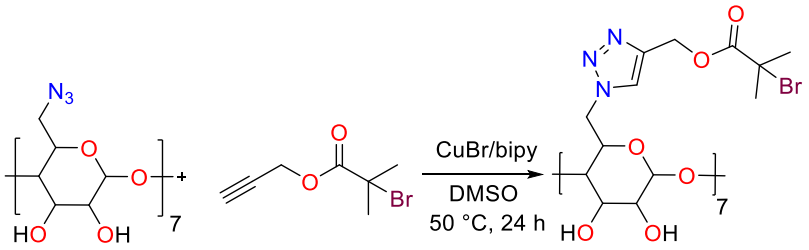

Scheme II.4.4 Schematic representation of the synthetic approach to per-6-deoxy-6-((1,2,3-triazol-4-yl)methyl 2-bromoisobutyrate)-*β*-cyclodextrin.

A solution of *β*-CD-$(N_3)_7$ (500 mg, 0.381 mmol, propargyl 2-bromoisobutyrate (626 mg, 3.00 mmol), bipy (953 mg, 6.00 mmol) in DMSO (5 ml) was deoxygenated by three freeze-pump-thaw cycles. The solution was then transferred *via* cannula under nitrogen into a Schlenk tube, previously evacuated and filled with nitrogen, containing CuBr (438 mg, 3.00 mmol). The resulting solution was stirred at 50 °C for 24 h. When the reaction was completed, the reaction mixture was purged with air for 1 h. The solution was precipitated in 40 mL of methyl *tert*-butyl ether (MTBE) and centrifuged at 8000 rpm for 5 min. The solvent was decanted and fresh MTBE was added, mixed and centrifuged again. This procedure was repeated 4 times in order to remove DMSO, excess propargyl initiator and Cu/bipy) residues. The final product could be recovered as beige powder

(355 mg, yield: 65%). As can be seen in the MALDI-TOF spectrum many side reactions occurred.

II.4.3.5 Synthesis of *per*-6-thio-*β*-cyclodextrin (*β*-CD-(SH)$_7$)

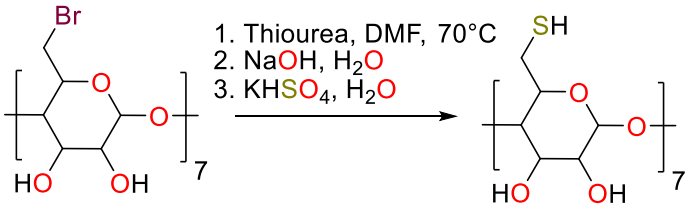

Scheme II.4.5 Schematic representation of the synthetic approach to *β*-CD-(SH)$_7$

***β*-CD-(Br)$_7$** (5.00 g, 3.17 mmol) and thiourea (2.50 g, 33.3 mmol) were dissolved in DMF (50 mL) and the mixture was heated to 70 °C under argon atmosphere. After 24 h, DMF was removed under reduced pressure and the obtained brown oil was dissolved in water (200 mL). Sodium hydroxide (2.22 g, 55.5 mmol) was then added and the reaction mixture was heated to a gentle reflux under nitrogen atmosphere. After 1 h, the resulting suspension was acidified with aqueous KH_SO_4 forming a white precipitate which was then filtered and washed thoroughly with water and dried under vacuum. Compound *β*-CD-SH$_7$ was recovered as white powder (yield: 3.20 g, 81%).

^{1}H NMR (400 MHz, DMSO-*d*$_6$, 298 K, ppm): *δ* =5.91 (*d*, 7 H, 6.8 Hz), 5.81 (*d*, 7 H, 2 Hz), 4.93(*d*, 7 H, 3.3 Hz), 3.68 (*t*, 7 H, 8.5 Hz), 3.61 (*t*, 7 H, 9.2 Hz), 3.29-3.40 (*m*, 14 H, overlap with H_2O), 3.19 (*m*, 7H), 2.75 (*m*, 7 H), 2.13 (*t*, 7 H, 8.3 Hz)

II.4.3.6 Synthesis of 2-(2-Bromoisobutyryloxy) ethyl acrylate

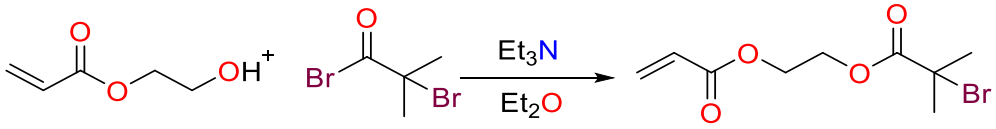

Scheme II.4.6 Schematic representation of the synthetic approach to 2-(2-Bromoisobutyryloxy) ethyl acrylate

Hydroxyethyl acrylate (10.0 mL, 10.1 g, 871 mmol) and triethylamine (17.0 mL, 12.3 g, 122 mmol) were dissolved in dichloromethane (DCM) (150 mL) and cooled down to 0 °C in an ice-water bath. A solution of *α*-bromoisobutyryl bromide (BIBB) (12.9 mL, 24.0 g, 104 mmol) in 20 mL DCM was added dropwise over a period of 20 min. The mixture was allowed to stir for 1 h at 0 °C after which it was allowed to reach room temperature and stirring was continued overnight. The solution was washed 3 x 50 mL 10% HCl solution, 3 x 50 mL saturated $NaHCO_3$ solution, 3 x 50 mL water and subsequently dried over $MgSO_4$. After evaporating the solvent *via* rotary evaporation, the product was purified by column chromatography on silica gel using petroleum ether: ethyl acetate (5:1) affording a colourless oil. (yield: 81% , 18.7 g).

^{1}H NMR (400 MHz, $CDCl_3$, 298 K, ppm): δ = 6.43 (*dd*, 1 H, 1.4 Hz, 17.4 Hz), 6.13 (*dd*, 1 H, 10.5 Hz, 17.4 Hz), 5.86 (*dd*, 1 H, 1.4Hz, 10.5 Hz), 4.41 (*s*, 4 H), 1.92 (*s*, 6 H)

II.4.3.7 Synthesis of *per*-6-deoxy-6-(thio-propanoyl-oxy-ethyl 2-bromoisobutyrate)-*β*-cyclodextrin (CD_7-Michael)

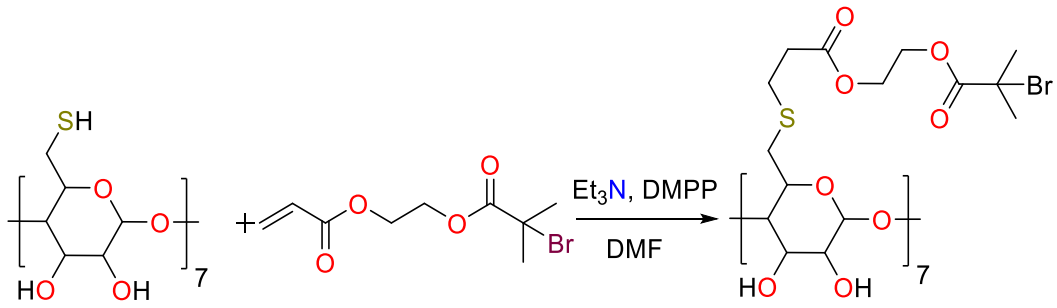

Scheme II.4.7 Schematic representation of the synthetic approach to *per*-6-deoxy-6-(thio-propanoyl-oxy-ethyl 2-bromo-2-methylpropanoate)-*β*-cyclodextrin

Per-6-thio-*β*-cyclodextrin (500 mg, 0.401 mmol), 2-(2-Bromoisobutyryloxy) ethyl acrylate (1.49 g, 5.62 mmol), dimethylphenylphosphine (20 µL, 19.3 mg, 0.140 mmol), triethylamine (0.100 mL, 72.6 mg, 7.18 mmol) were dissolved in 15 mL of dimethylformamide (DMF). A drop of water was added to the reaction mixture and the mixture was allowed to stir at room temperature for 5 h. The solution was precipitated in 100 mL of methyl *tert*-butyl ether (MTBE) and centrifuged at 8000 rpm for 5 min. The solvent was decanted and fresh MTBE was added, mixed and centrifuged again. This procedure was repeated 4 times in order to remove DMF and excess 2-(2-bromoisobutyryloxy) ethyl acrylate. Subsequently the product was dried under vacuum

yielding a fine beige (769 mg, yield: 62%). As can be seen in the MALDI-TOF spectrum many side reactions occurred.

II.4.3.8 Synthesis of allyl 2-bromoisobutyrate

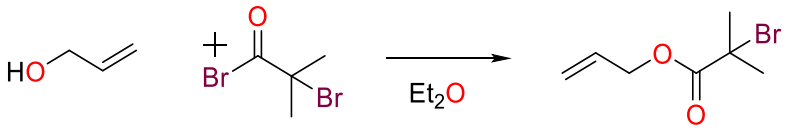

Scheme II.4.8 Schematic representation of the synthetic approach to allyl 2-bromoisobutyrate

Allyl alcohol (16.2 mL, 16.4 g, 282 mmol) and triethylamine (47.2 mL, 34.2 g, 339 mmol) were dissolved in diethyl ether (150 mL) and cooled down to 0 °C in an ice-water bath. A solution of *α*-bromoisobutyryl bromide (BIBB) (29.0 mL, 54.0 g, 234 mmol) in 20 mL diethyl ether was added dropwise over a period of 20 min. The mixture was allowed to stir for 1 h at 0 °C after which it was allowed to reach room temperature and stirring was continued overnight. The solution was washed 3 x 50 mL 10% HCl solution, 3 x 50 mL 5% NaOH solution, 3 x 50 mL water and subsequently dried over $MgSO_4$. After evaporating the solvent *via* rotary evaporation, the product was purified by column chromatography using chloroform as the eluent affording a colourless oil. (yield: 76% , 23 g).

^{1}H NMR (400 MHz, $CDCl_3$, 298 K, ppm): δ = 5.9 (*ddt*, 1 H, 5.5 Hz, 10.6 Hz, 17.2 Hz), 5.35 (*dq*, 1 H, 1.5 Hz, 17.2 Hz), 5.24 (*dq*, 1 H, 1.3 Hz, 10.6 Hz), 4.63 (*dt*, 2 H, 1.4 Hz, 5.6 Hz), 1.91 (*s*, 6 H)

II.4.3.9 Synthesis of *per*-6-deoxy-6-(thiopropyl-2-bromo-2-methylpropanoate)-*β*-cyclodextrin (CD_7-Radical = I7)

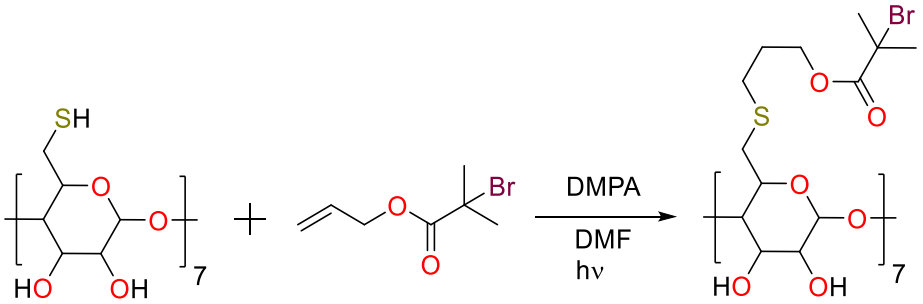

Scheme II.4.9 Schematic representation of the synthetic approach to *per*-6-deoxy-6-(thiopropyl-2-bromo-2-methylpropanoate)-*β*-cyclodextrin (*CD_7-Radical = I7*)

Per-6-thio-*β*-cyclodextrin (2.50 g, 2.01 mmol), and dithiotreitol (DTT, 618 mg, 4 mmol) were dissolved in 40 mL anhydrous DMF under Ar and heated to 60 °C. After 60 h de reaction mixture was allowed to cool down to room temperature and allyl 2-bromoisobutyrate (14.5 g, 70.2 mmol), 2,2-dimethoxy-2-phenylacetophenone (DMPA, 179 mg, 7.02 mmol) were added to the reaction mixture and stirring was continued for 5 h under UV irradiation (365 nm). The solution was precipitated in 500 mL of methyl *tert*-butyl ether (MTBE) in ten 50 mL centrifuge tubes and centrifuged at 8000 rpm for 5 min. The solvent was decanted and all precipitated fractions collected in two 50 mL centrifuge tubes and fresh MTBE was added, mixed and centrifuged again. This procedure was repeated 4 times in order to remove DMF and allyl 2-bromoisobutyrate. Subsequently the product was dried under vacuum, yielding a fine beige solid. (3.7 g, yield: 68%).

^{1}H NMR (400 MHz, DMSO-d_6, 298 K, ppm): δ = 5.90 (*d*, 7 H, 5.6 Hz), 5.8 (*m*, 7 H), 4.85 (m, 7 H), 4.22 (*t*, 14 H, 5.2 Hz), 3.85 (*m*, 7 H), 3.57 (*m*, 7 H), 3.33 (*m*, 14 H), 3.09 (*d*, 7 H, 10.6 Hz), 2.82 (*m*, 7 H), 2.69 (*m*, 14 H), 1.90 (*s*, 56 H)

MALDI-TOF MS m/z: calculated for $C_{91}H_{147}Br_7O_{42}S_7K^+$:2733.12; found: 2733.36

II.4.3.10 General procedure for SET-LRP

A Schlenk tube was charged with same ratio of first block monomer (420 eq), pre-activated Cu(0) wire (5 cm), $CuBr_2$ (0.33 mg, 0.28 eq) and Me_6TREN (4.53 mg, 1.33 eq) in DMSO (1 ml) and then the mixture was degassed by gentle bubbling of argon gas

for 30 min. Pre-degassed CD-initiator in 1 ml (40 mg, 1 eq) was then added *via* gas tight syringe sequentially. The Schlenk tube was sealed and the reaction mixture was allowed to polymerise at 25°C. Sampling was carried out using a degassed syringe to check the conversion of MA. After it reached to full conversion, the second block solution (70 eq in 0.5 mL DMSO) was then degassed with argon for 20 min and subsequently transferred *via* cannula to the Schlenk tube under argon protection to polymerise. A sample was taken for ^{1}H NMR and GPC analysis to check full monomer conversion again. When the ^{1}H NMR result confirmed nearly full conversion, the last block (70 eq in 0.5 mL DMSO) was added into the polymerisation solution. Catalyst residues were removed by filtering through a column of neutral alumina prior to THF GPC analysis.

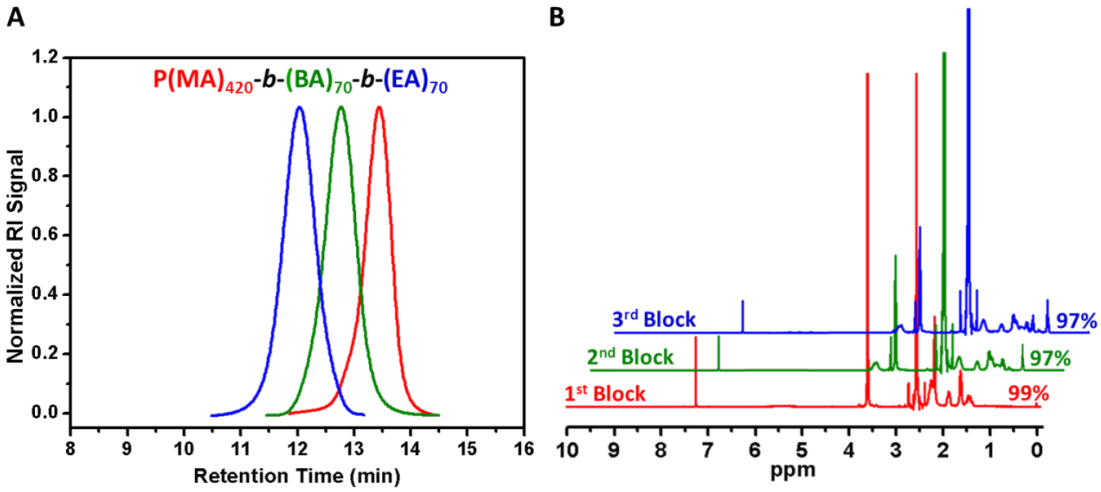

Figure II.4.1 GPC traces of M42B7E7 (A); and ^{1}H NMR spectra displaying full conversion for each block (B).

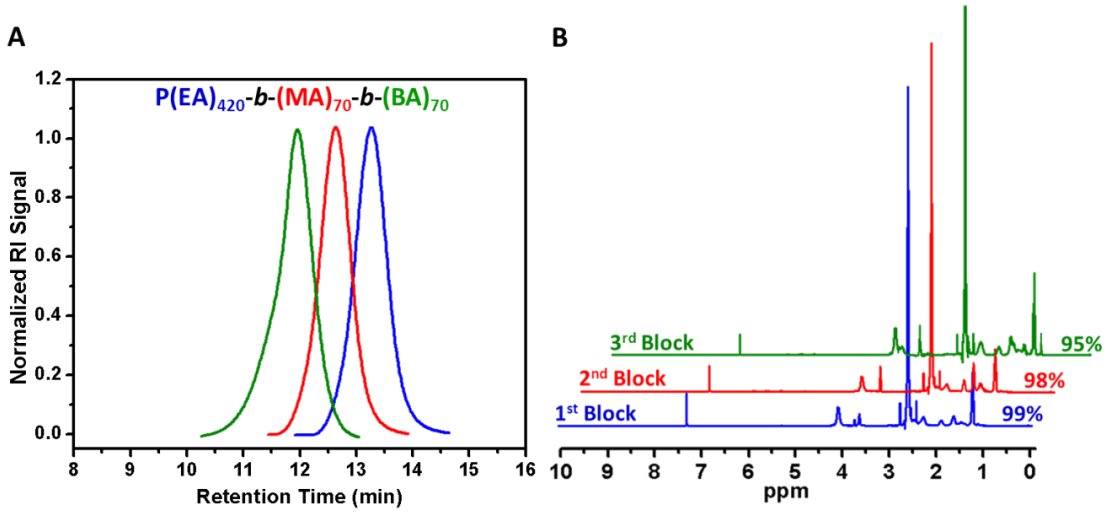

Figure II.4.2 GPC traces of E42M7B7 (A); and ^{1}H NMR spectra displaying full conversion for each block (B).

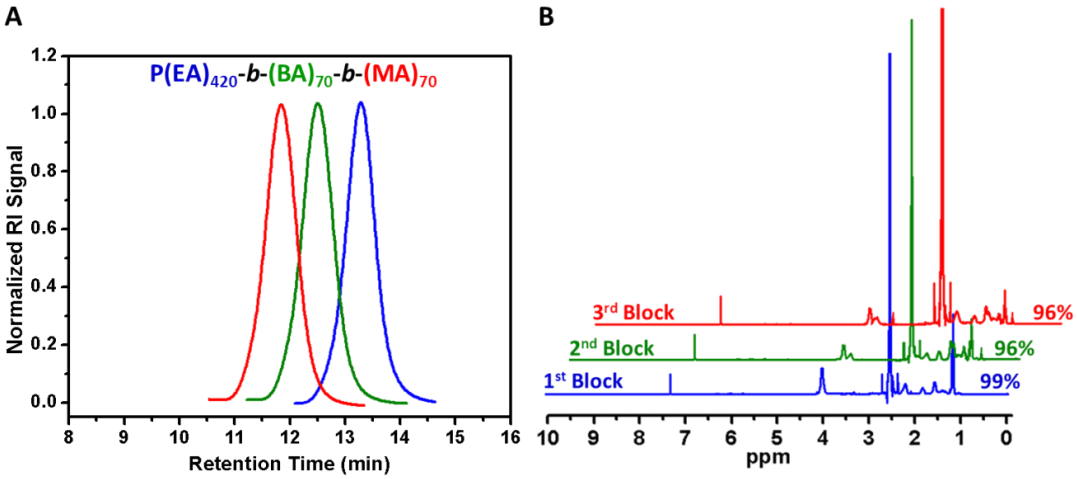

Figure II.4.3 GPC traces of E42B7M7 (A); and ^{1}H NMR spectra displaying full conversion for each block (B).

II.5 References

(1) Lutz, J.-F.; Lehn, J.-M.; Meijer, E. W.; Matyjaszewski, K.; Takeuchi, M. *Nat. Rev. Mater.* **2016**, *1* (5), 16024.

(2) Badi, N.; Lutz, J. F. *Chem. Soc. Rev.* **2009**, *38* (12), 3383.

(3) Lutz, J. F.; Ouchi, M.; Liu, D. R.; Sawamoto, M. *Science (80-.).* **2013**, *341* (6146), 628.

(4) Hadjichristidis, N.; Iatrou, H.; Pitsikalis, M.; Mays, J. *Prog. Polym. Sci.* **2006**, *31* (12), 1068.

(5) Matyjaszewski, K.; Tsarevsky, N. V. *Nat. Chem.* **2009**, *1* (4), 276.

(6) Anastasaki, A.; Nikolaou, V.; Nurumbetov, G.; Wilson, P.; Kempe, K.; Quinn, J. F.; Davis, T. P.; Whittaker, M. R.; Haddleton, D. M. *Chem. Rev.* **2016**, *116* (3), 835.

(7) Gao, H.; Ohno, S.; Matyjaszewski, K. *J. Am. Chem. Soc.* **2006**, *128* (47), 15111.

(8) Ohno, K.; Wong, B.; Haddleton, D. M. *J. Polym. Sci. Part A Polym. Chem.* **2001**, *39* (13), 2206.

(9) Zhang, Q.; Su, L.; Collins, J.; Chen, G.; Wallis, R.; Mitchell, D. A.; Haddleton, D. M.; Becer, C. R. *J. Am. Chem. Soc.* **2014**, *136* (11), 4325.

(10) Zhang, Z. X.; Liu, X.; Xu, F. J.; Loh, X. J.; Kang, E. T.; Neon, K. G.; Li, J. *Macromolecules* **2008**, *41* (16), 5967.

(11) Zhang, Z.-X.; Liu, K. L.; Li, J. *Macromolecules* **2011**, *44* (5), 1182.

(12) Song, X.; Wen, Y.; Zhu, J. ling; Zhao, F.; Zhang, Z. X.; Li, J. *Biomacromolecules* **2016**, *17* (12), 3957.

(13) Stenzel, M. H.; Davis, T. P. *J. Polym. Sci. Part A Polym. Chem.* **2002**, *40* (24), 4498.

(14) Zhang, L.; Stenzel, M. H. *Aust. J. Chem.* **2009**, *62* (8), 813.

(15) Gody, G.; Maschmeyer, T.; Zetterlund, P. B.; Perrier, S. *Macromolecules* **2014**, *47* (10), 3451.

(16) Gody, G.; Barbey, R.; Danial, M.; Perrier, S. *Polym. Chem.* **2015**, *6* (9), 1502.

(17) Zetterlund, P. B.; Gody, G.; Perrier, S. *Macromol. Theory Simulations* **2014**, *23* (5), 331.

(18) Barner-Kowollik, C.; Davis, T. P.; Stenzel, M. H. *Aust . J . Chem* **2006**, *59*, 719.

(19) Zhang, Q.; Collins, J.; Anastasaki, A.; Wallis, R.; Mitchell, D. A.; Becer, C. R.; Haddleton, D. M. *Angew. Chemie - Int. Ed.* **2013**, *52* (16), 4435.

(20) Zhang, Q.; Wilson, P.; Li, Z.; McHale, R.; Godfrey, J.; Anastasaki, A.; Waldron, C.; Haddleton, D. M. *J. Am. Chem. Soc.* **2013**, *135* (19), 7355.

(21) Zhang, Q.; Anastasaki, A.; Li, G.-Z.; Haddleton, A. J.; Wilson, P.; Haddleton, D.

M. *Polym. Chem.* **2014**, *5* (12), 3876.

(22) Aksakal, R.; Resmini, M.; Becer, C. R. *Polym. Chem.* **2016**, *7* (43), 6564.

(23) Aksakal, R.; Resmini, M.; Becer, C. R. *Polym. Chem.* **2016**, *7* (1), 171.

(24) Kolb, H. C.; Finn, M. G.; Sharpless, K. B. *Angew. Chem. Int. Ed.* **2001**, *40* (11), 2004.

(25) Barner-Kowollik, C.; Du Prez, F. E.; Espeel, P.; Hawker, C. J.; Junkers, T.; Schlaad, H.; Van Camp, W. *Angew. Chemie Int. Ed.* **2011**, *50* (1), 60.

(26) Rostovtsev, V. V.; Green, L. G.; Fokin, V. V.; Sharpless, K. B. *Angew. Chemie Int. Ed.* **2002**, *41* (14), 2596.

(27) Nair, D. P.; Podgorski, M.; Chatani, S.; Gong, T.; Xi, W. X.; Fenoli, C. R.; Bowman, C. N. *Chem. Mater.* **2014**, *26* (1), 724.

(28) Hoyle, C. E.; Bowman, C. N. *Angew. Chemie Int. Ed.* **2010**, *49* (9), 1540.

(29) Uygun, M.; Tasdelen, M. A.; Yagci, Y. *Macromol. Chem. Phys.* **2010**, *211* (1), 103.

(30) Percec, V.; Guliashvili, T.; Ladislaw, J. S.; Wistrand, A.; Stjerndahl, A.; Sienkowska, M. J.; Monteiro, M. J.; Sahoo, S. *J. Am. Chem. Soc.* **2006**, *128* (43), 14156.

Chapter 3

Influence of molecular architecture on glycopolymer lectin binding

This chapter describes the synthesis and characterisation of radical initiators for SET-LRP and their use for the synthesis of mannose containing star glycopolymers with varying arm number and length. 2 sets of star glycopolymers were successfully synthesised and characterised via ^{1}H-NMR and GPC. The first set encompasses 5 star glycopolymers with a different amount of arms per molecule but with equal arm length. For the second set of 5, the amount of sugars per molecule was kept constant. The obtained star glycopolymers were subsequently evaluated for their lectin-binding affinity towards a series of a mix of both newly and previously studied C-type lectins present on dendritic and Langerhans cells via Surface Plasmon Resonance (SPR). In general, it is noticeable that binding activity and avidity increases with both the number of arms and the arm length of the glycopolymers.

SPR measurements were performed by Dr. G. Yilmaz and Miss A. Monaco

Parts of this chapter have been published: Oz, Y.; Abdouni, Y.; Yilmaz, G.; Becer, C. R.; Sanyal, A. *Polym. Chem*. 2019, 10 (24), 3351.

III Influence of molecular architecture on glycopolymer lectin binding

III.1 Introduction

Over the last two decades, a plethora of synthetic glycostructures have been synthesised and evaluated as possible biomimetics for the glycocalyx.[1,2] Significance of the cellular glycocalyx is demonstrated by its role in major biological events such as protection against and recognition of pathogens, intercellular recognition and signal transduction.[3,4] Glycoproteins and glycolipids which constitute the main building blocks of the glycocalyx are of significant importance from a biological point of view, however their synthetic complexity limits their use in biological studies. Their complexity originates from an inherent highly branched nature, this branched nature however, offers a great interaction ability towards lectins (or carbohydrate-binding proteins) with high specificity.[5,6] Apart from this favourable specificity, lectin binding avidity can be notably enhanced by what is known as “the glycocluster effect”. The glycocluster effect is defined as the significant increase in binding affinity towards lectins, originating from multivalent protein-carbohydrate interactions working cooperatively.[7,8] Over the last years, polymer chemists have greatly exploited this glycocluster effect, employing precision synthesis techniques in the hopes of finding new molecular architectures with improved binding avidity.[9] Factors that influence this binding avidity include: saccharide density, backbone flexibility, glycopolymer length but also recently we’ve shown that linker flexibility has a not to be ignored effect.[10,11]

The introduction of precision synthesis in polymer chemistry, enabled the production of different nonlinear molecular architectures ranging from dendritic, brush, graft, hyperbranched, star shaped and even cyclic polymers.[12] In particular, star polymers can be achieved *via* three distinct synthetic routes. These synthetic routes encompass a core-first approach, a coupling-onto approach or lastly an arm-first

approach. Synthetically speaking, the coupling-onto method would require a high coupling efficiency. The arm-first approach on the other hand, generally gives a broad distribution of arms per molecule and for this reason, a core-first approach is often preferred as it offers an augmented control over the number of arms.[13,14] Stenzel and coworkers, employed a core-first approach for the synthesis of 4-arm star glycopolymers. In their work it was confirmed that not only glycopolymer length and thus molecular weight, but also backbone rigidity has an important influence on binding affinity towards lectins.[15,16] Mitchel *et al.* furthermore showed the possible use of star glycopolymers in immune response modulation by influencing cytokine expression.[17]

As mentioned *vide supra*, lectins are proteins capable of binding carbohydrates with great specificity. Here newly synthesised glycopolymeric structures were tested towards one class of lectins, namely C-type lectins. C-type lectin receptors constitute a large family of both transmembrane and secreted proteins that contain one or more carbohydrate recognition domains known as C-type lectin-like domains (CTLD) which are calcium dependent in nature.[18] A subdivision of these lectins has been classified as pattern recognition receptors as they induce immune response regulation by specific pathogen- or damage-associated molecule activation. CLRs that function in this way, employed in this study, comprise the dendritic cell-specific intracellular adhesion molecules (ICAM)-3 grabbing non-integrin (DC-SIGN or CD209), the liver/lymph node-specific ICAM-3 grabbing non-integrin (L-SIGN, DC-SIGNR or CD209L), the C-type lectin-like receptor -1 (CLEC-1) and the dendritic cell-associated C-type lectin-2 (Dectin-2).[19–21] Other C-type lectins are involved in the detection and clearance of dead and dying cells, both crucial processes for the maintenance of organ and tissue homeostasis. These include soluble (secreted) C-type lectins such as the mannose-binding lectin (MBL) but also surfactant protein-D (SP-D), both members of the collectin family which facilitates dead cell clearance by recognition of mannose structures among other motifs.[22] Furthermore membrane-bound CLRs such as the dendritic and epithelial cell receptor (DEC205) and the dendritic cell natural killer (NK) lectin group receptor 1 (DNGR1) are among those able to detect cell-death.[23–25] Lastly the Langerhans cell-specific C-type lectin (Langerin or CD207) plays an important protective role, prompting uptake and degradation of viral particles such as the recognition of the HIV glycoproteins.[26,27]

This chapter describes the synthesis and characterisation of two series of novel star glycopolymers starting from star initiators recently developed in the own group. Subsequently these mannose containing star glycopolymers have been tested towards

their ability to effectively bind the above mentioned newly and previously studied C-type lectins, found on dendritic and Langerhans cells.

III.2 Results and discussion

III.2.1 Synthesis of a mannose glycomonomer

The first step in making glycopolymers is the synthesis of a suitable glycomonomer. Here we synthesised a mannose glycomonomer as previously published.[28] The mannose glycomonomer that we synthesised here is an acrylate that has shown to polymerise really well using SET-LRP in the past.[28,29] To achieve this, *D*-mannose was treated with propargyl alcohol in the presence of silica supported sulphuric acid. Subsequently 3-azidopropyl acrylate was prepared by reacting sodium azide with 3-bromopropanol and the resulting 3-azidopropanol was then reacted with acryloyl chloride. Finally mannose acrylate was achieved by 'clicking' the propargyl-*D*-mannose to 3-azidopropyl acrylate using the well-known copper(I)-catalysed azide-alkyne cycloaddition (CuAAC) "click" reaction.

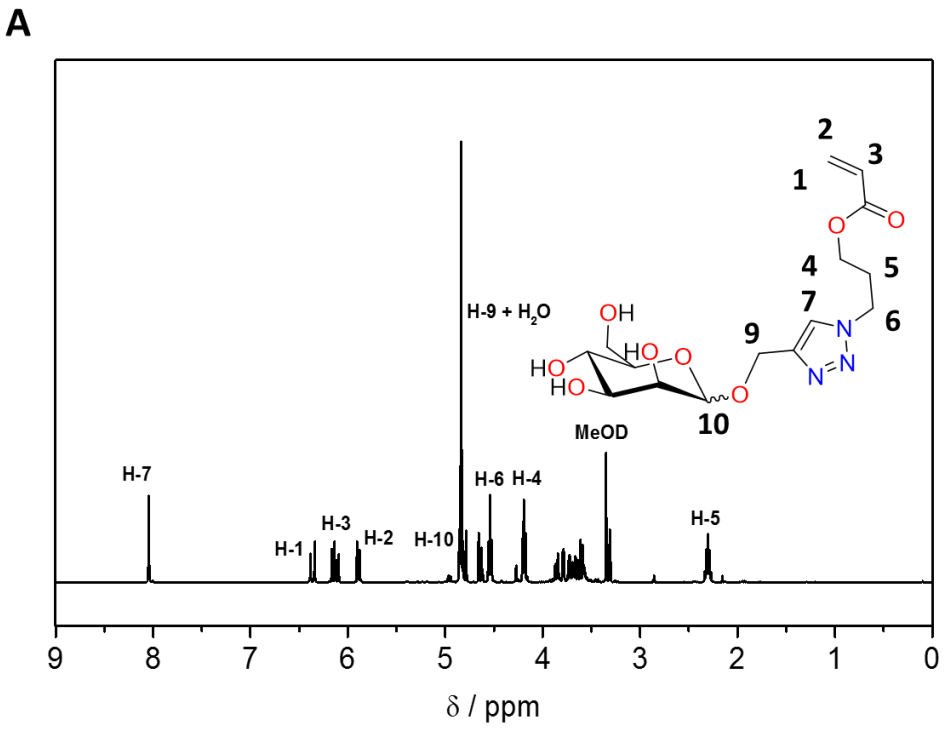

Figure III.2.1 A) ^{1}H-NMR spectrum of *D*-mannose acrylate in MeOD.

III.2.2 Synthesis of initiators

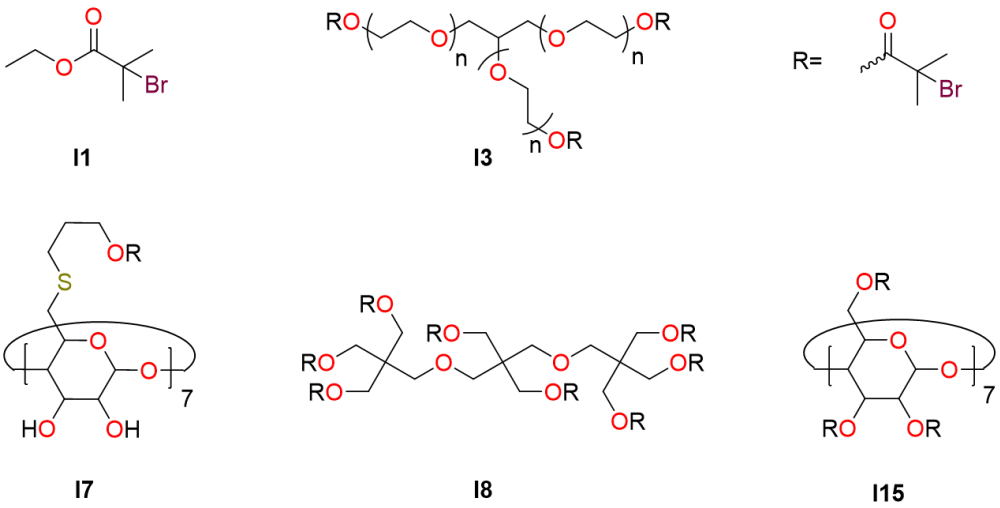

Figure III.2.2 Chemical structures of the various SET-LRP initiators synthesised and used in this chapter.

For the synthesis of the anticipated star glycopolymers, appropriate SET-LRP star initiators had to be synthesised. Initiator I1, which is the popularly used ethyl *α*-bromoisobutyrate, was bought from Sigma-Aldrich and is the only non-newly synthesised initiator. Secondly initiator I3, which is a water-soluble three arm initiator based on commercially available glycerol ethoxylate (M_n ~ 1000 g/mol) and which has three initiating sites, was prepared by Dr. Resat Aksakal and used as received (after removing inhibitor on basic alumina).[30] Initiator I7 was prepared as described in Chapter 2 and is the first initiator in this Chapter which is based on *β*-cyclodextrin containing 7 initiating sites.

Initiator I8, is based on tripentaerythritol, a commercially available molecule containing 8 primary hydroxyls. Solubility of tripentaerythritol proved to be cumbersome in dry DMF and NMP. For this reason a mixture of dichloromethane (DCM) and pyridine was used, which resulted in a fine suspension of the product. The hydroxyl groups were consequently converted into SET-LRP initiators by addition of *α*-bromoisobutyryl bromide (BIBB).

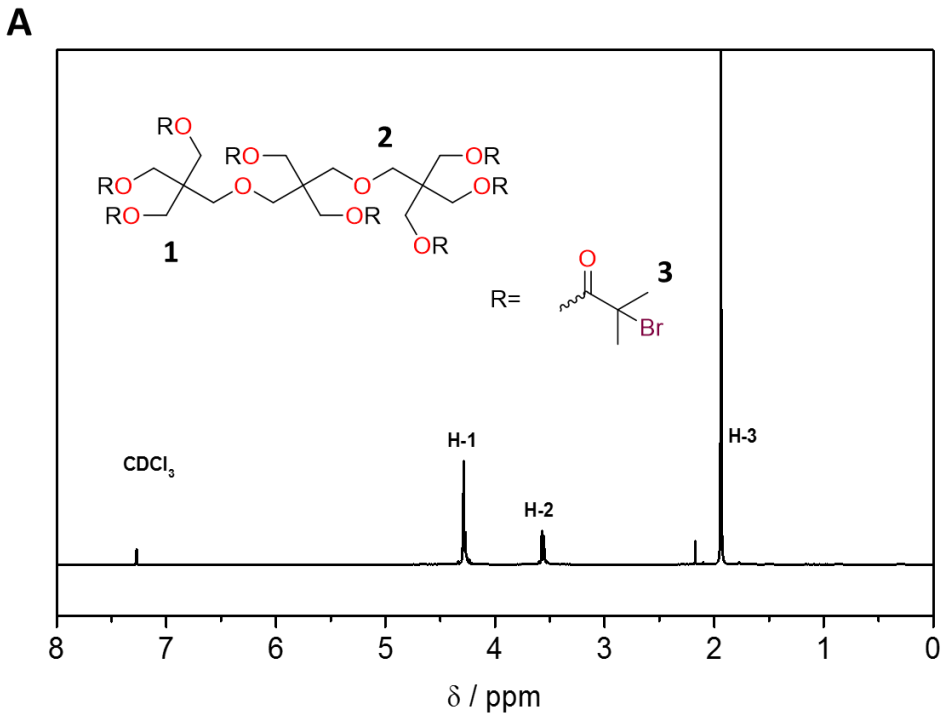

Figure III.2.3 A) ^{1}H-NMR spectrum of initiator I8, the tripentaerythritol initiator

Lastly, initiator I15, the second *β*-cyclodextrin based initiator, was prepared according to literature as well.[29] Here, *β*-cyclodextrin was dissolved in *N*-methyl-2-pyrrolidone (NMP) and reacted with BIBB forming a mixture of products with different degrees of substitution. The primary hydroxyls were all converted, however conversion of the secondary hydroxyls at the secondary rim region of the *β*-cyclodextrin gave rise to sterical problems, limiting reactivity of adjacent secondary hydroxyls. MALDI-TOF analysis shed light on the amount of actual esterifications showing an average of 15 initiating sites per initiator I15 molecule.

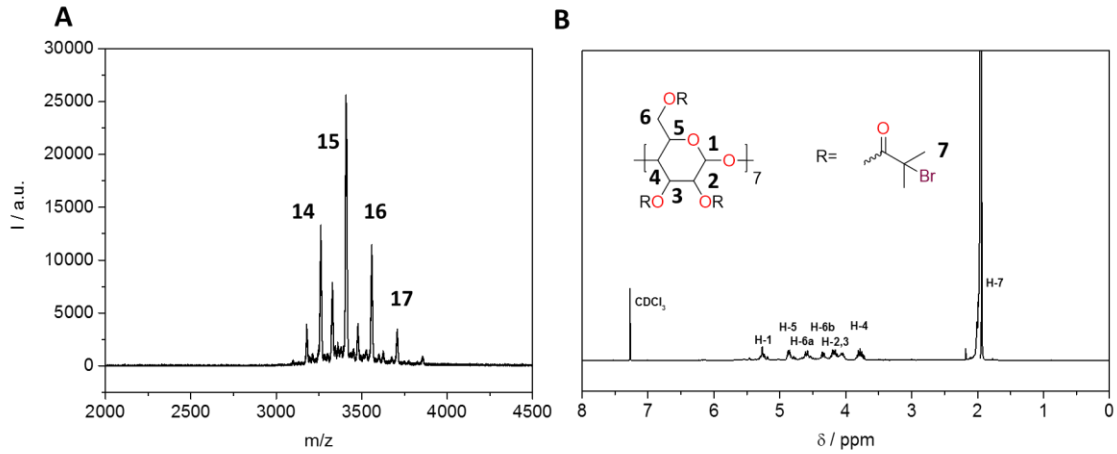

Figure III.2.4 A) MALDI-TOF mass spectrum of initiator I15 depicting the different degrees of substitution. The minor peaks in between the major peaks are due to bromine loss. B) ^{1}H-NMR spectrum of initiator I15.

III.2.3 Synthesis of glycopolymers

Two sets of star glycopolymers were subsequently prepared using SET-LRP in DMSO. The first set of glycopolymers (set S1) was generated with a different amount of arms per molecule but with equal arm length to obtain a similar size of star glycopolymers. The second set of glycopolymers (set S2) on the other hand also has a different amount of arms per molecule but an equal glycovalency per molecule. During the polymerisation, monomer concentration was deliberately kept low too avoid star-star coupling between polymers, as bimolecular radical termination is a very common side reaction. Additionally, detailed kinetic investigations were not the focus of this work but were performed to determine the reaction time needed to reach 50% conversion for set S2.

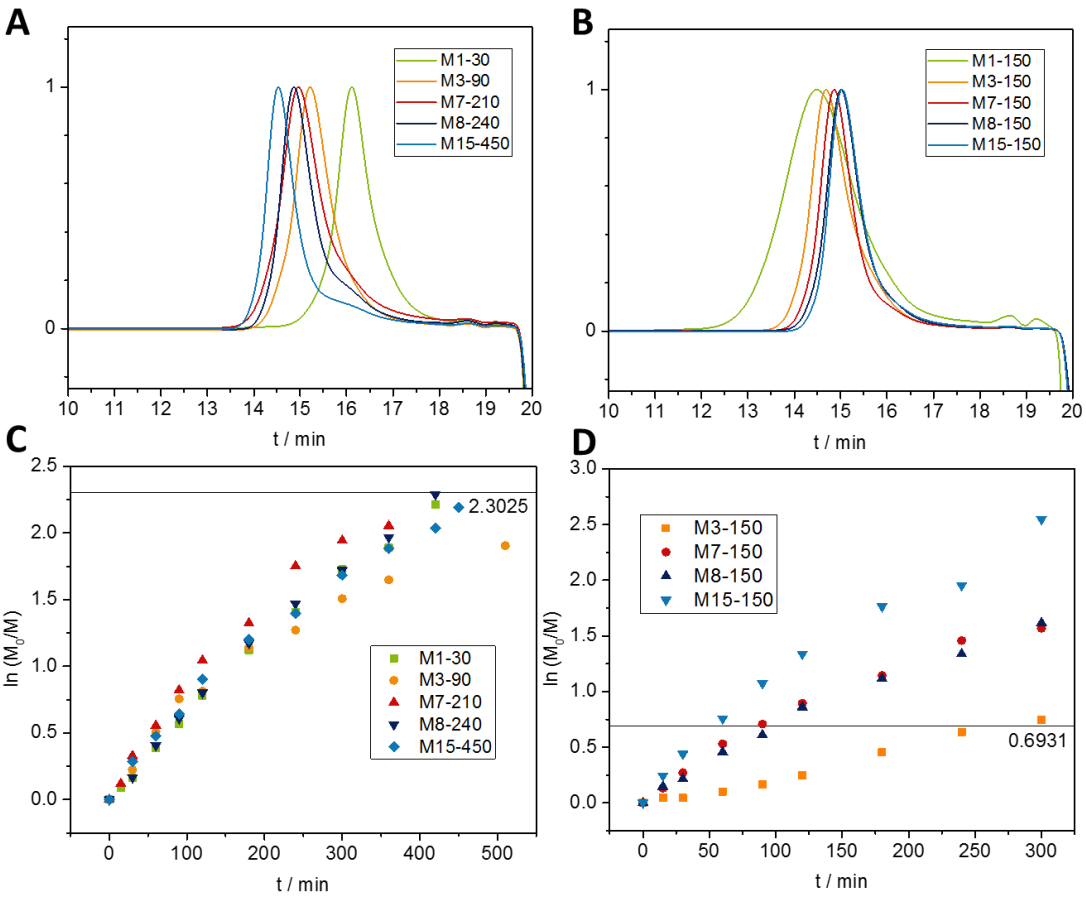

Figure III.2.5 A) GPC chromatograms of set S1. B) GPC chromatograms of set S2. C) Kinetic plots of set S1. D) Kinetic plots of set S2.

Set S1 was polymerised using initiators I1-I15 corresponding to 1;3;7;8 and 15 arm star glycopolymers respectively, details on the polymerisation procedures can be found in experimental section III.4. All polymerisations were stopped at max 90% conversion except polymer M7-210 which seemed to be more prone to termination reactions as can be deduced from the kinetic plots (**Figure III.2.5 C**). For this reason the polymerisation of M7-210 was stopped after 8h at approximately 85.6 % conversion. Overall all glycomonomer conversions were found to be within 85 % and 90% as determined by ^{1}H-NMR. GPC chromatograms in DMF show an absence of star-star coupling however tailing can be observed for the polymers with a high amount of arms which can be attributed to a high local density of radicals around the star glycopolymer molecules (**Figure III.2.5 A**). Dispersities furthermore, were found to be rather high (1.36-1.69) which is in correspondence with the tailing observed earlier for polymers M7-210 to M15-450. As seen in **Figure III.2.5 A**, the GPC traces show a clear shift in molecular weight with increasing amount of arms per molecule. However number average molecular weights M_n compared to PMMA standards are found to be lower than

expected, as is often observed for star polymers due to the smaller hydrodynamic radius compared to a linear polymer of same molecular weight.[31]

Table III.2.1 Summary of monomer conversions, number average molar masses (M_n), peak molar masses (M_p) and dispersities (Đ) of the synthesised star glycopolymers.

Set	Code	Initiator	Star	DP	ρ^a (%)	$M_{n,NMR}{}^b$ (g.mol^{-1})	$M_{n,GPC}{}^c$ (g.mol^{-1})	$M_{p,GPC}{}^c$ (g.mol^{-1})	Đ
S1	**M1-30**	I1	Linear	30	89.3	10200	7500	10300	1.36
	M3-90	I3	Three arm	90	85.6	30200	24600	25300	1.39
	M7-210	I7	Seven arm	210	87.3	71150	18000	32800	1.69
	M8-240	I8	Eight arm	240	89.8	82100	20500	36400	1.51
	M15-450	I15	Fifteen arm	450	88.6	152400	44200	51900	1.59
S2	**M1-150**	I1	Linear	150	56.8	32050	30300	54700	2.26
	M3-150	I3	Three arm	150	54.5	32000	26300	43800	1.51
	M7-150	I7	Seven arm	150	54.3	33150	23900	36400	1.43
	M8-150	I8	Eight arm	150	54.3	32000	20400	31100	1.43
	M15-150	I15	Fifteen arm	150	50.2	31500	19450	30600	1.41

Conversion (ρ) obtained from ^{1}H NMR; [b] $M_{n,NMR} = ([M]_o/[I]_o \times \rho \times M_{mon} + M_I)$; [c] Determined by DMF GPC (relative to PMMA stn.).

Set S2 was polymerised with the same initiators I1-I15. A set of glycopolymers was polymerised using a monomer to initiating molecule ratio of 300/1, in order to determine the kinetics of the reactions for which then for each polymerisation the polymerisation time at 50 % conversion was determined *via* ^{1}H-NMR. Using the kinetic data, the same reactions were repeated using the same polymerisation conditions and then stopped at 50 % conversion. All polymerisations reached 50 % conversion within 3 h of polymerisation time except polymer M1-150 which took 29 h, as can be explained by the low concentration of propagating radicals compared to polymers M3-150 to M15-150. GPC chromatograms in DMF represent molecular weights that are quite close to each other (**Figure III.2.5 B**). Interestingly here, we can see a clear effect of hydrodynamic radius on measured molecular weight. Peak molecular weights (M_p) display a clear downward trend with increasing number of arms.[31] Dispersities of polymers M3-150 to M15-150 are lower than those of polymers M3-150 to M15-150 which can be explained by the shorter amount of polymerisation time and thus termination reactions. Polymers M1-150 and M3-150 , however, have higher dispersities than polymers M1-30 and M3-90 owing to a slower propagation rate and thus higher chance of competing side

reactions. After reaction, all polymers were dialysed against water to remove remaining glycomonomer and other impurities and measured by ^{1}H-NMR in D_2O (**Figure III.2.6**).

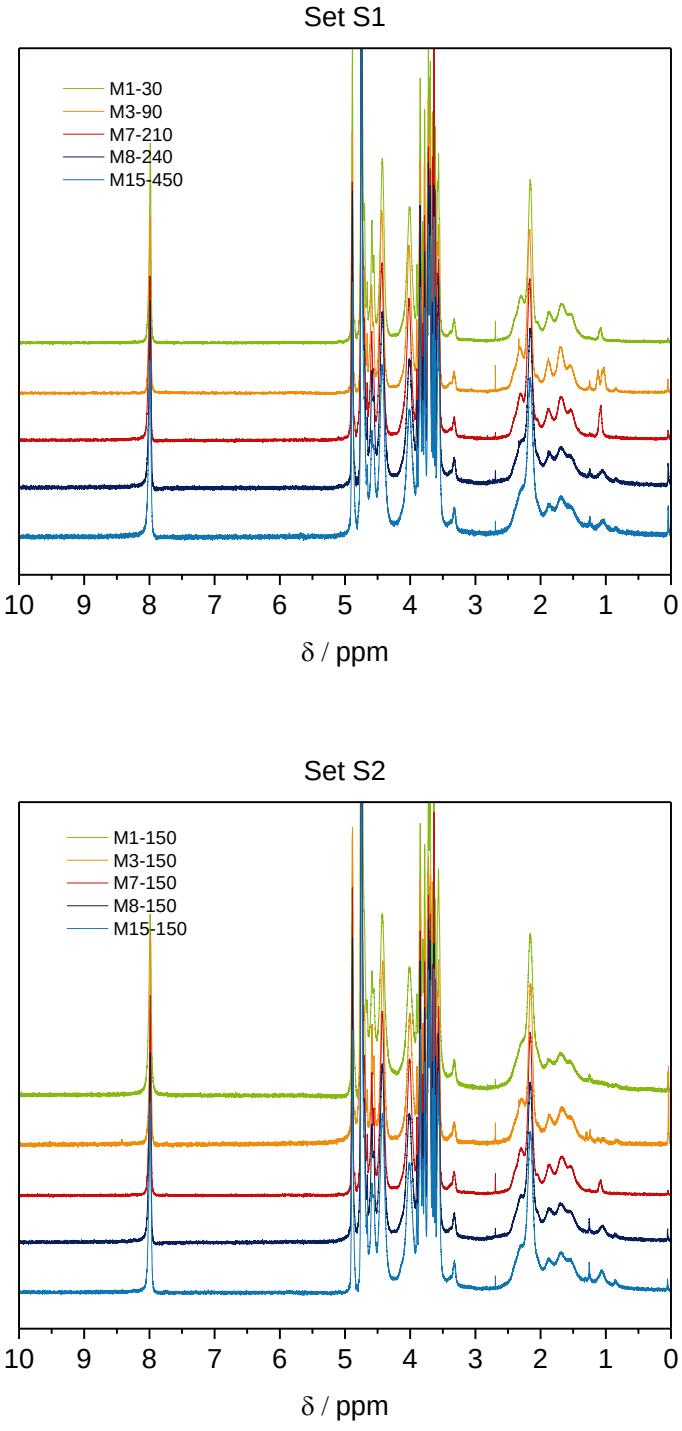

Figure III.2.6 ^{1}H-NMR in D_2O of sets S1 and S2 showing the purity of the synthesised star glycopolymers, with clear visibility of the triazole peak at 8.0 ppm and disappearance of the vinyl protons between 6.5 and 5.5 ppm.

III.2.4 Surface Plasmon Resonance

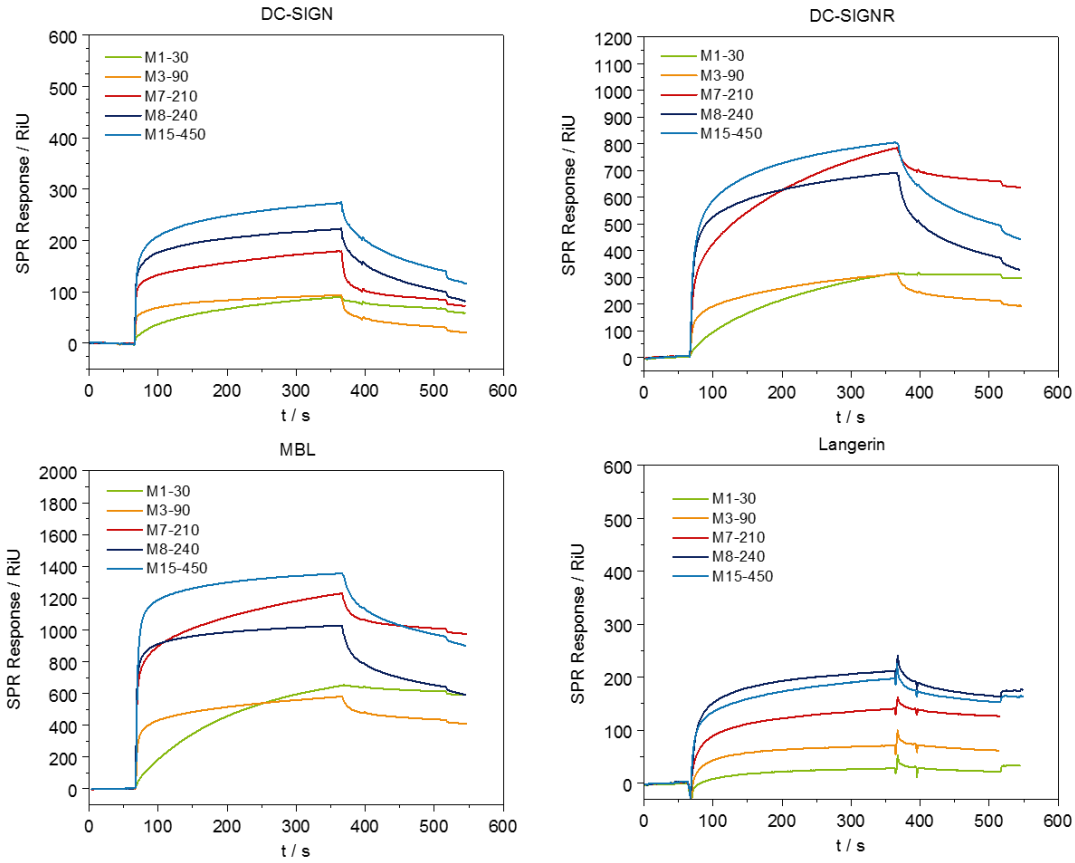

Figure III.2.7 Comparison of glycopolymer set S1 surface plasmon resonance (SPR) lectin binding results with DC-SIGN, DC-SIGNR, MBL and Langerin at a concentration of 4000 nM.

Sets S1 and S2 were tested using SPR for their ability to bind a series of 9 different lectins which can be found on dendritic and Langerhans cells, known from literature to bind mostly mannose or other carbohydrates. The SPR results for sets S1 and S2, show that no significant binding interaction could be detected for the aforementioned glycopolymers with CLEC-1, a lectin that acts as an inhibitory receptor in dendritic cells, which is able to dampen T-cell responses and for which specific carbohydrate binding affinity is not known yet.[32] Also DNGR-1, which is known to bind F-actin exposed by dying cells and which furthermore facilitates cross-presentation of antigens associated with dead cells by dendritic cells, showed no binding towards the mannose containing glycopolymers.[33] Hence, we can safely state that no binding pockets are present for mannose binding on these lectins. DEC-205, which role in antigen uptake, processing and presentation has been well characterised, showed only poor binding capability limited to polymers M8-240 and M15-450.[34] However, binding for these polymers was not strong enough to be able to determine the kinetic parameters.

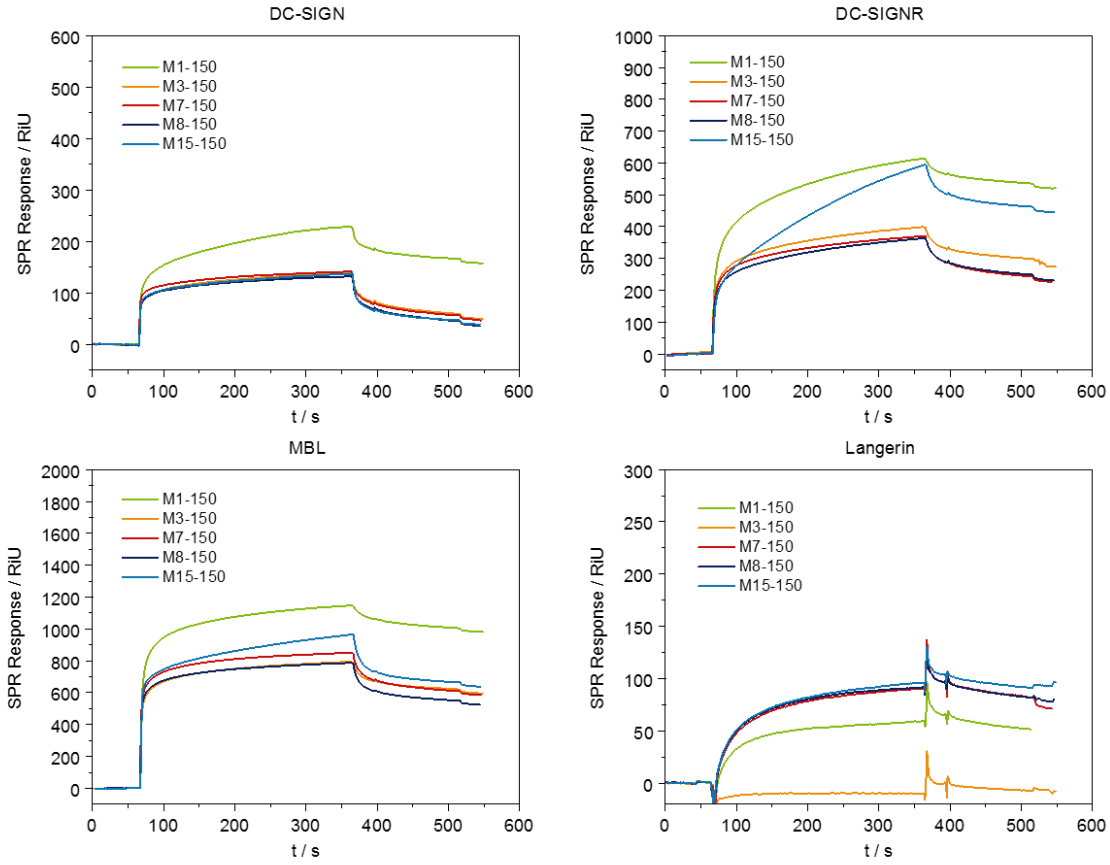

Figure III.2.8 Comparison of glycopolymer set S2 surface plasmon resonance (SPR) lectin binding results with DC-SIGN, DC-SIGNR, MBL and Langerin at a concentration of 4000 nM.

As expected, the SPR results reveal that the mannose containing glycopolymers display a relatively high and strong binding affinity with the other lectins. **Figure III.2.9A**, which shows results for set S1 comprising of polymers with a different amount of arms per molecule but of equal arm length, indicates that the association constants (K_a) increase with the number of arms per glycopolymer reaching the highest K_a values for M15-450. This tends to be true for Langerin, SP-D and Dectin-2 although M8-240 (with 8 arms) seems to have an optimal amount of arms for the lectins DC-SIGN and MBL, both known to bind mannose really well. As seen in **Table III.4.1** and **Table III.4.3** for DC-SIGN and MBL the K_a values of M8-240 is one order of magnitude higher than the K_a value of M15-450 and two orders of magnitude higher than linear M1-30. DC-SIGNR (or L-SIGN) is the only lectin in this sample collection with a preference for M7-210 however it must be noted that all K_a values for DC-SIGNR are around 10^7 M^{-1}. Dissociation rate constants k_d are in generally very low for entire set S1, indicating that the interacted mannose units on the arms tend to remain bound or that rebinding of released mannose units occurs rather than the dissociation of the complex when the buffer runs over the surface.

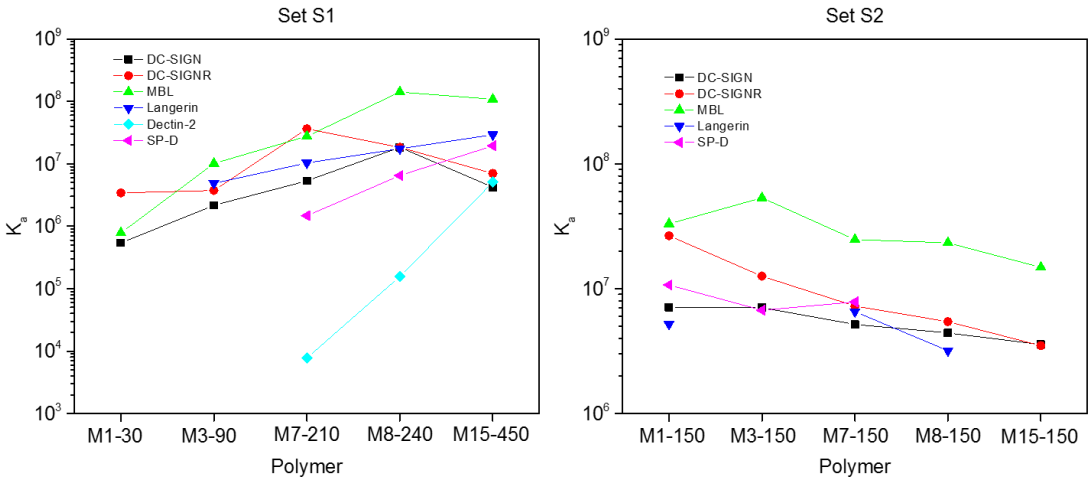

Figure III.2.9 Graphical representation of association constants (K_a) for glycopolymer set S1 and S2 with various lectins, as determined by SPR.

Star glycopolymer set S2 on the other hand, shows a nice decreasing trend in lectin binding affinity with increasing amount of arms and thus decreasing arm length (**Figure III.2.9B**). Surprisingly, even though the glycopolymers in set S2 exhibit very similar binding trends according to their R_{max} values, linear M1-150 demonstrates the highest K_a value and thus highest binding affinity for almost all lectins except MBL and Langerin. Langerin, which functions as an innate anti-viral defence mechanism and an antigen receptor that's involved in adaptive immune responses, shows a preferential binding to polymer M7-150.[35] However also here it must be noted that the difference with M1-150 is rather small. Furthermore, particularly lower dissociation rate constants (k_d) were observed for M1-150 with all lectins, which means that M1-150 binds more strongly than other glycopolymers in set S2. We can attribute this decrease in set S2 to a reduction in polymer arm length, which limits the ability of the polymers to reach different receptors.[10]

III.3 Conclusion

In summary, two sets of novel star shaped mannose containing glycopolymers were synthesised *via* SET-LRP starting from a series of star polymer initiators previously developed in the research group. Both sets of initiators and corresponding glycopolymers were fully characterised *via* ^{1}H-NMR, GPC and MALDI-TOF mass spectrometry. Lectin binding studies were performed *via* surface plasmon resonance (SPR), towards a series of newly and previously studied lectins. SPR measurements showed that molecular architecture (number and length of the star glycopolymer arms) has a significant effect on the association constants between the glycopolymer and the lectin. Overall, we can conclude that binding strength increases with both the number of arms and the arm length of the glycopolymers. In addition to the confirmation that increased glycovalency increases overall binding ability and avidity, the SPR results also revealed that different glycopolymer architectures can have different binding profiles towards different lectins.

III.4 Experimental section

III.4.1 Materials

Tris(2-(dimethylamino)ethyl)amine (Me_6TREN) was previously synthesised within the group. *D*-Mannose glycomonomer was synthesised as previously reported.[36,37] All other reagents and solvents were obtained at the highest purity available from Sigma Aldrich Chemical Company unless stated otherwise.

III.4.2 Instruments and analysis

Proton (^{1}H-NMR) nuclear magnetic resonance spectroscopy (Bruker DPX-400/600) was used to determine the chemical structure of the synthesised initiators and polymers. Samples were dissolved at 10 mg/mL concentration in $CDCl_3$, DMSO-d_6, D_2O or MeOD-d_4 as solvent. Monomer conversion was calculated by the disappearance of vinyl protons (H_2C=CH-CO–) (≈ 6.5-5.5 ppm) compared to the monomer's triazole proton (≈ 8.2-7.9 ppm).

GPC measurements were conducted on an Agilent 1260 infinity system operating in DMF with 5mM NH_4BF_4 and equipped with refractive index detector and variable wavelength detector, 2 PLgel 5 µm mixed-C columns (300×7.5mm), a PLgel 5 mm guard column (50x7.5mm) and an autosampler. The instrument was calibrated with linear narrow poly(methyl methacrylate) standards. All samples were passed through basic alumina to remove any copper residues and filtered with a 0.2 µm Nylon 66 before analysis.

Matrix assisted laser desorption/ionisation – time of flight mass spectroscopy (MALDI-TOF MS) was performed using a Bruker Daltonics Autoflex MALDI-ToF mass spectrometer, equipped with a nitrogen laser at 337 nm with positive ion ToF detection. Polymer samples were measured as follows; solutions in acetonitrile of trans-2-[3-(4-tert-Butylphenyl)-2-methyl-2-propenylidene]malononitrile (DCTB, ≥98%) as matrix (30 mg·mL^{-1}), potassium trifluoroacetate (KTFA) as cationisation agent (10 mg·mL^{-1}) and sample (10 mg·mL^{-1}) were spotted separately on the MALDI plate (0.7 µL each) and mixed on the plate. Spectra were recorded in reflectron mode and the mass spectrometer was calibrated with a peptide mixture up to 6000 Da.

Surface Plasmon Resonance (SPR) - The extent of interaction between the glycopolymers and lectins were performed on a BIAcore 3000 system (GE Healthcare). The proteins (0.025 mg/ml) were immobilised *via* a standard amino coupling protocol onto a CM5 sensor chip which was activated by flowing a 1:1 mixture of 0.1 M N-hydroxysuccinimide and 0.1 M N-ethyl-N'-(dimethylaminopropyl)carbodiimide over the chip for 6 min at 25 °C at a flow rate of 20 µL/min after the system equilibration with HEPES filtered buffer (10 mM HEPES, 150 mM NaCl, 5 mM $CaCl_2$) supplemented with 0.005% TWEEN® 20 at pH 7.4. Subsequently, channels 1 (blank), 2, 3 and 4 were blocked by following a solution of ethanolamine (1 M pH 8.5) for 10 min at 5 µL/min to remove remaining reactive groups on the channels. Sample solutions were prepared at varying concentrations (4000 nM-250 nM) in the same HEPES buffer to calculate the binding kinetics. Sensorgrams for each glycopolymer concentration were recorded with a 300 seconds injection of polymer solution (on period) followed by 150 seconds of buffer alone (off period). Regeneration of the sensor chip surfaces was performed using 10 mM HEPES pH 7.4, 150 mM NaCl, 10 mM EDTA, 0.01% P20 surfactant solution. Kinetic data was evaluated using a single set of sites (1:1 Langmuir Binding) model and also Biavalent model in the BIAevalulation 3.1 software.

III.4.3 Experimental procedures

III.4.3.1 Synthesis of 3-azido-propan-1-ol

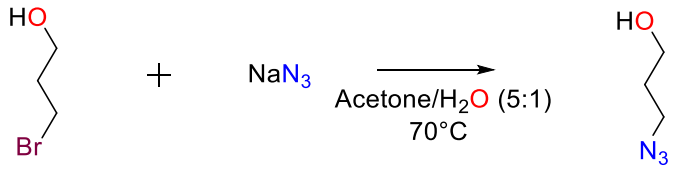

Scheme III.4.1 Schematic representation of the synthetic approach to 3-azidopropan-1-ol

3-bromopropan-1-ol (7.00 g, 50.4 mmol) was dissolved in a solution of acetone (250 mL) and water (50 mL) along with sodium azide (1.6 eq., 5.56 g, 85.6 mmol) and refluxed overnight at temperature of 70 °C. The organic solvent was removed by rotary evaporation. 50 mL water was added to the remaining water phase and was then extracted with diethyl ether (3X50 mL). The resulting ether phase was then back

extracted with water (50 mL) and dried over magnesium sulphate. The organic solvent was removed by rotary evaporation. The product was recovered as a colourless liquid and used directly (yield: 64%).

^{1}H NMR (400 MHz, D_2O, 298 K, ppm): δ =3.66 (*t*, 2 H, 6.3 Hz), 4.41 (*t*, 2 H, 6.8 Hz), 1.81 (*quin*, 2 H, 6.5 Hz).

^{13}C NMR (100 MHz, D_2O, 298 K, ppm): δ = 58.78 (O-CH_2), 47.93 (CH_2-N_3), 30.49 (C-CH_2-C).

III.4.3.2 Synthesis of 3-azidopropyl acrylate

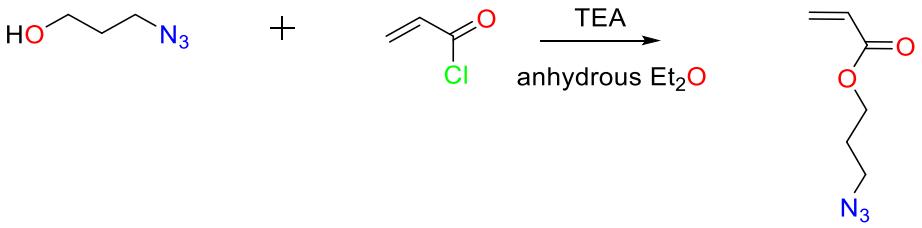

Scheme III.4.2 Schematic representation of the synthetic approach to 3-azidopropyl acrylate

A solution of 3-azido-propan-1-ol (6.10 g, 60.3 mmol), TEA (11.8 mL, 84.5 mmol), hydroquinone (30 mg) and anhydrous diethyl ether (200 mL) was cooled in an ice water bath. Acryloyl chloride (5.88 mL, 72.4 mmol) in 20 mL diethyl ether was added dropwise into the solution. The mixture was stirred in the ice bath for 1 h and then at ambient temperature overnight. The ammonium salts were removed by filtration and the residue was extracted sequentially with aqueous solution of hydrochloric acid (10 v%, 3X50 mL), water (2X50 mL), 5 wt% aqueous NaOH (3X50 mL) and water (2X50 mL) and dried over magnesium sulphate. The organic solvent was removed by rotary evaporation. The product was recovered as a yellow liquid and used directly (yield: 45%).

^{1}H NMR (400 MHz, $CDCl_3$, 298 K, ppm): δ =6.42 (*dd*, 1 H, 1.4, 17.3 Hz), 6.12 (*dd*, 1 H,10.4, 17.3 Hz), 5.85 (*dd*, 1 H, 1.4, 10.4 Hz), 4.25 (*t*, 2 H, 6.2 Hz), 3.41 (*t*, 2 H, 6.7 Hz), 1.96 (*quin*, 2 H, 6.4 Hz).

III.4.3.3 Synthesis of 1-(2′-Propargyl) D-Mannose

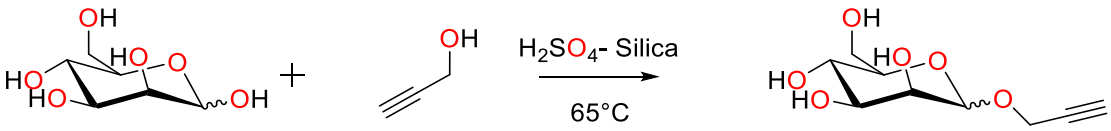

Scheme III.4.3 Schematic representation of the synthetic approach to 1-(2′-propargyl) D-Mannose

1-(2′-Propargyl) D-Mannose was prepared according to the procedure reported by Mukhopadhyay *et al*.[38] A suspension solution of *D*-Mannose (12.0 g, 66.6 mmol), propargyl alcohol (19.4 mL, 333 mmol) and H_2SO_4-silica (333 mg) was stirred at 65 °C overnight. After cooling to ambient temperature, the reaction mixture was transferred to a silica gel column and eluted with $CHCl_3$-MeOH (8:1) to remove the excess propargyl alcohol. 1-(2′-Propargyl) *D*-Mannose was obtained as a white solid after drying under vacuum (8.01 g, yield: 55 %). 1-(2′-propargyl) *D*-Mannose was found as an anomeric mixture in a ratio of 10:1 (α/β).

^{1}H NMR (400 MHz, CD_3OD, 298 K, ppm): *δ:* 4.96 (*d*, 1H, 1.6 Hz), 4.27 (*d*, 2H, 2.5 Hz), 3.84 (*dd*, 1H, 2.3, 11.8 Hz), 3.79 (*dd*, 1H, 1.8, 3.1 Hz), 3.66 (*m*, 3H), 3.51 (*m*, 1H), 2.85 (*t*, 1 H, 2.4 Hz)

III.4.3.4 Synthesis of *D*-Mannose glycomonomer

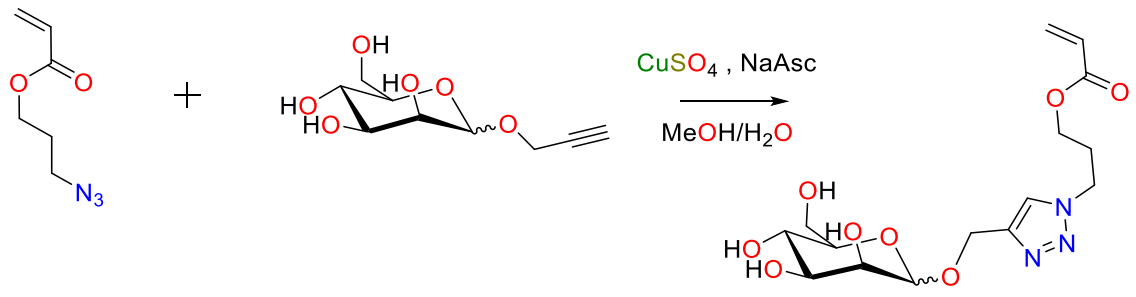

Scheme III.4.4 Schematic representation of the synthetic approach to the *D*-Mannose glycomonomer

1-(2′-propargyl) *D*-mannose (3.64 g, 16.7 mmol) and 3-azidopropyl acrylate (2.85 g, 18.3 mmol) were dissolved in MeOH/H_2O (2:1 vol/vol, 60 mL), aqueous solution of $CuSO_4 \cdot 5H_2O$ (624 mg, 2.50 mmol) and (+)-sodium L-ascorbate (625 mg, 3.15 mmol)

were added into the reaction solution. The reaction mixture was stirred at ambient temperature for 24 h and then the methanol was removed *in vacuo* and the residue mixture was freeze dried in order to remove water. The purification of the obtained product was done by silica gel column chromatography using DCM-MeOH (8:1) as eluent. After removal of the solvent, the product was obtained as a white sticky solid (1.62 g, yield: 58.2%).

^{1}H NMR (D_2O, 298 K, 400 MHz): δ =8.07, 8.06 (s, overlapped, 1 H, NC*H*=C), 6.37 (dd, J=1.8, 15.5 Hz), 6.36 (dd, J=1.6, 15.7 Hz) (anomeric 1 H, CH_2=C), 6.14 (dd, J=10.4, 6.9 Hz), 6.13(dd, J=10.4, 7.0 Hz) (anomeric, 1 H, CH_2=C*H*C=O), 5.89 (dd, 1 H, J=1.5, 8.9 Hz, CH_2=C), 4.70-5.05 (m, CH_2-OH, H-1 of mannose , overlap with H_2O), 4.64 (d, 1 H, J=12.3 Hz, CH_2-OH), 4.55 (t, 2 H, J=6.9 Hz, CH_2-N), 4.19 (t, 2 H, J=6.0 Hz, C=O-O-CH_2), 3.40-3.92 (m, H residues of mannose), 2.30 (m, 2H, CH_2-CH_2-CH_2) ppm.

III.4.3.5 Synthesis of Initiator I3 (tri-O-(2-bromo-2-methyl propionyl)-glycerol ethoxylate)[30]

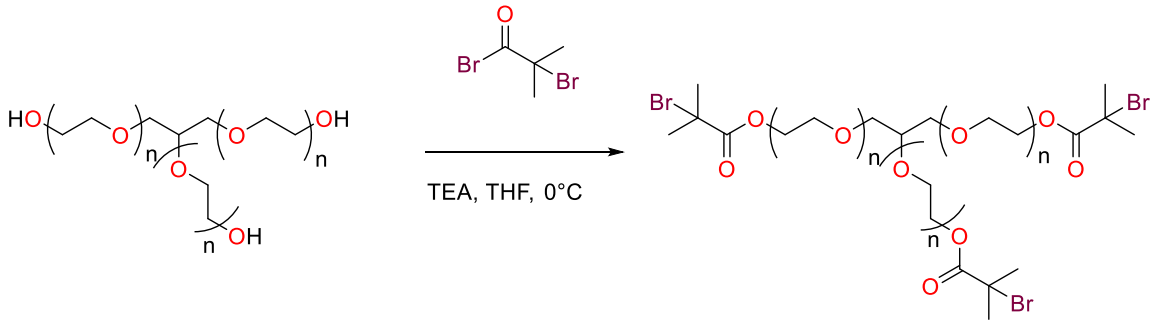

Scheme III.4.5 Schematic representation of the synthetic approach to Initiator I3 (tri-O-(2-bromo-2-methyl propionyl)-glycerol ethoxylate)

Glycerol ethoxylate (26.40 mL, 30.04 mmol), TEA (22.35 mL, 160.35 mmol) and dry THF (250 mL) were added to a round bottom flask equipped with stirring bar and cooled down to 0°C in an ice-bath. BIBB (16.7 mL, 135.11 mmol) was dissolved in dry THF (50 mL) and the mixture was slowly added to the reaction under Ar over a period of 1 hour. The resulting suspension was allowed to warm up to ambient temperature and furthermore allowed to stir overnight. The salts were removed via filtration and subsequently washed with 30 mL of THF. The resulting filtrate was collected and concentrated *in vacuo*, precipitated twice in hexane and subsequently redissolved in

DCM and passed over a basic alumina column. The initiator was found as a transparent viscous oil. (Yield = 29.0 mL, 78%).

^{1}H NMR (400 MHz, $CDCl_3$, 298 K, ppm): δ = 4.32 (t, 6H), 3.76-3.71 (m, 7H), 3.69-3.58 (broad, 72H), 3.58- 3.48 (m, 4H), 1.96 (s, 18H).
MALDI-TOF MS m/z: calculated for $C_{55}H_{103}O_{26}Br_3{}^+K^+$: 1455.392 Da; found, 1456.1

III.4.3.6 Synthesis of Initiator I8 (Octa-O-(2-bromo-2-methylpropionyl)-tripentaerythritol)

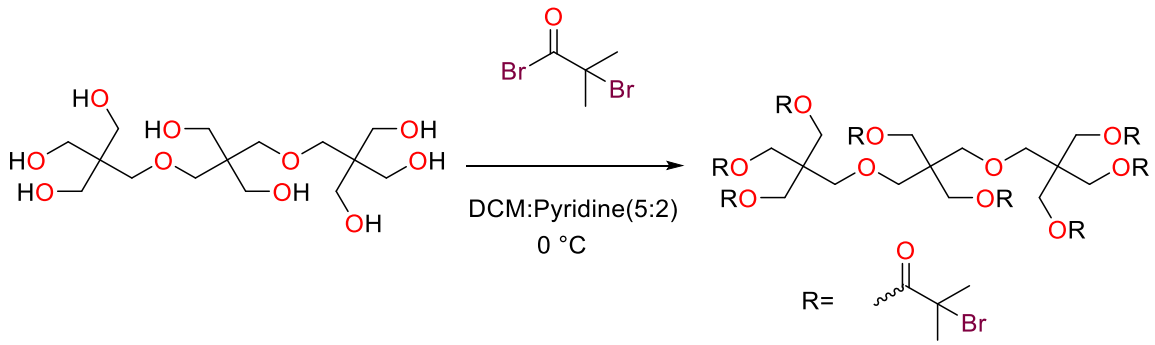

Scheme III.4.6 Schematic representation of the synthetic approach to initiator I8 (Octa-O-(2-bromo-2-methylpropionyl)-tripentaerythritol)

Tripentaerythritol (10.0 g, 26.8 mmol) was suspended in dry DCM (200 mL), followed by the addition of pyridine (100 mL) and cooled in an ice-water bath to 0 °C. BIBB (53 mL, 429 mmol) dissolved in dry DCM (50 mL) at 0 °C was added dropwise to the tripentaerythritol solution under magnetic stirring. The reaction continued 2 days at room temperature. The salts were filtered of and the filtrate was then washed sequentially with an aqueous solution of hydrochloric acid (10 v%, 3X100 mL), with a saturated $NaHCO_3$ aqueous solution (3X100 mL) and water (3X100mL). The solution was passed over silica and then concentrated by rotary evaporation. The initiator was found as a beige solid (Yield: 19 g, 45 %).

^{1}H NMR (400 MHz, $CDCl_3$, 298 K, ppm): δ = 4.29 (*s*, 12 H), 4.27 (*s*, 4 H), 3.57 (*s*, 4 H), 3.55 (*s*, 4H), 1.94 (*s*, 36 H), 1.93 (*s*, 12 H).
MALDI-TOF MS m/z: calculated for $C_{47}H_{72}Br_8O_{18}$ H^+: 1564.8; found, 1564.31

III.4.3.7 Synthesis of Initiator I15 (Hepta-(2, 3, 6-tri-O-(2-bromo-2-methylpropionyl)-*β*-cyclodextrin)

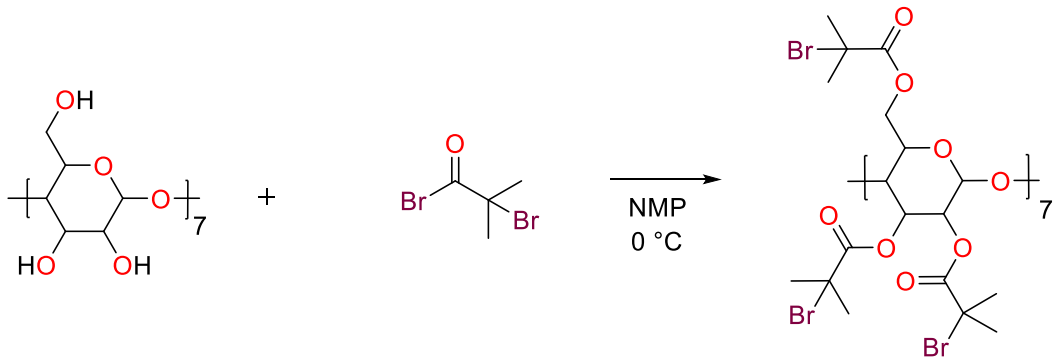

Scheme III.4.7 Schematic representation of the synthetic approach to initiator I15 (Hepta-(2, 3, 6-tri-O-(2-bromo-2-methylpropionyl)-*β*-cyclodextrin).

Initiator I15 was synthesised according to literature through the esterification of *β*-cyclodextrin with *α*-bromoisobutyryl bromide (BIBB) in 1-methyl-2-pyrrolidone (NMP).[29] *β*-cyclodextrin was recrystallized twice from water and dried in vacuum overnight at 100 °C. Anhydrous recrystallized *β*-cyclodextrin (5.67 g, 5.00 mmol) was dissolved in 40 ml anhydrous NMP and cooled in an ice-water bath to 0 °C. BIBB (51.9 mL, 420 mmol) dissolved in anhydrous NMP (30 mL) at 0 °C was added dropwise to the *β*-cyclodextrin solution under magnetic stirring. The reaction temperature was kept at 0 °C for 3h and was then allowed to rise to ambient temperature. The reaction was allowed to continue for 3 days. The brown syrup was concentrated under vacuum and subsequently diluted with 100 mL dichloromethane. The solution was then washed sequentially with a saturated $NaHCO_3$ aqueous solution (3X70 mL) and water (3X70mL). The dichloromethane was removed by rotary evaporation and the resulting syrup was diluted with 20 mL of acetone and precipitated in 1L of ice cold water. This purification procedure was repeated 5 times. Finally beige solid was obtained after drying under vacuum (12 g). The average degree of substituted hydroxyl groups at the periphery, determined by ^{1}H-NMR and MALDI-TOF spectrometry was 15.

^{1}H NMR (400 MHz, $CDCl_3$, 298 K, ppm): δ = 5.27 (m, 7 H), 4.86 (m, 7 H), 4.59 (m, 7 H), 4.34 (m, 7 H), 4.18 (m, 7 H), 4.06 (m, 7 H), 3.78 (m, 7 H), 1.96 (broad s, 90 H) ppm. MALDI-TOF MS m/z: calculated for $C_{102}H_{145}Br_{15}O_{50}K^+$: 3408.86 found, 3408.21

III.4.3.8 SET-LRP polymerisations

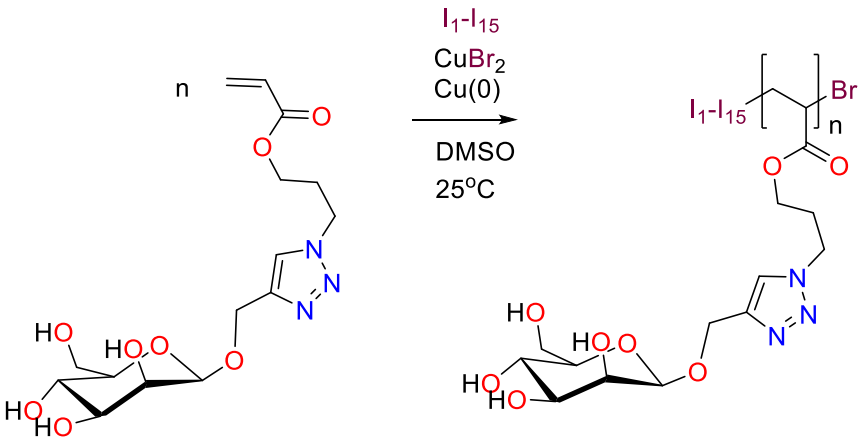

Scheme III.4.8 Schematic representation of the homopolymerisation of the Mannose glycomonomer using initiators I1-I15

III.4.3.8.1 SET-LRP of M1-30

A Schlenk tube was charged with initiator I1 (ethyl *α*-bromoisobutyrate, 3.93 µL, 0.0267 mmol, 1 eq.), mannose glycomonomer (300 mg, 0.804 mmol, 30 eq.), Me_6TREN (1.36 µL, 0.19 eq), $CuBr_2$ (0.239 mg, 0.04 eq.) in DMSO (2 mL), sealed with a rubber septum and subsequently degassed by gentle bubbling of Ar gas for 15 min. The polymerisation was then started by addition of pre-activated Cu(0) wire (5 cm) wrapped around a stirring bar under a positive Ar pressure and quickly sealed again and the reaction mixture was allowed to polymerise at 25˚C. Sampling was carried out using a degassed syringe to check the conversion of mannose glycomonomer. The reaction was allowed to polymerise for 420 min until 89.3% conversion.

III.4.3.8.2 SET-LRP of M3-90

A Schlenk tube was charged with initiator I3 (tri-O-(2-bromo-2-methyl propionyl)-glycerol ethoxylate, 13 mg, 9.15 µmol, 1 eq.), mannose glycomonomer (307.6 mg, 0.824 mmol, 90 eq.), Me_6TREN (1.39 µL, 0.57 eq), $CuBr_2$ (0.245 mg, 0.12 eq.) in DMSO (2 mL), sealed with a rubber septum and subsequently degassed by gentle bubbling of Ar gas for 15 min. The polymerisation was then started by addition of pre-activated Cu(0) wire (5 cm) wrapped around a stirring bar under a positive Ar pressure and quickly sealed again and the reaction mixture was allowed to polymerise at 25˚C. Sampling was carried out using a degassed syringe to check the conversion of mannose glycomonomer. The reaction was allowed to polymerise for 510 min until 85.6% conversion.

III.4.3.8.3 SET-LRP of M7-210

A Schlenk tube was charged with initiator I7 (per-6-deoxy-6-(thiopropyl-2-bromo-2-methylpropanoate)-β-cyclodextrin, 10.5 mg, 3.89 µmol, 1 eq.), mannose glycomonomer (305.3 mg, 0.817 mmol, 210 eq.), Me_6TREN (1.38 µL, 1.33 eq), $CuBr_2$ (0.244 mg, 0.28 eq.) in DMSO (2 mL), sealed with a rubber septum and subsequently degassed by gentle bubbling of Ar gas for 15 min. The polymerisation was then started by addition of pre-activated Cu(0) wire (5 cm) wrapped around a stirring bar under a positive Ar pressure and quickly sealed again and the reaction mixture was allowed to polymerise at 25˚C. Sampling was carried out using a degassed syringe to check the conversion of mannose glycomonomer. The reaction was allowed to polymerise for 360 min until 87.3% conversion.

III.4.3.8.4 SET-LRP of M8-240

A Schlenk tube was charged with initiator I8 (Octa-O-(2-bromo-2-methylpropionyl)-tripentaerythritol, 5.8 mg, 3.70 µmol, 1 eq.), mannose glycomonomer (332.2 mg, 0.889 mmol, 240 eq.), Me_6TREN (1.50 µL, 1.52 eq), $CuBr_2$ (0.265 mg, 0.32 eq.) in DMSO (2 mL), sealed with a rubber septum and subsequently degassed by gentle bubbling of Ar gas for 15 min. The polymerisation was then started by addition of pre-activated Cu(0) wire (5 cm) wrapped around a stirring bar under a positive Ar pressure and quickly sealed again and the reaction mixture was allowed to polymerise at 25˚C. Sampling was carried out using a degassed syringe to check the conversion of mannose glycomonomer. The reaction was allowed to polymerise for 420 min until 89.8% conversion.

III.4.3.8.5 SET-LRP of M15-450

A Schlenk tube was charged I15 (Hepta-(2, 3, 6-tri-O-(2-bromo-2-methylpropionyl)-*β*-cyclodextrin, 6.2 mg, 1.84 µmol, 1 eq.), mannose glycomonomer (309.1 mg, 0.827 mmol, 450 eq.), Me_6TREN (1.40 µL, 2.85 eq), $CuBr_2$ (0.246 mg, 0.6 eq.) in DMSO (2 mL), sealed with a rubber septum and subsequently degassed by gentle bubbling of Ar gas for 15 min. The polymerisation was then started by addition of pre-activated Cu(0) wire (5 cm) wrapped around a stirring bar under a positive Ar pressure and quickly sealed again and the reaction mixture was allowed to polymerise at 25˚C. Sampling was carried out using a degassed syringe to check the conversion of mannose glycomonomer. The reaction was allowed to polymerise for 450 min until 88.6% conversion.

III.4.3.8.6 SET-LRP of M1-150

A Schlenk tube was charged with initiator I1 (ethyl *α*-bromoisobutyrate, 0.39 µL, 0.00267 mmol, 1 eq.), mannose glycomonomer (300 mg, 0.804 mmol, 300 eq.),

Me_6TREN (1.36 µL, 0.19 eq), $CuBr_2$ (0.239 mg, 0.04 eq.) in DMSO (2 mL), sealed with a rubber septum and subsequently degassed by gentle bubbling of Ar gas for 15 min. The polymerisation was then started by addition of pre-activated Cu(0) wire (5 cm) wrapped around a stirring bar under a positive Ar pressure and quickly sealed again and the reaction mixture was allowed to polymerise at 25˚C. Sampling was carried out using a degassed syringe to check the conversion of mannose glycomonomer. The polymerisation was monitored until the monomer conversion reached 56.8% at 29 h.

III.4.3.8.7 SET-LRP of M3-150

A Schlenk tube was charged with initiator I3 (tri-O-(2-bromo-2-methyl propionyl)-glycerol ethoxylate, 5 mg, 3.52 µmol, 1 eq.), mannose glycomonomer (394.4 mg, 1.06 mmol, 300 eq.), Me_6TREN (0.536 µL, 0.57 eq), $CuBr_2$ (94.4 µg, 0.12 eq.) in DMSO (2 mL), sealed with a rubber septum and subsequently degassed by gentle bubbling of Ar gas for 15 min. The polymerisation was then started by addition of pre-activated Cu(0) wire (5 cm) wrapped around a stirring bar under a positive Ar pressure and quickly sealed again and the reaction mixture was allowed to polymerise at 25˚C. Sampling was carried out using a degassed syringe to check the conversion of mannose glycomonomer. The polymerisation was monitored until the monomer conversion reached 54.5% at 300 min.

III.4.3.8.8 SET-LRP of M7-150

A Schlenk tube was charged with initiator I7 (*per*-6-deoxy-6-(thiopropyl-2-bromo-2-methylpropanoate)-*β*-cyclodextrin, 10 mg, 3.71 µmol, 1 eq.), mannose glycomonomer (415.3 mg, 1.11 mmol, 300 eq.), Me_6TREN (1.31 µL, 1.33 eq), $CuBr_2$ (0.231 mg, 0.28 eq.) in DMSO (2 mL), sealed with a rubber septum and subsequently degassed by gentle bubbling of Ar gas for 15 min. The polymerisation was then started by addition of pre-activated Cu(0) wire (5 cm) wrapped around a stirring bar under a positive Ar pressure and quickly sealed again and the reaction mixture was allowed to polymerise at 25˚C. Sampling was carried out using a degassed syringe to check the conversion of mannose glycomonomer. The polymerisation was monitored until the monomer conversion reached 54.3% at 90 min.

III.4.3.8.9 SET-LRP of M8-150

A Schlenk tube was charged with initiator I8 (Octa-O-(2-bromo-2-methylpropionyl)-tripentaerythritol, 5.8 mg, 3.70 µmol, 1 eq.), mannose glycomonomer (415.29 mg, 1.11 mmol, 300 eq.), Me_6TREN (1.50 µL, 1.52 eq), $CuBr_2$ (0.265 mg, 0.32 eq.) in DMSO (2 mL), sealed with a rubber septum and subsequently degassed by gentle bubbling of Ar gas for 15 min. The polymerisation was then started by addition of pre-activated Cu(0) wire (5 cm) wrapped around a stirring bar under a positive Ar pressure

and quickly sealed again and the reaction mixture was allowed to polymerise at 25˚C. Sampling was carried out using a degassed syringe to check the conversion of mannose glycomonomer. The polymerisation was monitored until the monomer conversion reached 54.3% at 90 min.

III.4.3.8.10 SET-LRP of M15-150

A Schlenk tube was charged I15 (Hepta-(2, 3, 6-tri-O-(2-bromo-2-methylpropionyl)-*β*-cyclodextrin, 12 mg, 3.56 µmol, 1 eq.), mannose glycomonomer (398.8 mg, 1.07 mmol, 300 eq.), Me_6TREN (2.71 µL, 2.85 eq), $CuBr_2$ (0.477 mg, 0.6 eq.) in DMSO (2 mL), sealed with a rubber septum and subsequently degassed by gentle bubbling of Ar gas for 15 min. The polymerisation was then started by addition of pre-activated Cu(0) wire (5 cm) wrapped around a stirring bar under a positive Ar pressure and quickly sealed again and the reaction mixture was allowed to polymerise at 25˚C. Sampling was carried out using a degassed syringe to check the conversion of mannose glycomonomer. The polymerisation was monitored until the monomer conversion reached 50.2% at 60 min.

III.4.4 Kinetic data obtained *via* SPR

Table III.4.1 Polymer interactions with DC-SIGN

Polymer	k_a [$M^{-1}s^{-1}$]	k_d [s^{-1}]	K_A[M^{-1}]	K_D [M]	R_{max} [RU]
M1-30	$1.23x10^3$	$2.26x10^{-3}$	$5.42x10^5$	$1.84x10^{-6}$	90
M3-90	$1.16x10^4$	$5.34x10^{-3}$	$2.16x10^6$	$4.62x10^{-7}$	95
M7-210	$1.45x10^4$	$2.72x10^{-3}$	$5.33x10^6$	$1.88x10^{-7}$	180
M8-240	$7.65x10^4$	$4.16x10^{-3}$	$1.84x10^7$	$5.44x10^{-8}$	220
M15-450	$1.39x10^4$	$3.29x10^{-3}$	$4.22x10^6$	$2.37x10^{-7}$	275
M1-150	$1.02x10^4$	$1.43x10^{-3}$	$7.09x10^6$	$1.41x10^{-7}$	230
M3-150	$2.3x10^4$	$3.26x10^{-3}$	$7.05x10^6$	$1.42x10^{-7}$	140
M7-150	$1.83x10^4$	$3.53x10^3$	$5.18x10^6$	$1.93x10^{-7}$	140
M8-150	$1.84x10^4$	$4.16x10^{-3}$	$4.43x10^6$	$2.26x10^{-7}$	130
M15-150	$1.45x10^4$	$4.07x10^{-3}$	$3.57x10^6$	$2.8x10^{-7}$	140

Table III.4.2 Polymer interactions with DC-SIGNR

Polymer	k_a [$M^{-1}s^{-1}$]	k_d [s^{-1}]	K_A[M^{-1}]	K_D [M]	R_{max} [RU]
M1-30	471	$1.38x10^{-4}$	$3.41x10^{6}$	$2.93x10^{-7}$	315
M3-90	$2.93x10^{3}$	$7.8x10^{-4}$	$3.75x10^{6}$	$2.67x10^{-7}$	310
M7-210	$3.2x10^{3}$	$8.79x10^{-5}$	$3.64x10^{7}$	$2.75x10^{-8}$	785
M8-240	$4.7x10^{4}$	$2.56x10^{-3}$	$1.83x10^{7}$	$5.45x10^{-8}$	690
M15-450	$1.21x10^{4}$	$1.73x10^{-3}$	$7.02x10^{6}$	$1.43x10^{-7}$	805
M1-150	$1.22x10^{4}$	$4.59x10^{-4}$	$2.65x10^{7}$	$3.78x10^{-8}$	610
M3-150	$1.14x10^{4}$	$9.05x10^{-4}$	$1.26x10^{7}$	$7.93x10^{-8}$	400
M7-150	$8.94x10^{3}$	$1.23x10^{-3}$	$7.26x10^{6}$	$1.38x10^{7}$	370
M8-150	$5.58x10^{3}$	$1.02x10^{-3}$	$5.44x10^{6}$	$1.84x10^{-7}$	360
M15-150	$1.32x10^{3}$	$3.78x10^{-4}$	$3.5x10^{6}$	$2.86x10^{-7}$	590

Table III.4.3 Polymer interactions with MBL

Polymer	k_a [$M^{-1}s^{-1}$]	k_d [s^{-1}]	K_A[M^{-1}]	K_D [M]	R_{max} [RU]
M1-30	354	$4.53x10^{-4}$	$7.81x10^{5}$	$1.28x10^{-6}$	650
M3-90	$7.65x10^{3}$	$7.55x10^{-4}$	$1.01x10^{7}$	$9.88x10^{-8}$	580
M7-210	$1.51x10^{4}$	$5.48x10^{-4}$	$2.75x10^{7}$	$3.64x10^{-8}$	1230
M8-240	$2.34x10^{5}$	$1.66x10^{-3}$	$1.41x10^{8}$	$7.08x10^{-9}$	1025
M15-450	$1.51x10^{5}$	$1.4x10^{-3}$	$1.08x10^{8}$	$9.3x10^{-9}$	1355
M1-150	$2.9x10^{4}$	$8.75x10^{-4}$	$3.31x10^{7}$	$3.02x10^{-8}$	1150
M3-150	$7.29x10^{4}$	$1.36x10^{-3}$	$5.34x10^{7}$	$1.87x10^{-8}$	795
M7-150	$3.1x10^{4}$	$1.26x10^{-3}$	$2.47x10^{7}$	$4.05x10^{-8}$	850
M8-150	$3.2x10^{4}$	$1.37x10^{-3}$	$2.33x10^{7}$	$4.3x10^{-8}$	790
M15-150	$1.32x10^{4}$	$8.94x10^{-4}$	$1.48x10^{7}$	$6.68x10^{-8}$	1000

Table III.4.4 Polymer interactions with Langerin

Polymer	k_a [$M^{-1}s^{-1}$]	k_d [s^{-1}]	K_A[M^{-1}]	K_D [M]	R_{max} [RU]
M1-30	-	-	-	-	-
M3-90	$7.96x10^3$	$1.63x10^{-3}$	$4.88x10^6$	$2.05x10^{-7}$	70
M7-210	$8.23x10^3$	$7.96x10^{-4}$	$1.03x10^7$	$9.67x10^{-8}$	240
M8-240	$7.31x10^3$	$4.19x10^{-4}$	$1.74x10^7$	$5.74\ x10^{-8}$	210
M15-450	$8.78x10^3$	$3.01x10^{-4}$	$2.92x10^7$	$3.42x10^{-8}$	320
M1-150	$1.02x10^4$	$1.95x10^{-3}$	$5.2x10^6$	$1.92x10^{-7}$	55
M3-150	-	-	-	-	-
M7-150	$5.8\ x10^3$	$9.85\ x10^{-4}$	$6.56\ x10^6$	$1.52\ x10^{-7}$	94
M8-150	$6.69x10^3$	$2.1x10^{-3}$	$3.19x10^6$	$3.14x10^{-7}$	90
M15-150	-	-	-	-	-

Table III.4.5 Polymer interactions with SP-D

Polymer	k_a [$M^{-1}s^{-1}$]	k_d [s^{-1}]	K_A[M^{-1}]	K_D [M]	R_{max} [RU]
M1-30	-	-	-	-	-
M3-90	-	-	-	-	-
M7-210	891	$6.07\ x10^{-4}$	$1.47\ x10^6$	$6.81\ x10^{-7}$	168
M8-240	$2.25x10^4$	$3.47x10^{-3}$	$6.48\ x10^6$	$1.54\ x10^{-7}$	120
M15-450	$3.32\ x10^4$	$1.71x10^{-3}$	$1.94\ x10^7$	$5.16\ x10^{-8}$	187
M1-150	$8.6\ x10^3$	$8.05\ x10^{-4}$	$1.07\ x10^7$	$9.35\ x10^{-8}$	77
M3-150	$6.17\ x10^3$	$9.19\ x10^{-4}$	$6.72\ x10^6$	$1.49\ x10^{-7}$	42
M7-150	$1.69\ x10^4$	$2.16\ x10^{-3}$	$7.83\ x10^6$	$1.28\ x10^{-7}$	50
M8-150	-	-	-	-	-
M15-150	-	-	-	-	-

Table III.4.6 Polymer interactions with Dectin-2

Polymer	k_a [$M^{-1}s^{-1}$]	k_d [s^{-1}]	K_A[M^{-1}]	K_D [M]	R_{max} [RU]
M1-30	-	-	-	-	-
M3-90	-	-	-	-	-
M7-210	18.8	$2.43x10^{-3}$	$7.75 x10^{3}$	$1.29x10^{-4}$	95
M8-240	433	$2.76x10^{-3}$	$1.57x10^{5}$	$6.37x10^{-6}$	210
M15-450	73.5	$1.45x10^{-5}$	$5.07x10^{6}$	$1.97x10^{-7}$	310
M1-150	-	-	-	-	-
M3-150	-	-	-	-	-
M7-150	-	-	-	-	-
M8-150	-	-	-	-	-
M15-150	-	-	-	-	-

III.5 References

(1) Abdouni, Y.; Yilmaz, G.; Becer, C. R. *Macromol. Rapid Commun.* **2017**, *38* (24), 1700212.

(2) Purcell, S. C.; Godula, K. *Interface Focus* **2019**, *9* (2), 20180080.

(3) Gamblin, D. P.; Scanlan, E. M.; Davis, B. G. *Chem. Rev.* **2009**, *109* (1), 131.

(4) Ting, S. R. S.; Chen, G.; Stenzel, M. H. *Polym. Chem.* **2010**, *1* (9), 1392.

(5) Gabius, H.-J.; André, S.; Kaltner, H.; Siebert, H.-C. *Biochim. Biophys. Acta - Gen. Subj.* **2002**, *1572* (2–3), 165.

(6) Gabius, H.-J.; André, S.; Jiménez-Barbero, J.; Romero, A.; Solís, D. *Trends Biochem. Sci.* **2011**, *36* (6), 298.

(7) Kiessling, L. L.; Gestwicki, J. E.; Strong, L. E. *Angew. Chemie Int. Ed.* **2006**, *45* (15), 2348.

(8) Lundquist, J. J.; Toone, E. J. *Chem. Rev.* **2002**, *102* (2), 555.

(9) Yilmaz, G.; Becer, C. R. *Eur. Polym. J.* **2013**, *49* (10), 3046.

(10) Kiessling, L. L.; Grim, J. C. *Chem. Soc. Rev.* **2013**, *42* (10), 4476.

(11) Yilmaz, G.; Uzunova, V.; Hartweg, M.; Beyer, V.; Napier, R.; Remzi Becer, C. *Polym. Chem.* **2018**, *9*, 611.

(12) Lutz, J.-F.; Lehn, J.-M.; Meijer, E. W.; Matyjaszewski, K.; Takeuchi, M. *Nat. Rev. Mater.* **2016**, *1* (5), 16024.

(13) Gao, H.; Ohno, S.; Matyjaszewski, K. *J. Am. Chem. Soc.* **2006**, *128* (47), 15111.

(14) Anastasaki, A.; Nikolaou, V.; Nurumbetov, G.; Wilson, P.; Kempe, K.; Quinn, J. F.; Davis, T. P.; Whittaker, M. R.; Haddleton, D. M. *Chem. Rev.* **2016**, *116* (3), 835.

(15) Chen, Y.; Chen, G.; Stenzel, M. H. *Macromolecules* **2010**, *43* (19), 8109.

(16) Chen, Y.; Lord, M. S.; Piloni, A.; Stenzel, M. H. *Macromolecules* **2015**, *48* (2), 346.

(17) Mitchell, D. A.; Zhang, Q.; Voorhaar, L.; Haddleton, D. M.; Herath, S.; Gleinich, A. S.; Randeva, H. S.; Crispin, M.; Lehnert, H.; Wallis, R.; Patterson, S.; Becer, C. R. *Chem. Sci.* **2017**, *8* (10), 6974.

(18) Brown, G. D.; Willment, J. A.; Whitehead, L. *Nat. Rev. Immunol.* **2018**, *18* (6), 374.

(19) Khoo, U.-S.; Chan, K. Y. K.; Chan, V. S. F.; Lin, C. L. S. *J. Mol. Med.* **2008**, *86* (8), 861.

(20) Léger, P.; Tetard, M.; Youness, B.; Cordes, N.; Rouxel, R. N.; Flamand, M.; Lozach, P. Y. *Traffic* **2016**, *17* (6), 639.

(21) Kerscher, B.; Willment, J. A.; Brown, G. D. *Int. Immunol.* **2013**, *25* (5), 271.

(22) Martin, M.; Blom, A. M. *Immunol. Rev.* **2016**, *274* (1), 218.

(23) Sancho, D.; Reis e Sousa, C. *Curr. Opin. Immunol.* **2013**, *25* (1), 46.

(24) Cao, L.; Shi, X.; Chang, H.; Zhang, Q.; He, Y. *Proc. Natl. Acad. Sci. U. S. A.* **2015**, *112* (23), 7237.

(25) Hanč, P.; Schulz, O.; Fischbach, H.; Martin, S. R.; Kjær, S.; Reis e Sousa, C. *EMBO J.* **2016**, *35* (22), 2484.

(26) de Witte, L.; Nabatov, A.; Pion, M.; Fluitsma, D.; de Jong, M. A. W. P.; de Gruijl, T.; Piguet, V.; van Kooyk, Y.; Geijtenbeek, T. B. H. *Nat. Med.* **2007**, *13* (3), 367.

(27) Berg, L. M. van den; Cardinaud, S.; Aar, A. M. G. van der; Sprokholt, J. K.; Jong, M. A. W. P. de; Zijlstra-Willems, E. M.; Moris, A.; Geijtenbeek, T. B. H. *J. Immunol.* **2015**, *195* (4), 1763.

(28) Zhang, Q.; Collins, J.; Anastasaki, A.; Wallis, R.; Mitchell, D. A.; Becer, C. R.; Haddleton, D. M. *Angew. Chemie - Int. Ed.* **2013**, *52* (16), 4435.

(29) Zhang, Q.; Su, L.; Collins, J.; Chen, G.; Wallis, R.; Mitchell, D. A.; Haddleton, D. M.; Becer, C. R. *J. Am. Chem. Soc.* **2014**, *136* (11), 4325.

(30) Aksakal, R.; Resmini, M.; Becer, C. R. *Polym. Chem.* **2016**, *7* (1), 171.

(31) Burns, J. A.; Haddleton, D. M.; Becer, C. R. In *Progress in Controlled Radical Polymerization: Materials and Applications*; 2012; Vol. 1101, pp 81–98.

(32) Lopez Robles, M. D.; Pallier, A.; Huchet, V.; Le Texier, L.; Remy, S.; Braudeau, C.; Delbos, L.; Moreau, A.; Louvet, C.; Brosseau, C.; Royer, P.-J.; Magnan, A.; Halary, F.; Josien, R.; Cuturi, M.-C.; Anegon, I.; Chiffoleau, E. *Blood Adv.* **2017**, *1* (9), 557.

(33) Ahrens, S.; Zelenay, S.; Sancho, D.; Hanč, P.; Kjær, S.; Feest, C.; Fletcher, G.; Durkin, C.; Postigo, A.; Skehel, M.; Batista, F.; Thompson, B.; Way, M.; Reis e Sousa, C.; Schulz, O. *Immunity* **2012**, *36* (4), 635.

(34) Shrimpton, R. E.; Butler, M.; Morel, A.-S.; Eren, E.; Hue, S. S.; Ritter, M. A. *Mol. Immunol.* **2009**, *46* (6), 1229.

(35) van der Vlist, M.; Geijtenbeek, T. B. H. *Immunol. Cell Biol.* **2010**, *88* (4), 410.

(36) Oz, Y.; Abdouni, Y.; Yilmaz, G.; Becer, C. R.; Sanyal, A. *Polym. Chem.* **2019**, *10* (24), 3351.

(37) Zhang, Q.; Anastasaki, A.; Li, G.-Z.; Haddleton, A. J.; Wilson, P.; Haddleton, D. M. *Polym. Chem.* **2014**, *5* (12), 3876.

(38) Roy, B.; Mukhopadhyay, B. *Tetrahedron Lett.* **2007**, *48* (22), 3783.

Chapter 4

Supramolecular PEI-glycoconjugates for targeted *sa*RNA delivery

Messenger RNA (mRNA) has become a promising platform for both therapeutics and vaccines. More specifically, self-amplifying RNA (saRNA) is particularly advantageous as it provides a higher protein expression and also dose minimisation. In this chapter, we present the synthesis of a novel mannosylated polyethylenimine (PEI), enabled by the host-guest interaction between β-cyclodextrin and adamantane. For this we firstly modified transfection grade PEI, to obtain adamantane bearing PEIs (adaPEI). We have modified β-cyclodextrin to contain 7 mannose moieties and investigated the host-guest complexation between the two systems. We show that the host-guest complexation does not interfere with the electrostatic interaction with saRNA, and observed that while increasing the degree of mannosylation decreases transfection efficiency in vitro, it increases the number of cells expressing GFP by 8-fold in human skin explants. Furthermore, we found that increasing the ratio of glycopolymer to saRNA also enhanced the percentage of transfected cells ex vivo. We identified that these mannosylated PEIs specifically increased protein expression in the epithelial cells resident in human skin in a mannose dependent manner.

Biological experiments were performed and written by Dr. A. K. Blakney (I.C.)

Parts of this chapter have been published:

Oz, Y., Abdouni, Y., Yilmaz, G., Becer, C. R. & Sanyal, A. Magnetic glyconanoparticles for selective lectin separation and purification. *Polym. Chem.* **10**, 3351–3361 (2019).

IV Supramolecular PEI-glycoconjugates for targeted *sa*RNA delivery

IV.1Introduction

Recent advances and investment in RNA technology have enabled messenger RNA (*m*RNA) to become a clinically viable platform for both vaccines and protein replacement therapeutics. Self-amplifying *m*RNA (*sa*RNA) has emerged as a next-generation approach, and has several advantages compared to both *m*RNA and plasmid DNA (*p*DNA). Because *sa*RNA vectors are derived from the alphavirus genome,[1] they are able to self-replicate in the cytoplasm, resulting in amplification of the delivered dose of RNA and higher magnitude and duration of protein expression than *m*RNA.[2–4] Compared to *p*DNA, *sa*RNA is a minimal genetic vector and does not pose the risk of integration or insertional mutagenesis.[5] While a number of *m*RNA vaccines and therapeutics are currently being tested in the clinic,[6] there have not yet been any non-viral RNA replicons tested in human clinical trials.[7]

*sa*RNA has previously been formulated with a variety of delivery platforms, including lipid nanoparticles (LNPs),[8,9] a cationic nanoemulsion, cationic polymers[10,11] and ionisable dendrimers.[2] These formulations are not tailored for targeting of certain cell populations, but rather increased overall cellular uptake and expression of the *sa*RNA. Liang et al. previously observed that while neutrophils, monocytes and dendritic cells infiltrate the injection site and take up the RNA, it was mainly monocytes and dendritic cells that translated *m*RNA formulated in LNPs.[12] Both *si*RNA and *m*RNA have previously been targeted to leukocytes using the ASSET platform, in which LNPs are coated in monoclonal antibodies to target specific leukocyte subsets.[13] Furthermore, siRNA has been directly conjugated to a synthetic triantennary N-acetylgalactosamine (GalNAc)-based ligand that directly targets hepatocytes *in vivo*.[14] In this chapter, we sought a delivery platform that enabled tailoring of glycosylation without the use of

expensive monoclonal antibodies or direct conjugation to *sa*RNA, which is much larger in size than *si*RNA and unlikely to be taken up by cells without complexation.

Host-guest interactions between β-cyclodextrin (CD) and adamantane (Ad) have been previously used as a gene delivery platform for intravenous delivery of *p*DNA, wherein polyethylene glycol (PEG) was conjugated to adamantane in order to reduce toxicity of a poly(ethyleneimine) (PEI) formulation.[15] β-Cyclodextrin and adamantane are known to form a specific and stable complex in aqueous environments through the interaction between adamantane and the hydrophobic cavity of β-cyclodextrin.[16–18] Glycosylation of β-cyclodextrins has been performed previously, and allows for a facile approach for attaching a variety of glycan groups.[18,19] Given the ease of chemistry and biocompatibility of β-cyclodextrin-adamantane complexes, we chose this host-guest pair as a platform for glycosylation of PEI as a targeted delivery vehicle for *sa*RNA.

Here, we have developed a mannosylated PEI complex enabled by the host-guest interaction between β-cyclodextrin and adamantane. We designed and synthesised a library of PEI polymers with varying degrees of mannosylation. We then characterised the polymers and the polyplexes formed when complexed with *sa*RNA for size, charge and transfection efficiency *in vitro*. After identifying the optimal ratio of PEI to *sa*RNA, we then tested these formulations *ex vivo* in a clinically relevant human skin explant model to characterise the transfection efficiency. Finally, we observed how the degree of mannosylation and ratio of polymer to *sa*RNA affected cellular expression and identified which cellular subsets are targeted.

IV.2Results and discussion

IV.2.1 Synthesis of a mannose bearing *β*-cyclodextrin (CD-Man$_7$)

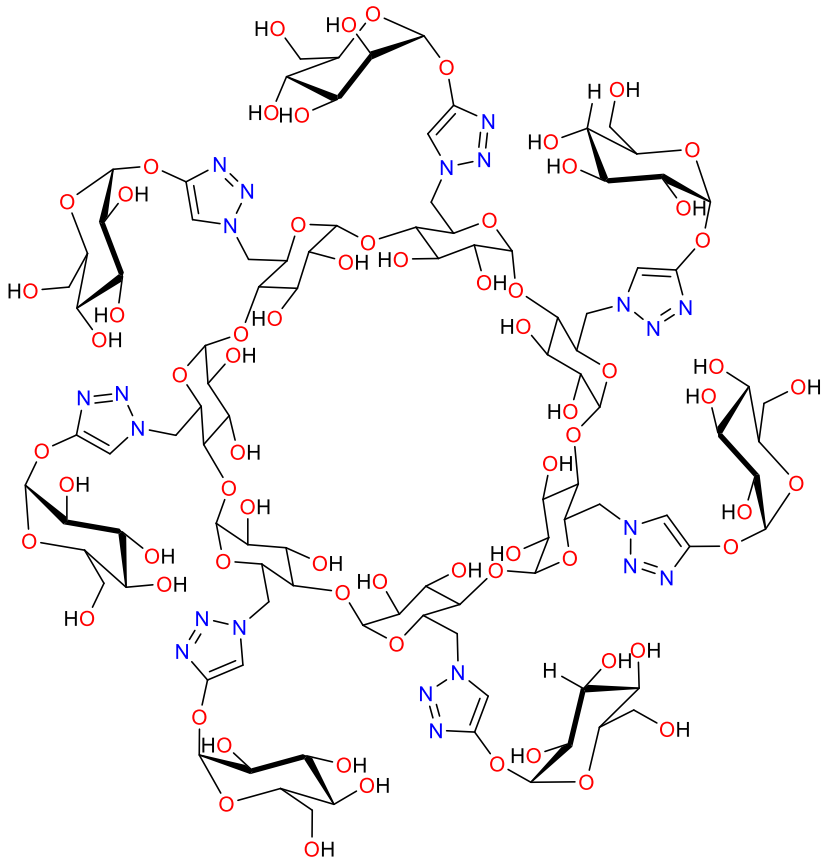

Figure IV.2.1 Chemical representation of the *β*-cyclodextrin based mannose glycocluster (CD-Man$_7$).

Following the successful (and unsuccessful) synthesis of *β*-cyclodextrin derivatives in Chapter 2, we realised the modification of only the primary rim face of the *β*-cyclodextrin would still allow hydrophobic moieties to enter the cavity of the *β*-cyclodextrin. For this reason we decided to repeat the synthesis of *per*-(6-deoxy-6-bromine)-*β*-cyclodextrin and utilise it as a scaffold for a mannose bearing glycocluster (CD-Man$_7$). This heptavalent glycocluster has been published elsewhere but we've updated the synthesis procedure to achieve this glycocluster.[20] Starting from *per*-(6-deoxy-6-bromine)-*β*-cyclodextrin we again performed the azidation as in Chapter 2 using sodium azide in DMF, achieving *per*-(6-deoxy-6-azido)-β-cyclodextrin. In Chapter 3, we demonstrated the synthesis of propargyl-*D*-mannose *via* a Fischer type glycosylation

using silica supported sulphuric acid. Eventually both compounds, per-(6-deoxy-6-bromine)-*β*-cyclodextrin and propargyl-*D*-mannose, were clicked together *via* the copper (I)-catalysed azide-alkyne cycloaddition (CuAAC) in DMSO using bipy as a ligand. In the original recipe, the DMSO was concentrated *in vacuo*, and then the compounds were purified by precipitation in cold methanol. This proved unsuccessful in our case and thus we opted to purify the cyclodextrins using dialysis against water. Propargyl-*D*-mannose which was added in excess was removed this way, eventually obtaining the desired product after freeze-drying the remaining water, as a white solid.

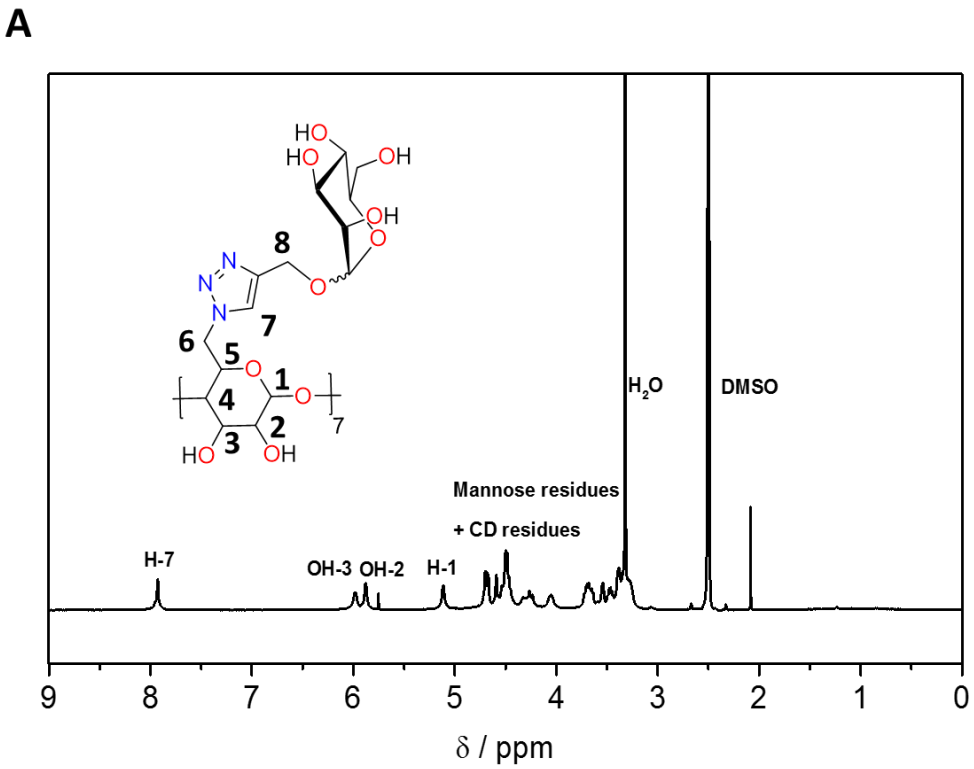

Figure IV.2.2 A) ^{1}H-NMR spectrum of CD-Man$_7$ in DMSO-d_6

IV.2.2 Synthesis of a polymeric mannose bearing *β*-cyclodextrin (CD-(*p*Man$_8$)$_7$)

In Chapter 2 we were able to demonstrate the synthesis of a novel *β*-cyclodextrin based SET-LRP initiator. In Chapter 3, we utilised this novel initiator for the synthesis of a *β*-cyclodextrin with 7 polymeric arms bearing mannose moieties successfully. Here we've utilised the same procedure, anticipating to achieve a *β*-cyclodextrin with polymeric arms bearing 10 mannose units on average. Kinetic experiments in Chapter 3

(**Figure III.2.5**) revealed that when using the same reaction conditions as in section **III.4.3.8.3**, an average arm length of around 10 mannose glycomonomers per arm would be achieved after 60 min. The experiment was thus repeated and the polymerisation was stopped after 60 min. ^{1}H-NMR then revealed the conversion of the mannose glycomonomers as 27.5% (8.3 monomers per arm) by comparing the triazole peak to the vinyl protons. Molecular weight of the polymer was then determined *via* NMR and was revealed to be 24499 Da on average.

IV.2.3 Synthesis of adamantane bearing linear PEI

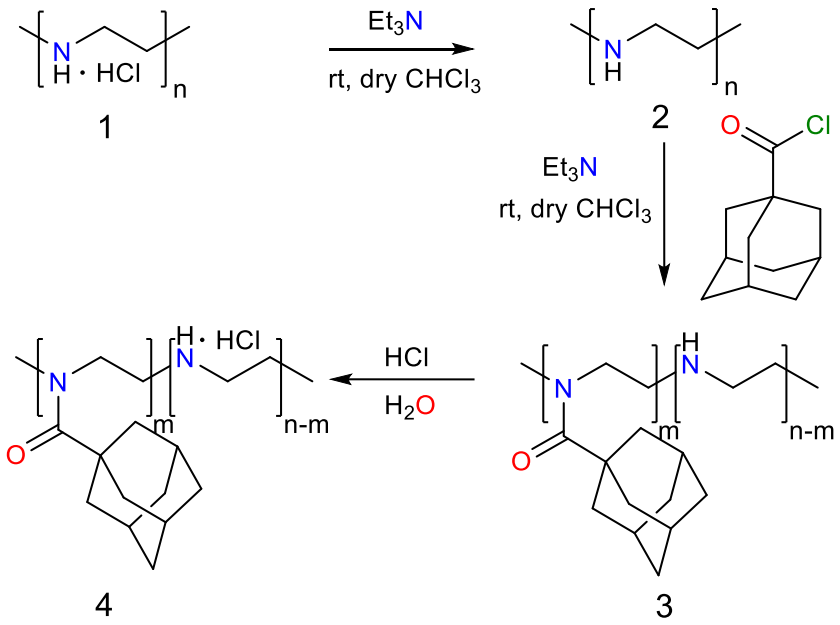

Scheme IV.2.1 Synthesis route towards adamantane bearing linear PEI (*ada*PEI)

A library of different PEI based polymers were successfully modified to contain appending adamantane units along the backbone. For this, commercially available PEI was first deprotonated using triethylamine in dry chloroform. Achieving good dissolution proved to be cumbersome in this case and thus the reaction medium (before adding the 1-adamantane carbonyl chloride solution) was sonicated for 30 min in order to achieve a really fine suspension of (deprotonated) linear PEI. Subsequently the deprotonated linear PEI solution was reacted with 1-adamantane carbonyl chloride *via* a simple nucleophilic substitution reaction (**Scheme IV.2.1**). ^{1}H-NMR samples were taken, clearly showing the PEI peak (*-CH_2-CH_2-)* around 3 ppm and the adamantane residues between 1.5 and 2 ppm (**Figure IV.2.3**).

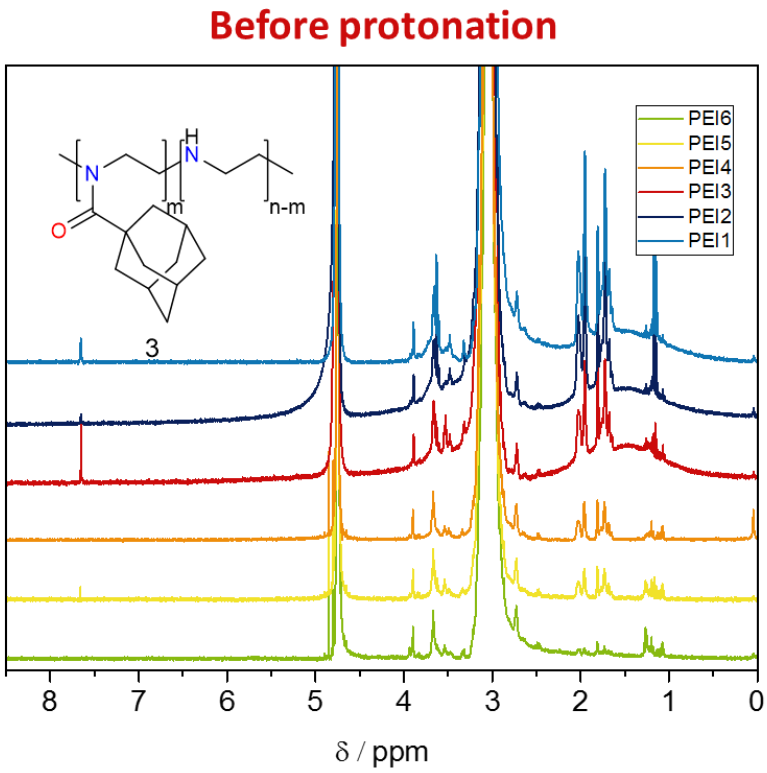

Figure IV.2.3 ^{1}H-NMR spectrum of the unprotonated *ada*PEIs in D_2O

The obtained *ada*PEI polymers were subsequently dissolved in water and protonated by addition of a 32% HCl solution and precipitated in acetone. The resulting protonated *ada*PEI polymers were furthermore characterised using ^{1}H-NMR in order to determine the average adamantane content per polymer chain together with the change in molecular weight (**Table IV.2.1**). Protonation shifts the PEI peak (*-CH_2-CH_2-)* from around 3.0 ppm to around 3.5 ppm as can be seen in **Figure IV.2.4**. Percentages in **Table IV.2.1** are defined as the percentage of monomer units along the polymer backbone. ^{1}H-NMR analysis revealed that there is a huge discrepancy between the amount of adamantyl groups added to the reaction and adamantyl actually found along the polymer chain.

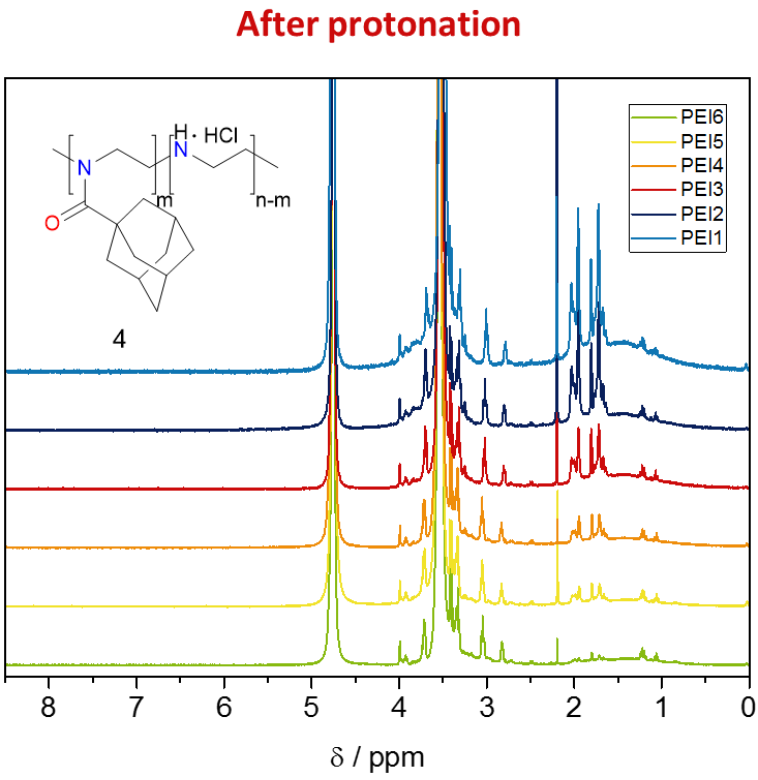

Figure IV.2.4 ^{1}H-NMR spectrum of the protonated *ada*PEIs in D_2O

Table IV.2.1 Characteristics of synthesised *ada*PEI polymers

***glyco*PEI**	**% Adamantane,** theoretical	**% Adamantane,** Experimental, NMR	**# Adamantanes per chain**	**MW *ada*PEI (Da)**
PEI_1	40	2.18	10.96	41393
PEI_2	20	1.71	8.58	41088
PEI_3	10	0.94	4.76	40603
PEI_4	5	0.54	2.72	40344
PEI_5	2.5	0.37	1.83	40232
PEI_6	1.25	0.14	0.71	40090

IV.2.4 Synthesis of *glyco*PEI: Complexation of *ada*PEI with CD-(*p*Man$_8$)$_7$

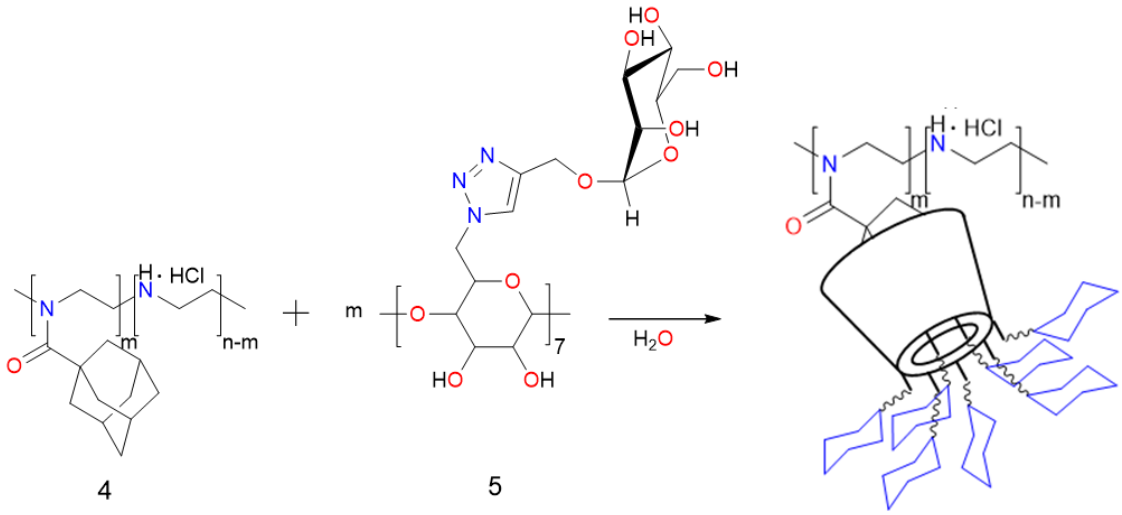

Scheme IV.2.2 Synthetic approach towards mannose glycocluster decorated linear PEI (glycoPEI)

The next big step in achieving linear PEI decorated with mannose glycoclusters was achieving the host-guest complexation of both entities with each other. As the host-guest interaction of CD-Man$_7$ with adamantane hadn't been studied before we decided to do isothermal titration calorimetry (ITC) measurements in order to prove the host-guest interaction. ITC works by promptly measuring the heat which is either released or absorbed during a molecular binding event measured by a sensitive calorimeter during gradual titration of the ligand into the sample cell. For this we first titrated normal *β*-cyclodextrin with rimantadine, an adamantane amino derivative), in order to see if we'd achieve the same binding affinity as reported in literature (Figure IV.2.5). We found an association constant K_a equal to 5.37 x 10^4 M^{-1}, which is in the same range as those values found in literature (see section **I.3.1**). Confident in the measurements we then measured the interaction of rimantadine with CD-Man$_7$, we inspected a reduction in binding affinity, as one face of the *β*-cyclodextrin is blocked from possible interactions. ITC revealed an association constant K_a of 1.41 x 10^4 M^{-1}. This is a four-fold decrease as compared to the binding affinity of *β*-cyclodextrin, but still in the same order of magnitude.

Confident in the complexation between the *ada*PEIs with CD-Man$_7$, we proceeded with the synthesis. For this, aqueous solutions of the different *ada*PEIs and the aqueous solutions of both CD-Man$_7$ and CD-(*p*Man$_8$)$_7$ were prepared and mixed in accordance with **Table IV.2.2**. PEI7 in this case was achieved by complexation between

*ada*PEI3 and CD-(*p*Man$_8$)$_7$. The obtained solutions were then freeze-dried to achieve the desired mannosylated *glyco*PEIs.

Table IV.2.2 Quantities used in *glyco*PEI synthesis

***glyco*PEI**	***ada*PEI**	**m (*ada*PEI)**	**m (CD-Man$_7$)**
PEI1	PEI1	30.4 mg	22.89 mg
PEI2	PEI2	30.2 mg	17.90 mg
PEI3	PEI3	30.1 mg	10.00 mg
PEI4	PEI4	30.1 mg	5.75 mg
PEI5	PEI5	30.5 mg	3.95 mg
PEI6	PEI6	30.0 mg	1.51 mg
PEI7	PEI3	30.1 mg	86.00 mg

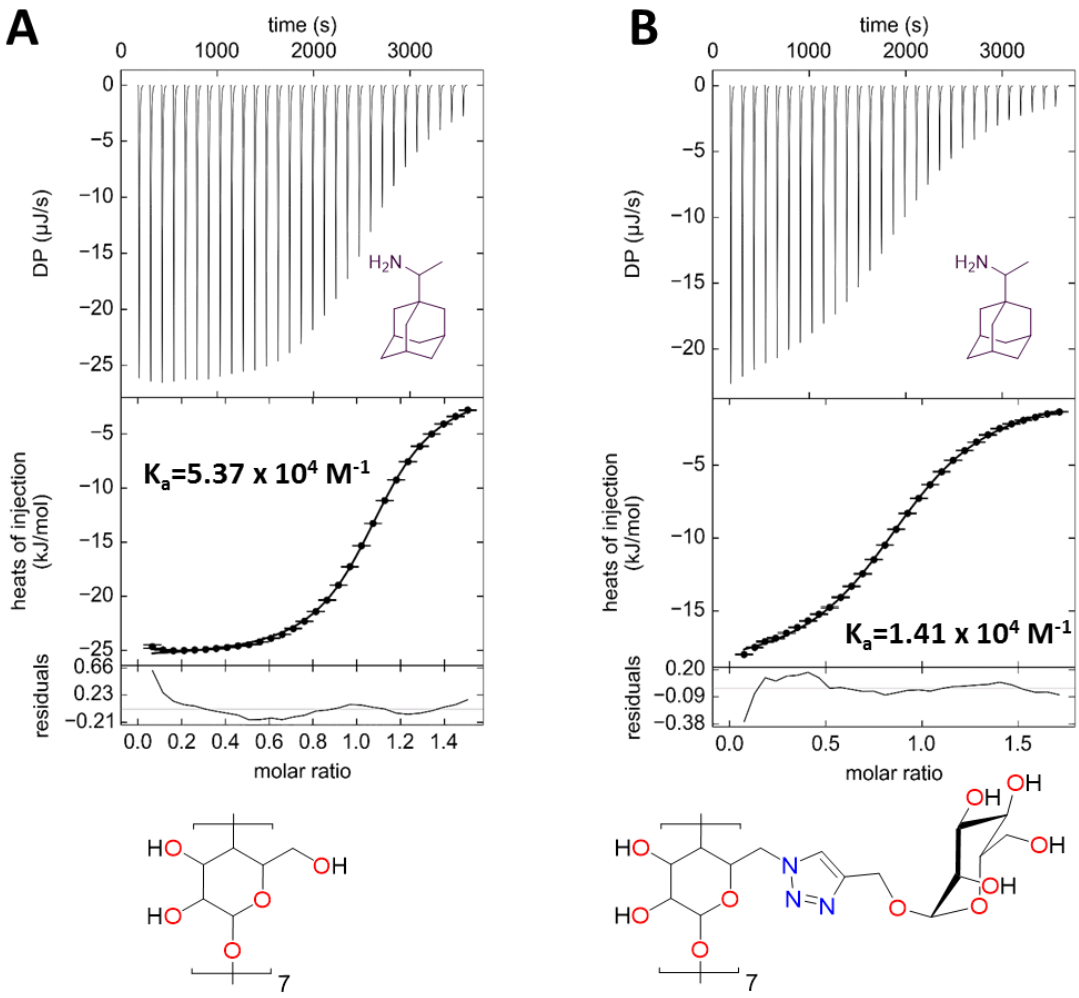

Figure IV.2.5 A) ITC measurements of *β*-cyclodextrin titrated with rimantadine and B) ITC measurements of CD-Man$_7$ titrated with rimantadine.

The host-guest interaction between the *ada*PEIs and CD-Man$_7$ was studied using a combination of ^{1}H-NMR and NOESY NMR. ^{1}H-NMR revealed that the adamantane peaks shifted as a result of a change in chemical environment caused by the host-guest complexation (**Figure IV.2.6**). The anticipated host-guest complexation between the adamantyl groups and CD-Man$_7$ as NOESY experiments furthermore revealed cross-peaks between the signals at 4 – 4.4 ppm assigned to the inner protons of the CD-Man$_7$ cavity and the signals at 1.8 – 2.4 ppm assigned to the adamantane which was not present when taken NOESY from the respective pure products (**Figure IV.2.7**). The resulting solutions were subsequently freeze-dried, resulting in a fine powder which is easily dissolvable for use in RNA transfection.

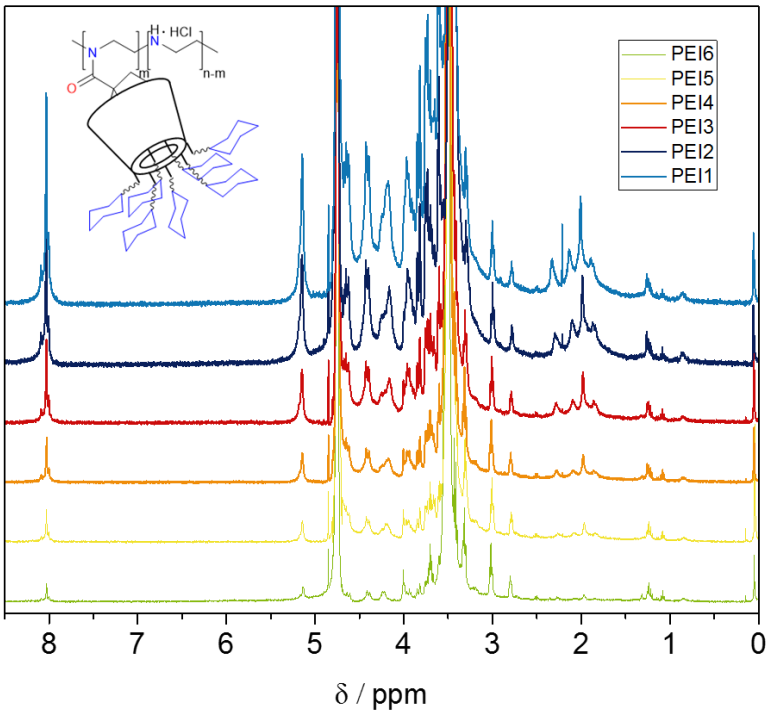

Figure IV.2.6 ^{1}H-NMR spectra of the protonated *ada*PEIs in D_2O

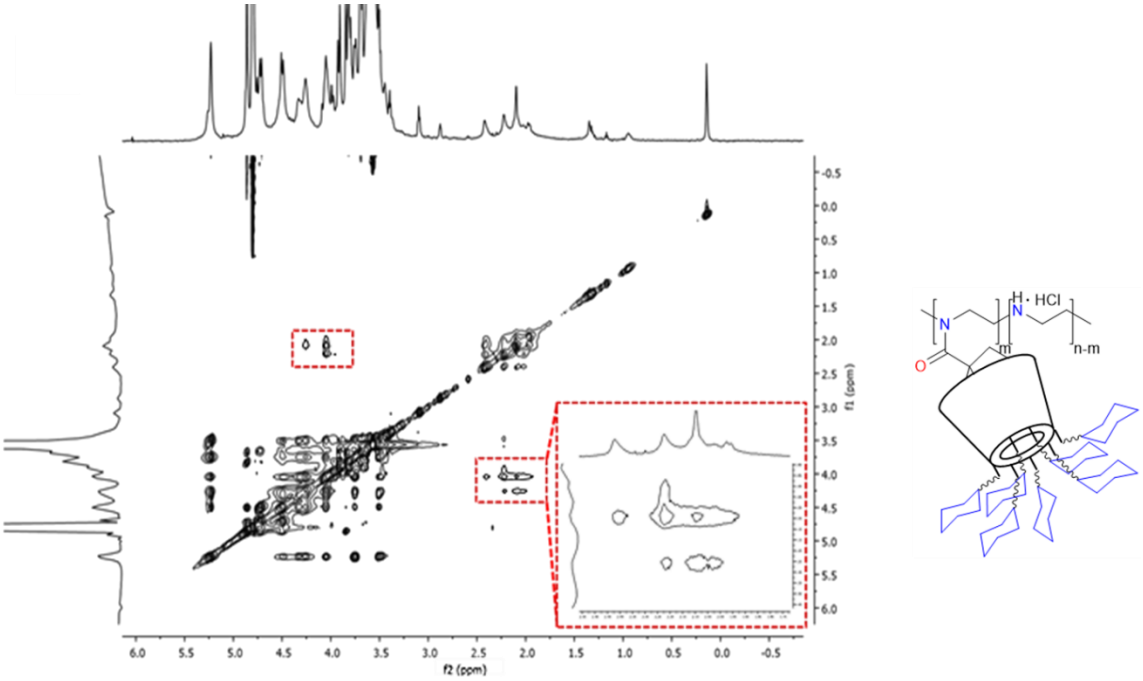

Figure IV.2.7 2D NOESY-NMR spectrum of the *ada*PEI3 and CD-Man$_7$, clearly showing cross peaks between the signals at 4.0 – 4.3 ppm assigned to the inner protons of the CD-Man$_7$ cavity and the signals at 1.9 – 2.4 ppm assigned to the adamantane.

IV.2.5 Particle size and charge after complexation with *sa*RNA*

Particle sizes and charges were characterised after complexation with *sa*RNA **(Figure IV.2.8**). All particles were between 50-200 nm in size, with a slight trend of increasing size with increasing degree of mannosylation. All particles were positively charged after *sa*RNA complexation, indicating that the host-guest interaction does not interfere with the cationic charges or further condensation of *sa*RNA molecules.

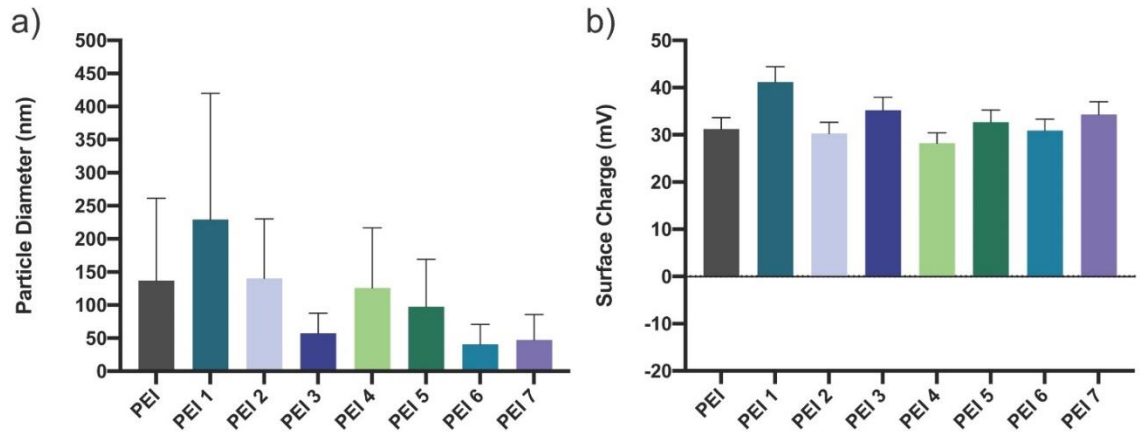

Figure IV.2.8 Particle size and zeta potential of *ada*PEI-CD-Man$_7$/*sa*RNA polyplexes as determined by DLS. a) Particle diameter and b) zeta potential of complexes prepared at a ratio of 5:1 polymer to RNA (w/w). Bars represent mean ± standard deviation for n=3.

IV.2.6 Increasing mannosylation of PEI decreases transfection efficiency in vitro*

In order to investigate the effects of the ratio of PEI to *sa*RNA and degree of mannosylation on transfection efficiency *in vitro*, we prepared polyplexes with *sa*RNA and PEI polymers with and without mannosylation (**Figure IV.2.9**). We observed similar transfection efficiency between the 5:1 and 20:1 ratios of polymer to *sa*RNA (w/w) *in vitro* (**Figure IV.2.9.a**). We postulate that this is because the glycopolymers are saturated with *sa*RNA even at lower ratios of polymer to RNA, which is supported by the zetasizer data (**Figure IV.2.8**) wherein even at a ratio of 5:1, the particles exhibit a positive charge. Thus, adding more polymer does not increase the transfection efficiency.

We then compared how the degree of mannosylation affected transfection efficiency, using either unmodified PEI, PEI with varying amounts of CD-Man$_7$ (PEI$_{1\text{-}6}$) or PEI with CD-(*p*Man$_8$)$_7$ (PEI$_7$) (**Figure IV.2.9.b**). Because changing the mass ratio of polymer to *sa*RNA changes the amount of available positively charges amines, we used a fixed ratio of PEI to *sa*RNA of 5:1 (w/w) and then normalised the molar amount of PEI in each formulation for PEI$_{1\text{-}7}$. We observed that PEI had the highest transfection efficiency, ~10^6 RLU, whereas all of the mannosylated PEIs were lower, between 1-5x10^5 RLU. In addition, increasing the degree of mannosylation decreased the transfection efficiency *in vitro*, as PEI$_6$ had the highest transfection efficiency of the mannosylated PEIs, and PEI$_1$ had the lowest. We hypothesise that this is due to sterical hindrance

cause by increasing degree of mannosylation which may limit the access that *sa*RNA has to the amine groups on PEI. Furthermore, while HEK cells can be induced to express the mannose receptor,[21] they do not naturally express it, thus these experiments exhibit how the structure of the polyplexes affects non-mannose mediated uptake. Overall, we observed that the ratio of mannosylated PEI to *sa*RNA did not affect transfection, but that increasing the degree of mannosylation interfered with *in vitro* transfection efficiency in a non-mannose dependent manner.

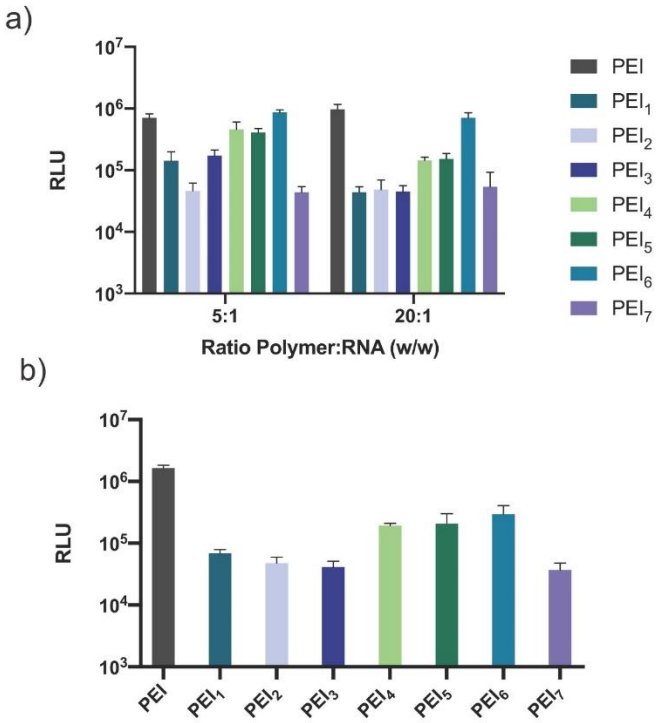

Figure IV.2.9 In vitro transfection efficiency of *ada*PEI-CD-Man_7 complexes with fLuc saRNA in HEK293T.17 cells after 24 hours. a) Transfection with complexes prepared at a ratio of total polymer complex to RNA of either 5:1 or 20:1 (w/w) or b) normalised to the molar amount of PEI in the complex. Bars represent mean ± standard deviation for n=3.RLU = Relative Light Unit.

IV.2.7 Increasing ratio of mannosylated PEI to RNA increases the percentage of resident epithelial cells expressing *sa*RNA*

Because *in vitro* transfection efficiency does not generally correlate well with *in vivo* efficacy,[22] we sought to test these glycopolymers in a clinically translational human skin explant model (**Figure IV.2.10**). Human skin explants have previously been shown to be a viable model for optimization of nucleic acid formulations,[9] and contain many cell

types with the mannose receptor including dendritic cells, fibroblasts, and macrophages.[23–27] We first prepared formulations with either RNA alone, PEI or mannosylated PEI ($PEI_{1\text{-}6}$) (**Figure IV.2.10a**) at a ratio of 5:1 polymer to *sa*RNA (w/w). We were surprised to observe that the polyplexes did not enhance the percentage of $eGFP^+$ in skin explants, even with unmodified PEI (**Figure IV.2.10b**). We observed a similar effect for PEI with CD-$(p\text{Man}_8)_7$ - only ~1% of cells expressed GFP and there was no observed benefit to naked RNA alone. We then tested whether increasing the ratio of PEI_1 to saRNA had any effect on the percentage of cells expressing GFP (**Figure IV.2.10c**). We observed that increasing the ratio of PEI_1 to saRNA to 10:1 and 20:1 (w/w) did indeed increase the number of GFP^+ cells to 5% and 8%, with p=0.018 and 0.00038, respectively. This enhancement is superior to previously studied LNP formulations.[9]

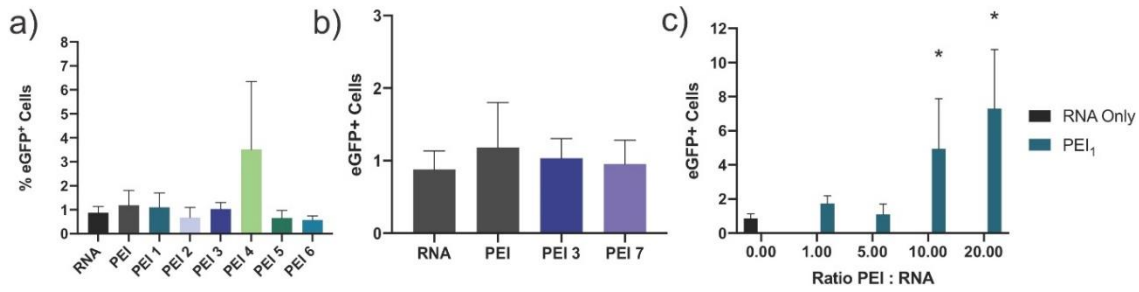

Figure IV.2.10 Percentage of eGFP+ cells in human skin explants after treatment with saRNA/*ada*PEICD-Man7 complexes after 72 hours in culture. a) Complexes at a ratio of 5:1 (complex to RNA, w/w) with PEI1-6, b) Complexes at a ratio of 5:1 (complex to RNA, w/w) comparing the effect of polymannosylated CD, c) Varying the ratio of complexes to RNA from 1:1 to 20:1 (w/w) of PEI1. Bars represent the mean ± standard deviation for n=3. * indicates significance of $p<0.05$.

We then characterised which cells were expressing the *sa*RNA using a flow cytometry panel capable of identifying epithelial cells (CD45-), fibroblasts (CD90+), NK cells (CD56+), leukocytes (CD45+), Langerhans cells (CD1a+), monocytes (CD14+) dendritic cells (CD11c+), T cells (CD3+) and B cells (CD19+). As previously observed the majority of cells that make up the skin are epithelial cells, fibroblasts and dendritic cells, and leukocytes, Langerhans cells, B cells, monocytes and T cells to a lesser extent (**Figure IV.2.11**). While epithelial cells make up ~64% of the total cells, they make up only 16% of the cells expressing the *sa*RNA alone. However, when the *sa*RNA was complexed with mannosylated PEI_1 at a ratio of 20:1 (w/w), it was expressed in ~33% of epithelial cells. Furthermore, increasing the ratio of PEI_1 to *sa*RNA led to proportional increases in the percentage of epithelial cells expressing GFP. GFP was expressed in either a similar or lesser percentage of the other cell types. Overall, we observed that

increasing the ratio of mannosylated PEI to *sa*RNA increased the number of cells expressing saRNA in human skin explants, and we identified that epithelial cells were specifically targeted by these polyplexes.

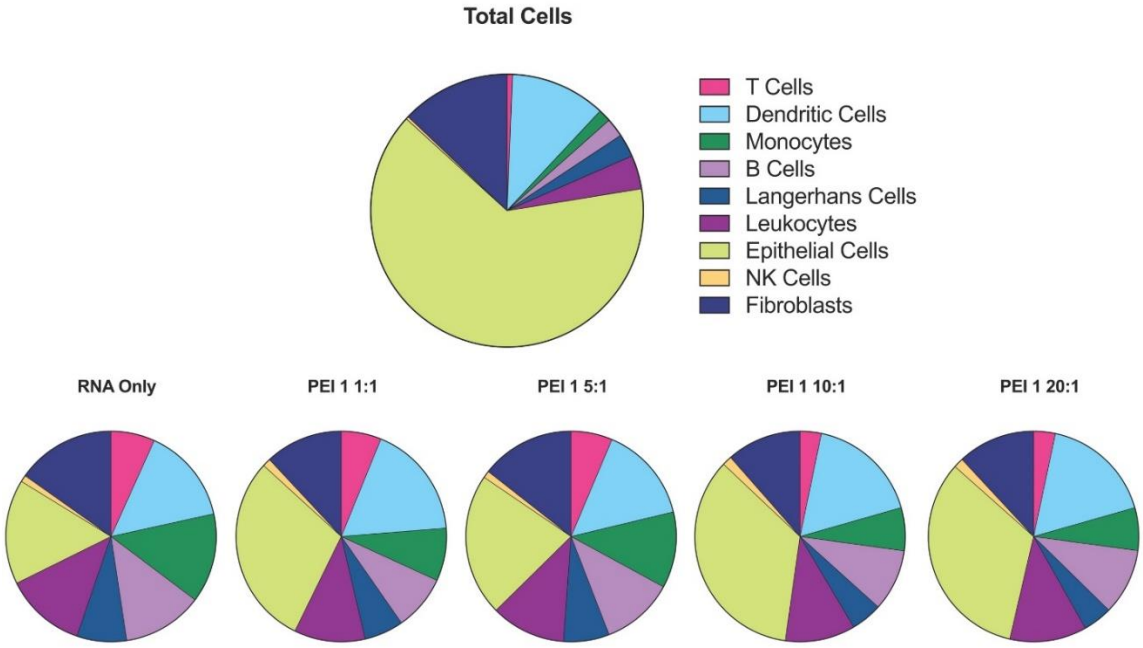

Figure IV.2.11 Phenotypic identity of eGFP+ cells in human skin explants after ID injection of GFP saRNA/PEI-Ad-CD-Man7 complexes at varying ratios of PEI1 to saRNA. Cells were identified using the following antibodies: epithelial cells (CD45-), fibroblasts (CD90+), NK cells (CD56+), leukocytes (CD45+), Langerhans cells (CD1a+), monocytes (CD14+), dendritic cells (CD11c+), T cells (CD3+) and B cells (CD19+).

IV.2.8 Increasing degree of mannosylation enhances uptake into epithelial cells in human skin explants*

Given our observation that increasing the ratio of mannosylated PEI to *sa*RNA enhanced the number of cells expressing saRNA, we then studied whether the degree of mannosylation affected cellular uptake and expression *ex vivo* (**Figure IV.2.12**). We prepared polyplexes at a fixed ratio of 20:1 (w/w) of PEI to *sa*RNA and again evaluated which cells were expressing GFP. We observed that at a ratio of 20:1, the PEI formulations (both unmodified and mannosylated) increased the percentage of GFP^+ cells to ~8%. Increasing the degree of mannosylation had a trend of increasing the percentage of epithelial cells expressing GFP (**Figure IV.2.12**), although only the

$PEI_{1,2,4,6}$ groups were found to be statistically significantly higher. While the mannose receptor is primarily known to be expressed by macrophages, dendritic cells, fibroblasts and keratinocytes, it has previously been shown to be expressed by vaginal epithelial cells.[28] It is possible that human skin epithelial cells also express the mannose receptor, leading to increased polyplex uptake and *sa*RNA expression in these cells. However, in these studies we quantified the percentage of cells *expressing* the *sa*RNA, not the percentage of cellular uptake, so it is possible that there is increased uptake into cells that are known to express the mannose receptor. In the context of RNA vaccines, it has yet to be defined as to which cells are desired to express the protein; we hypothesize that overall increased protein expression will result in increased immunogenicity. Overall, we show that increasing the degree of mannosylation increases protein expression, specifically in epithelial cells of human skin explants.

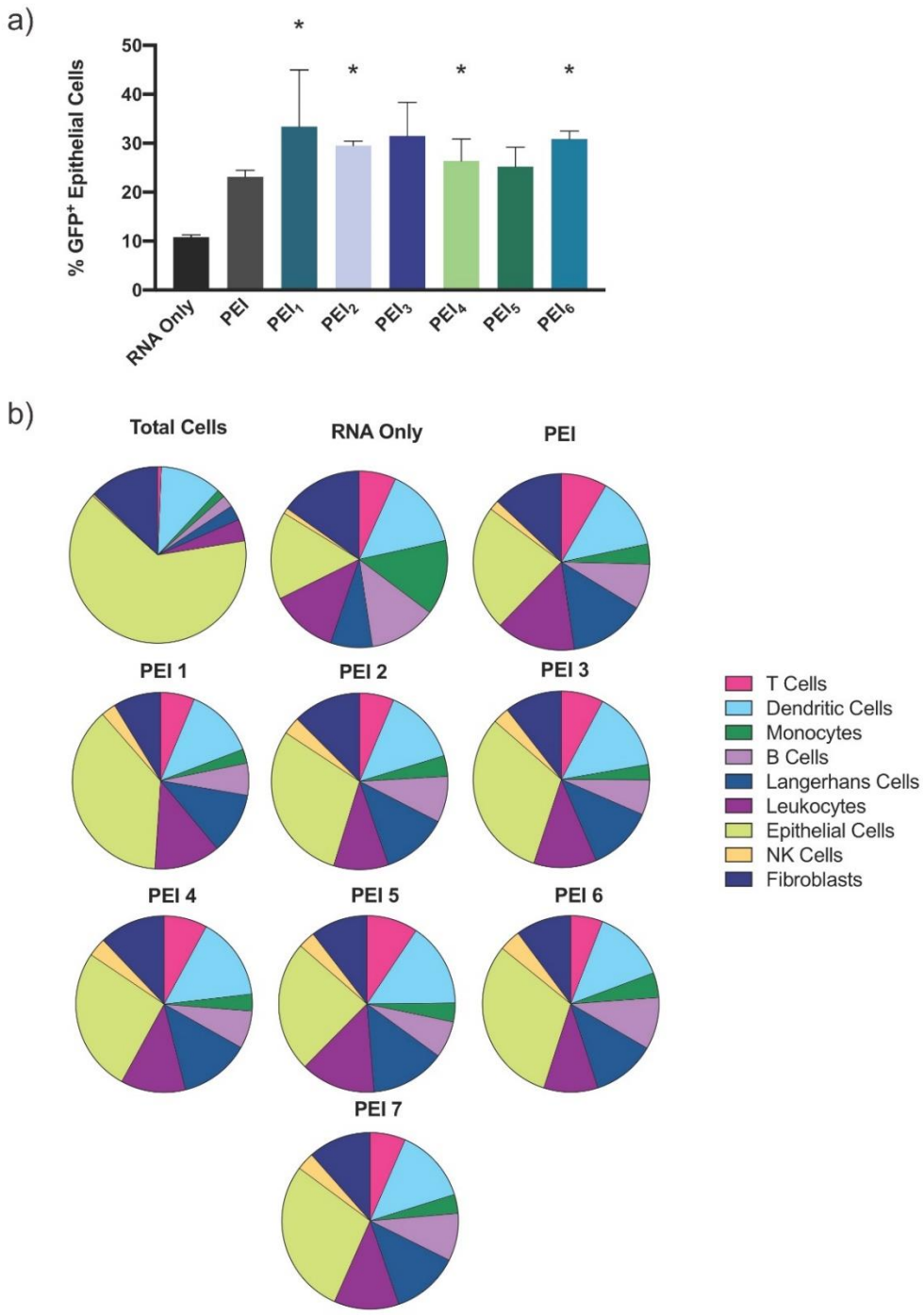

Figure IV.2.12 Phenotypic identity of eGFP+ cells in human skin explants after ID injection of saRNA/*ada*PEI-CD-Man7 complexes prepared at a ratio of 20:1 (w/w) with PEI1-7 after 72 hours in culture. a) % of GFP+ epithelial cells in human skin explants. Bars represent the mean ± standard deviation for n=3. * indicates significance of $p<0.05$. b) Phenotypes of cells expressing GFP. Cells were identified using the following antibodies: epithelial cells (CD45-), fibroblasts (CD90+), NK cells (CD56+), leukocytes (CD45+), Langerhans cells (CD1a+), monocytes (CD14+), dendritic cells (CD11c+), T cells (CD3+) and B cells (CD19+).

IV.3Conclusion

In this chapter, we have shown the successful synthesis and characterisation of a library of mannosylated linear PEI polymers enabled by the host-guest interaction between *β*-cyclodextrin and adamantane. For this we firstly modified transfection grade PEI, to obtain adamantane bearing PEIs (*ada*PEI) by reacting the linear PEI polymer with adamantane carbonyl chloride. We have modified *β*-cyclodextrin to contain 7 mannose moieties and investigated the host-guest complexation between the two systems. The resulting complexes were subsequently used for targeted *sa*RNA delivery. We show that while increasing the degree of mannosylation stifles *in vitro* transfection efficiency, it enhances the percentage of cells expressing the *sa*RNA in human skin explants. Furthermore, we found that increasing the ratio of polymer to *sa*RNA also enhanced the protein expression *ex vivo*, which was specifically due to an increase in epithelial cell expression. We observed that increasing the degree of mannosylation also increased expression specifically in epithelial cells. We anticipate that this platform, which enables glycosylation of PEI through host-guest chemistry, is a highly clinically translational delivery vehicle and is dually useful for targeting specific cell types for *sa*RNA delivery and expression.

IV.4 Experimental section

IV.4.1 Materials

PEI MAX (Transfection grade linear polyethylenimine hydrochloride, MW 40,000) was purchased from Polysciences, Inc. Dry triethylamine (TEA) (≥99.5%) equipped with septum, 1-adamantane carbonyl chloride and $CuBr_2$ were purchased from Sigma Aldrich and used as received. Tris(2-(dimethylamino)ethyl)amine (Me_6TREN) was synthesised according to literature procedures and stored at 4°C prior to use. Cyclodextrin initiator, mannose glycomonomer and heptamannose *β*-cyclodextrin (CD-Man_7) were synthesised as previously reported and stored at -20 °C prior to use.[20,29] All other reagents and solvents were purchased from Sigma Aldrich at the highest purity available and used without further purification unless stated otherwise.

IV.4.2 Instruments and analysis

Proton (^{1}H) Nuclear Magnetic Resonance (^{1}H-NMR) spectra were recorded on a 400 MHz Bruker Avance III spectrometer using DMSO-d_6, $CDCl_3$, MeOD-d_4 or D_2O as the solvent at 300K. 2D Nuclear Overhauser Effect SpectroscopY (NOESY) NMR experiments were performed on a 600 MHz Bruker Avance NEO spectrometer in D_2O at a temperature of 303 K using the states-TPPI method with a 5ms Z-gradient spoil pulse in the mixing time and zero-quantum suppression using the method of M.J. Thrippleton & J.Keeler.[30] Mixing time was set to 0.3 s, spectra were recorded using 20 scans per t1 increment and the spectral width was set to 8 x 8 ppm.

Isothermal Titration Calorimetry (ITC) experiments were performed at 25 °C using a MicroCal PEAQ-ITC microcalorimeter (Malvern-Panalytical, U.K.). Solutions were prepared in water. In a typical experiment, 19 injections of 2.0 µL of titrant were titrated into the sample cell over 2 s with a stirring speed of 750 rpm and 120 s separation to ensure thermal equilibration. Data were baseline adjusted by subtracting background data obtained from equivalent injections of titrant into solution. The titration curves were analysed using the integrated public-domain software packages NITPIC, SEDPHAT, and GUSSI.

GPC measurements were conducted on an Agilent 1260 infinity system operating in DMF with 5mM NH_4BF_4 and equipped with refractive index detector and variable wavelength detector, 2 PLgel 5 μm mixed-C columns (300×7.5mm), a PLgel 5 mm guard column (50x7.5mm) and an autosampler. The instrument was calibrated with linear narrow poly(methyl methacrylate) standards. All samples were passed through basic alumina to remove any copper residues and filtered with a 0.2 μm Nylon 66 before analysis.

Dynamic Light Scattering (DLS). The hydrodynamic diameters (D_h, the volume weight diameter of the distribution) evolution were determined characterised by a Malvern Zetasizer Nano ZS instrument equipped with a He−Ne laser at 633 nm. DLS measurements were performed by dissolving polymer samples at 1 mg/ml in deionised water and all the samples were passed through a 0.22 μm nylon filter before measurement. For complex samples, polymers were dissolved separately in deionised in water and mixed together at different molar ratio. Then the samples were stirred overnight at room temperature and filtered using a 0.22 nylon filter before analysis. All the samples were measured three times at 25 °C.

IV.4.3 Experimental procedures

IV.4.3.1 Synthesis of a heptamannose-*β*-cyclodextrin (CD-Man*7*)

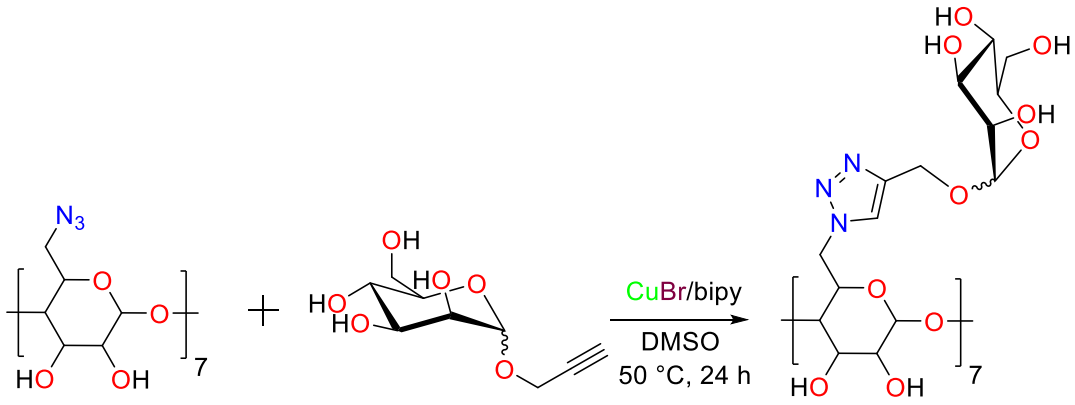

Scheme IV.4.1 Schematic representation of the synthetic approach to CD-$(Man)_7$.

β-CD-$(N_3)_7$ (1.96 g , 1.5 mmol), 1-(2‘-propargyl)-D-Mannose (2.61 g ,12 mmol) were dissolved in DMSO (20 mL) in a Schlenk tube. Bipyridine (0,37 g , 0.0024 mmol) and CuBr (0.17 g ,0.0012 mmol) were added. The resulting mixture was evacuated and filled with argon and 3 freeze-pump-thaw cycles were performed to eliminate oxygen from the reaction mixture. The mixture was then allowed to stir at 50 °C for 24 h. After the reaction, water was added to the reaction medium and the resulting mixture was dialysed against water. After dialysis, the resulting clear solution was freeze dried.

^{1}H NMR (DMSO-d6, 298 K, 400 MHz): δ = 7.95, 7.92 (s, overlapped, 7 H, NCH=C), 5.80-6.10 (m, 14 H, OH-2, OH-3 of CD), 5.10 (s, 7 H, H-1), 3.00-5.00 (m, CD & mannose residues, overlap with H_2O) ppm.

IV.4.3.2 Synthesis of a polymeric mannose bearing β-cyclodextrin (CD-(*p*Man$_8$)$_7$)

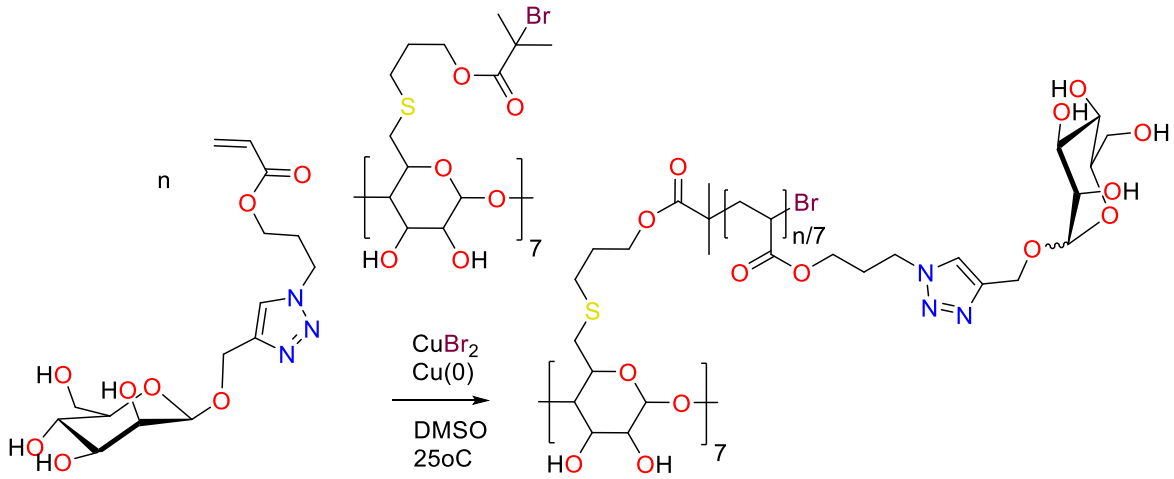

Scheme IV.4.2 Schematic representation of the homopolymerisation of the mannose glycomonomer achieving a polymeric mannose bearing *β*-cyclodextrin (CD-(*p*Man$_8$)$_7$

A Schlenk tube was charged with CD$_7$-initiator (10.0 mg, 2696.88 g/mol, 3.71 µmol), mannose glycomonomer (291 mg, 373.36 g/mol, 779 µmol, 30 eq. per initiating site), Me$_6$TREN (1.32 µL, 4.93 µmol, 0.19 eq. per initiating site), CuBr$_2$ (232 µg, 1.04 µmol, 1.04 eq. per initiating site) in DMSO (2 mL), sealed with a rubber septum and subsequently degassed by gentle bubbling of Ar gas for 15 min. The polymerisation was then started by addition of pre-activated Cu(0) wire (5 cm) wrapped around a stirring bar under a positive Ar pressure and quickly sealed again and the reaction mixture was allowed to polymerise for 1 h at 25˚C. Sampling was carried out using a degassed syringe to check the conversion of mannose glycomonomer. NMR samples was dissolved in DMSO-*d$_6$* and conversion was determined as 27.5% (8.3 monomers per arm) by comparing the triazole peak to the vinyl protons. After polymerisation the glycopolymer CD-*p*(Man$_8$)$_7$ was dialysed against water to remove excess glycomonomer and further impurities. Molecular weight of the polymer was then determined *via* ^{1}H NMR and was revealed to be 24.5 kDa on average.

IV.4.3.3 General procedure for *ada*PEI synthesis.

Linear polyethylenimine hydrochloride 40 kDa (PEI, 100 mg, 2.5 x 10^{-6} mol) was

suspended in 40 mL dry $CHCl_3$ in a 100 mL RBF under Ar, equipped with stirring bar and sonicated for 30 min. Subsequently the suspension was stirred and 1 mL of dry TEA was added. Afterwards, the suspension was sonicated for 30 min until a fine suspension was achieved. A solution of adamantane carbonyl chloride (50 mg, 2.515 x 10^{-4} mol, 0.2 eq. per repeating unit) in 10 mL dry $CHCl_3$ was prepared and subsequently added to the suspension. The mixture was allowed to stir overnight at ambient temperature. After the reaction the suspension was filtered over the MilliPore and washed with 2 x 30 mL $CHCl_3$ and an NMR sample was taken in D_2O. Subsequently the filtered residue was dissolved in 10 mL H_2O to which 1 mL of a 32% HCl solution in water was added. The solution was subsequently precipitated in acetone, filtered over the MilliPore and dried under vacuum. An NMR sample was taken in D_2O and average amount of adamantanes per chain were calculated by comparing the CH_2- peak to the amount of adamantane protons. Quantities for synthesis of other *ada*PEIs can be found in **Table IV.4.1.**

Table IV.4.1 Quantities used in adaPEI synthesis

***ada*PEI**	**PEI**	**Eq. of adamantane per monomer unit added**	**m (1-adamantane carbonyl chloride)**
PEI1	100 mg	0.4	99.93 mg
PEI2	100 mg	0.2	49.96 mg
PEI3	100 mg	0.1	24.98 mg
PEI4	100 mg	0.05	12.49 mg
PEI5	100 mg	0.025	6.25 mg
PEI6	100 mg	0.0125	3.13 mg

IV.4.3.4 Synthesis of *glyco*PEI: Complexation of *ada*PEI with CD-Man_7

A solution of *ada*PEI2 (30.2 mg, 41088 g/mol, 0.734 µmol) and CD-Man_7 (17.9 mg, 2836.53 g/mol, 6.26 µmol, 8.58 eq. per polymer chain) was prepared in 10 mL H_2O amounting to a 1 / 1 ratio of cyclodextrin derivative per adamantane and sonicated until the solution became clear. Subsequently the solution was transferred to a 20 mL glass vial and freeze-dried. An NMR sample was made by dissolving 10 mg in D_2O for Nuclear Overhauser Effect Spectroscopy (NOESY). Quantities for synthesis of other *ada*PEIs can be found in the Supporting Information **Table IV.2.2**.

IV.4.3.5 Synthesis of *glyco*PEI: Complexation of *ada*PEI with CD-(*p*Man$_8$)$_7$

A solution of *ada*PEI3 (30.1 mg, 40603 g/mol, 0.741 µmol) and CD-(*p*Man$_8$)$_7$ (86 mg, 24499 g/mol, 3.51 µmol, 4.75 eq. per polymer chain) was prepared in 10 mL H_2O amounting to a 1 / 1 ratio of gycopolymer CD-(*p*Man$_8$)$_7$ per adamantane and sonicated until the solution became clear. Subsequently the solution was transferred to a 20 mL glass vial and freeze-dried.

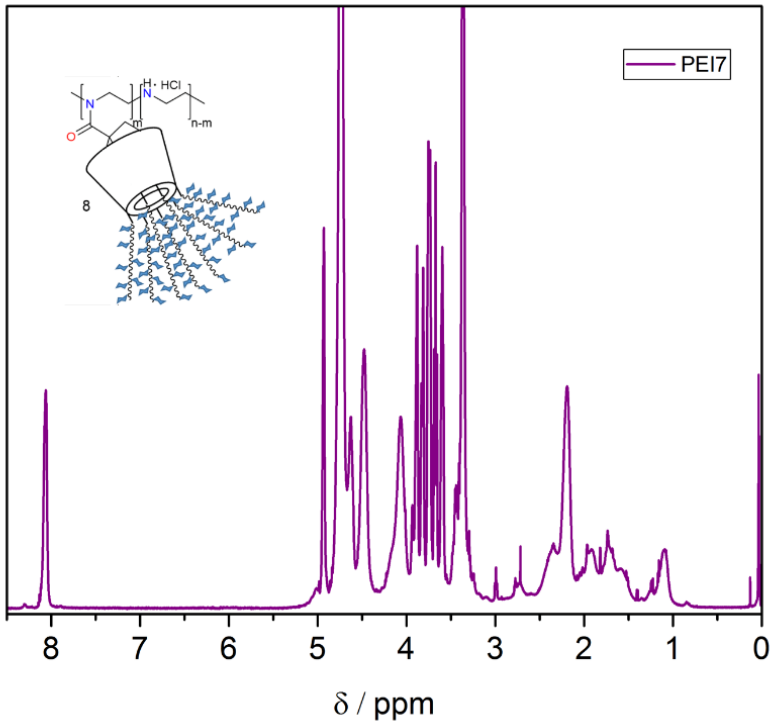

Figure IV.4.1 ^{1}H-NMR spectrum of the *glyco*PEI7 (adaPEI3 complexed with CD-(*p*Man$_8$)$_7$.

IV.4.3.6 *sa*RNA synthesis and purification*

Self-amplifying RNA encoding the non-structural proteins (NSPs) from the Venezuelan Equine Encephalitis Virus (VEEV) and either firefly luciferase (fLuc) or enhanced green fluorescent protein (eGFP) was prepared using *in vitro* transcription. *p*DNA was transformed into *Eschericia coli* and cultured in 50 mL of LB broth with 1 mg/mL carbenicillin (Sigma Aldrich, UK) and isolated using a Plasmid Plus Maxiprep kit (QIAGEN, UK). pDNA concentration and purified were quantified on a NanoDrop One (ThermoFisher, UK) and then linearised using MluI for 2 h at 37 °C and heat inactivated

at 80 °C for 20 min. Co-transcriptionally capped *sa*RNA, used for *in vitro* experiments, was synthesised using 1 µg of linearised DNA template in a mMessage mMachine reaction (Promega, UK) according to the manufacturer's protocol, and purified using a MEGAclear column (Invitrogen, UK) according to the manufacturer's protocol. For *ex vivo* experiments, uncapped *in vitro* RNA transcripts were synthesised using 1 µg of linearised DNA template in a MEGAScript reaction (Promega, UK) according to the manufacturer's protocol. Transcripts were then purified by overnight LiCl precipitation at -20 °C, pelleted by centrifugation at 14,000 RPM for 20 min, washed with 70% EtOH, centrifuged at 14,000 RPM for 5 min, and then resuspended in UltraPure H_2O. Purified transcripts were then capped using the ScriptCap™ and m^7G Capping System (CellScript, Madison, WI, USA) and ScriptCap™ 2'-O-Methyltransferase Kit (CellScript, Madison, WI, USA) simultaneously according to the manufacturer's protocol. Capped transcripts were then purified again by LiCl precipitation and stored at -80 °C in a buffer of 10 mM HEPES with 100 mg/mL trehalose until use.

IV.4.3.7 Particle complexation and characterisation*

Stock solutions of glycopolymers were prepared at a concentration of 5 mg/mL in ultrapure H_2O and purified using a 0.22 µm syringe filter (Millipore, Sigma, UK). saRNA complexes were prepared by mixing the RNA and polymer in 20 mM HEPES buffer (pH 7.4) with 5% glucose, with a ratio of polymer to RNA of 5:1 (w/w) unless otherwise specified. The solution was immediately vortexed for 30 seconds and then allowed to rest for 10 minutes prior to use.

Polyplexes were prepared in a volume of 800 µL of 20 mM HEPES with 5% glucose for particle size and charge analysis, and characterised on a Zetasizer NanoZS (Malvern Instruments, UK) with Zetasizer 7.1 software (Malvern Instruments, UK) in a clear disposable 1 mL cuvette. The polyplexes were analysed using the following settings: a material refractive index of 1.529, absorbance of 0.010, dispersant viscosity of 0.8820 cP, refractive index of 1.330 and dielectric constant of 79. Each sample was analysed three times for up to 100 runs or until the measurement stabilised.

IV.4.3.8 *In vitro* transfection and luciferase assay*

HEK 293T.17 cells (ATCC, USA) were plated at a density of 50,000 cells/well 48 hours prior to transfection. The polyplexes were added to each well in a total volume of 100 µL with a total dose of 100 ng of RNA in 20 mM HEPES with 5% glucose with n=3. The cells were then incubated with the polyplexes for 4 hours, and then the media was replaced with 100 µL of complete Dulbecco's Modified Eagle's Medium (cDMEM) (with 10% fetal bovine serum (FBS), 5 mg/mL L-glutamine, 5 mg/mL penicillin streptomycin (ThermoFisher, UK)). After 24 hours, 50 uL of media was removed and 50 uL of ONE-Glo™ luciferase substrace (Promega, UK) was added, and the total 100 µL was transferred to a white 96-well plate and analyzed on a FLUOstar Omega plate reader (BMG LABTECH, UK) with a gain of 4000. The average of the media only wells were subtracted from each sample measurement.

IV.4.3.9 Human skin explant culture and digestion*

Surgically resected specimens of human skin tissue were collected at Charing Cross Hospital, Imperial College London, UK. All tissues were collected after receiving signed, informed consent from all patients under protocols approved by the Local Research Ethics Committee. The tissue was obtained from patients undergoing elective abdominoplasty, breast reduction or mastectomy surgeries. Tissue was refrigerated until arrival in the laboratory. The subcutaneous layer of fat was completely removed, and the remaining skin layers were trimmed into ~1 cm^2 sections. Explants were cultured in 10 mL of cDMEM in a petri dish at 37 °C and 5% CO_2, and the media was refreshed daily.

Explants were injected with 2 µg of saRNA in a volume of 50 µL intradermally (ID) using a Micro-Fine Demi 0.3 mL syringe (Becton Dickinson, UK). After 3 days, skin was digested as previously described.[9] Briefly, explants were minced well with scissors and incubated in 2 mL DMEM supplemented with 1 mg/mL collagenase P (Sigma, UK) and 5 mg/mL dispase II (Sigma, UK) for 4 hours at 37°C on a rotational shaker. Digests were then filtered through a 70 µm cell strainer and centrifuged for 5 min at 1750 RPM. Cells were resuspended in 100 µL of FACS buffer (PBS + 2.5% FBS) and stained with 100 µL of Aqua Live/Dead Stain (ThermoFisher, UK) diluted 1:400 in FACS buffer for 20 min on ice. Cells were then washed with 1 mL of FACS buffer, centrifuged at 1750 RPM for 5 min and stained with a panel of antibodies to identify cellular phenotypes for 30

minutes. Cells were then washed with 1 mL of FACS buffer, centrifuged at 1750 RPM for 5 minutes and resuspended in 250 µL of PBS. Cells were fixed with 250 µL of 3% paraformaldehyde for a total concentration of 1.5% and refrigerated until flow cytometry analysis.

IV.4.3.10 Flow cytometry analysis*

Single cell suspensions were analyzed on a LSRFortessa™ (BD Biosciences, UK) using FACSDiva software (BD Biosciences, UK) with 100,000 acquired events. Gating was performed as previously described.[9] GFP^+ cells and phenotypes were quantified using FlowJo Version 10 (FlowJo LLC, Oregon, USA).

IV.4.3.11 Statistical analysis*

Graphs and statistical analysis of *in vitro* and *ex vivo* data were prepared in GraphPad Prism, version 8.0. Statistical analysis was performed using a two-tailed t test or a one way ANOVA adjusted for multiple comparisons with $\alpha=0.05$ used to indicate significance.

IV.5 References

(1) Perri, S.; Greer, C. E.; Thudium, K.; Doe, B.; Legg, H.; Liu, H.; Romero, R. E.; Tang, Z.; Bin, Q.; Dubensky, T. W.; Vajdy, M.; Otten, G. R.; Polo, J. M. *J. Virol.* **2003**, *77* (19), 10394.

(2) Chahal, J. S.; Khan, O. F.; Cooper, C. L.; McPartlan, J. S.; Tsosie, J. K.; Tilley, L. D.; Sidik, S. M.; Lourido, S.; Langer, R.; Bavari, S.; Ploegh, H. L.; Anderson, D. G. *Proc. Natl. Acad. Sci. U. S. A.* **2016**, *113* (29), E4133.

(3) Geall, A. J.; Verma, A.; Otten, G. R.; Shaw, C. A.; Hekele, A.; Banerjee, K.; Cu, Y.; Beard, C. W.; Brito, L. A.; Krucker, T.; O'Hagan, D. T.; Singh, M.; Mason, P. W.; Valiante, N. M.; Dormitzer, P. R.; Barnett, S. W.; Rappuoli, R.; Ulmer, J. B.; Mandl, C. W. *Proc. Natl. Acad. Sci. U. S. A.* **2012**, *109* (36), 14604.

(4) Bogers, W. M.; Oostermeijer, H.; Mooij, P.; Koopman, G.; Verschoor, E. J.; Davis, D.; Ulmer, J. B.; Brito, L. A.; Cu, Y.; Banerjee, K.; Otten, G. R.; Burke, B.; Dey, A.; Heeney, J. L.; Shen, X.; Tomaras, G. D.; Labranche, C.; Montefiori, D. C.; Liao, H. X.; Haynes, B.; Geall, A. J.; Barnett, S. W. *J. Infect. Dis.* **2015**, *211* (6), 947.

(5) Evans, C. F.; Dolter, K. E.; Song, J.; Luxembourg, A.; Bernard, R.; Hannaman, D. *Mol. Ther.* **2008**, *16*, S91.

(6) Pardi, N.; Hogan, M. J.; Porter, F. W.; Weissman, D. *Nat. Rev. Drug Discov.* **2018**, *17* (4), 261.

(7) Lundstrom, K. *Vaccines* **2016**, *4* (4), 39.

(8) McCullough, K. C.; Bassi, I.; Milona, P.; Suter, R.; Thomann-Harwood, L.; Englezou, P.; Démoulins, T.; Ruggli, N. *Mol. Ther. - Nucleic Acids* **2014**, *3*, e173.

(9) Blakney, A. K.; McKay, P. F.; Ibarzo Yus, B.; Hunter, J. E.; Dex, E. A.; Shattock, R. J. *ACS Nano* **2019**, *13* (5), 5920.

(10) Démoulins, T.; Milona, P.; Englezou, P. C.; Ebensen, T.; Schulze, K.; Suter, R.; Pichon, C.; Midoux, P.; Guzmán, C. A.; Ruggli, N.; McCullough, K. C. *Nanomedicine Nanotechnology, Biol. Med.* **2016**, *12* (3), 711.

(11) Blakney, A. K.; Yilmaz, G.; McKay, P. F.; Becer, C. R.; Shattock, R. J. *Biomacromolecules* **2018**, *19* (7), 2870.

(12) Liang, F.; Lindgren, G.; Lin, A.; Thompson, E. A.; Ols, S.; Röhss, J.; John, S.; Hassett, K.; Yuzhakov, O.; Bahl, K.; Brito, L. A.; Salter, H.; Ciaramella, G.; Loré, K. *Mol. Ther.* **2017**, *25* (12), 2635.

(13) Veiga, N.; Goldsmith, M.; Granot, Y.; Rosenblum, D.; Dammes, N.; Kedmi, R.; Ramishetti, S.; Peer, D. *Nat. Commun.* **2018**, *9* (1), 4493.

(14) Willoughby, J. L. S.; Chan, A.; Sehgal, A.; Butler, J. S.; Nair, J. K.; Racie, T.;

Shulga-Morskaya, S.; Nguyen, T.; Qian, K.; Yucius, K.; Charisse, K.; van Berkel, T. J. C.; Manoharan, M.; Rajeev, K. G.; Maier, M. A.; Jadhav, V.; Zimmermann, T. S. *Mol. Ther.* **2018**, *26* (1), 105.

(15) Pun, S. H.; Bellocq, N. C.; Liu, A.; Jensen, G.; Machemer, T.; Quijano, E.; Schluep, T.; Wen, S.; Engler, H.; Heidel, J.; Davis, M. E. *Bioconjug. Chem.* **2004**, *15* (4), 831.

(16) Miyauchi, M.; Harada, A. *J. Am. Chem. Soc.* **2004**, *126* (37), 11418.

(17) Wang, J.; Jiang, M. *J. Am. Chem. Soc.* **2006**, *128* (11), 3703.

(18) Yilmaz, G.; Uzunova, V.; Napier, R.; Becer, C. R. *Biomacromolecules* **2018**, *19* (7), 3040.

(19) Kauscher, U.; Ravoo, B. J. *Beilstein J. Org. Chem.* **2012**, *8* (1), 1543.

(20) Zhang, Q.; Su, L.; Collins, J.; Chen, G.; Wallis, R.; Mitchell, D. A.; Haddleton, D. M.; Becer, C. R. *J. Am. Chem. Soc.* **2014**, *136* (11), 4325.

(21) Vigerust, D. J.; Vick, S. *J. Clin. Cell. Immunol.* **2015**, *06* (03), 1.

(22) Hajj, K. A.; Ball, R. L.; Deluty, S. B.; Singh, S. R.; Strelkova, D.; Knapp, C. M.; Whitehead, K. A. *Small* **2019**, *15* (6), 1805097.

(23) McKenzie, E. J.; Taylor, P. R.; Stillion, R. J.; Lucas, A. D.; Harris, J.; Gordon, S.; Martinez-Pomares, L. *J. Immunol.* **2007**, *178* (8), 4975.

(24) Wollenberg, A.; Mommaas, M.; Oppel, T.; Schottdorf, E. M.; Günther, S.; Moderer, M. *J. Invest. Dermatol.* **2002**, *118* (2), 327.

(25) Hespanhol, R. C.; Soeiro, M. de N. C.; Meuser, M. B.; Meirelles, M. de N. S. L.; Côrte-Real, S. *J. Histochem. Cytochem.* **2005**, *53* (1), 35.

(26) Lee, S. H.; Charmoy, M.; Romano, A.; Paun, A.; Chaves, M. M.; Cope, F. O.; Ralph, D. A.; Sacks, D. L. *J. Exp. Med.* **2018**, *215* (1), 357.

(27) Linehan, S. A. *BMC Immunol.* **2005**, *6* (1), 4.

(28) Fanibunda, S. E.; Modi, D. N.; Gokral, J. S.; Bandivdekar, A. H. *PLoS One* **2011**, *6* (11), e28014.

(29) Oz, Y.; Abdouni, Y.; Yilmaz, G.; Becer, C. R.; Sanyal, A. *Polym. Chem.* **2019**, *10* (24), 3351.

(30) Thrippleton, M. J.; Keeler, J. *Angew. Chemie Int. Ed.* **2003**, *42* (33), 3938.

Chapter 5

Single-chain folding glyconanoparticles, a supramolecular system

In this chapter, we describe the physicochemical characterisation of amphiphilic glycopolymers synthesised via Single-Electron Transfer – Living Radical Polymerisation (SET-LRP). Depending on the chemical composition of the polymer, these glycopolymers are able to fold into multi-chain or single-chain polymeric nanoparticles (SCPNs). The folding of these polymers is first of all based on the amphiphilicity of the glycopolymers and furthermore on the supramolecular formation of helical supramolecular stacks of benzene-1,3,5-tricarboxamides (BTAs) stabilised by threefold hydrogen bonding and π- π stacking along the polymer chain. The obtained polymeric nanoparticles were subsequently evaluated for their lectin-binding affinity towards a series of mannose- and galactose-binding lectins via Surface Plasmon Resonance (SPR).

SPR measurements were performed by Dr. G. Yilmaz and Miss A. Monaco, SAXS measurements were performed by Dr. G.M. ter Huurne

Parts of this chapter have been performed in close collaboration with Dr. G.M. ter Huurne and Dr. A.R.A. Palmans at the T.U. Eindhoven, Netherlands

V Single-chain folding glyconanoparticles, a supramolecular system

V.1 Introduction

Recent advances in polymer science, ranging from sequence-controlled polymers to single-chain folding polymeric nanoparticles have made it possible to mimic Nature's machinery closer than ever by introducing new levels of structural control and even function into our polymer chains.[1,2] Myriad macromolecules common in Nature such as proteins, nucleic acids and glycans are built upon basic principles of a limited number of 'monomers' (amino acids, nucleic acids and carbohydrates) orderly attached to one another, which translates further to a controlled folding and finally delivers specific function.[3]

Due to the significant difficulty in synthesis of complex glycans, owing to their inherently branched structure, polymer chemists have sought ways of synthesizing possible biomimetics for these highly functional structures.[4] Myriad synthetic glycostructures have been synthesised and evaluated in biological platforms, both in vitro and ex vivo.[5] The significance of these highly branched carbohydrates is evidenced by their major role in cellular processes such as signal transduction, intercellular recognition but also for other processes such as the protection against and recognition of pathogens.[6,7] Lectins or carbohydrate binding proteins form interesting targets thanks to the processes they affect. Lectin binding affinity (to synthetic glycostructures) can notably be enhanced by what is known as the "glycocluster effect". The glycocluster effect can be defined as the increase in binding affinity originating from multivalent lectin-carbohydrate interactions.[8,9] This glycocluster effect has extensively been exploited by polymer chemists in the hopes of discovering new molecular designs with improved binding avidity.[10–12]

After a surge in sequence-controlled glycopolymers over the last decade it has become clear that also in glycopolymer science, the next stage in the design of improved architectures would be the introduction of single-chain folding polymer technology.[13–15] A plethora of novel polymeric structures based on the reversible and/or non-reversible folding ability of polymeric nanoparticles have paved the way for glycoscience to step up its game into this new exciting field.[16,17] Altintas *et al.*, state that two main approaches can be followed, namely 'selective point folding' and 'repeat unit folding'. Repeat unit folding is the synthetically most accessible of the two, however it results in a less-defined and chaotic collapse. For the design of single-chain polymeric glyconanoparticles it is important however that the intramolecular linkages are compatible with the medium in which these structures are dissolved and thus have to be stable in water. Stenzel *et al.*, have taken the lead into these glyco-SCPNs by employing covalent techniques such as the use of 'click'-inspired thiol-Michael additions and light-induced profluorescent nitrile-imine-mediated tetrazole-*ene* cycloadditions.[18–20]

Another means of inducing the collapse of a polymer chain into a single-chain polymeric nanoparticle, is the use of solvophobic effects. By synthesizing amphiphilic random copolymers of poly(ethylene glycol) (PEG) and alkyl pendant groups, Terashima *et al.*, were able to induce reversible single-chain folding in water.[21,22] Other supramolecular interactions that are heavily exploited include the use of hydrogen bonding groups.[23–25] Benzene-1,3,5-tricarboxamides (BTAs) have proven to be a versatile platform for the control of single polymer chain conformations, as BTAs have the inherent ability to self-assemble into supramolecular polymers *via* π-π stacking and threefold hydrogen bonding.[26–28]

As mentioned *vide supra*, lectins are able to bind glycans with great specificity. Here, newly developed glycopolymeric nanoparticles are evaluated towards C-type lectins and two galactose binding lectins called Galectin-3 and RCA. C-type lectin receptors (CLRs) form a large family composed of both secreted and transmembrane proteins containing calcium dependent carbohydrate recognition domains known as C-type lectin-like domains (CTLD).[29] The dendritic cell-specific intracellular adhesion molecules (ICAM)-3 grabbing non-integrin (DC-SIGN or CD209), the liver/lymph node-specific ICAM-3 grabbing non-integrin (L-SIGN, DC-SIGNR or CD209L), the C-type lectin-like receptor -1 (CLEC-1) and the dendritic cell-associated C-type lectin-2 (Dectin-2) are important members of a subdivision classified as pattern recognition receptors.[30–32] The mannose-binding lectin (MBL) and also surfactant protein-D (SP-D) are both C-type lectins which are members of the collectin family and are involved in the detection

and clearance of dying and dead cells.[33] These processes are crucial for the maintenance of tissue and organ homeostasis. Other lectins in this study that are able to detect cell-death include the dendritic and epithelial cell receptor (DEC205) and the dendritic cell natural killer (NK) lectin group receptor 1 (DNGR1) which are membrane-bound CLRs. [34–36] The last C-type lectin in this study is the Langerhans cell-specific C-type lectin (Langerin or CD207). Langerin plays an important protective role in the recognition of HIV glycoproteins and more in general, prompts the uptake and degradation of viral particles. [37,38] The other two lectins, Galectin-3 and RCA_{120} are both galactose binding lectins. Galectin-3 is part of the Galectin family which affects numerous biological processes such as immune reaction, development and metastasis.[39] Ricinus communis agglutinin or RCA_{120} on the other hand, is a lectin present in castor beans, known in popular culture for its highly toxic properties.[40]

In this work we present the synthesis and physicochemical characterisation of novel chain folding glycopolymers based on both amphiphilicity of the glycopolymer chain and through the use of BTAs along the polymer chain *via* the 'repeat unit folding' method. Finally the mannose and galactose containing nanoparticles were tested for their binding ability towards the lectins mentioned above, in order to investigate the influence of nanoparticle formation on binding affinity.

V.2 Results

V.2.1 Synthesis of a galactose glycomonomer

Similar as in Chapter 3, the first step in making glycopolymers is the synthesis of a suitable glycomonomer. In this chapter, we synthesised a galactose glycomonomer using similar conditions as in Chapter 3. The galactose glycomonomer that we synthesised here is also an acrylate which polymerises similarly as the previously made mannose glycomonomer. To achieve this, *D*-galactose was treated with propargyl alcohol in the presence of silica supported sulphuric acid. Because of the different position of the hydroxyl group at the C2, the propargylation (which can visually be seen by dissolution of the sugar into the reaction medium) took longer up to 2 days instead of overnight. Subsequently 3-azidopropyl acrylate was prepared by reacting sodium azide with 3-bromopropanol and the resulting 3-azidopropanol was then reacted with acryloyl chloride as previously reported in Chapter 3. Finally galactose acrylate was achieved by 'clicking' the propargyl-*D*-galactose to 3-azidopropyl acrylate using the well-known copper (I)-catalysed azide-alkyne cycloaddition (CuAAC) "click" reaction.

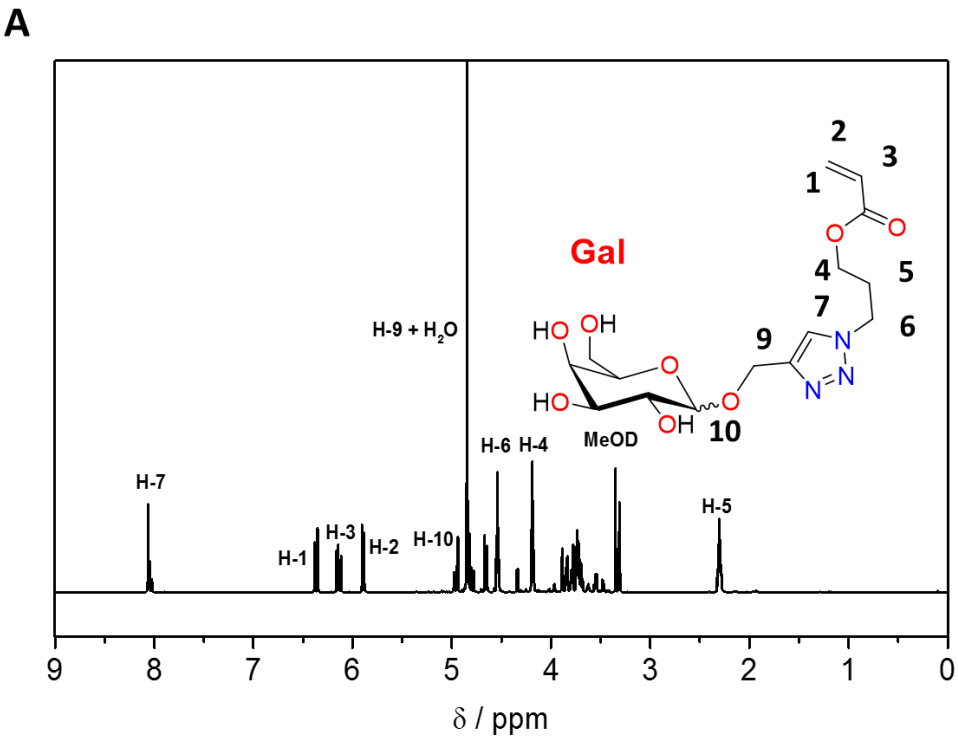

Figure V.2.1 A) ^{1}H-NMR spectrum of *D*-galactose acrylate in MeOD

V.2.2 Synthesis of a BTA monomer

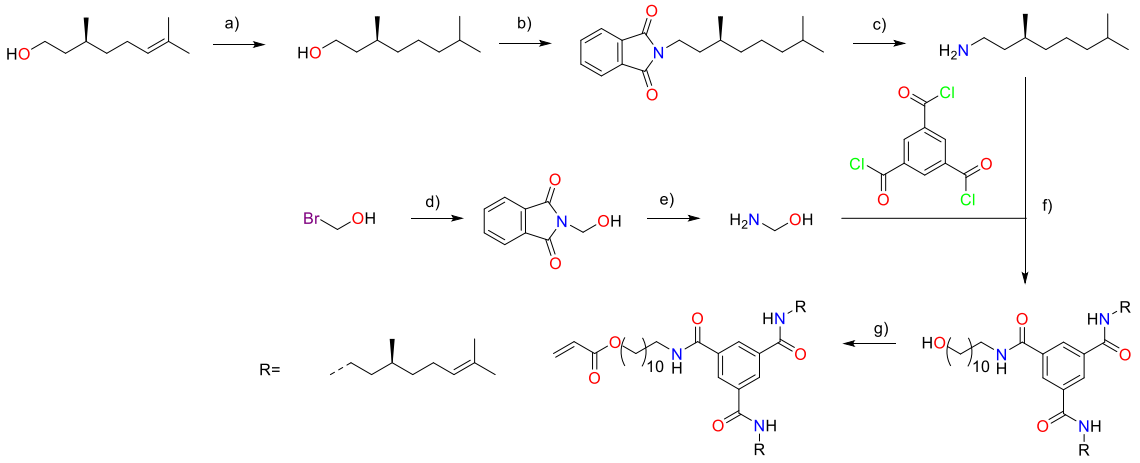

Scheme V.2.1 Synthesis of BTA acrylate: a) H_2, Pd/C (cat.), EtOAc; b) phthalimide, DIAD, PPh_3, Et_2O; c) H_2NNH_2•H_2O, THF, 90 ˚C; d) potassium phthalimide, DMF, 70 ˚C; e) H_2NNH_2•H_2O, THF, 90 ˚C; f) Et_3N, $CHCl_3$, 0 ˚C; g) acryloyl chloride, Et_3N, CH_2Cl_2, 0 ˚C.

In this Chapter, we worked in close collaboration with the group of prof. E.W. Meijer at the Eindhoven University of Technology, especially with prof. Dr. Anja R.A. Palmans and Dr. Gijs M. ter Huurne who are experts in the field of supramolecular polymerisations and single-chain folding polymeric nanoparticles. They were so kind to provide us with a compound described further as BTA-OH (a chiral BTA-bearing alcohol) synthesised as reported.[41] After receipt of the BTA-OH we subsequently converted it using acryloyl chloride in dichloromethane and purified *via* column chromatography, achieving the desired BTA acrylate.

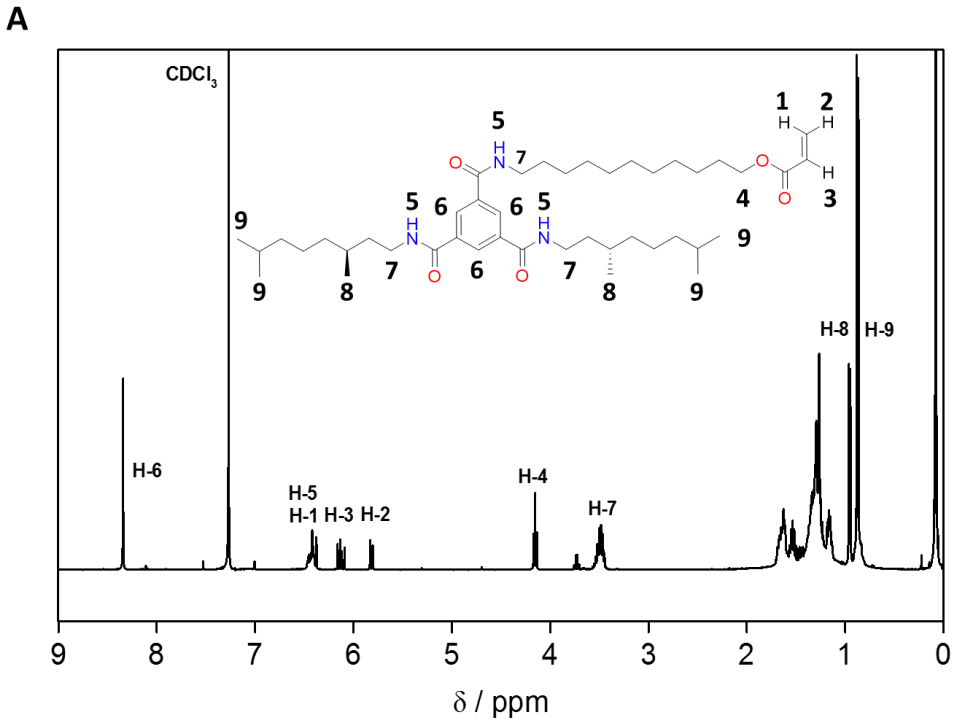

Figure V.2.2 A) ^{1}H-NMR spectrum of BTA acrylate in $CDCl_3$

V.2.3 Synthesis and characterisation of the copolymers

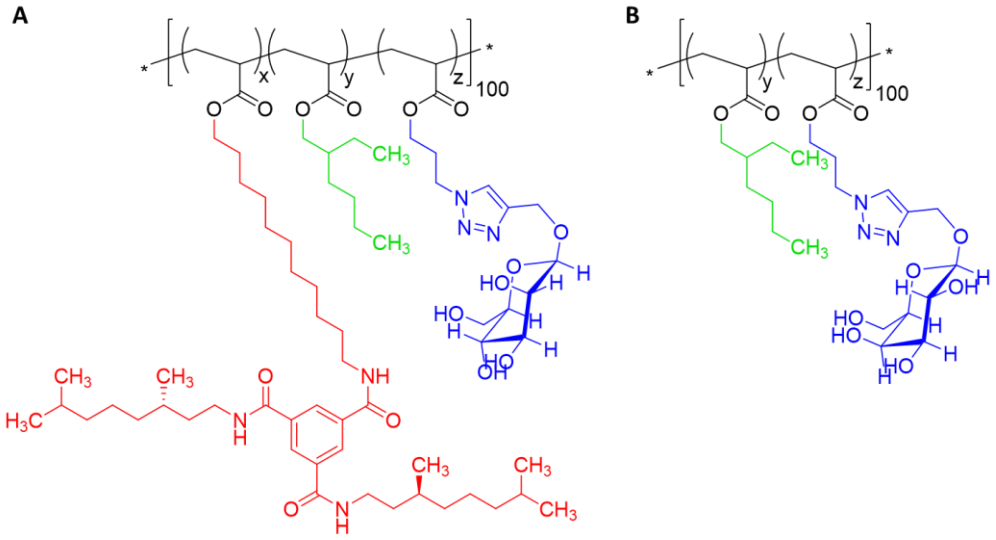

Figure V.2.3 Chemical structures of the amphiphilic glycopolymers A) Set 1 containing mannose acrylate, ethyl hexyl acrylate and BTA acrylate B) Set 2 containing galactose acrylate and ethyl hexyl acrylate

Previous studies using BTAs to induce supramolecular folding of a copolymer chain, used polyethylene glycol chains in order to make the particles water soluble. In this work water solubility is not achieved using PEG grafts but the highly water soluble nature of carbohydrates grafted along the polymer backbone. Three distinct sets of glycopolymers were prepared using conventional SET-LRP. Set 1A consists of glycopolymers containing an acrylic mannose monomer and 2-ethylhexyl acrylate (EHA), Set 1B on the other hand contains and additional acrylic monomer displaying a benzene-1,3,5-tricarboxamide (BTA) (**Fig V.2.3A**). Finally Set 2 consists of polymers containing an acrylic galactose monomer and EHA (**Figure V.2.3B**). Both glycomonomers (mannose acrylate and galactose acrylate) were synthesised as previously published and as reported in Chapter 3 and section V.2.1.[42] The third acrylic monomer containing a chiral BTA was achieved by reacting BTA-OH (which was synthesised as previously reported) with acryloyl chloride resulting in a chiral BTA-acrylate as discussed in section V.2.2.[28]

The synthesis of the glycopolymers was then accomplished *via* SET-LRP in DMSO. The goal was to achieve glycopolymers with a length of roughly 100 monomer units. For this a Schlenk tube was charged with ethyl α-bromoisobutyrate as the initiator, Me_6TREN, $CuBr_2$, the relevant glycomonomer, EHA, DMSO and in the case of Set 1b the BTA-acrylate, all with a combined monomer to initiator ratio of 200:1. The resulting

mixture was then degassed by bubbling Ar gas through the solution. The polymerisation was then started by addition of a pre-activated Cu(0) wire (5 cm) wrapped around the stirring bar under a positive Ar pressure and quickly sealed again and the reaction mixture was allowed to polymerise at 25˚C. The conversion of all polymers was monitored using ^{1}H-NMR by comparing the signals of the vinyl protons (H_2C=CH-CO–)(≈ 6.5-5.5 ppm) to the glycomonomer's triazole proton (≈ 8.2-7.9 ppm) and the polymerisation was stopped at roughly 50% conversion by removing the Cu(0) wire. The resulting glycopolymers were then dialysed against water to remove the remaining glycomonomers and subsequently gradually dialysed against a mixture of water/THF (2:1) to (1:2) to remove the remaining EHA and BTA-acrylate.

The resulting glycopolymers were furthermore analysed *via* ^{1}H-NMR and GPC to determine the chemical composition and polymer properties (**Table V.2.1**). ^{1}H-NMR spectra revealed that the hydrophobic content of the polymers (EHA and BTA) was higher than anticipated. Gel permeation chromatography was performed using DMF as eluent and PMMA standards and revealed slightly elevated dispersities (*Đ*) ranging between 1.23 and 1.65, attributed to the long reaction times (+24h) as the hydrophobic monomers are not good monomers for SET-LRP.

Table V.2.1 Summary of monomer conversions (*ρ*), degree of polymerisation (DP), glycopolymer composition (CHO = carbohydrate, EHA = ethylhexyl acrylate, BTA = BTA acrylate), number average molar masses as determined by NMR ($M_{n,NMR}$) and by GPC ($M_{n,GPC}$) and dispersities (*Đ*) of glycopolymer Set 1 and Set 2.

Polymer	ρ^{a}_{NMR} (%)	*DP*	Composition,$_{theo}$ (%)			Composition,$_{NMR}$ (%)			$M_{n,NMR}$[b] (g.mol^{-1})	$M_{n,GPC}$[c] (g.mol^{-1})	*Đ*
			CHO	EHA	BTA	CHO	EHA	BTA			
Set 1 Mannose glycopolymers											
M90-10	73	146	90	10	-	83.8	16.2	-	50200	35600	1.29
M85-15	68	136	85	15	-	74.9	25.1	-	44500	34000	1.29
M80-20	74	148	80	20	-	68	32	-	46500	38200	1.29
M75-25	58	116	75	25	-	67.7	32.3	-	36400	25000	1.27
M70-30	54	108	70	30	-	67	33	-	34400	20900	1.58
M100-0-0	51	102	100	-	-	100	-	-	38300	20600	1.48
M97-0-2.5	75	150	97.5	-	2.5	97.7	-	2.3	55650	28500	1.23
M95-0-5	58	116	95	-	5	95.7	-	4.3	42600	29700	1.28
M90-0-10	40	80	90	-	10	84.6	-	15.4	27700	17500	1.56
M80-17-2.5	49	98	80	17.5	2.5	71	26.8	2.2	45270	23700	1.22
M72-23-5	53	106	72.5	22.5	5	71.6	22.2	6.1	46400	23350	1.66
M75-15-10	40	80	75	15	10	71.8	14.3	13.8	31700	17850	1.62
Set 2 Galactose glycopolymers											
G100-0	200	50	100	0	-	100	-	-	37500	24100	1.40
G95-5	200	66	95	5	-	89.1	10.9	-	46760	32500	1.53
G90-10	200	59	90	10	-	86	14	-	41100	33400	1.39
G85-15	200	51	85	15	-	81.5	18.5	-	34700	28000	1.35
G80-20	200	54	80	20	-	76	24	-	35600	26600	1.29

Conversion (*ρ*) obtained from ^{1}H-NMR; [b] $M_{n,NMR}$ = (Based on conversion and composition as calculated by ^{1}H-NMR); [c] Determined by DMF GPC (relative to PMMA stn.).

V.2.4 Sample preparation procedure

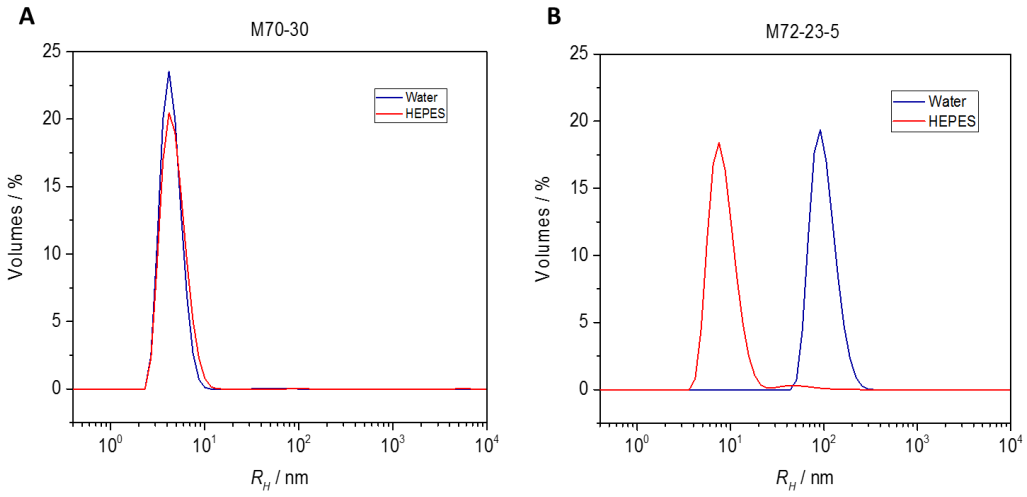

Figure V.2.4 DLS volumes size distribution of mannose glycopolymers ($c_{polymer}$ = 1 mg mL^{-1} in water and HEPES buffered saline, T = 20 ˚C), A) polymer M70-30 containing mannose and EHA and B) polymer M72-23-5 containing mannose, EHA and BTA

Preliminary DLS results performed on the samples revealed that the sample preparation procedure showed to be crucial for the dissolution and desired chain folding and aggregation behaviour of the amphiphilic glycopolymers (**Figure V.2.1**). In this work, dissolution of the amphiphilic glycopolymers was performed both in HEPES buffered saline and in deionized water. HEPES buffered saline was used here as it is more representative for the physiological environment and for later SPR measurements. Dissolution was facilitated by three cycles of the following: 45 min of sonication at 60 ˚C and subsequent heating for 45 min at 95 ˚C. Subsequently, the samples were allowed to slowly cool down overnight in the oven and afterwards the samples were filtered using a 100 nm PVDF filter. As can be seen from de DLS graphs, non-BTA containing polymers are easily dissolved with a low hydrodynamic radius (< 10 nm) both in HEPES buffered saline and in water. On the other hand BTA containing polymers proved to dissolve better in HEPES buffer saline and HEPES buffer saline showed to disrupt intermolecular interactions more easily.

V.2.5 Conformation of the glycopolymers

The effect of glycopolymer composition on the conformation in solution of the particles was studied using small-angle X-ray scattering (SAXS) experiments. At lower *q* values the acquired scattering profiles were levelling off as is typical for small polymeric nanoparticles in solution.

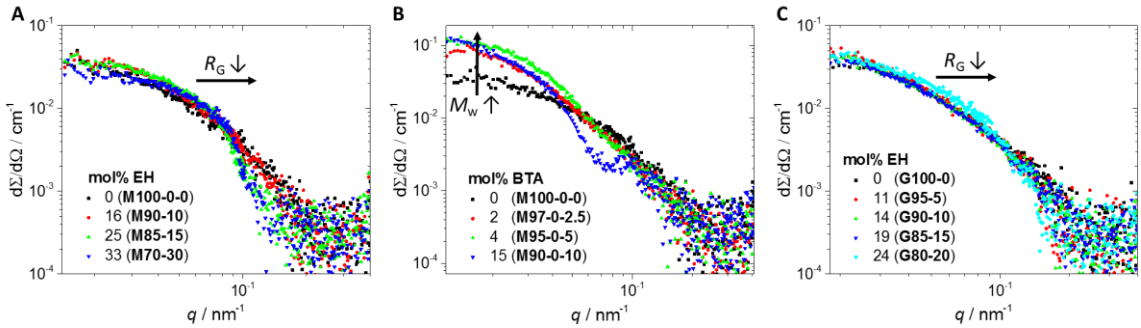

Figure V.2.5 Comparison of the SAXS curves for the synthesised glycopolymers ($c_{polymer}$ = 1 mg mL^{-1} in HEPES buffered saline, T = 20 ˚C) with (A) Set 1a consisting of mannose glycopolymers and EHA, (B) Set 1b comprised of mannose glycopolymers containing BTA and (C) Set 2 consisting of galactose glycopolymers and EHA.

Table V.2.2 Overview of the effect of EHA (ethylhexyl acrylate) content on the Aggregation Number (N_{agg}) and the Radius of Gyration (R_G) for Set 1A

Polymer	EHA content	Estimated N_{agg}	R_G
	mol%	-	nm
M100-0-0	0	1.1	4.1
M90-10	16	1.0	3.8
M85-15	25	1.1	3.4
M70-30	33	1.0	2.6

In glycopolymer Set 1A, the point at which the curves start to decay shifts to higher *q* values as a function of hydrophobic content which shows that the particles become smaller (**Figure V.2.2A** and **Table V.2.2**). Furthermore it can be seen that the slope of decay becomes steeper when increasing the EHA content indicating more compact particles. Apart from these observations, the scattering profiles for all polymers in Set 1A remained featureless. Based on these observations, we can conclude that the incorporation of more EHA results in smaller and more compact single-chain nanoparticles.

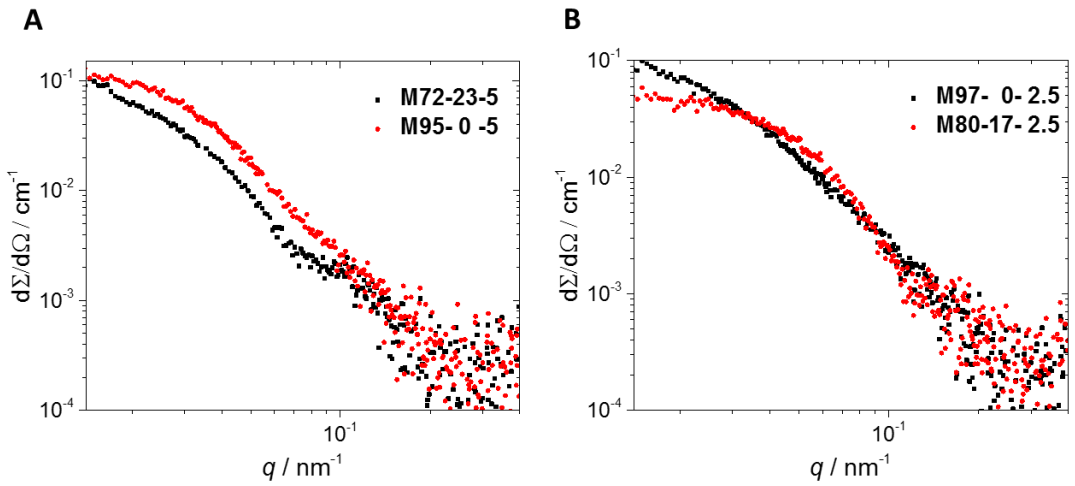

Figure V.2.6 Comparison of the SAXS curves for BTA containing glycopolymers ($c_{polymer}$ = 1 mg mL^{-1} in HEPES buffered saline, T = 20 ˚C) with (A) polymers with 5% BTA, (B) polymers with 2.5% BTA

Table V.2.3 Overview of the effect of the BTA content on the Aggregation Number (N_{agg}) and the Radius of Gyration (R_G) for Set 1B

Polymer	BTA content	Estimated N_{agg}	R_G
	mol%	-	nm
M100-0-0	0	1.0	4.1
M97-0-2.5	2	1.8	6.1
M95-0-5	4	2.9	5.5
M90-0-10	15	6.9	9.0

When BTA's are added to the polymer composition such as in Set 1B, additional features appear. Looking at the polymers only containing mannose and BTA we can first of all observe that with increasing BTA content the value at $q \rightarrow 0$, becomes higher, which indicates a higher mass of the formed particles (**Figure V.2.2B** and **Table V.2.3**). Secondly, increasing the BTA content shifts the point at which the curves starts to decay to lower q values, this indicates an increase in particle size. For polymer M90-0-10, an additional decay can be observed which indicates the presence of an additional small internal structure. As with the increase in EHA, adding more BTA and thus hydrophobic content to the polymer composition results in more compact particles. We can conclude that the incorporation of more BTAs, induces clustering of the glycopolymers into small multi-chain polymeric nanoparticles.

Table V.2.4 Comparison of the effect of the BTA and EHA content on the Aggregation Number (N_{agg}) and the radius of gyration (R_G) for Set 1b

Polymer	BTA content	EH content	Estimated N_{agg}	R_G
	mol%	mol%	-	nm
M95-0-5	4	0	2.9	5.5
M72-23-5	6	22	3.2	7.2
M97-0-2.5	2	0	1.8	6.1
M80-17-2.5	2	27	1.6	3.7

Adding EHA to the BTA polymers gives similar results as Set 1A, meaning the point at which the curves start to decay shifts to higher *q* values and the slope of decay becomes steeper (**Figure V.2.3** and **Table V.2.4**). It can also be noted that the intensity at low *q* values is similar when adding EHA to the BTA glycopolymers, which indicates the aggregation number remains unaffected. As with Set 1A we can conclude that adding more EHA results in smaller and more compact nanoparticles.

Table V.2.5 Overview of the effect of EHA content on the Aggregation Number (N_{agg}) and the radius of gyration (R_G) for Set 2

Polymer	BTA content	Estimated N_{agg}	R_G
	mol%	-	nm
G100-0	0	1.0	4.0
G95-5	11	1.0	4.4
G90-10	14	1.0	4.1
G85-15	19	1.2	4.3
G80-20	24	1.1	3.5

In resemblance with glycopolymer Set 1A, Set 2 (which contains galactose containing polymers) reveals that the incorporation of more EHA results in slightly smaller and more compact single-chain nanoparticles (**Figure V.2.2C** and **Table V.2.5**).

V.2.6 Folding of the BTA containing glycopolymers

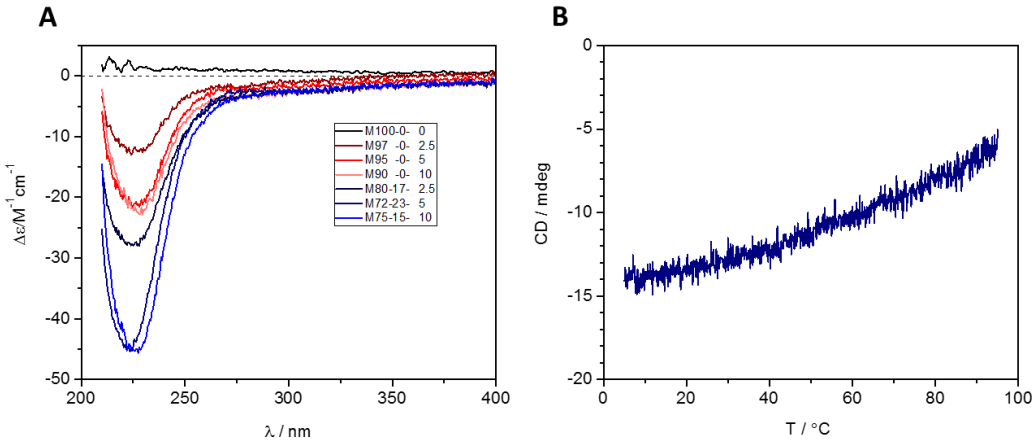

Figure V.2.7 (A) Comparison of the molar CD spectra obtained for Set 1b (c_{BTA} = 50 µM in HEPES buffered saline, T = 20 ˚C) as a function of the incorporation of BTA and EHA and (B) Influence of temperature on the CD intensity (c_{BTA} = 50 µM in HEPES buffered saline, λ = 225 nm, *l* = 5mm)

Chiral BTA grafts are able to fold a polymer backbone into a compact polymeric nanoparticle. Threefold hydrogen bonds facilitate and stabilise the formation of helical assemblies with a preferred handedness, induced by the chiral sidechains. In order to monitor the presence of these structured assemblies, circular dichroism (CD) spectroscopy can be used as a valuable tool. The intensity of the CD signal is directly proportional to the fraction of BTA effectively present in the helical stacks. For all the glycopolymers containing BTA, negative CD effects were detected in HEPES buffered saline with identical shapes, with a maximum at 225 nm (**Figure V.2.4A**). This observation indicates that the same conformation is adopted by the BTA's amides within left-handed self-assembled helices. The other glycopolymers without BTA, do not exhibit CD activity in the range of 200 – 400 nm. Set 1B can be split in 2 glycopolymer samples, a sample without EHA and a sample with EHA. Glycopolymers containing 2.5% and 5% BTA residues, feature similar CD effects in both subsets (Δε = – 22 M^{-1} cm^{-1} for M90-0-10 and M95-0-5 and Δε = – 45 M^{-1} cm^{-1} for M72-23-5 and M80-17-2.5), whereas 10% BTA exhibits a much lower intensity and thus a reduction in BTA self-assembly. Addition of EHA to the glycopolymer composition dramatically enhances the folding ability of the BTA moieties resulting in a two-fold increase in CD effect compared to non-EHA containing glycopolymers. **Figure V.2.6B** shows the temperature dependence of the CD effect in the range between 5 ˚C and 95 ˚C. It can be noted that with increasing temperature, the CD effect experiences a gradual decrease which is in agreement with

previous research. Remarkably, even at high temperatures (> 90 ˚C) a strong CD effect can still be observed in buffer.

V.2.7 Lectin binding studies

Set 1 and Set 2 were subjected to SPR measurements in order to evaluate their ability to bind a series of 9 different lectins found on dendritic and Langerhans cells, known from literature to bind specific carbohydrates. No considerable binding interaction could be detected for the mannose containing polymers with the lectins CLEC-1 and DNGR-1. These lectins respectively have roles in dendritic cells as an inhibitory receptor and as a facilitator in the cross-presentation of antigens associated with dead cells.

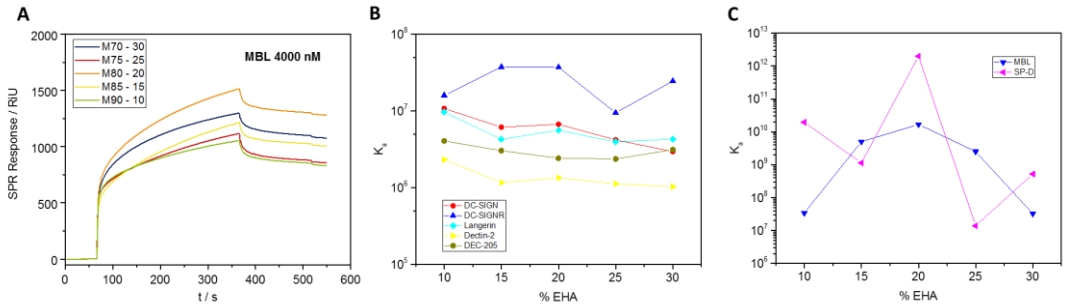

Figure V.2.8 A) SPR sensorgram of Set 1a with MBL ($c_{polymer}$ = 4000 nM). B and C) Graphical representation of association constants (K_a) for glycopolymer Set 1a with various lectins, as determined by SPR.

Set 1a consisting of mannose glyco-SCPNs, shows a clear decreasing trend in binding affinity between the glycopolymers and the lectins DC-SIGN, Langerin, Dectin-2 and DEC-205 with increasing EHA content (**Figure V.2.5B**). MBL (or the mannose binding lectin) on the other hand, experiences a maximal binding affinity at 20% EHA content, which can be explained by an optimal distance between sugar residues and thus increase in binding affinity (**Figure V.2.5C**). However, SP-D (a lectin found to be involved in the recognition of viral particles) doesn't present a clear trend in terms of EHA content of the glycopolymer. It should be noted however that binding affinity of the glycopolymers with SP-D and MBL is very high, with K_a's ranging between 10^7 1/M to even 10^{12} 1/M.

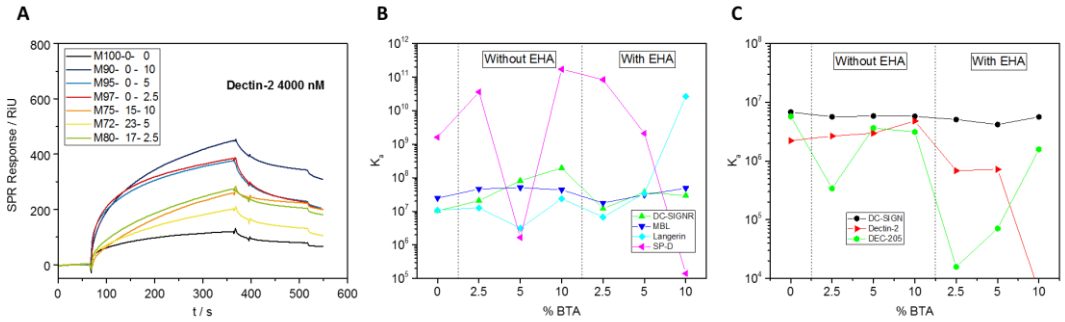

Figure V.2.9 A) SPR sensorgram of Set 1b with Dectin-2 ($c_{polymer}$ = 4000 nM). B and C) Graphical representation of association constants (K_a) for glycopolymer Set 1b with various lectins, as determined by SPR.

Moving further to the BTA containing glycopolymers of Set 1b, conclusions become a bit more difficult (**Figure V.2.6**). However, when comparing association constants K_a between polymers with or without EHA but with similar BTA content we can conclude that addition of more EHA results in a slightly reduced binding affinity. This observation was most pronounced in lectin binding affinity results for the lectin Dectin-2 as can be seen in **Figure V.2.6A**. This observation is in agreement with the findings in glycopolymer Set 1a. We can furthermore see that upon addition of more BTA to the glycopolymer composition, an increase in binding affinity is attained. This increase in binding affinity can be seen in both the series with and without EHA within this set. **Figure V.2.7** shows binding affinity of Set 2 consisting of galactose glyco-SCPNs. Set 2 shows a minimum binding affinity at 10 % EHA content for lectin RCA_{120} with a binding constant K_a around 2.37 x 10^5 1/M. The exact opposite appears for the lectin Galectin-3. For Galectin-3, 10 % experiences maximal binding at around 4.5 x 10^6 1/M.

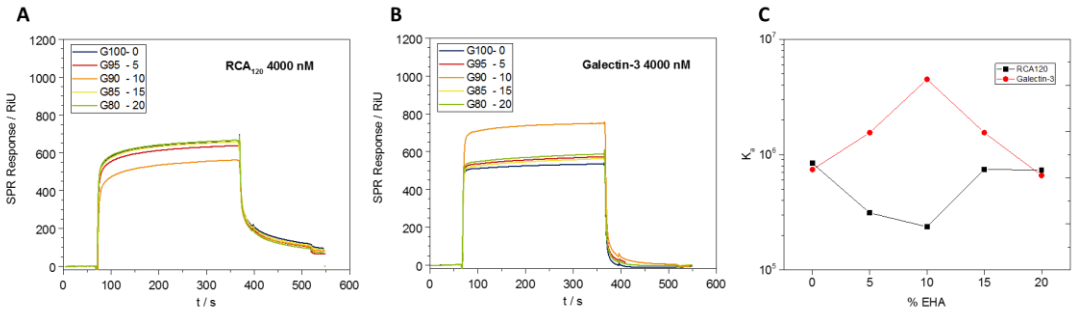

Figure V.2.10 A) SPR sensorgram of Set 2 with RCA_{120} ($c_{polymer}$ = 4000 nM) B) SPR sensorgram of Set 2 with Galectin-3 ($c_{polymer}$ = 4000 nM) B) Graphical representation of association constants (K_a) for glycopolymer Set 2 with RCA_{120} and Galectin-3, as determined by SPR.

V.3 Discussion

SAXS measurements were performed on the amphiphilic glycopolymers. All amphiphilic glycopolymers (without BTA) proved to have masses (determined with SAXS in solution) in close agreement with the mass values based on the composition as determined by NMR. For this reason we can conclude that all the non-BTA containing glycopolymers (mannose and galactose) fold into single-chain nanoparticles, independent of the exact composition of the glycopolymer. This is furthermore evidenced by DLS measurements which gave similar results. BTA containing glycopolymers on the other hand show higher masses with an aggregation number (N_{agg}) averaging between 1 to 7 polymer chains per aggregate.

These findings are furthermore evidenced by the CD spectroscopy experiments. CD spectroscopy measurements were performed to see the influence of using carbohydrates as solubilizing agent instead of PEG graft along the polymer chain. Disruption of the intermolecular forces between glycopolymers chains (BTA self-assembly) proved to be very difficult as can be seen in **Figure V.2.4B**. When the solution is heated up to 95 ˚C, still about one third of the BTA moieties are present in helical stacks. Interestingly the intensity of the CD signal increases significantly when sugars are used instead of PEG chains (PEG: $|\Delta\varepsilon|$ = - 23 M^{-1} cm^{-1} to carbohydrates = - 45 M^{-1} cm^{-1}) for polymers both containing 5% BTA and additional hydrophobic monomers.[43] Non-BTA glycopolymers however show a much lower CD intensity, especially for polymers with a BTA content over 10 %. Where for PEG graft based polymers, the magnitude of the CD signal increases with increasing BTA content, we found that folding becomes worse for glycopolymers with increasing BTA content resulting in a lower amount of BTA incorporated into stacks. Similar as with the increase in EHA content, we can conclude from SAXS and CD measurements that higher BTA content results in a less compact and more elongated particle due to a worse folding of the BTA particles.

Moving back to the relationship between particle composition and lectin binding affinity, it's become clear that particle size and morphology have great impact on glycopolymer interactions. From SPR measurements we could conclude that in increase in EHA content results in a slightly reduced binding affinity between the glyconanoparticles and the lectins. This can be explained by the more compact and globular conformation the glycopolymer chains adopt upon addition of EHA which limits the freedom to adopt an optimal conformation to reach different binding pockets. Secondly, as can be seen from the SPR binding results, increasing BTA content actually

shows an increase in binding affinity. Also these findings can be explained from a physicochemical point of view. As increasing EHA content contracts the nanoparticles size, increasing the BTA content results in bigger particles composed of multiple polymer chains and thus a morphologically less controlled and less compact nanoparticle. This demonstrates the highly dynamic nature of protein glycopolymer interactions, where a balance should be found between optimal binding distance and flexibility to adopt the desired conformation.

V.4 Conclusion

In a pursuit of controlling the dynamic chain folding of polymeric glyconanoparticles, mannose and galactose amphiphilic glycopolymers were synthesised and characterised containing both hydrophobic pendants (ethyl hexyl) and supramolecular motifs (BTA). Physicochemical properties were investigated using ^{1}H-NMR, GPC, DLS, CD spectroscopy and SAXS. The results have shown that addition of more EHA to the glycopolymer composition results in more compact single-chain polymeric nanoparticles and that the amphiphilic glycopolymers adopt a more compact spherical conformation, having a radius of gyration ranging between 2.6 and 4.4 nm. Addition of more BTA on the other hand, makes the glyconanoparticles more compact, however, it induces clustering of the copolymers into small multi-chain polymeric nanoparticles with radii of gyration between 3.7 and 9 nm composed of 1 to 7 glycopolymer chains. Lectin binding studies were performed towards a series of lectins found on dendritic and Langerhans cells and towards two galactose binding lectins, RCA_{120} and Galectin-3. All mannose containing glyconanoparticles have great binding affinity towards the lectins DC-SIGN, DC-SIGNR, Langerin, Dectin-2 and DEC-205. Especially SP-D and MBL showed extremely high binding constants K_a of up to 10^{10}-10^{12} 1/M. We found that addition of EHA (and thus more compact nanoparticles) results in a reduction in binding affinity and addition of low amounts of BTAs furthermore results in an increase in binding affinity.

V.5 Experimental section

V.5.1 Materials

Tris(2-(Dimethylamino)ethyl)amine (Me_6TREN) was previously synthesised within the group. *D*-Mannose glycomonomer was synthesised as previously reported.[42,44]All other reagents and solvents were obtained at the highest purity available from Sigma Aldrich Chemical Company unless stated otherwise. HEPES buffered saline was prepared by dissolving HEPES (2.38 g), NaCl (8.77 g), $CaCl_2$ (0.74 g) in 1 L water. Once everything was dissolved, the pH was adjusted until a pH of 7.4.

V.5.2 Instruments and analysis

Proton (^{1}H-NMR) nuclear magnetic resonance spectroscopy (Bruker DPX-400/600) was used to determine the chemical structure of the synthesised initiators and polymers. Samples were dissolved at 10 mg/mL concentration in $CDCl_3$, DMSO-d_6, D_2O or MeOD-d_4 as solvent. Monomer conversion was calculated by the disappearance of vinyl protons (H_2C=CH-CO–) (≈ 6.5-5.5 ppm) compared to the mannose glycomonomer's triazole proton (≈ 8.2-7.9 ppm). Polymer compositions were calculated based on the comparison of the triazole proton (≈ 8.2-7.9 ppm), with the BTAs aromatic and amide protons (≈ 8.3-8.9 ppm) and the methyl protons of the BTA and ethyl hexyl acrylate after subtraction of the backbone peaks (≈ 0.5-1.1 ppm).

GPC measurements were conducted on an Agilent 1260 infinity system operating in DMF with 5mM NH_4BF_4 and equipped with refractive index detector and variable wavelength detector, 2 PLgel 5 µm mixed-C columns (300×7.5mm), a PLgel 5 mm guard column (50x7.5mm) and an autosampler. The instrument was calibrated with linear narrow poly(methyl methacrylate) standards. All samples were passed through basic alumina to remove any copper residues and filtered with a 0.2 µm Nylon 66 before analysis.

Dynamic light scattering (DLS) measurements were performed using a Malvern µV Zetasizer equipped with an 830 nm laser and a scattering angle of 90° at a temperature of 20 °C. Samples were prepared at 1 mg/mL and filtered with a 0.2 µm

PVDF-filter (Whatman) to prevent the presence of dust. A fluorescence cell with a 1 cm path length was used for the measurements.

Small-angle X-ray scattering (SAXS) was performed on a SAXSLAB Ganesha system using a GeniX-Cu ultra-low divergence source producing X-ray photons with a wavelength of 1.54 Å and a flux of 1 x 10^8 ph/s. Scattering patterns were collected using a Pilatus 300K silicon pixel detector. Sample-to-detector distances of 0.13, 0.73 m, and 1.53 m were used giving an observed q range of $1.3 \cdot 10^{-3}$ $nm^{-1} \leq q \leq 2.4$ nm^{-1}. The solutions (typically 1 mg/mL) were measured in 2 mm quartz capillaries, typically measurement times were: 1 h at a sample-to-detector distance of 0.13 m, 5 h at 0.73 m, and 9 h at 1.53 m. The SAXSgui software package was used to radially average the resulting 2D images to obtain the intensity *I (q)* vs. *q* profiles. Standard data reduction procedures, i.e. subtraction of the solvent's contribution, were performed using the same software. The curves were fitted using the SasView 4.1.2 software packages. A polymer excluded volume model was used to fit the scattering curves.

Circular dichroism spectroscopy measurements were performed on a Jasco J-815 circular dichroism (CD) spectropolarimeter equipped with a PFD-425S/15 Peltier-type temperature controller. A quartz cuvette with an optical path length of 1 mm was used. The molar circular dichroism Δε was calculated using Δε= CD effect / (32980 x c_{BTA} x *l*), in which *c* is the concentration of the BTAs attached to the polymer backbone and *l* is the optical pathway.

Surface Plasmon Resonance (SPR) - The extent of interaction between the glycopolymers and lectins were performed on a BIAcore 3000 system (GE Healthcare). The proteins (0.025 mg/ml) were immobilized *via* a standard amino coupling protocol onto a CM5 sensor chip which was activated by flowing a 1:1 mixture of 0.1 M N-hydroxysuccinimide and 0.1 M N-ethyl-N'-(dimethylaminopropyl)carbodiimide over the chip for 6 min at 25 °C at a flow rate of 20 µL/min after the system equilibration with HEPES filtered buffer (10 mM HEPES, 150 mM NaCl, 5 mM $CaCl_2$) supplemented with 0.005% TWEEN® 20 at pH 7.4. Subsequently, channels 1 (blank), 2, 3 and 4 were blocked by following a solution of ethanolamine (1 M pH 8.5) for 10 min at 5 µL/min to remove remaining reactive groups on the channels. Sample solutions were prepared at varying concentrations (4000 nM-250 nM) in the same HEPES buffer to calculate the binding kinetics. Sensorgrams for each glycopolymer concentration were recorded with a 300 seconds injection of polymer solution (on period) followed by 150 seconds of buffer alone (off period). Regeneration of the sensor chip surfaces was performed using 10 mM HEPES pH 7.4, 150 mM NaCl, 10 mM EDTA, 0.01% P20 surfactant solution. Kinetic

data was evaluated using a single set of sites (1:1 Langmuir Binding) model and also Biavalent model in the BIAevalulation 3.1 software.

V.5.3 Experimental procedures

V.5.3.1 Synthesis of 1-(2′-Propargyl) *D*-Galactose

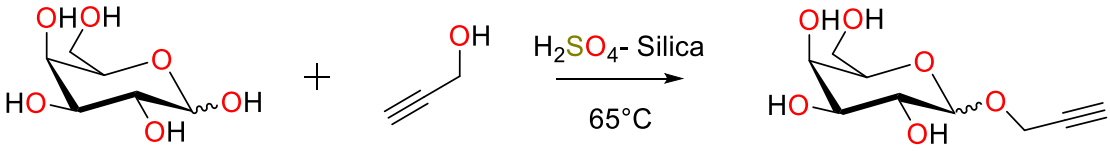

Scheme V.5.1 Schematic representation of the synthetic approach to the *D*-galactose glycomonomer

1-(2′-Propargyl) *D*-Galactose was prepared according to the procedure reported by Mukhopadhyay *et al*.[45] A suspension solution of *D*-Galactose (12 g, 66.6 mmol), propargyl alcohol (19.4 mL, 333 mmol) and H_2SO_4-silica (500 mg) was stirred at 65 °C for two days. After cooling to ambient temperature, the reaction mixture was transferred to a silica gel column and eluted with $CHCl_3$-MeOH (8:1) to remove the excess propargyl alcohol. 1-(2′-Propargyl) *D*-galactose was obtained as white hygroscopic solid after drying under vacuum (6.5 g, yield: 45 %). 1-(2′-propargyl)-*D*-galactose was found as an anomeric mixture in a ratio of 4:1 (*β/α*).

^{1}H NMR (400 MHz, CD_3OD, 300 K, ppm): *δ*: 5.03 (*d*, 1H, 3.9 Hz), 4.42 (m, 1H), 4.30 (*d*, 2H, 2.3 Hz), 3.90 (*d*, 1H, 3 Hz), 3.85-3.65 (*m*, 3H), 3.60-3.40 (*m*, 1H), 2.84 (*t*, 1 H, 2.3 Hz)

V.5.4 Synthesis of *D*-Galactose glycomonomer

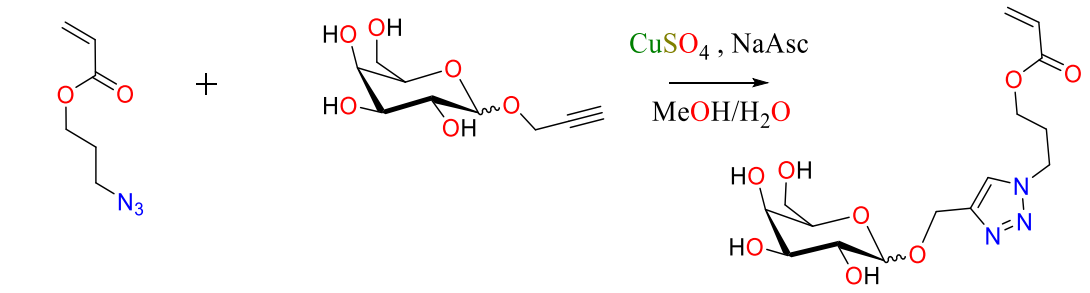

Scheme V.5.2 Schematic representation of the synthetic approach to the *D*-galactose glycomonomer

To a solution of 3-azidopropyl acrylate (3.16 g, 20.3 mmol) and 1-(2′-propargyl) *D*-galactose (4.04 g, 18.5 mmol) and a spatula tip of hydroquinone in MeOH/H_2O (2:1 vol/vol, 180 mL), an aqueous solution of $CuSO_4 \cdot 5H_2O$ (624 mg, 2.5 mmol) and (+)-sodium *L*-ascorbate (625 mg, 3.15 mmol) were sequentially added. The mixture was stirred at ambient temperature for 24 h. The methanol was removed via rotary evaporator and residue mixture was freeze dried in order to remove water. The obtained green solid was purified by silica gel column chromatography using dichloromethane-MeOH (10:1) as eluent. The relevant fractions were collected and after removal of solvent pure *D*-galactose glycomonomer was isolated as white solid (4.78 g, yield: 69.1%). The obtained unprotected *D*-galactose glycomonomer is an anomeric mixture.

^{1}H NMR (400 MHz, CD_3OD, 300 K, ppm): δ =8.05 (*s*, 1 H), 6.37 (*dd*, 1H, 1.4, 17.3 Hz), 6.14 (*dd*, 1H, 10.4, 17.3 Hz), 5.89 (*dd*, 1H, 1.4, 10.4 Hz), 4.94 (*d*, 1H, 3.6 Hz), 4.90-4.60 (*m*, 2H, overlap with H_2O), 4.54 (*t*, 2 H, 6.8 Hz), 4.19 (*t*, 2 H, 6.1 Hz), 4.00-3.40 (*m*, 6 H, galactose residues), 2.3 (*quin*, 2 H, 6.3 Hz)

V.5.5 Synthesis *of (S,S)*-BTA acrylate

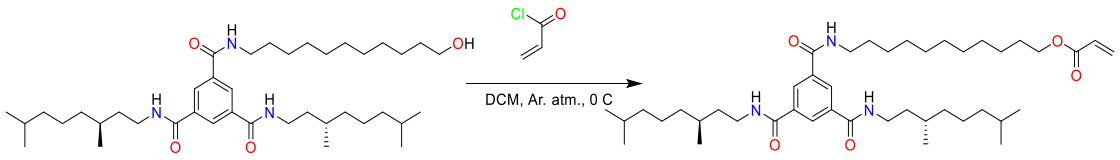

Scheme V.5.3 Schematic representation of the synthetic approach to the BTA-acrylate monomer

(*S*,*S*)-BTA-C_{11}-OH (2.86 g, 4.35 mmol) and triethylamine (0.750 mL, 5.38 mmol) were dissolved in 25 mL of dry DCM and the solution was placed under an argon atmosphere. The mixture was cooled using an ice bath before a solution of acryloyl chloride (0.55 mL, 5.63 mmol) in 20 mL dry DCM was added in a dropwise fashion. The reaction was stirred overnight and washed with 1 M HCl (2x), saturated $NaHCO_3$ (2x) and brine subsequently. After drying the organic layer over $MgSO_4$, the product was purified *via* column chromatography (silica, elution: 15% EtOAc in $CHCl_3$). After removal of the solvent *in vacuo*, the product was obtained as a white wax (yield: 80%).

^{1}H-NMR (400 MHz, $CDCl_3$): δ 8.31 (s, 3H), 6.46 (*t*, 1H), 6.42 (*t*, 2H) 6.40 (*dd*, 1H, 1.5, 17.3 Hz), 6.13 (*dd*, 1H, 10.4, 17.3 Hz), 5.82 (*dd*, 1H, 1.5, 10.4 Hz), 5.54 (m, 1H), 4.13 (t, *J* = 6.7 Hz, 2H), 3.54 – 3.37 (m, 6H), 1.94 (m, 3H), 1.73 – 1.06 (m, 40H), 0.93 (d, *J* = 6.5 Hz, 6H), 0.86 (d, *J* = 6.6 Hz, 12H).

V.5.6 General procedure for the SET-LRP polymerisation of Set 1

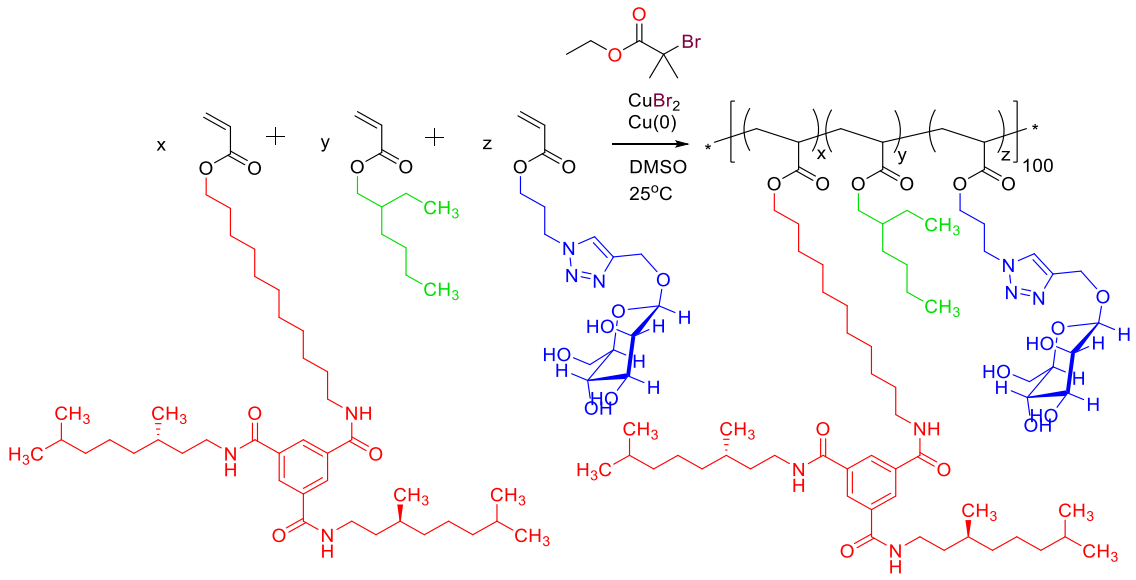

Scheme V.5.4 Schematic representation of the polymerisation procedure for Set 1

A Schlenk tube was charged with initiator ethyl *α*-bromoisobutyrate, 1.17 µL, 0.00803 mmol, 1 eq.), mannose glycomonomer (480 mg, 1.28 mmol, 160 eq.), ethyl hexyl acrylate (47.12 µL, 0.28 mmol, 35 eq), BTA acrylate (28.61 mg, 0.402 mmol, 5 eq), Me_6TREN (0.408 µL, 0.19 eq), $CuBr_2$ (0.35 mg, 0.04 eq.) in DMSO (2 mL), sealed with a rubber septum and subsequently degassed by gentle bubbling of Ar gas for 15 min. The polymerisation was then started by addition of pre-activated Cu(0) wire (5 cm)

wrapped around a stirring bar under a positive Ar pressure and quickly sealed again and the reaction mixture was allowed to polymerise at 25˚C. Sampling was carried out using a degassed syringe to check the conversion of mannose glycomonomer. The polymerisation was allowed to continue to polymerise until at least 50% conversion was reached.

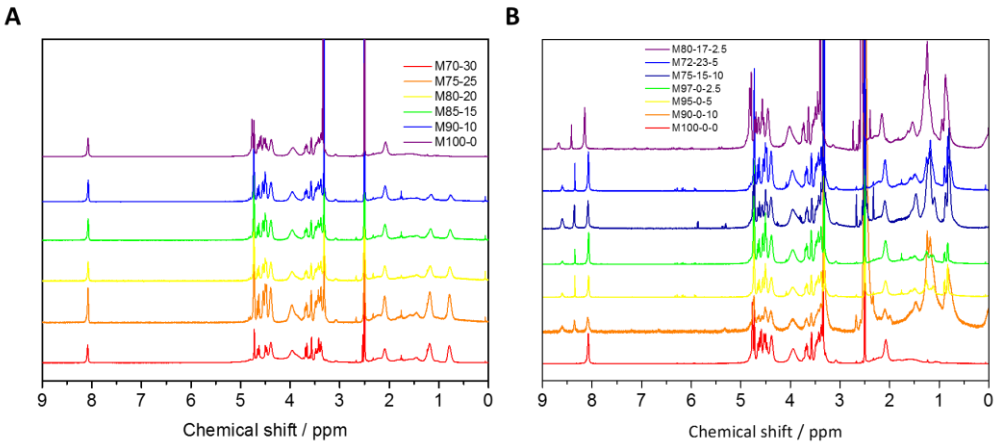

Figure V.5.1 A) ^{1}H-NMR in DMSO-d_6 of Set 1A showing the purity of the synthesised star glycopolymers, with clear visibility of the triazole peak at 8.0 ppm and disappearance of the vinyl protons between 6.5 and 5.5 ppm, B) ^{1}H-NMR in DMSO-d_6 of Set 1B showing the purity of the synthesised star glycopolymers, with clear visibility of the triazole peak at 8.0 ppm and disappearance of the vinyl protons between 6.5 and 5.5 ppm

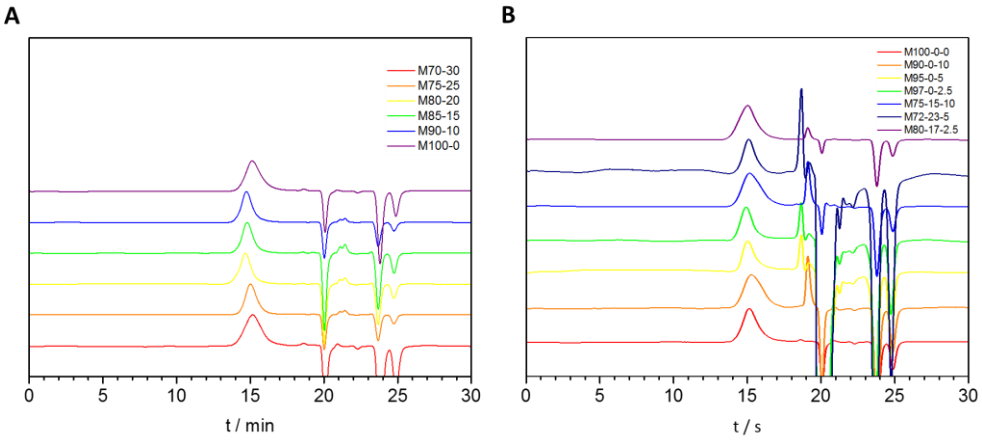

Figure V.5.2 A) GPC chromatograms of Set 1A. B) GPC chromatograms of Set 1B.

V.5.7 General procedure for the SET-LRP polymerisation of Set 2

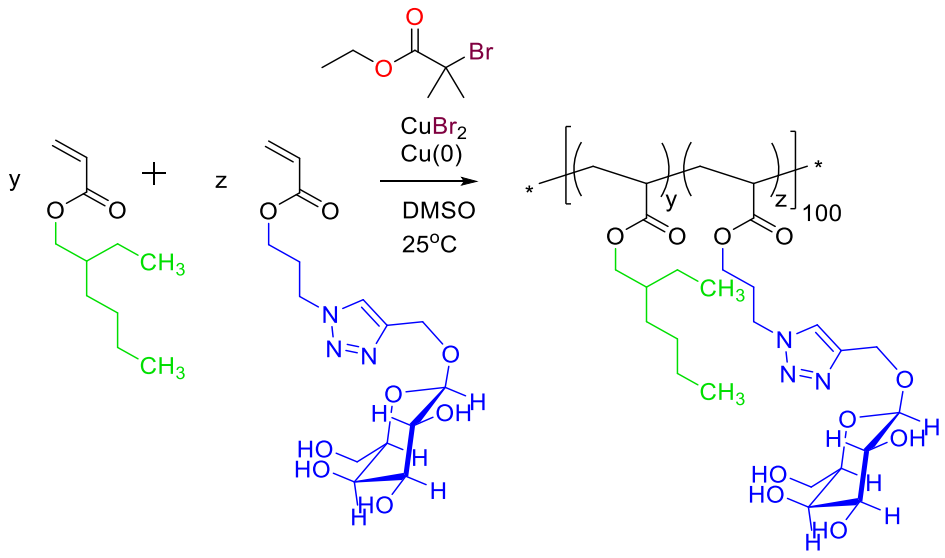

Scheme V.5.5 Schematic representation of the polymerisation procedure for Set 2

A Schlenk tube was charged with initiator ethyl α-bromoisobutyrate, 1.17 µL, 0.00803 mmol, 1 eq.), galactose glycomonomer (480 mg, 1.28 mmol, 160 eq.), ethyl hexyl acrylate (53.85 µL, 0.231 mmol, 40 eq), Me_6TREN (0.408 µL, 0.19 eq), $CuBr_2$ (0.35 mg, 0.04 eq.) in DMSO (2 mL), sealed with a rubber septum and subsequently degassed by gentle bubbling of Ar gas for 15 min. The polymerisation was then started by addition of pre-activated Cu(0) wire (5 cm) wrapped around a stirring bar under a positive Ar pressure and quickly sealed again and the reaction mixture was allowed to polymerise at 25˚C. Sampling was carried out using a degassed syringe to check the conversion of the monomers by comparing the acrylate peaks to the triazole proton. The polymerisation was allowed to continue to polymerise until at least 50% conversion was reached.

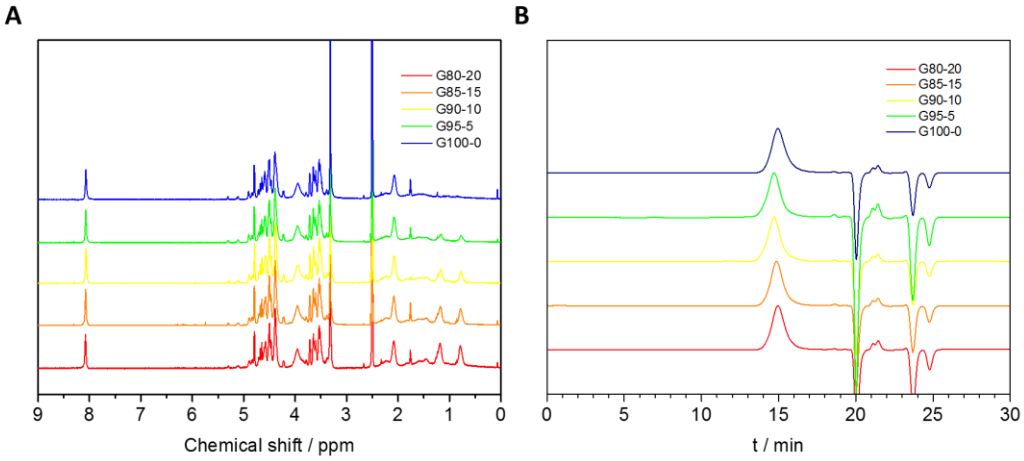

Figure V.5.3 A) ^{1}H-NMR in DMSO-d_6 of Set 2 showing the purity of the synthesised star glycopolymers, with clear visibility of the triazole peak at 8.0 ppm and disappearance of the vinyl protons between 6.5 and 5.5 ppm, B) GPC chromatograms of Set 2.

V.5.8 DLS measurements

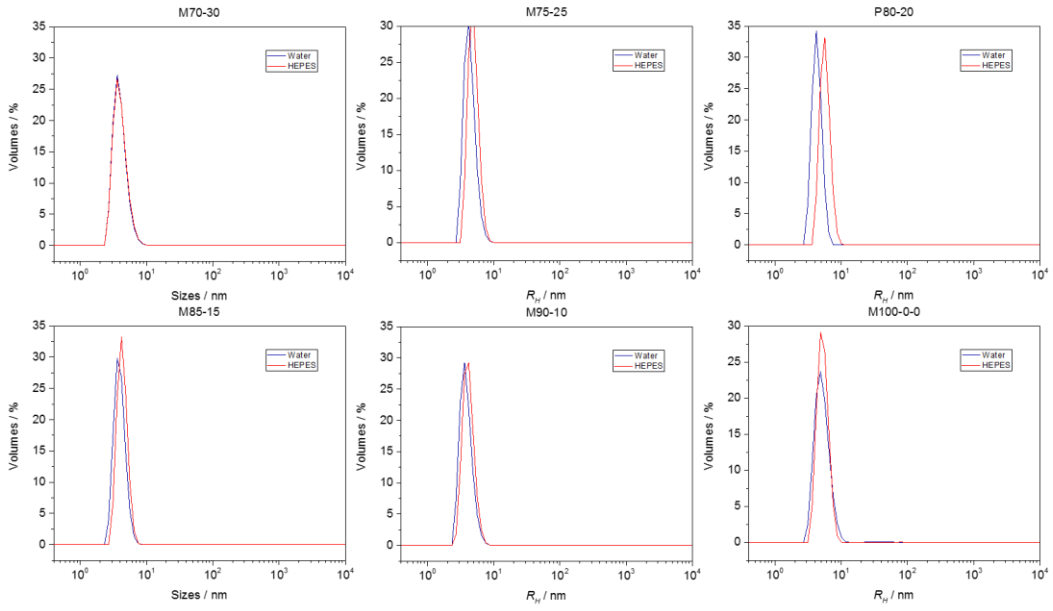

Figure V.5.4 Volume distribution of the hydrodynamic radius (R_H) of Set 1A (filtered with a 200 nm PVDF filter)

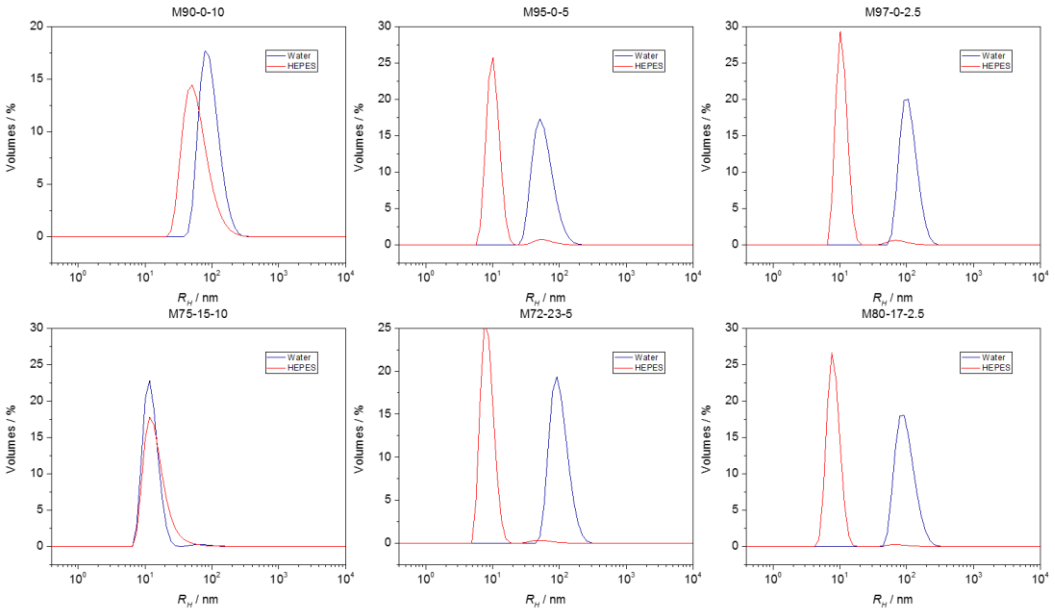

Figure V.5.5 Volume distribution of the hydrodynamic radius (R_H) of Set 1B (filtered with a 200 nm PVDF filter)

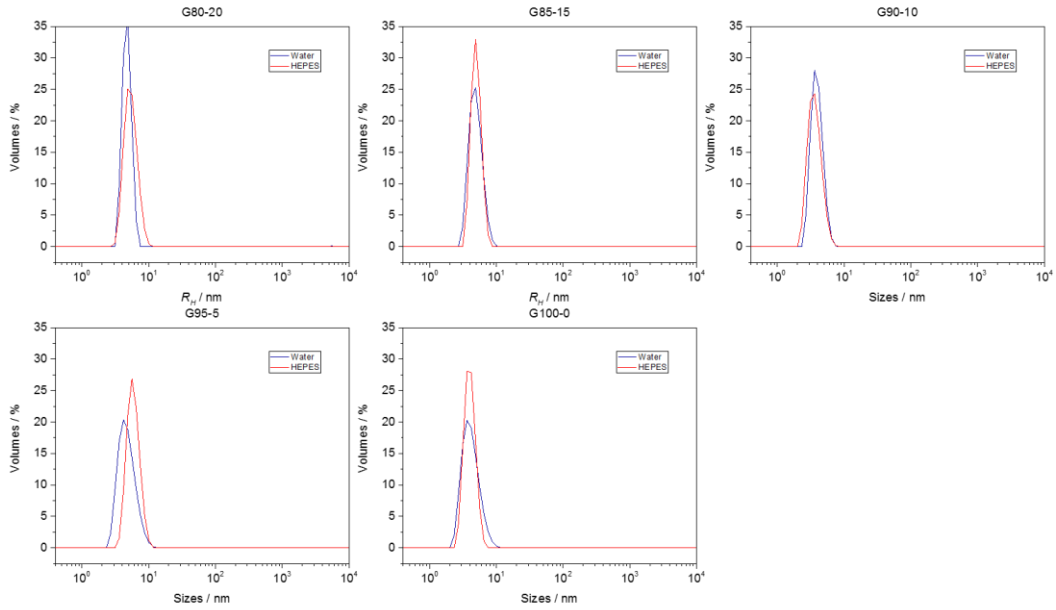

Figure V.5.6 Volume distribution of the hydrodynamic radius (R_H) of Set 2 (filtered with a 200 nm PVDF filter)

V.5.9 SAXS measurements

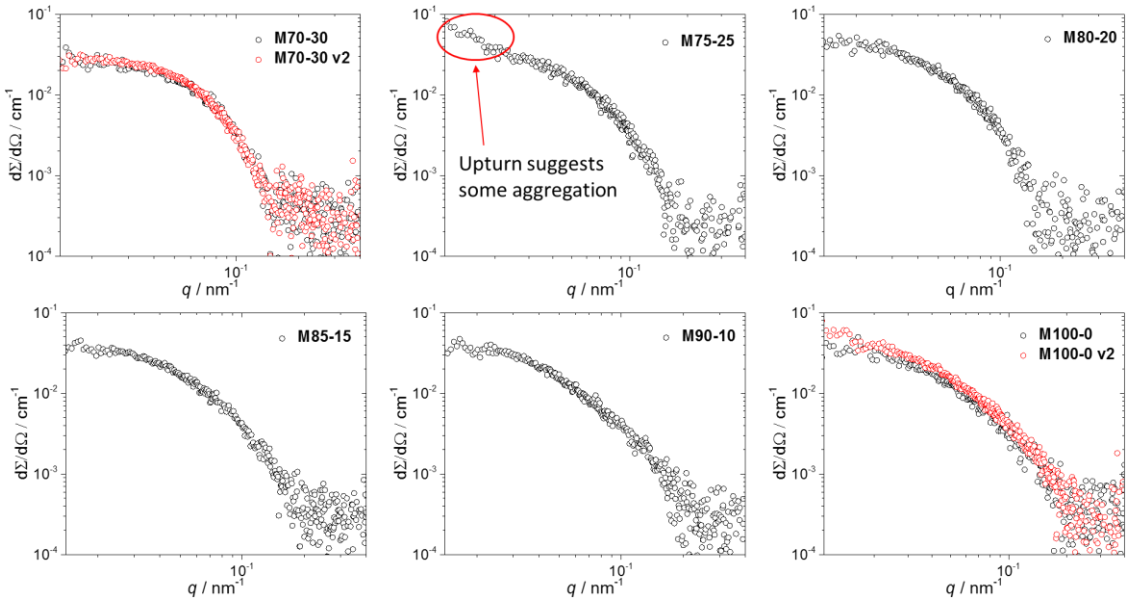

Figure V.5.7 Small-angle X-ray scattering curves of Set 1A (filtered with a 200 nm PVDF filter)

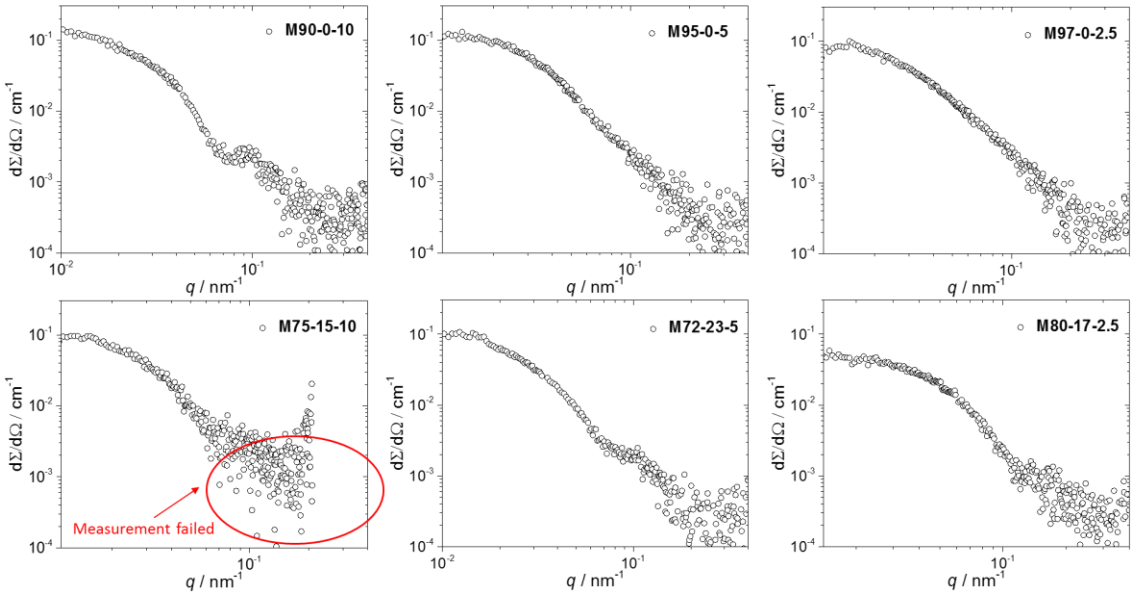

Figure V.5.8 Small-angle X-ray scattering curves of Set 1B (filtered with a 200 nm PVDF filter)

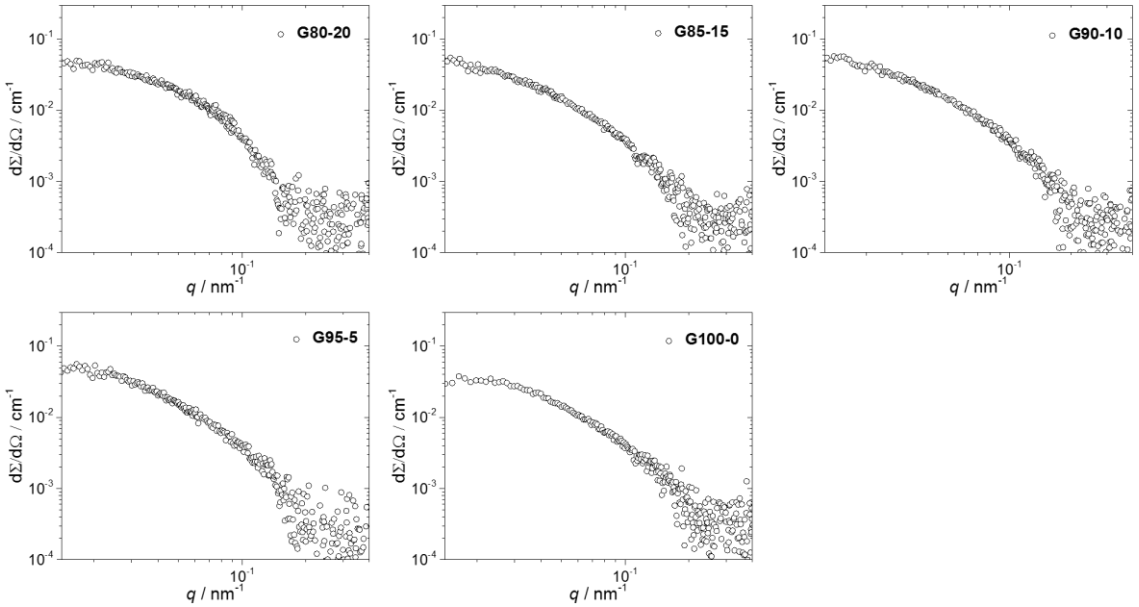

Figure V.5.9 Small-angle X-ray scattering curves of Set 2 (filtered with a 200 nm PVDF filter)

V.5.10 Kinetic data obtained *via* SPR

Table V.5.1 Polymer interactions with DC-SIGN

Polymer	k_a [$M^{-1}s^{-1}$]	k_d [s^{-1}]	K_A[M^{-1}]	K_D [M]	R_{max} [RU]
M100-0-0	$2.69x10^{-4}$	$3.95x10^{-3}$	$6.8x10^{6}$	$1.47x10^{-7}$	120
M90-0-10	$6.03x10^{3}$	$1.05x10^{-3}$	$5.76x10^{6}$	$1.74x10^{-7}$	325
M95-0-5	$6.41x10^{3}$	$1.19x10^{-3}$	$5.83x10^{6}$	$1.85x10^{-7}$	420
M97-0-2.5	$9.12x10^{3}$	$1.61x10^{-3}$	$5.66x10^{6}$	$1.77x10^{-7}$	350
M75-15-10	$7.56x10^{3}$	$1.34x10^{-3}$	$5.62x10^{6}$	$1.78x10^{-7}$	300
M80-17-2.5	$1.29x10^{4}$	$2.53x10^{-3}$	$5.08x10^{6}$	$1.97x10^{-7}$	200
M72-23-5	$8.97x10^{3}$	$2.14x10^{-3}$	$4.18x10^{6}$	$2.39x10^{-7}$	280
M70-30	$6.77x10^{3}$	$2.28x10^{-3}$	$2.97x10^{6}$	$3.37x10^{-7}$	185
M75-25	$2.18x10^{4}$	$4.73x10^{-3}$	$4.21x10^{6}$	$2.17x10^{-7}$	120
M80-20	$1.81x10^{4}$	$2.69x10^{-3}$	$6.73x10^{6}$	$1.49x10^{-7}$	165
M85-15	$1.64x10^{4}$	$2.66x10^{-3}$	$6.17x10^{6}$	$1.62x10^{-7}$	150
M90-10	$3.41x10^{4}$	$3.17x10^{-3}$	$1.08x10^{7}$	$9.29x10^{-8}$	160

Table V.5.2 Polymer interactions with DC-SIGNR

Polymer	k_a [$M^{-1}s^{-1}$]	k_d [s^{-1}]	K_A[M^{-1}]	K_D [M]	R_{max} [RU]
M100-0-0	$8.8x10^{3}$	$8.55x10^{-4}$	$1.03x10^{7}$	$9.71x10^{-8}$	250
M90-0-10	$4.82x10^{3}$	$2.48x10^{-5}$	$1.95x10^{8}$	$5.14x10^{-9}$	1300
M95-0-5	$3.88x10^{3}$	$4.74x10^{-5}$	$8.18x10^{7}$	$1.22x10^{-8}$	1400
M97-0-2.5	$6.33x10^{3}$	$3.03x10^{-4}$	$2.09x10^{7}$	$4.78x10^{-8}$	1000
M75-15-10	$4.26x10^{3}$	$1.45x10^{-4}$	$2.94x10^{7}$	$3.4x10^{-4}$	1000
M80-17-2.5	$2.83x10^{3}$	$2.34x10^{-4}$	$1.21x10^{7}$	$8.3x10^{-8}$	800
M72-23-5	$3.27x10^{3}$	$8.81x10^{-5}$	$3.71x10^{7}$	$2.67x10^{-8}$	840
M70-30	$2.83x10^{3}$	$1.15x10^{-4}$	$2.46x10^{7}$	$4.07x10^{7}$	270
M75-25	$1.53x10^{3}$	$1.65x10^{-4}$	$9.48x10^{6}$	$1.05x10^{-7}$	350
M80-20	$2.77x10^{3}$	$7.45x10^{-5}$	$3.71x10^{7}$	$2.69x10^{-8}$	710
M85-15	$2.08x10^{3}$	$5.56x10^{-5}$	$3.75x10^{7}$	$2.67x10^{-8}$	650
M90-10	$3.71x10^{3}$	$2.31x10^{-4}$	$1.6x10^{7}$	$6.24x10^{-8}$	540

Table V.5.3 Polymer interactions with MBL

Polymer	k_a [$M^{-1}s^{-1}$]	k_d [s^{-1}]	K_A[M^{-1}]	K_D [M]	R_{max} [RU]
M100-0-0	$1.57x10^{4}$	$6.35x10^{-4}$	$2.47x10^{7}$	$4.05x10^{-8}$	650
M90-0-10	$8.24x10^{3}$	$1.89x10^{-4}$	$4.37x10^{7}$	$2.29x10^{-8}$	2800
M95-0-5	$9.81x10^{3}$	$1.93x10^{-4}$	$5.09x10^{7}$	$1.96x10^{-8}$	2200
M97-0-2.5	$1.22x10^{4}$	$2.64x10^{-4}$	$4.63x10^{7}$	$2.16x10^{-8}$	1800
M75-15-10	$8.2x10^{3}$	$1.67x10^{-4}$	$4.91x10^{7}$	2.04x10-^{8}	3000
M80-17-2.5	$9.22x10^{3}$	$5.2x10^{-4}$	$1.77x10^{7}$	$5.64x10^{-8}$	1700
M72-23-5	$1.49x10^{4}$	$4.81x10^{-4}$	$3.09x10^{7}$	$3.23x10^{-8}$	2100
M70-30	$7.14x10^{3}$	$2.19x10^{-4}$	$3.25x10^{7}$	$3.08x10^{-8}$	1300
M75-25	$4.01x10^{3}$	$1.59x10^{-6}$	$2.52x10^{9}$	$3.98x10^{-10}$	1100
M80-20	$6.13x10^{3}$	$3.65x10^{-7}$	$1.68x10^{10}$	$5.96x10^{-11}$	1510
M85-15	$4.25x10^{3}$	$8.46x10^{-7}$	$5.02x10^{9}$	$1.99x10^{-10}$	1210
M90-10	$1.01x10^{4}$	$2.95x10^{-4}$	$3.41x10^{7}$	$2.93x10^{-8}$	1050

Table V.5.4 Polymer interactions with Langerin

Polymer	k_a [$M^{-1}s^{-1}$]	k_d [s^{-1}]	K_A[M^{-1}]	K_D [M]	R_{max} [RU]
M90-0-10	$6.41x10^3$	$2.69x10^{-4}$	$2.38x10^7$	$4.2x10^{-8}$	450
M70-30	$8.43x10^3$	$1.96x10^{-3}$	$4.31x10^6$	$2.32x10^{-7}$	240
M95-0-5	$9.31x10^3$	$9.14x10^{-4}$	$3.14x10^6$	$3.19x10^{-7}$	360
M75-25	$8.57x10^3$	$2.16x10^{-3}$	$3.97x10^6$	$2.52x10^{-7}$	210
M80-20	$9.79x10^3$	$1.75x10^{-3}$	$5.61x10^6$	$1.78x10^{-7}$	260
M90-10	$1.17x10^4$	$1.21x10^{-3}$	$9.69x10^6$	$1.03x10^{-7}$	230
M85-15	$7.35x10^3$	$1.71x10^{-3}$	$4.29x10^6$	$2.33x10^{-7}$	265
M100-0-0	$8.29x10^3$	$7.64x10^{-4}$	$1.09x10^7$	$9.21x10^{-8}$	190
M97-0-2.5	$6.54x10^3$	$5.15x10^{-4}$	$1.27x10^7$	$7.87x10^{-8}$	330
M75-15-10	$5.07x10^3$	$1.93x10^{-7}$	$2.63x10^{10}$	$3.8x10^{-11}$	390
M80-17-2.5	$5.14x10^3$	$7.58x10^{-4}$	$6.78x10^6$	$1.47x10^{-7}$	250
M72-23-5	$5.67x10^3$	$1.64x10^{-3}$	$3.45x10^7$	$2.9x10^{-8}$	265

Table V.5.5 Polymer interactions with Dectin-2

Polymer	k_a [$M^{-1}s^{-1}$]	k_d [s^{-1}]	K_A[M^{-1}]	K_D [M]	R_{max} [RU]
M90-0-10	$3.81x10^3$	$7.95x10^{-4}$	$4.79x10^6$	$2.09x10^{-7}$	450
M70-30	$3.09x10^3$	$3.01x10^{-3}$	$1.03x10^6$	$3.74x10^{-7}$	110
M95-0-5	$6.08x10^3$	$2.05x10^{-3}$	$2.97x10^6$	$3.37x10^{-7}$	380
M75-25	$7.51x10^3$	$6.63x10^{-3}$	$1.13x10^6$	$8.82x10^{-7}$	65
M80-20	$5.31x10^3$	$3.93x10^{-3}$	$1.35x10^6$	$7.4x10^{-7}$	200
M90-10	$6.7x10^3$	$2.87x10^{-3}$	$2.33x10^6$	$4.28x10^{-7}$	280
M85-15	$3.98x10^3$	$3.41x10^{-3}$	$1.17x10^6$	$8.57x10^{-7}$	220
M100-0-0	$5.43x10^3$	$2.45x10^{-3}$	$2.22x10^6$	$4.51x10^{-7}$	120
M97-0-2.5	$4.55x10^3$	$1.71x10^{-3}$	$2.66x10^6$	$3.75x10^{-7}$	380
M75-15-10	7.54	$1.24x10^{-3}$	$6.1x10^3$	$1.64x10^{-4}$	260
M80-17-2.5	956	$1.4x10^{-3}$	$6.85x10^5$	$1.46x10^{-6}$	275
M72-23-5	$1.39x10^3$	$1.94x10^{-3}$	$7.2x10^5$	$1.39x10^{-6}$	200

Table V.5.6 Polymer interactions with DEC-205

Polymer	k_a [$M^{-1}s^{-1}$]	k_d [s^{-1}]	K_A[M^{-1}]	K_D [M]	R_{max} [RU]
M90-0-10	$1.24x10^4$	$3.99x10^{-3}$	$3.12x10^6$	$3.21x10^{-7}$	190
M70-30	$2.39x10^4$	$7.62x10^{-3}$	$3.14x10^6$	$3.19x10^{-7}$	160
M95-0-5	$1.56x10^4$	$4.27x10^{-3}$	$3.65x10^6$	$2.74x10^{-7}$	165
M75-25	$1.75x10^4$	$7.33x10^{-3}$	$2.38x10^6$	$4.2x10^{-7}$	155
M80-20	$1.69x10^4$	$6.95x10^{-3}$	$2.43x10^6$	$4.11x10^{-7}$	180
M90-10	$8.81x10^3$	$2.16x10^{-3}$	$4.08x10^6$	$2.45x10^{-7}$	170
M85-15	$2.09x10^4$	$6.84x10^{-3}$	$3.05x10^6$	$3.28x10^{-7}$	170
M100-0-0	$4.37x10^3$	$7.62x10^{-4}$	$5.74x10^6$	$1.47x10^{-7}$	140
M97-0-2.5	$1.16x10^3$	$3.39x10^{-3}$	$3.41x10^5$	$2.93x10^{-6}$	170
M75-15-10	$3.71x10^5$	0.235	$1.58x10^6$	$6.33x10^{-7}$	180
M80-17-2.5	16.7	$1.06x10^{-3}$	$1.58x10^4$	$6.35x10^{-7}$	140
M72-23-5	332	$4.68x10^{-3}$	$7.1x10^4$	$1.41x10^{-5}$	120

Table V.5.7 Polymer interactions with SP-D

Polymer	k_a [$M^{-1}s^{-1}$]	k_d [s^{-1}]	K_A[M^{-1}]	K_D [M]	R_{max} [RU]
M75-25	706	$5.05x10^{-5}$	$1.4x10^7$	$7.15x10^{-8}$	450
M85-15	785	$6.86x10^{-7}$	$1.14x10^9$	$8.74x10^{-10}$	710
M80-17-2.5	$1.39x10^3$	$1.66x10^{-8}$	$8.36x10^{10}$	$1.2x10^{-11}$	1330
M70-30	$1.12x10^3$	$2.14x10^{-6}$	$5.26x10^8$	$1.9x10^{-9}$	435
M80-20	$1.56x10^3$	$7.78x10^{-10}$	$2x10^{12}$	$5x10^{-13}$	820
M90-10	$1.4x10^3$	$7.14x10^{-8}$	$1.96x10^{10}$	$5.1x10^{-11}$	480
M72-23-5	$1.93x10^3$	$9.2x10^{-7}$	$2.1x10^9$	$4.77x10^{-10}$	1480
M100-0-0	$2.91x10^3$	$1.81x10^{-6}$	$1.61x10^9$	$6.21x10^{-10}$	80
M90-0-10	$2.07x10^3$	$1.22x10^{-8}$	$1.71x10^{11}$	$5.86x10^{-12}$	1435
M95-0-5	$6.9x10^3$	$4.14x10^{-3}$	$1.66x10^6$	$6.02x10^{-7}$	170
M97-0-2.5	$1.47x10^4$	$4.09x10^{-7}$	$3.59x10^{10}$	$2.79x10^{-11}$	555
M75-15-10	24.8	$1.77x10^{-4}$	$1.4x10^5$	$7.13x10^{-6}$	1200

V.6 References

(1) Abdouni, Y.; Yilmaz, G.; Becer, C. R. *Macromol. Rapid Commun.* **2017**, *38* (24), 1700212.

(2) Lutz, J.-F.; Lehn, J.-M.; Meijer, E. W.; Matyjaszewski, K.; Takeuchi, M. *Nat. Rev. Mater.* **2016**, *1* (5), 16024.

(3) Pieters, B. J. G. E.; Van Eldijk, M. B.; Nolte, R. J. M.; Mecinović, J. *Chem. Soc. Rev.* **2016**, *45* (1), 24.

(4) Becer, C. R. *Macromol. Rapid Commun.* **2012**, *33* (9), 742.

(5) Spain, S. G.; Cameron, N. R. *Polym. Chem.* **2011**, *2* (1), 60.

(6) Gamblin, D. P.; Scanlan, E. M.; Davis, B. G. *Chem. Rev.* **2009**, *109* (1), 131.

(7) Ting, S. R. S.; Chen, G.; Stenzel, M. H. *Polym. Chem.* **2010**, *1* (9), 1392.

(8) Kiessling, L. L.; Gestwicki, J. E.; Strong, L. E. *Angew. Chemie Int. Ed.* **2006**, *45* (15), 2348.

(9) Lundquist, J. J.; Toone, E. J. *Chem. Rev.* **2002**, *102* (2), 555.

(10) Yilmaz, G.; Becer, C. R. *Eur. Polym. J.* **2013**, *49* (10), 3046.

(11) Yilmaz, G.; Uzunova, V.; Hartweg, M.; Beyer, V.; Napier, R.; Remzi Becer, C. *Polym. Chem.* **2018**, *9*, 611.

(12) Kiessling, L. L.; Grim, J. C. *Chem. Soc. Rev.* **2013**, *42* (10), 4476.

(13) Mavila, S.; Eivgi, O.; Berkovich, I.; Lemcoff, N. G. *Chem. Rev.* **2016**, *116* (3), 878.

(14) Huo, M.; Wang, N.; Fang, T.; Sun, M.; Wei, Y.; Yuan, J. *Polymer*. June 2015, pp A11–A21.

(15) Lyon, C. K.; Prasher, A.; Hanlon, A. M.; Tuten, B. T.; Tooley, C. A.; Frank, P. G.; Berda, E. B. *Polym. Chem.* **2015**, *6* (2), 181.

(16) Altintas, O.; Barner-Kowollik, C. *Macromol. Rapid Commun.* **2016**, *37* (1), 29.

(17) Huurne, G. M. ter; Palmans, A. R. A.; Meijer, E. W. *CCS Chem.* **2019**, 64.

(18) Espeel, P.; Du Prez, F. E. *Macromolecules* **2015**, *48* (1), 2.

(19) Kröger, A. P. P.; Komil, M. I.; Hamelmann, N. M.; Juan, A.; Stenzel, M. H.; Paulusse, J. M. J. *ACS Macro Lett.* **2019**, *8* (1), 95.

(20) Wuest, K. N. R.; Lu, H.; Thomas, D. S.; Goldmann, A. S.; Stenzel, M. H.; Barner-Kowollik, C. *ACS Macro Lett.* **2017**, *6* (10), 1168.

(21) Terashima, T.; Sugita, T.; Fukae, K.; Sawamoto, M. *Macromolecules* **2014**, *47* (2), 589.

(22) Terashima, T.; Sawamoto, M. In *Single-Chain Polymer Nanoparticles*; Wiley-VCH Verlag GmbH & Co. KGaA: Weinheim, Germany, 2017; pp 313–339.

(23) Cantekin, S.; De Greef, T. F. A.; Palmans, A. R. A. *Chem. Soc. Rev.* **2012**, *41*

(18), 6125.

(24) Mes, T.; Van Der Weegen, R.; Palmans, A. R. A.; Meijer, E. W. *Angew. Chemie - Int. Ed.* **2011**, *50* (22), 5085.

(25) ter Huurne, G. M.; Gillissen, M. A. J.; Palmans, A. R. A.; Voets, I. K.; Meijer, E. W. *Macromolecules* **2015**, *48* (12), 3949.

(26) Gillissen, M. A. J.; Terashima, T.; Meijer, E. W.; Palmans, A. R. A.; Voets, I. K. *Macromolecules* **2013**, *46* (10), 4120.

(27) Stals, P. J. M.; Gillissen, M. A. J.; Paffen, T. F. E.; De Greef, T. F. A.; Lindner, P.; Meijer, E. W.; Palmans, A. R. A.; Voets, I. K. *Macromolecules* **2014**, *47* (9), 2947.

(28) ter Huurne, G. M.; de Windt, L. N. J.; Liu, Y.; Meijer, E. W.; Voets, I. K.; Palmans, A. R. A. *Macromolecules* **2017**, *50* (21), 8562.

(29) Brown, G. D.; Willment, J. A.; Whitehead, L. *Nat. Rev. Immunol.* **2018**, *18* (6), 374.

(30) Khoo, U.-S.; Chan, K. Y. K.; Chan, V. S. F.; Lin, C. L. S. *J. Mol. Med.* **2008**, *86* (8), 861.

(31) Léger, P.; Tetard, M.; Youness, B.; Cordes, N.; Rouxel, R. N.; Flamand, M.; Lozach, P. Y. *Traffic* **2016**, *17* (6), 639.

(32) Kerscher, B.; Willment, J. A.; Brown, G. D. *Int. Immunol.* **2013**, *25* (5), 271.

(33) Martin, M.; Blom, A. M. *Immunol. Rev.* **2016**, *274* (1), 218.

(34) Sancho, D.; Reis e Sousa, C. *Curr. Opin. Immunol.* **2013**, *25* (1), 46.

(35) Cao, L.; Shi, X.; Chang, H.; Zhang, Q.; He, Y. *Proc. Natl. Acad. Sci. U. S. A.* **2015**, *112* (23), 7237.

(36) Hanč, P.; Schulz, O.; Fischbach, H.; Martin, S. R.; Kjær, S.; Reis e Sousa, C. *EMBO J.* **2016**, *35* (22), 2484.

(37) de Witte, L.; Nabatov, A.; Pion, M.; Fluitsma, D.; de Jong, M. A. W. P.; de Gruijl, T.; Piguet, V.; van Kooyk, Y.; Geijtenbeek, T. B. H. *Nat. Med.* **2007**, *13* (3), 367.

(38) Berg, L. M. van den; Cardinaud, S.; Aar, A. M. G. van der; Sprokholt, J. K.; Jong, M. A. W. P. de; Zijlstra-Willems, E. M.; Moris, A.; Geijtenbeek, T. B. H. *J. Immunol.* **2015**, *195* (4), 1763.

(39) Dumic, J.; Dabelic, S.; Flögel, M. *Biochim. Biophys. Acta - Gen. Subj.* **2006**, *1760* (4), 616.

(40) Meng, X. L.; Fang, Y.; Wan, L. S.; Huang, X. J.; Xu, Z. K. *Langmuir* **2012**, *28* (38), 13616.

(41) Terashima, T.; Mes, T.; De Greef, T. F. A.; Gillissen, M. A. J.; Besenius, P.; Palmans, A. R. A.; Meijer, E. W. *J. Am. Chem. Soc.* **2011**, *133* (13), 4742.

(42) Oz, Y.; Abdouni, Y.; Yilmaz, G.; Becer, C. R.; Sanyal, A. *Polym. Chem.* **2019**, *10* (24), 3351.

(43) ter Huurne, G. M.; Vantomme, G.; van den Bersselaar, B. W. L.; Thota, B. N. S.;

Voets, I. K.; Palmans, A. R. A.; Meijer, E. W. *J. Polym. Sci. Part A Polym. Chem.* **2019**, *57* (3), 411.

(44) Zhang, Q.; Anastasaki, A.; Li, G.-Z.; Haddleton, A. J.; Wilson, P.; Haddleton, D. M. *Polym. Chem.* **2014**, *5* (12), 3876.

(45) Roy, B.; Mukhopadhyay, B. *Tetrahedron Lett.* **2007**, *48* (22), 3783.

Chapter 6

Overview and Future Prospects

In this short chapter, we reflect on what has been achieved in this PhD thesis, what could be improved and what the future beholds in this exciting field of glycopolymer chemistry.

VI Overview and Future Prospects

In this PhD thesis, we have successfully demonstrated the synthesis, characterisation and use of new polymeric structures with novel architectures and proven their relevancy in biological applications. For me the beauty of this thesis lies in the fact that as a polymer chemist I was able to successfully combine the three core Natural Sciences of today, meaning the beautiful discipline of ***Chemistry***, studying substances, their composition, properties, structures and how they react with other substances, but also ***Physics***, studying matter, energy, forces and the interactions between them, and then lastly ***Biology***, the study of life and living organisms, most probably the study with which most people can relate and understand its importance through *Medicine* and *Pharmacology*.

In a first project, we were able to demonstrate (*by trial and error*) the successful synthesis of a novel *β*-Cyclodextrin and its use in the sequence-controlled polymerisation of a series of acrylates. The original goal was to use these systems for the polymerisation of saccharide bearing acrylates, however the combination of both star initiators, which demand more dilute reaction conditions, and sequence-controlled polymerisations, which demand very high conversion rates, proved to be cumbersome when applying to glycomonomers, as they have a slower propagation rate as compared to other acrylates. As discussed in Section I.5, Solid-Phase synthesis (as employed by the group of Hartmann) proved to be much more attractive to achieve sequence-defined oligomers, as the desired compounds can be optimised to display optimal distances between carbohydrates.

In the second project, we explored the influence of molecular architecture of glycopolymers on lectin binding, meaning how star polymer design and thus amount of glycopolymer arms has an effect on binding affinity. We demonstrated that for polymers with an equal amount of carbohydrates per molecule, an increase in amount of arms lowers the binding affinity, thus we concluded (as established before) that this is due a reduction in glycopolymer arm length. We furthermore demonstrated that when arm length is kept the same, an increase in amount of arms results in an increase in binding

affinity, and thus for future designs, it is beneficial to include more arms per glycopolymer.

In a third project, we investigated the synthesis and use of glycosylated polyethylenimine (*glyco*PEI) for self-amplifying RNA (*sa*RNA) transfection both *in vitro* and *ex vivo*. Nature's toolbox, for the synthesis of various biomolecules, exploits all types of chemical and physical interactions to achieve function in life. One of the tools that is not heavily exploited yet synthetically by humans, is the use of supramolecular interactions to achieve functional and biologically relevant materials (apart from drug delivery *via* polymersomes). Here we glycosylated PEI by covalently attaching adamantane moieties and subsequently exploiting these adamantane through modified *β*–cyclodextrin host-guest interactions. We showed that although *in vitro* transfection efficiency stifles, glycosylation of the PEIs does enhance the percentage of cells expressing *sa*RNA *ex vivo* in human skin explants. Increasing mannosylation, did increase *sa*RNA in epithelial cells specifically, demonstrating our intended targeted delivery.

Lastly, the pièce de résistance, the project combining all three core Natural Sciences, was the synthesis and physicochemical characterisation of single-chain folding glyconanoparticles and applying them in lectin binding studies. We were able to demonstrate that increasing the hydrophobic content along the polymer chain results in more compact nanoparticles, which unfortunately meant paying a penalty in lectin-binding affinity. We were also able to show here that using the directional supramolecular interactions of benzene-1,2,3-tricarboxamides (BTA) can be beneficial in lectin-binding affinity, as they induce clustering of glycopolymer chains into small multi-chain nanoparticles, illustrating the fine balance between intermolecular and intramolecular interactions.

It should be clear, that when designing new glycopolymeric systems in the future (be it for drug delivery or as adjuvants or vaccines), molecular architecture plays an important role and not only 'the type of sugar which is used'. We are still a long way from achieving absolute control over structure and function as Nature has, but Science has achieved tremendous steps forward over the past decade. Undoubtedly, when all characteristics for ideal binding affinity (in specific cases) are understood, the novel tools of sequence-control and single-chain folding nanotechnology should be able to offer us specifically tailored macromolecules in the same way as we are able to make specifically tailored small molecules in pharmacology.